Mesoporous silica particles and macrocyclic ligands as modulators of polyphenol oxidase activity in food systems.

DOCTORAL THESIS

Presented by:
Sara Muñoz Pina

Supervised by:
Ana Mª Andrés Grau
Ángel Luís Argüelles Foix
José Vicente Ros Lis

September 2021

UNIVERSITAT POLITÈCNICA DE VALÈNCIA

IIAD
INSTITUTO DE INGENIERÍA DE ALIMENTOS PARA EL DESARROLLO

UNIVERSITAT POLITÈCNICA DE VALÈNCIA

INSTITUTO UNIVERSITARIO DE INGENIERÍA DE ALIMENTOS PARA EL DESARROLLO

Mesoporous silica particles and macrocyclic ligands as modulators of polyphenol oxidase activity in food systems.

DOCTORAL THESIS

Presented by

Sara Muñoz Pina

Supervisors

Dra. Ana Mª Andrés Grau

Dr. Ángel Luís Argüelles Foix

Dr. José Vicente Ros Lis

September 2021

Dra. Ana Mª Andrés Grau, Catedrática de Universidad perteneciente al Departamento de Tecnología de Alimentos de la Universidad Politécnica de València,

Dr. Ángel Luís Argüelles Foix, profesor titular del Departamento de Tecnología de Alimentos de la Universitat Politècnica de València,

Dr. José Vicente Ros Lis, profesor titular del Departamento de Química inorgánica de la Universitat de València,

CONSIDERAN: que la memoria titulada "Mesoporous silica particles and macrocyclic ligands as modulators of polyphenol oxidase activity in food systems" que presenta Dª Sara Muñoz Pina, para aspirar al grado Doctor de la Universitat Politècnica de València, y que ha sido realizada bajo su dirección en el Instituto Universitario de Ingeniería de Alimentos para el Desarrollo de la Universitat Politècnica de València, reúne las condiciones adecuadas para constituir su tesis doctoral, por lo que AUTORIZAN a la interesada para su presentación.

Valencia, junio de 2021

Fdo.: Ana Mª Andrés Grau Fdo.: Ángel Luís Argüelles Foix Fdo.: José Vicente Ros Lis

A mis padres,

por permitirme soñar,

por permitirme ser quien quiero ser.

AGRADECIMIENTOS

En primer lugar, me gustaría agradecer a mis tres directores, Ana Andrés, Ángel Argüelles y José Vicente Ros, por contar conmigo y confiar en mí. Ana, gracias por tener siempre la puerta de tu despacho abierta para ayudarme y apoyarme, no solo en temas científicos sino personales. Ha sido un placer ser tu doctoranda y aprender tanto de ti. Ángel, gracias por tu cariño y por tu apoyo, gracias por anteponer siempre mi bienestar y no dudar en echarme una mano cuando lo he necesitado. A José Vicente, por todo lo aprendido en estos años.

A mi familia, porque nada de esto hubiera sucedido sin ellos. Mil gracias a mi padre, de ti saqué mi vena científica, la pasión por aprender y la curiosidad por indagar en lo no conocido. Aunque nunca podré saber tanto de química como tú, espero que estés orgulloso de mi. Gracias a mi madre, mi apoyo incondicional, la que siempre ha confiado en que yo puedo con todo y nunca ha dejado de creer en mí. Gracias a mis hermanos, gracias por ser los mejores, por quererme y apoyar todas mis aventuras, gracias por estar siempre conmigo, no sabéis cuanto os quiero.

Gracias a ti, Alberto, tú eres parte de esta tesis casi tanto como yo. Sabes que no habría podido hacerlo sin ti. Has leído cada una de estas palabras, has estado a mi lado siempre, tanto en los buenos como en los malos momentos, y siempre has estado para darme un abrazo y un decirme ¡tú puedes! Eres el mejor compañero de vida que he podido elegir. Millones de gracias. Te quiero.

Gracias a mis chicos L1-05, Mariola, Ruth, Diego y Aitana. He aprendido infinidad con vosotros, me he reído todos los días a vuestro lado y me habéis apoyado siempre. No me olvido de ti Ever. Contigo he pasado infinidad de horas en el lab. Gracias por estar siempre ahí y ayudarme en mis "crisis", ¡nos vemos en México! Gracias a Leydi por todos los momentos que hemos pasado juntas. Gracias a Juan,

por todas las risas y por tu super apoyo. Gracias a todos los de la "planta 1", los que aún seguís por estos pasillos y los que habéis pasado en algún momento por aquí: Carolina, Andrea, Quim, Janaina, Sara, Laura, Victoria, Ángela, Claudia, Stevens, etc.

Gracias a todos los técnicos del IIAD que siempre me han ayudado en todo lo que he necesitado. Especial mención a Vir. Gracias por ayudarme tanto, por todos esos ratos de conversaciones en tu despacho y por seguir preocupándote por mí.

Gracias a Ana Heredia, por confiar en mí para tu proyecto y por todo lo que he aprendido junto a ti.

A mis "tesinandas" Dafne y Élia, ha sido un placer y una grata experiencia trabajar con vosotras.

Gracias a Ramón Martínez, Enrique García España y Pedro Amorós por haber colaborado en esta tesis. En concreto a los chicos del "cubo rojo": Eli, Santi, Cris F., Carmen, Mar, Cris, Luis y Adri. Santi, gracias por ayudarme tanto, sobre todo en la parte final de la tesis. A mis chicas: Eli, Carol y Nataly, gracias por vuestra ayuda y cariño, por todas esas tardes juntas, sabéis que habéis sido fundamentales.

Gracias a mis queridos "futuros millonarios": Borja, Javi, Juan, Lara y Valeriano. No sabéis cuanto me habéis ayudado y lo agradecida que estoy.

Gracias Ana, por todas las meriendas y paseos de desahogo juntas.

Muchas gracias a mis amigas, gracias por estar desde pequeñas a mi lado, por celebrar cada uno de mis éxitos como si fuera vuestro y por apoyarme siempre.

Gracias a la autora de mi fantástica portada: One. Contigo empezó todo en 2008 y con tu portada termina esta etapa. No podría estar más feliz de haberme cruzado contigo. Gracias Paula, por ser como eres y estar siempre conmigo.

Y, por último, gracias a Nala y Canelo, por ser la alegría de la casa.

ABSTRACT

The browning of injured fruit and vegetable tissues can cause undesirable changes and consumers' rejection resulting in high economic losses and food waste. This damage, known as enzymatic browning, is mainly caused by the polyphenol oxidase enzyme (PPO) which oxidize the phenolic compounds found in these tissues into reddish pigments named melanonids. Thus, preventing PPO activity in post-harvest processing fruits and vegetables including their juices has received a lot of attention from the food industry. Nonetheless, the current alternatives have some drawbacks such as negative effects on the nutritional quality of products or high cost. Hence, the purpose of this doctoral thesis is focused on the development and evaluation of new non-thermal strategies for PPO inhibition and prevention of the enzymatic browning. For this purpose, two different strategies were addressed; On one hand, several macrocyclic polyamine compounds were selected and evaluated. The chemical structure was found to strongly influence the inhibitor power, and two different compounds were found to be efficient against the enzymatic browning with IC_{50} of 10 µM and 0.30 mM. Their effectiveness was proved in cloudy apple juice resulting in a delay of the enzymatic browning and the loss of total phenolic compounds. On the other hand, the development and application of mesoporous silica particles functionalized with diverse chemical groups were studied. The results showed that both the structure of the material and the type of functionalization are decisive. The UVM-7 support offered the strongest inhibition of the PPO. The functionalisation with thiol groups enhanced the inhibitor power stopping the enzymatic browning in cloudy apple juice. Alternatively, amine groups, although showing less inhibitory power, were able to immobilise the enzyme. Finally, the UVM-7 support was magnetized for easily elimination of the medium, thus preventing the juice filtration need. Cloudy apple juice treated with magnetized

UVM-7 functionalized with thiol groups maintained the initial concentration of both vitamin C and flavonoids. Moreover, the antioxidant capacity and the total phenolic content remained almost unchanged.

RESUMEN

El oscurecimiento de los tejidos de frutas y verduras dañados puede provocar cambios indeseables y el rechazo por parte del consumidor. Este deterioro, conocido como pardeamiento enzimático, es causado principalmente por la enzima polifenol oxidasa (PPO), que oxida los compuestos fenólicos en pigmentos rojizos llamados melanoides. De esta forma, la prevención de la actividad de PPO en el procesamiento postcosecha tanto en frutas y verduras como en sus licuados, ha recibido desde siempre mucha atención por parte de la industria alimentaria. Sin embargo, los tratamientos actuales presentan diversos inconvenientes, entre los que podemos destacar los efectos negativos en la calidad nutricional de los productos y su elevado coste. El cometido de esta tesis doctoral se centra en el desarrollo y evaluación de nuevas estrategias no térmicas para la inhibición de la PPO con el objetivo final de detener el pardeamiento enzimático. Para esto se abordaron dos estrategias diferentes. Por un lado, se seleccionaron y evaluaron varias poliaminas macrocíclicas. Se determinó que la estructura química influye fuertemente en el poder inhibidor, existiendo dos compuestos altamente eficaces contra el pardeamiento enzimático, los cuales presentan IC_{50} de 10 µM y 0.30 mM. Su eficacia se validó en zumo de manzana recién licuado retrasando el pardeamiento enzimático y la pérdida de compuestos fenólicos totales. Por otro lado, se estudió el desarrollo y aplicación de partículas de sílice mesoporosas funcionalizadas con diversos grupos químicos. Los resultados mostraron que tanto la estructura del material como la funcionalización son determinantes. El soporte UVM-7 ofreció la inhibición más fuerte sobre la enzima PPO, y una vez funcionalizado con grupos tiol este aumentó notablemente su poder inhibidor, deteniendo el pardeamiento enzimático en zumo de manzana. Por el contrario, los grupos amino, aunque mostraron menor poder inhibidor, fueron capaces de inmovilizar a la enzima y

eliminarla del medio. Finalmente, el soporte UVM-7 fue magnetizado para su fácil eliminación del medio, evitando así la etapa de filtración. El soporte UVM-7 magnetizado y funcionalizado con tioles logró mantener la concentración inicial de vitamina C y flavonoides en el zumo de manzana. Además, la capacidad antioxidante y el contenido de fenoles totales se mantuvieron casi sin cambios.

RESUM

L'enfosquiment de fruïtes i verdures provoca un alt rebuig per part del consumidor. Aquest fet genera grans pèrdues econòmiques i un gran desaprofitament d'aliments. Aquest deteriorament, conegut com enfosquiment enzimàtic, és causat principalment per l'enzim polifenol oxidasa (PPO), que oxida els compostos fenòlics en pigments vermellosos anomenats melanoïdines. D'aquesta manera, la prevenció de l'activitat de la PPO en el processament postcollita tant en fruites i verdures com en els seus liquats, ha rebut des de sempre molta atenció per part de la indústria alimentària. No obstant això, els tractaments actuals presenten diversos inconvenients, entre els quals podem destacar els efectes negatius en la qualitat nutricional dels productes o el seu elevat cost. L'objectiu d'aquesta tesi doctoral es centra en el desenvolupament i avaluació de noves estratègies no tèrmiques per a la inhibició de la PPO amb la finalitat de detindre el enfosquiment enzimàtic. Per això s'aborden dues estratègies diferents. D'una banda, es va seleccionar i avaluar diverses poliamines macrocícliques. Determinat que l'estructura química influeix fortament en el poder inhibidor, existint dos compostos altament eficaços contra el enfosquiment enzimàtic, els quals presenten IC_{50} de 10 µM i 0.30 mM. La seua eficàcia es va validar en el suc de poma recentment liquat retardant el enfosquiment enzimàtic i la pèrdua de compostos fenòlics totals. D'altra banda, es va estudiat el desenvolupament i aplicació de partícules de sílice mesoporoses funcionalitzades amb diversos grups químics. Els resultats van mostrar que tant l'estructura del material com la funcionalització foren determinants. El suport UVM-7 va oferir la inhibició més forta sobre l'enzim PPO, i una vegada funcionalitzat amb grups tiol aquest va augmentar notablement el seu poder inhibidor, detenint el enfosquiment enzimàtic en el suc de poma. Tot i això, els grups amina, encara que mostren menys poder inhibidor, foren capaços d'immobilitzar

l'enzim i eliminar-la del medi. Finalment, el suport UVM-7 va ser magnetitzat per la seva fàcil eliminació del mig, evitant així l'etapa de filtració. El suport UVM-7 magnetitzat i funcionalitzat amb grups tiol va aconseguir mantindre la concentració inicial de vitamina C i flavonoides en el suc de poma. A més, la capacitat antioxidant i el contingut de fenols totals es van mantindre quasi sense canvis.

PREFACE

Justification of the study

Enzymatic browning is one of the most important reactions in food technology affecting foods rich in phenolic compounds like fruits, vegetables, and seafood. This chemical alteration is a complex process catalysed by the polyphenol oxidase enzyme (PPO) in which phenolic compounds are oxidized giving rise to reddish-brownish pigments called melanonids. This undesirable phenomenon not only alters the original colour of the food but affects its taste and nutritional value. Besides, the colour change causes rejection by the consumer leading to high amounts of food waste and economic losses for the industry.

Within the agri-food sector, the most affected industry by enzymatic browning is the one dedicated to the production of fruit and vegetable juices. When squeezing the fruit, cell membranes break releasing both PPO and polyphenols located initially in different organelles (plastids and vacuoles). In addition, the large amount of oxygen in the blend accelerates the enzymatic reaction. Thus, one of the critical points faced by this sector is to avoid or at least minimize as much as possible the enzymatic browning. Traditionally, thermal pasteurization has been used to inactivate the PPO however rising the temperatures above 60°C negatively affects thermosensitive nutrients such as vitamins, carotenoids, and anthocyanins. Other non-thermal treatments have been developed, yet the high investment needed, or the elevated cost of production have limited their implementation.

Thus, with the high demands of consumers, the low-profit margins of the industry, and the great environmental awareness, it is necessary to keep searching for an alternative that preserves the nutritional, and organoleptic properties of juices, also offering a viable alternative for the industry.

Dissertation outline

The present Doctoral Thesis is a papers compendium-style thesis structured in 7 sections: Introduction, Hypothesis and Objectives, Work Plan, Experimental Methodology, Results and Discussion, Concluding Remarks and Future Perspectives. The aim of the Introduction is to compile the enzymatic browning features. A description of the enzymatic browning process, its origin, drawbacks and, current strategies for the inhibition of PPO were gathered and documented. The Hypothesis and Objectives, in the form of research questions, include the specific aims related to the different papers. In the Work Plan section, diagrams summarising the experimental plan are provided. More descriptive information is found in the Experimental Methodology section. A total of 5 scientific papers conforms the Results and Discussion divided in 2 different chapters. Finally, the Concluding Remarks are stated followed by a short comment on possible Future Perspectives.

Dissemination of the results

- International journals

Published:

Muñoz-Pina, S., Ros-Lis, J. V., Argüelles, Á., Coll, C., Martínez-Máñez, R., & Andrés, A. (2018). Full inhibition of enzymatic browning in the presence of thiol-functionalised silica nanomaterial. *Food chemistry*, 241, 199-205.

Muñoz-Pina, S., Ros-Lis, J. V., Argüelles, Á., Martínez-Máñez, R., & Andrés, A. (2020). Influence of the functionalisation of mesoporous silica material UVM-7 on polyphenol oxidase enzyme capture and enzymatic browning. *Food chemistry*, 310, 125741.

Muñoz-Pina, S., Ros-Lis, J. V., Delgado-Pinar, E., Martínez-Camarena, A., Verdejo, B., García-España, E., Argüelles, A. & Andrés, A. (2020). Inhibitory Effect of Azamacrocyclic Ligands on Polyphenol Oxidase in Model and Food Systems. *Journal of Agricultural and Food Chemistry*, 68 (30), 7964-7973.

Submitted or under preparation:

Muñoz-Pina, S., Duch-Calabuig, A., Ros-Lis, J. V., Verdejo, B., García-España, E., Argüelles, A. & Andrés, A. (2021). A tetraazahydroxypyridinone derivative as inhibitor of apple juice enzymatic browning and oxidation. *LWT - Food Science and Technology* (submitted).

Muñoz-Pina, S., Duch-Calabuig, A., Ruiz de Assín E., Ros-Lis, J. V., Amorós, P., Argüelles, A. & Andrés, A. (2021). Bioactive compounds and enzymatic browning inhibition in cloudy apple juice by a new magnetic UVM-7-SH mesoporous material (under preparation).

- *Book chapters*

Muñoz-Pina, S., Ros-Lis, J. V., Argüelles, Á., & Andrés, A. (2020). Use of Nanomaterials as Alternative for Controlling Enzymatic Browning in Fruit Juices. In Nanoengineering in the Beverage Industry: Volumen 20: The Science of beverages (pp. 163-196). Elsevier.

- *International conferences*

Oral presentation - Muñoz-Pina, S., Ros-Lis, J. V., Argüelles, Á., Coll, C., & Andrés, A. (2016). PPO-substrate interaction study in presence of silica nanomaterials. X International Workshop on Sensors and Molecular Recognition. 7-8 July, Valencia, Spain.

Poster - Muñoz-Pina, S., Ros-Lis, J. V., Argüelles, Á., Coll, C., Martínez-Máñez, R., & Andrés, A. (2017). Enzymatic browning study in presence of UVM-7 functionalized with thiol groups. XI International Workshop on Sensors and Molecular Recognition. 6-7 July, Valencia, Spain.

Poster - Muñoz-Pina, S., Ros-Lis, J. V., Argüelles, Á., Coll, C., & Andrés, A. (2018). Interaction study between PPO and mesoporous silica nanoparticles with diverse functionalization. XII International Workshop on Sensors and Molecular Recognition. 5-6 July, Valencia, Spain.

Poster - Muñoz-Pina, S., Ros-Lis, J. V., Verdejo, B., García-España, E., Argüelles, A. & Andrés, A. (2019). Supramolecular inhibitors of polyphenol oxidase based on polyamines. XIII International Workshop on Sensors and Molecular Recognition. 4-5 July, Valencia, Spain.

TABLE OF CONTENTS

LIST OF FIGURES

Figure 5.31. Antioxidant capacity measured by three different methodologies (DPPH●, ABTS●+, and FRAP) of cloudy apple juice. Dotted line indicates the initial value in the juice at t=0. *After removing the material after 10 min in contact with the cloudy apple juice. $^{a-c}$ Different lowercase letters indicate significant differences among times for $p<0.05$ compared with the control t=0. $^{A-C}$ Different capital letters indicate significant differences among compounds at the same time for $p<0.05$; in this case both time 10 and 10* (before and after removing the material) are compared with control t=10 min..... 271

LIST OF TABLES

1. INTRODUCTION

BOOK CHAPTER

Muñoz-Pina, S. et al. (2020). Use of Nanomaterials as Alternative for Controlling Enzymatic Browning in Fruit Juices. In Nanoengineering in the Beverage Industry: Volumen 20: The Science of beverages (pp. 163-196). Elsevier.

1. Introduction

1.1. Polyphenol oxidase and enzymatic browning

1.1.1. Polyphenol oxidase structure and activity

Polyphenol oxidase (PPO) is a term that includes a large number of copper-containing enzymes, comprising catechol oxidase (EC 1.10.3.1), tyrosinase (EC 1.14.18.1), and laccase (E.C. 1.10.3.2). It was first discovered by Schoenbein in 1856 in mushroom but it is widely distributed in nature as can be found in bacteria, fungi, animals, and plants[1].

This metalloprotein belongs to the oxidoreductase family and it is characterised for having in its active centre two copper ions linked each one to three histidines being a type 3 copper enzyme (see Figure. 1.1)[2]. This enzyme catalyses the oxidation of phenolic substrates into quinones and depending on the source of the enzyme, it may act over monophenols and/or diphenols, so its general name is polyphenol oxidase. As an example, tyrosinase can act over both types of substrates, whereas, catechol oxidase from plant sources shows only o-diphenol oxidase activity[3].

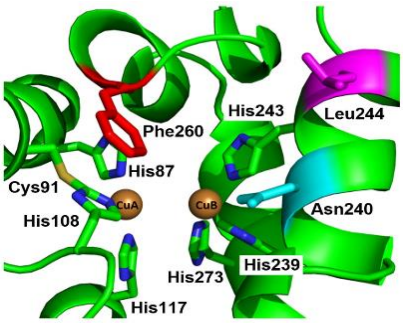

***Figure 1.1** . Example of an active center from PPO. (Source: Panis et al., 2020)[2]*

During oxidation, the PPO centre active can undergo three different stages: met-, oxy- and deoxy-tyrosinase, although only met- and oxy-tyrosinase are bonded to oxygen and capable of catalyse the oxidation of polyphenols (see Figure 1.2)[4]. Both forms have catecholase/diphenolase activity, which means the capacity to convert *o*-diphenols into *o*-quinones, but only the oxi-tyrosinase form exhibit cresolase/monophenolase activity[5,6]. At the end of one cycle,

two molecules of catechol are oxidized, and one molecular oxygen is reduced to water resulting in the formation of two quinone products (see Figure 1.2).

On the other hand, the genetic structure of the PPO varies on the food species, cultivar, maturity, and age generating diverse isoenzymes[7,8]. The structural differences between the isoenzymes cause each of them to have differences on electrophoretic mobility, optimal temperature, and pH, as well as differences in the substrate specificity[9–11]. For instance, apples analysed under the same pH and same substrate showed differences on their activity where higher activity was found for Starking Delicious (0.45 u/mL) and the lowest for Golden Delicious and Fuji (0.18 – 0.14 U/mL)[12]. Besides, in comparison with other varieties of fruits, apples have higher activity than lulo, mango, and passion fruit (0.13, 0.016, and 0.01 respectively) under the same conditions[13].

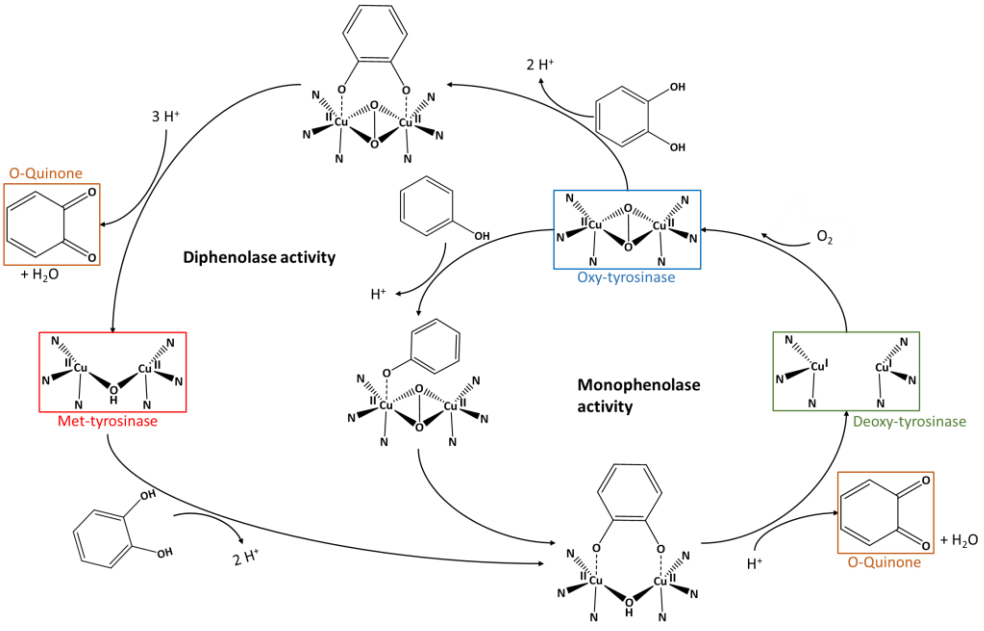

***Figure 1.2**. Monophenolase and diphenolase cycle of tyrosinase enzyme.*

The enzymatic browning process, which occurs in fruits (e.g., apricots, pears, bananas, and grapes), vegetables (e.g., potatoes, mushrooms, and lettuce), and in seafood (e.g., shrimps, spiny lobsters, and crabs), is associated mainly to the Polyphenol Oxidase activity. Its effect results in the generation of brown pigments which are in some cases essential and desirable[14]. As an examples, it is used to remove phenols from wastewater, for the treatment of some diseases as Parkinson's disease and it is a quality parameter in chocolate or tea[15–17]. However, in most foods these reactions generate not only colour changes but also adverse effects on taste, flavour, and nutritional value[18].

Fruit juices are the most affected by the enzymatic browning considering that, when the fruit is liquefied, the cells break releasing all polyphenols and PPO into a medium with a high concentration of oxygen. As consumer acceptance of these products depends on their organoleptic properties, and colour is one of the most important attributes in juices and beverages. Thus, enzymatic browning has a great impact over the food industry, due to the consequent quality and economic losses.

1.1.2. The process of enzymatic browning

Enzymatic browning is a complex process divided into three parts: enzymatic hydroxylation, enzymatic oxidation, and non-enzymatic polymerization. In the first step, the enzyme catalyses the hydroxylation of monophenols to *o*-dihydroxyphenols and in the second one, the PPO catalyses the oxidation of *o*-dihydoxyphenols into *o*-quinones. Finally, a non-enzymatic reaction provokes the polymerization of these *o*-quinones (either with proteins and amino acids or between them) giving rise to reddish-brownish pigments called melanonids, which are the reason for colour change[19,20].

The main factors that influence enzymatic browning are the concentration and source of both the active enzyme and phenolic compounds. Yet also other factors such as pH, temperature, and oxygen concentration are relevant.

Active form of PPO: As pointed out, PPO is present in the tissues of most plants and animals, but especially in fruits and vegetables [21]. Nevertheless, its presence *per se* does not determine the level of enzymatic browning suffering by food. One characteristic of the PPO is its ability to exist in an inactive or latent state form with a C-terminal domain blocking its catalytic site (see Figure 1.3)[22,23]. PPO can be released from latency, or been activated, due to the presence of anionic surfactant, acidification, proteolytic treatment, or senescence[24]. The latent forms of PPO are not capable of oxidate any substrate unless they are activated, delaying thus the enzymatic browning[25,26]. Some food where these two forms (active and latent) have been found are lettuce, apricot, pulp mango, and truffles[27–30].

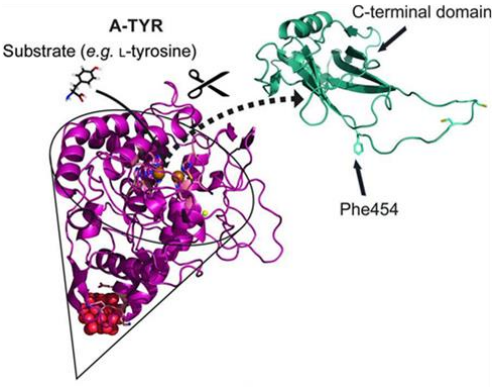

Figure 1.3. *Illustration of the activation process. (Source: Mauracher et al. 2014)*[23]

Concentration of phenolic compounds: The enzymatic browning is highly correlated with the concentration of phenolic compounds in food matrices. In this way, foods such as apples or avocado will be more susceptible to suffer enzymatic browning than others due to their high content. There are

an immense variety of these compounds presents in fruits and vegetables, but they vary among species, cultivar, maturity status and climatic/environmental conditions[31]. However, among all the phenolic compounds found, only a small number serves as direct substrates for PPO[32]. Besides, the substrate specificity differs depending on the PPOs source and not always is the majority compound. For examples, catechin is the major phenolic substrate in grapes however its PPO showed higher activity for caffeic acid. The PPO activity in peach was greater for catechin and in apples, chlorogenic acid is a key substrate although PPO revealed higher specificity for 4- methylcatechol[26,32,33].

pH: PPO activity also depends on the pH of the medium, which affects its structural conformation and thus binding of substrates and the catalysis. Generally, the optimum pH for PPO activity is between 4.0–8.0 and decreases until being almost inexistent below pH 3[10]. These values depend on the isoenzyme and even in the same fruit or vegetable at various stages of maturity have been reported to differ in optimum pH of activity[34]. It is interesting to note that some PPOs show a narrow pH optimum (field bean, 4.0), while others have a wider pH range or even multiple pH optima[26]. As an example, Red Fuji apple PPOs variety had the highest activity at pH 8.00, while Golden Delicious and Granny Smith at 4.50 and 7.50–8.00, respectively[35]. Hence, fruits with high acidic content like lemons, oranges and so, low enzymatic browning occurs.

Temperature: Temperature plays also a significant role in affecting the catalytic activity of PPO, as it influences the solubility of oxygen and may lead to enzyme denaturation. The PPO activity stops reversibly below 7 °C and can be destroyed partial or total when exposed at 70 - 90 °C[36]. The optimum

T also varies widely but is mostly in the range of 20–45 °C with few exceptions such as plums (65 °C) or strawberry (50 °C)[1,26].

Oxygen: Finally, the presence of oxygen is required for oxidation to occur as the reaction only starts when the PPO and the O_2 meet. Thus, those matrices with greater accessibility to oxygen will brown more.

Therefore, the combination of all these factors is necessary for food to suffer in a greater or lesser extent the enzymatic browning. Among all foods, fruits and vegetables are those that present all these requirements to be the most susceptible to browning (high concentrations of active PPO and polyphenols at an adequate pH). PPO and polyphenols are physically separated as PPO is mainly found in plastids while polyphenols are located in vacuoles. When there is a cell disruption in the matrix, PPO, polyphenols, and oxygen meet and starts the enzymatic browning. This tissue damage usually happens during harvesting, handling and post-harvest processing[12].

Hence, controlling and maintaining the organoleptic and nutritional properties of juices has been always a crucial target in the processing industry of fruits and vegetables, especially in their juices/beverages.

1.2. Strategies for the control of enzymatic browning in fruits and vegetables juices.

Over the years, the industry has adopted different methods and technologies to reduce enzymatic browning and, therefore, to decrease quality losses. Table 1.1 summarizes several approaches to avoid enzymatic browning during the preparation of juices, some of which are well-established technologies, and some others are still under development. As pointed in section 1.1.2, the

enzymatic browning depends on the concentration of the active enzyme, the phenolic compounds, pH, temperature, and the presence of oxygen. Thus, either variation of these factors or the inactivation/inhibition of the polyphenol oxidase enzyme (PPO) can be used to avoid the enzymatic browning and minimize product losses.

Among the strategies to interfere in the enzymatic browning process, we can highlight the removal of reactants such as oxygen or the denaturation of enzyme protein. In addition to the interaction with the copper prosthetic group and the interaction with the quinones formed during the oxidation process. However, heat treatments and the addition of anti-browning agents are still the most applied strategies[20].

Table 1.1. *Strategies for the control of enzymatic browning in fruits and vegetables juices and puree systems.*

Approach	Product	Reference
Thermal treatment	Apple juice	Wibowo et al., 2019[37]
	Strawberry puree	Aaby et al., 2018[38]
	Pomegranate juice	Vegara et al., 2013[39]
Ohmic heating	Apple juice	Abedelmaksoud et al., 2018[40]
	Watermelon juice	Makroo et al., 2017[41]
	Grape juice	Içier et al., 2008[42]
Microwave treatment	Avocado puree	Zhou et al., 2016[43]
	Apple puree	Picouet et al., 2009[44]
Reducing agents	Pear juice	Kolniak-Ostek et al., 2013[45]
	Grape juice	Wu 2014[46]
	Loquat juice	Ding et al., 2002[47]
Chelating agents	Pear puree	Lei Zhou et al., 2018[48]
	Apple juice	Du et al., 2012[49]
Acidulants	Pear puree	Lei Zhou et al., 2018[48]
	Pear juice	Jiang et al., 2016[51]
	Mango puree	Guerrero-Beltra et al., 2005[52]
Complexing agents	Apple juice	Martínez-Hernández et al.,2019[53]
	Apple juice	López-Nicolás et al., 2007[54]
Enzyme inhibitor	Apple puree	Sukhonthara et al., 2016[55]
	Apple juice	de la Rosa et al., 2011[56]
High-pressure processing	Carrot juice	Szczepańska et al., 2020[57]
	Blueberry juice	Zhu et al., 2017[59]
	Mango pulp	Kaushik et al., 2016[60]
Gamma irradiation	Grape juice	Carvalho Mesquita et al., 2020[61]
	Mango juice	Naresh et al., 2015[62]
Pulsed electric field	Apple juice	Wibowo et al., 2019[37]
	Apple juice	Zhang et al., 2018[63]
	Orange juice	Agcam et al., 2016[64]
Supercritical carbon dioxide	Apple juice	Murtaza et al., 2019[65]
	Apple juice	Marszałek et al., 2018[66]
Ultrasound	Bayberry juice	Cao et al., 2018[67]
	Strawberry juice	Bhat & Ming Goh 2017[68]
	Mango juice	Santhirasegaram et al. 2013[69]
Short-wave ultraviolet light	Melon juice	Fundo et al., 2019[70]
	Carrot juice	Türkmen el al., 2018[71]
	Apple and grape juice	Müller et al., 2014[72]
Cold plasma	Apple juice	Illera et al. 2019[73]

1.2.1. Thermal treatment

Thermal treatments, like pasteurization or sterilization, are the most commonly used methods by the juice industry due to their ability to both destroy microorganisms and inactivate enzymes. The inactivation of PPO, as well as other spoilage enzymes, can be achieved by subjecting the juice to high temperatures for an adequate length of time to denature the protein. Overall, the application of temperatures between 60-90^{o}C after the juice extraction destroys PPO catalytic activity stopping the polyphenol oxidation that produces brown colour; however, the time necessary for the PPO inactivation depends on the type of juice[38,39].

Conventional heat processes are classified according to their intensity as high temperature-long time (HTLT), high temperature-short time (HTST), mild temperature-long time (MTLT), and mild temperature-short time (MLST)[74]. Nowadays, HTLT is the most commonly used treatment in fruits and beverages with temperatures exceeding 80 °C and holding times above 30 seconds. Depending on the temperature used, it can be classified as pasteurization (temperature 80>T<100 °C), canning (temperature ca. 100 °C), or sterilization (temperature >100 °C)[75]. Juice pasteurization is able to reduce the strongest microorganism and also inactivates enzymes like PPO, POD (peroxidase), and PE (pectinesterase). However, juices with a pH above 4.5 need the strongest treatments to ensure proper shelf life and quality attributes since anthocyanins, vitamin C, and some carotenoids are thermolabile[76]. For instance, Radziejewska-Kubzdela & Biegańska-Marecik[77] reported a 40% reduction in ascorbic acid content and a 20% in total phenolics after pasteurization in cloudy apple juice. Besides, a decrease in most of the flavonoids was observed, not only in chlorogenic acid but also in catechin, epicatechin, and quercetin derivatives. Being the most affected quercetin derivatives with a reduction of 70 and 50 % respectively. In order to preserve these compounds, the industry developed

some alternatives: HTST (T≥80 °C and holding times ≤30 s), MTLT (T<80 °C and holding times >30 s), and MTST (T<80 °C and holding times ≤30 s) treatments. Nevertheless, highly thermolabile compounds such as ascorbic acid and some carotenoids are still lost in some juices[78,79]. Even minimizing the conditions (MTST), complete inhibition of PPO activity is not achieved, and some sensory and physicochemical properties are modified[74].

Thus, even though these treatments ensure safety and extend the shelf life of juices, the application of thermal treatments to inactivate PPO leads to a significant loss of the nutritional quality of the products. The destruction of thermosensitive nutrients such as vitamins, carotenoids, and anthocyanins[80,81] as well as the changes of colour, flavour, and texture are some of the drawbacks of applying thermal treatments[82]. It is a fact that researchers have optimized the time/temperature profile to minimize those effects in many fruit juices. However, as these parameters change with the raw material, it is still a great challenge for incipient beverages such as smoothies obtained from red fruits (blueberries, raspberries, grape, etc.) or new fruits (Cashew apple, Acerola, etc.).

The heating method affects the temperature distribution inside the food, and directly modifies the time-temperature relationship for enzyme deactivation[42]. Alternatively, to pasteurization or sterilization, where the heat is transferred through solid-liquid interfaces or between solid particles, ohmic heating (OH) has also been used in the food industry. OH consists of a conduction-heating technique for liquids and pumpable particles with sufficient conductivity, such as fruit and vegetable juices. This technique is defined as a process in which electric currents (100 V/cm) pass through the food system and dissipates as heat. During the process, occurs an internal energy transformation from electrical to thermal as an important number of ions start to move. The temperature rises rapidly, from seconds to minutes,

leading to safe products with high quality and added value[83]. In fact, OH has shown lower deterioration in carotenoids, antioxidants, and vitamin C in several juices than applying HT[84]. Nonetheless, OH requires electrodes in contact with the juices causing electrochemical reactions that lead to erosion and corrosion, some induced by the low pH of the juices. Furthermore, in OH electric conductivity is a crucial parameter that highly depends on the raw material. Many reports show the wide variability found in the electric conductivity of different fruits requiring adjustment according to the conductivity of the liquid. Thus, the cost and difficulties to control the process parameters, as well as lack of appropriate legislation, are the main issues for the implementation of these technologies[85,86].

1.2.2. Non- Thermal Treatments

1.2.2.1 Chemical agents

Alternative approaches based on the use of chemical treatments have been studied to control enzymatic browning in juices. These compounds are known as reducing agents (ascorbic acid and analogs, glutathione, L-cysteine), enzyme inhibitors (aromatic carboxylic acids, substituted resorcinols, anions, peptides, and sulphites), chelating agents (phosphates, EDTA, organic acids), acidulants (citric acid, phosphoric acid) and complexing agents (cyclodextrins)[87]. It is also possible to classify the different chemical treatments depending on whether they mainly affect the enzyme, the substrates, or the final products. The direct products of oxidation are *o*-quinones and they can be reduced again to *o*-diphenols (See Figure 1.4) or trapped in colourless complexes. As indicated above, these *o*-quinones polymerize into secondary products that are highly coloured compounds but much less reactive. Therefore, many compounds able to react with *o*-quinones have been investigated[88].

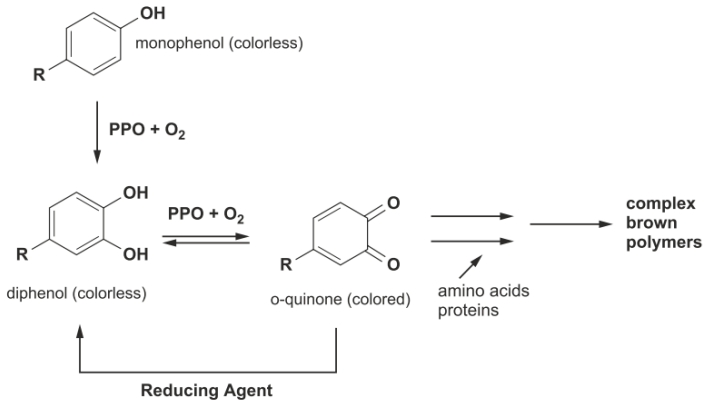

Figure 1.4. *Inhibition of the catalytic activity by reducing the o-quinones to colorless diphenol by reducing agents (Source: Jukanti, 2017)[26].*

Sulphites are the compounds most used so far by the food industry to control enzymatic browning. These chemicals are powerful inhibitors of PPO activity; however, an excess of sulphite-based formulations may cause adverse reactions, mainly in asthmatic people. Since it was reported by the Evaluations of the Joint FAO/WHO Expert Committee on Food Additives (JECFA) in 2008[90] that the intake of sulphites could be above safe limits, their use as food additives is not recommended.

Due to adverse health effects provoked by sulphites, researchers have been carrying out studies to find potent anti-browning agents that cause no damage to the organism. Like most enzymes, the activity of polyphenol oxidase is pH-dependent as the configuration of its structure changes with the pH. Thus, the addition of acids to the medium induces full inhibition. Besides, most of them not only reduce the pH but also have a secondary inhibition mechanism as chelators or reducing agents. This technique is extensively used, and the most employed acids are those found naturally, including ascorbic, citric, malic, and phosphoric acids.

An example would be the use of ascorbic acid; this acid is a potent antioxidant that lowers the pH and reduces the *o*-quinones formed to colourless catechols[51]. Is probably the most frequently used chemical product for browning control of fruit products, but its efficiency is highly dependent on its concentration in the commodities[91]. Furthermore, its effect is only temporary, as it irreversibly oxidizes to dehydroascorbic acid under either enzymatic or chemical oxidation conditions, and browning can then occur after depletion[36,92]. Another drawback of ascorbic acid would be its influence on the sensory properties of the products. This compound has a sour and bitter taste that at high concentrations can alter the flavour of the initial product. Besides, it has been studied how its concentration increases the unnatural odors in apple juice decreasing the fresh, fruity, and apple-like odors[93,94].

A similar but more powerful inhibitor would be kojic acid. This compound also acts as a reducing agent and as a non-competitive inhibitor. Its highest inhibitory influence has made it become a positive reference when testing new inhibitors against PPO[95]. However, its use in the food industry is not widespread due to the difficulty of large-scale production and its high cost[36].

In the case of citric acid, two different mechanisms modify the catalytic activity of the enzyme. Firstly, the lowering pH capacity, and secondly the acid also inhibits PPO by chelating the copper moiety of the enzyme[3]. However, acidulants are frequently used in combination with other types of antibrowning agents since it is very difficult to achieve complete inhibition for a long time only by reducing the pH. As an example, citric acid is added in conjunction with ascorbic acid or sodium sulphite for the inhibition of enzymatic browning[96].

Mixtures containing ascorbic acid are the most common combinations found both in literature and in trade. A clear example is the combination of plant proteases

with ascorbic acid described by Derardja et al. (2019)[28]. This study was carried out on apricot puree and the results reflected how the combinations were more effective than the application of ascorbic alone. A combination of 500 mg of ascorbic acid with 100 mg of papain causes a postharvest live improvement. When using only ascorbic acid, after 200h the browning decrease a 40%, on the contrary, the combination with proteases browning was reduced by 80%. This can be explained as ascorbic acid prevented the browning reactions that may occur before or during the proteolytic inactivation of PPO with the proteases. Regarding the combination of ascorbic acid with other compounds in fruit juices, Wang et al. (2014)[98] described the use of citric acid, ascorbic acid, and nitrogen in combination. The use of these compounds together causes a drop in the calculated browning index from 15.05 to 0.47.

Other compounds that seem to be effective in the control of enzymatic browning in fruit products are sulfur-containing compounds. These compounds are characterized by having one or more thiol groups on their structure such as L-cysteine, glutathione, mercaptoethanol, and thiourea. Nonetheless, among all these possible inhibitors, L-cysteine is the most effective one[99]. Despite sulphur-containing compounds prevent brown pigment formation the action mechanism is complex. Out of the many mechanisms of L-cysteine over PPO that have been proposed, the reaction with quinones intermediates and its reduction power of quinones, are the most acceptable ones[100]. However, in order to assure an effective inhibition, the needed concentration of cysteine is that high that produces an unwelcome odour[101], restricting its use in food processing.

On the other hand, several compounds have chemical structures closely related to o-diphenols and are able to interact directly with PPO. These enzyme inhibitors bind either to the active centre (competitive way) or to the allosteric site

(non-competitive way) of the PPO rending it incapable of catalysing the enzymatic reaction. These include methyl-substituted derivatives such as guaiacol and ferulic acid and m-diphenols such as 4-hexylresorcinol among others[95].

Since PPO is a metalloprotein in which copper is the prosthetic group, it is inhibited by a variety of chelating agents among the acids mentioned above. These include sodium diethyldithiocarbamate (DIECA), sodium azide, potassium ethylxanthate, and ethylene-diaminetetraacetate (EDTA)[89]. Sodium azide and DIECA are more powerful inhibitors than EDTA[102,103], however, these compounds are toxic and not allow in the food industry[104]. In contrast, EDTA is a chelating agent allowed for use in the food industry (E385). However as it does not present high effectiveness, this compound is usually used in conjunction with other reducing or acidifying agents, such as ascorbic or citric acid[105].

1.2.2.2. Other Physical Treatments

Due to consumer's demand for healthier and fresh-like products, it has raised the interest in exploring alternative food processing technologies that require minimal chemical additives with moderate effect on food quality. Nowadays, alternative methodologies or processing technologies involving non-thermal inactivation of enzymes are being widely investigated. As a result, several non/mild-thermal processing technologies have been developed aiming to achieve similar microbial and enzymatic inactivation, while extending the shelf-life of products. In this sense, finding non-thermal and non-chemical methods is a relevant challenge in the field.

The most studied and/or used methods so far are irradiation, high hydrostatic pressure, ultrafiltration, ultrasonication, and pulse electric fields.

In the first place, high-pressure processing (HPP), is a technique where food is subjected to elevated pressures (100-1000 MPa) over a short period with or without the addition of heat, to obtain a fresh-like, high quality and shelf-stable product[106]. HPP could preserve the nutritional value and the delicate sensory properties of fruit and vegetable juices due to its limited effect on low molecular-mass compounds[107]. However, this method is more efficient to inactivate microorganisms than to totally inactivate enzymes, which are more resistant[57]. Its use allows decreasing the temperature of thermal treatment, but it seems difficult to replace thermal treatments, besides this technique has a high cost when compared with traditional ones. As an example, there are some juices on the market treated by HPP, however, these juices must be stored under refrigeration and have less shelf-life.

Treatments based on the use of ultrasound (US), ultraviolet (UV), irradiation, and pulsed electric fields (PEF) are some of the approaches that could be applied for the inactivation of microorganisms and enzymes.

Over the last few years, ultrasonic technology has become to be a potentially beneficial food processing technique to destroy microorganisms and inactivate enzymes generally found in fruit and vegetable juices. The ultrasound application on food can offer a promising conservation approach without side effects on the food quality, nutritional quality, sensory properties, and visual attributes[108]. When applying high-power ultrasound at low frequencies (20–100 kHz) to a fruit juice, the ultrasound is propagated by the aqueous phase and an effect called cavitation occurs (formation and collapse of bubbles). Consequently, the so-called “tiny hotspot” is formed at a specific temperature and pressure providing the energy needed to destroy large molecules by liberating reactive radicals from the water. and producing the enzymatic inactivation. However, some new studies suggest that

inactivation is mainly caused by the rise in temperature over time rather than by the process applied[109].

Also, the application of ultraviolet light (UV) is an emerging technology for the treatment and disinfection of juices. When a juice is exposed to UV-C light, the proteins begin to form aggregates and therefore the enzymes begin to lose activity[110]. In the case of the microorganism present on the juice, the application of UV light at a wavelength of about 254 nm stops the DNA replication from having an effective treatment without chemicals. However, the penetration of UV-C light is compromised in coloured and turbid liquid foods and, besides, microorganisms can be protected by suspended solids in fruit juices[111].

Regarding ionizing radiation, it is a physical treatment that exposes the food directly to x-rays or gamma rays to improve food safety and quality. Irradiation inactivates microorganisms, guaranteeing disinfection and reduces the enzyme activity, so it would be a good option for extending the shelf-life of fruit and vegetable juices. However, among its disadvantages are the loss of nutrients from the juices during the processing, like vitamins, and the low acceptability by the consumer about the ingesting of irradiated foods. These reasons make this technology rarely used by industry[112].

Finally, pulsed electric fields (PEF), has also emerged in response to the claim for safe foods with a fresh-like quality and longer shelf-life and its capability of adaption to continuous processing[82]. Juice is introduced into a chamber that applies high voltage pulses (20-80 kV/cm) through two electrodes for a microsecond. Then, as a result, the cell membranes of microbial cells irreversibly lose their functionality through the process called electroporation, and the structures of the enzymes are also inactivated[113]. Still, the good result of this technique in the enzymatic inactivation depends on other factors such as electric field strength, treatment time,

electrical conductivity, and pH[114]. Nevertheless, PEF had demonstrated to be an alternative for heat treatments in liquid food due to the better response to the inactivation of enzymes and microorganisms. Odriozola-Serrano et al. (2009)[115] reported the influence of different PEF parameters on the total content of health-related compounds in strawberry juice. Their results revealed that the antioxidant potential of the juice was affected by the pulse width, pulse polarity, and frequency. PEF treatments conducted at 232 Hz with bipolar pulses of 1 ms produced strawberry juices with the highest content of health-related compounds. The same was also pointed out by Chen et al. (2013)[116] comparing several studies in fruit juices. Other authors[117] reviewed the effects of PEF on wine, and concluded that PEF successfully improved the phenolic and anthocyanin contents; however, the organoleptic characteristics changed depending on the parameters.

Although most studies have been focused on these technologies, it is worth mentioning other techniques whose application to this field is less developed, but they hold promise for food technology.

Supercritical CO_2 is another novel non-thermal technique that does not require the application of temperature (usually below 50 °C and pressures above 7.38 MPa). The gas enters the food matrix by a pressurization step penetrating the microbial cells, when depressurization proceeds, the gas rapidly expands inside the cells causing their totally destruction[118]. With respect to enzymes, the pressure change drops the pH and also causes conformational changes in their structure and therefore its inactivation[119].

Another approach found in the literature is based on membrane separation technique, also known as ultrafiltration. It allows the separation of some components at room temperature by applying a pressure gradient and can compete economically with conventional techniques. The membrane is capable of separating

the different components according to their size and structure; for example, the membrane retains solutes of high molecular weight and suspended solids. Its capacity to retain proteins has been wildly used in the milk industry to extract casein or other proteins as well as for developing new infant formulations[120,121]. Ultrafiltration also preserves beverages and dairy products to prevent microbial growth. Even though this technique could be applied to fruit juices for its facility to remove larger molecules like PPO, ultrafiltration also retains bioactive components, like polyphenols, sugars, vitamins, and proteins responsible for their organoleptic properties of drinks[122]. Furthermore, the easy and quickly membrane fouling affects negatively its filtration capacity and membrane life decreasing its application in the beverage industry[123].

A novel non-thermal and green food process technology with great potential applications for juices would be cold plasma. Gases are ionized at atmospheric pressure and room temperature generating plasma with high reactive particles such as charged molecules, photons, and free radicals. These chemical species are characterized by high antimicrobial efficiency and can also modify structures of several enzymes like PPO decreasing its activity[113]. Nevertheless, the water activity, protein and fat content, texture, pH, and type of the foods play an important role and is still in an early stage of development[124].

In short, all non-thermal treatments cited so far have shown good results to inactivate enzymes. However, they still have some limitations such as adverse health effects, negative effects in the nutritional quality of products, high cost, large machinery requirements, and low efficiency.

Thus, based on what has been commented, it is still necessary to search for new methods that are aligned with current social challenges. That is to say, methods

that are effective against enzymatic browning although non-altering food quality and with low environmental impact (see Table 1.2).

Table 1.2. *Scheme of the ideal attributes of an anti-browning treatment in comparison with the current ones. Green: positive effect, Orange: small effect, Red: negative effect.*

Approach	PPO inhibition	Bacterial inhibition	No remains in food	No alteration nutritional composition	pH stable	Sensorial acceptability	Low cost/easy to use	Safe
Ideal	●	●	●	●	●	●	●	●
Pasteurization	●	●	●	●	●	●	●	●
Other heating treatments	●	●	●	●	●	●	●	●
Sulphites	●	●	●	●	●	●	●	●
Acids (ascorbic, kojic or citric)	●	●	●	●	●	●	●	●
Chelating agents	●	●	●	●	●	●	●	●
HPP	●	●	●	●	●	●	●	●
PEF	●	●	●	●	●	●	●	●
Supercritical CO_2	●	●	●	●	●	●	●	●
Ultrafiltration	●	●	●	●	●	●	●	●

REFERENCES

(1) Panadare, D.; Rathod, V. K. Extraction and Purification of Polyphenol Oxidase: A Review. *Biocatalysis and Agricultural Biotechnology*. Elsevier Ltd April 1, 2018, pp 431–437.

(2) Panis, F.; Kampatsikas, I.; Bijelic, A.; Rompel, A. Conversion of Walnut Tyrosinase into a Catechol Oxidase by Site Directed Mutagenesis. *Sci. Rep.* **2020**, *10* (1), 1659.

(3) Mishra, B. B.; Gautam, S. Polyphonel Oxidases: Biochemical and Molecular Characterization, Distribution, Role and Its Control. *Enzym. Eng.* **2016**, *05* (01).

(4) Ramsden, C. A.; Riley, P. A. Tyrosinase: The Four Oxidation States of the Active Site and Their Relevance to Enzymatic Activation, Oxidation and Inactivation. *Bioorg. Med. Chem.* **2014**, *22* (8), 2388–2395.

(5) Kanteev, M.; Goldfeder, M.; Fishman, A. Structure-Function Correlations in Tyrosinases. *Protein Sci.* **2015**, *24* (9), 1360–1369.

(6) Rolff, M.; Schottenheim, J.; Decker, H.; Tuczek, F. Copper-O2 Reactivity of Tyrosinase Models towards External Monophenolic Substrates: Molecular Mechanism and Comparison with the Enzyme. *Chem. Soc. Rev.* **2011**, *40* (7), 4077–4098.

(7) Marques Silva, F. V.; Sulaiman, A. Polyphenoloxidase in Fruit and Vegetables: Inactivation by Thermal and Non-Thermal Processes. In *Encyclopedia of Food Chemistry*; Elsevier, 2018; pp 287–301.

(8) Lei, D.; Feng, Y.; Jiang, D. Characterization of Polyphenol Oxidase from Plants. *Prog. Nat. Sci.* **2004**, *14* (7), 553–561.

(9) Dirks-Hofmeister, M. E.; Singh, R.; Leufken, C. M.; Inlow, J. K.; Moerschbacher, B. M. Structural Diversity in the Dandelion (Taraxacum Officinale) Polyphenol Oxidase Family Results in Different Responses to Model Substrates. *PLoS One* **2014**, *9* (6), e99759.

(10) Taranto, F.; Pasqualone, A.; Mangini, G.; Tripodi, P.; Miazzi, M. M.; Pavan, S.; Montemurro, C. Polyphenol Oxidases in Crops: Biochemical, Physiological and Genetic Aspects. *International Journal of Molecular Sciences*. MDPI AG February 10, 2017, p 377.

(11) Kampatsikas, I.; Bijelic, A.; Pretzler, M.; Rompel, A. Three Recombinantly Expressed Apple Tyrosinases Suggest the Amino Acids Responsible for Mono- versus Diphenolase Activity in Plant Polyphenol Oxidases. *Sci. Rep.* **2017**, *7* (1), 1–13.

(12) Falguera, V.; Sánchez-Riaño, A. M.; Quintero-Cerón, J. P.; Rivera-Barrero, C. A.; Méndez-Arteaga, J. J.; Ibarz, A. Characterization of Polyphenol Oxidase Activity in Juices from 12 Underutilized Tropical Fruits with High Agroindustrial Potential. *Food Bioprocess Technol.* **2012**, *5* (7), 2921–2927.

(13) Falguera, V.; Pagán, J.; Ibarz, A. Effect of UV Irradiation on Enzymatic Activities and Physicochemical Properties of Apple Juices from Different Varieties. *LWT - Food Sci. Technol.* **2011**, *44* (1), 115–119.

(14) Corzo-Martínez, M.; Corzo, N.; Villamiel, M.; del Castillo, M. D. Chapter 4: Browning Reactions. In *Browning Reactions, in Food Biochemistry and Food Processing*; Simpson, B. K., Ed.; 2012; pp 56–83.

(15) Min, K.; Park, G. W.; Yoo, Y. J.; Lee, J. S. A Perspective on the Biotechnological Applications of the Versatile Tyrosinase. *Bioresour. Technol.* **2019**, *289*, 121730.

(16) Fang, J.; Sureda, A.; Silva, A. S.; Khan, F.; Xu, S.; Nabavi, S. M. Trends of Tea in Cardiovascular Health and Disease: A Critical Review. *Trends Food Sci. Technol.* **2019**, *88*, 385–396.

(17) Macedo, A. S. L.; Rocha, F. de S.; Ribeiro, M. da S.; Soares, S. E.; Bispo, E. da S. Characterization of Polyphenol Oxidase in Two Cocoa (Theobroma Cacao L.) Cultivars Produced in the South of Bahia, Brazil. *Food Sci. Technol.* **2016**, *36* (1), 56–63.

(18) Es-Safi, N.-E.; Eronique Cheynier, V.; Moutounet, M. Implication of Phenolic Reactions in Food Organoleptic Properties. *J. Food Compos. Anal.* **2003**, *16*, 535–553.

(19) Kanteev, M.; Goldfeder, M.; Chojnacki, M.; Adir, N.; Fishman, A. The Mechanism of Copper Uptake by Tyrosinase from Bacillus Megaterium. *JBIC J. Biol. Inorg. Chem.* **2013**, *18* (8), 895–903.

(20) Queiroz, C.; Mendes Lopes, M. L.; Fialho, E.; Valente-Mesquita, V. L. Polyphenol Oxidase: Characteristics and Mechanisms of Browning Control. *Food Rev. Int.* **2008**, *24* (4), 361–375.

(21) Moon, K. M.; Kwon, E. Bin; Lee, B.; Kim, C. Y. Recent Trends in Controlling the Enzymatic Browning of Fruit and Vegetable Products. *Molecules*. MDPI AG June 1, 2020.

(22) Laveda, F.; Núñez-Delicado, E.; García-Carmona, F.; Sánchez-Ferrer, A. Proteolytic Activation of Latent Paraguaya Peach PPO. Characterization of Monophenolase Activity. *J. Agric. Food Chem.* **2001**, *49* (2), 1003–1008.

(23) Mauracher, S. G.; Molitor, C.; Al-Oweini, R.; Kortz, U.; Rompel, A. Latent and Active AbPPO4 Mushroom Tyrosinase Cocrystallized with

Hexatungstotellurate(VI) in a Single Crystal. *Acta Crystallogr. Sect. D Biol. Crystallogr.* **2014**, *70* (9), 2301–2315.

(24) Winters, A. L.; Minchin, F. R.; Michaelson-Yeates, T. P. T.; Lee, M. R. F.; Morris, P. Latent and Active Polyphenol Oxidase (PPO) in Red Clover (Trifolium Pratense) and Use of a Low PPO Mutant to Study the Role of PPO in Proteolysis Reduction. *J. Agric. Food Chem.* **2008**, *56* (8), 2817–2824.

(25) Yoruk, R.; Marshall, M. R. Physicochemical Properties and Function of Plant Polyphenol Oxidase: A Review. *Journal of Food Biochemistry*. Blackwell Publishing Ltd November 1, 2003, pp 361–422.

(26) Jukanti, A. *Polyphenol Oxidases (PPOs) in Plants*; Springer Singapore, 2017.

(27) Chazarra, S.; Cabanes, J.; Escribano, J.; Garcia-Carmona, F. Partial Purification and Characterization of Latent Polyphenol Oxidase in Iceberg Lettuce (Lactuca Sativa L.). *J. Agric. Food Chem.* **1996**, *44* (4), 984–988.

(28) Derardja, A. eddine; Pretzler, M.; Kampatsikas, I.; Barkat, M.; Rompel, A. Purification and Characterization of Latent Polyphenol Oxidase from Apricot (Prunus Armeniaca L.). *J. Agric. Food Chem.* **2017**, *65* (37), 8203–8212.

(29) Cheema, S.; Sommerhalter, M. Characterization of Polyphenol Oxidase Activity in Ataulfo Mango. *Food Chem.* **2015**, *171*, 282–287.

(30) Benaceur, F.; Chaibi, R.; Berrabah, F.; Neifar, A.; Leboukh, M.; Benaceur, K.; Nouioua, W.; Rezzoug, A.; Bouazzara, H.; Gouzi, H.; et al. Purification and Characterization of Latent Polyphenol Oxidase from Truffles (Terfezia Arenaria). *Int. J. Biol. Macromol.* **2020**, *145*, 885–893.

(31) Serra, S.; Anthony, B.; Boscolo Sesillo, F.; Masia, A.; Musacchi, S. Determination of Post-Harvest Biochemical Composition, Enzymatic

Activities, and Oxidative Browning in 14 Apple Cultivars. *Foods* **2021**, *10* (1), 186.

(32) Nicolas, J.; Billaud, C.; Philippon, J.; Rouet-Mayer, M. A. BROWNING | Enzymatic – Biochemical Aspects. In *Encyclopedia of Food Sciences and Nutrition*; Elsevier, 2003; pp 678–686.

(33) Jang, J. H.; Moon, K. D. Inhibition of Polyphenol Oxidase and Peroxidase Activities on Fresh-Cut Apple by Simultaneous Treatment of Ultrasound and Ascorbic Acid. *Food Chem.* **2011**, *124* (2), 444–449.

(34) Vamos-Vigyázó, L. Polyphenol Oxidase and Peroxidase in Fruits and Vegetables. *C R C Crit. Rev. Food Sci. Nutr.* **1981**, *15* (1), 49–127.

(35) Liu, F.; Han, Q.; Ni, Y. Comparison of Biochemical Properties and Thermal Inactivation of Membrane-Bound Polyphenol Oxidase from Three Apple Cultivars (Malus Domestica Borkh). *Int. J. Food Sci. Technol.* **2018**, *53* (4), 1005–1012.

(36) Singh, B.; Suri, K.; Shevkani, K.; Kaur, A.; Kaur, A.; Singh, N. Enzymatic Browning of Fruit and Vegetables: A Review. In *Enzymes in Food Technology: Improvements and Innovations*; Springer Singapore, 2018; pp 73–78.

(37) Wibowo, S.; Essel, E. A.; De Man, S.; Bernaert, N.; Van Droogenbroeck, B.; Grauwet, T.; Van Loey, A.; Hendrickx, M. Comparing the Impact of High Pressure, Pulsed Electric Field and Thermal Pasteurization on Quality Attributes of Cloudy Apple Juice Using Targeted and Untargeted Analyses. *Innov. Food Sci. Emerg. Technol.* **2019**, *54*, 64–77.

(38) Aaby, K.; Grimsbo, I. H.; Hovda, M. B.; Rode, T. M. Effect of High Pressure and Thermal Processing on Shelf Life and Quality of Strawberry Purée and Juice.

Food Chem. **2018**, *260*, 115–123.

(39) Vegara, S.; Martí, N.; Mena, P.; Saura, D.; Valero, M. Effect of Pasteurization Process and Storage on Color and Shelf-Life of Pomegranate Juices. *LWT - Food Sci. Technol.* **2013**, *54*, 592–596.

(40) Abedelmaksoud, T. G.; Mohsen, S. M.; Duedahl-Olesen, L.; Elnikeety, M. M.; Feyissa, A. H. Optimization of Ohmic Heating Parameters for Polyphenoloxidase Inactivation in Not-from-Concentrate Elstar Apple Juice Using RSM. *J. Food Sci. Technol.* **2018**, *55* (7), 2420–2428.

(41) Makroo, H. A.; Saxena, J.; Rastogi, N. K.; Srivastava, B. Ohmic Heating Assisted Polyphenol Oxidase Inactivation of Watermelon Juice: Effects of the Treatment on PH, Lycopene, Total Phenolic Content, and Color of the Juice. *J. Food Process. Preserv.* **2017**, *41* (6), e13271.

(42) Içier, F.; Yildiz, H.; Baysal, T. Polyphenoloxidase Deactivation Kinetics during Ohmic Heating of Grape Juice. *J. Food Eng.* **2008**, *85* (5), 410–417.

(43) Zhou, L.; Tey, C. Y.; Bingol, G.; Bi, J. Effect of Microwave Treatment on Enzyme Inactivation and Quality Change of Defatted Avocado Puree during Storage. *Innov. Food Sci. Emerg. Technol.* **2016**, *37*, 61–67.

(44) Picouet, P. A.; Landl, A.; Abadias, M.; Castellari, M.; Viñas, I. Minimal Processing of a Granny Smith Apple Purée by Microwave Heating. *Innov. Food Sci. Emerg. Technol.* **2009**, *10* (4), 545–550.

(45) Kolniak-Ostek, J.; Oszmiański, J.; Wojdyło, A. Effect of L-Ascorbic Acid Addition on Quality, Polyphenolic Compounds and Antioxidant Capacity of Cloudy Apple Juices. *Eur. Food Res. Technol.* **2013**, *236* (5), 777–798.

(46) Wu, S. Glutathione Suppresses the Enzymatic and Non-Enzymatic Browning

in Grape Juice. *Food Chem.* **2014**, *160*, 8–10.

(47) Ding, C.-K.; Chachin, K.; Ueda, Y.; Wang, C. Y. Inhibition of Loquat Enzymatic Browning by Sulfhydryl Compounds. *Food Chem.* **2002**, *76*, 213–218.

(48) Zhou, L.; Liu, W.; Stockmann, R.; Terefe, N. S. Effect of Citric Acid and High Pressure Thermal Processing on Enzyme Activity and Related Quality Attributes of Pear Puree. *Innov. Food Sci. Emerg. Technol.* **2018**, *45*, 196–207.

(49) Du, Y.; Dou, S.; Wu, S. Efficacy of Phytic Acid as an Inhibitor of Enzymatic and Non-Enzymatic Browning in Apple Juice. *Food Chem.* **2012**, *135*, 580–582.

(50) Jiang, G.-H.; Kim, Y.-M.; Nam, S.-H.; Yim, S.-H.; Eun, J.-B. Enzymatic Browning Inhibition and Antioxidant Activity of Pear Juice from a New Cultivar of Asian Pear (Pyrus Pyrifolia Nakai Cv. Sinhwa) with Different Concentrations of Ascorbic Acid. *Food Sci. Biotechnol.* **2016**, *25* (1), 153–158.

(51) Jiang, G. H.; Kim, Y. M.; Nam, S. H.; Yim, S. H.; Eun, J. B. Enzymatic Browning Inhibition and Antioxidant Activity of Pear Juice from a New Cultivar of Asian Pear (Pyrus Pyrifolia Nakai Cv. Sinhwa) with Different Concentrations of Ascorbic Acid. *Food Sci. Biotechnol.* **2016**, *25* (1), 153–158.

(52) Guerrero-Beltra, J.; Swanson, B. G.; Barbosa-Caovas, G. V. Inhibition of Polyphenoloxidase in Mango Puree with 4-Hexylresorcinol, Cysteine and Ascorbic Acid. *LWT* **2005**, *38*, 625–630.

(53) Martínez-Hernández, G. B.; Álvarez-Hernández, M. H.; Artés-Hernández, F. Browning Control Using Cyclodextrins in High Pressure–Treated Apple Juice. *Food Bioprocess Technol.* **2019**, *12* (4), 694–703.

(54) López-Nicolás, J. M.; Núñez-Delicado, E.; Sánchez-Ferrer, L.; García-Carmona, F. Kinetic Model of Apple Juice Enzymatic Browning in the Presence of

Cyclodextrins: The Use of Maltosyl-b-Cyclodextrin as Secondary Antioxidant. *Food Chem.* **2007**, *101*, 1164–1171.

(55) Sukhonthara, S.; Kaewka, K.; Theerakulkait, C. Inhibitory Effect of Rice Bran Extracts and Its Phenolic Compounds on Polyphenol Oxidase Activity and Browning in Potato and Apple Puree. *Food Chem.* **2016**, *190*, 922–927.

(56) de la Rosa, L. A.; Alvarez-Parrilla, E.; Moyers-Montoya, E.; Villegas-Ochoa, M.; Ayala-Zavala, J. F.; Hernández, J.; Ruiz-Cruz, S.; González-Aguilar, G. A. Mechanism for the Inhibition of Apple Juice Enzymatic Browning by Palo Fierro (Desert Ironweed) Honey Extract and Other Natural Compounds. *LWT - Food Sci. Technol.* **2011**, *44* (1), 269–276.

(57) Szczepańska, J.; Barba, F. J.; Skąpska, S.; Marszałek, K. High Pressure Processing of Carrot Juice: Effect of Static and Multi-Pulsed Pressure on the Polyphenolic Profile, Oxidoreductases Activity and Colour. *Food Chem.* **2020**, *307*.

(58) Zhu, J.; Wang, Y.; Li, X.; Li, B.; Liu, S.; Chang, N.; Jie, D.; Ning, C.; Gao, H.; Meng, X. Combined Effect of Ultrasound, Heat, and Pressure on Escherichia Coli O157:H7, Polyphenol Oxidase Activity, and Anthocyanins in Blueberry (Vaccinium Corymbosum) Juice. *Ultrason. Sonochem.* **2017**, *37*, 251–259.

(59) Zhu, L.; Zhang, Y.-B. Crystallization of Covalent Organic Frameworks for Gas Storage Applications. *Molecules* **2017**, *22* (7), 1149.

(60) Kaushik, N.; Rao, P. S.; Mishra, H. N. Process Optimization for Thermal-Assisted High Pressure Processing of Mango (Mangifera Indica L.) Pulp Using Response Surface Methodology. *LWT - Food Sci. Technol.* **2016**, *69*, 372–381.

(61) Carvalho Mesquita, T.; Evangelista Vasconcelos Schiassi, M. C.; Maria Teixeira

Lago, A.; Careli-Gondim, Í.; Mesquita Silva, L.; de Azevedo Lira, N.; Elena Nunes Carvalho, E.; Carlos de Oliveira Lima, L. Grape Juice Blends Treated with Gamma Irradiation Evaluated during Storage. *Radiat. Phys. Chem.* **2020**, *168*.

(62) Naresh, K.; Varakumar, S.; Variyar, P. S.; Sharma, A.; Reddy, O. V. S. Effect of γ-Irradiation on Physico-Chemical and Microbiological Properties of Mango (Mangifera Indica L.) Juice from Eight Indian Cultivars. *Food Biosci.* **2015**, *12*, 1–9.

(63) Zhang, M.; Yang, N.; Guo, L.; Li, D.; Wu, S.; Wu, F.; Jin, Z.; Xu, X. Physicochemical Properties of Apple Juice Influenced by Induced Potential Difference (Induced Electric Field) during Disposable Continuous-Flow Treatment. *J. Food Eng.* **2018**, *234*, 108–116.

(64) Agcam, E.; Akyildiz, A.; Akdemir Evrendilek, G. A Comparative Assessment of Long-Term Storage Stability and Quality Attributes of Orange Juice in Response to Pulsed Electric Fields and Heat Treatments. *Food Bioprod. Process.* **2016**, *99*, 90–98.

(65) Murtaza, A.; Iqbal, A.; Linhu, Z.; Liu, Y.; Xu, X.; Pan, S.; Hu, W. Effect of High-Pressure Carbon Dioxide on the Aggregation and Conformational Changes of Polyphenol Oxidase from Apple (Malus Domestica) Juice. *Innov. Food Sci. Emerg. Technol.* **2019**, *54*, 43–50.

(66) Marszałek, K.; Woźniak, Ł.; Barba, F. J.; Skąpska, S.; Lorenzo, J. M.; Zambon, A.; Spilimbergo, S. Enzymatic, Physicochemical, Nutritional and Phytochemical Profile Changes of Apple (Golden Delicious L.) Juice under Supercritical Carbon Dioxide and Long-Term Cold Storage. *Food Chem.* **2018**, *268*, 279–286.

(67) Cao, X.; Cai, C.; Wang, Y.; Zheng, X. The Inactivation Kinetics of Polyphenol Oxidase and Peroxidase in Bayberry Juice during Thermal and Ultrasound Treatments. *Innov. Food Sci. Emerg. Technol.* **2018**, *45*, 169–178.

(68) Bhat, R.; Ming Goh, K. Sonication Treatment Convalesce the Overall Quality of Hand-Pressed Strawberry Juice. *Food Chem.* **2017**, *215*, 470–476.

(69) Santhirasegaram, V.; Razali, Z.; Somasundram, C. Effects of Thermal Treatment and Sonication on Quality Attributes of Chokanan Mango (Mangifera Indica L.) Juice. *Ultrason. Sonochem.* **2013**, *20* (5), 1276–1282.

(70) Fundo, J. F.; Miller, F. A.; Mandro, G. F.; Tremarin, A.; Brandão, T. R. S.; Silva, C. L. M. UV-C Light Processing of Cantaloupe Melon Juice: Evaluation of the Impact on Microbiological, and Some Quality Characteristics, during Refrigerated Storage. *LWT* **2019**, *103*, 247–252.

(71) Türkmen, F. U.; Takci, H. A. M. Ultraviolet-C and Ultraviolet-B Lights Effect on Black Carrot (Daucus Carota Ssp. Sativus) Juice. *J. Food Meas. Charact.* **2018**, *12* (2), 1038–1046.

(72) Müller, A.; Noack, L.; Greiner, R.; Stahl, M. R.; Posten, C. Effect of UV-C and UV-B Treatment on Polyphenol Oxidase Activity and Shelf Life of Apple and Grape Juices. *Innov. Food Sci. Emerg. Technol.* **2014**, *26*, 498–504.

(73) Illera, A. E.; Chaple, S.; Sanz, M. T.; Ng, S.; Lu, P.; Jones, J.; Carey, E.; Bourke, P. Effect of Cold Plasma on Polyphenol Oxidase Inactivation in Cloudy Apple Juice and on the Quality Parameters of the Juice during Storage. *Food Chem. X* **2019**, *3*, 100049.

(74) Petruzzi, L.; Campaniello, D.; Speranza, B.; Corbo, M. R.; Sinigaglia, M.; Bevilacqua, A. Thermal Treatments for Fruit and Vegetable Juices and

Beverages: A Literature Overview. *Compr. Rev. Food Sci. Food Saf.* **2017**, *16* (4), 668–691.

(75) Miller, F. A.; Silva, C. L. M. Thermal Treatment Effects in Fruit Juices. In *Advances in fruit processing technologies*; 2012; pp 363–383.

(76) Ağçam, E.; Akyildiz, A.; Dündar, B. Thermal Pasteurization and Microbial Inactivation of Fruit Juices. In *Fruit Juices: Extraction, Composition, Quality and Analysis*; Elsevier Inc., 2018; pp 309–339.

(77) Radziejewska-Kubzdela, E.; Biegańska-Marecik, R. A Comparison of the Composition and Antioxidant Capacity of Novel Beverages with an Addition of Red Cabbage in the Frozen, Purée and Freeze-Dried Forms. *LWT - Food Sci. Technol.* **2015**, *62* (1), 821–829.

(78) Mena, P.; Martí, N.; Saura, D.; Valero, M.; García-Viguera, C. Combinatory Effect of Thermal Treatment and Blending on the Quality of Pomegranate Juices. *Food Bioprocess Technol.* **2013**, *6* (11), 3186–3199.

(79) Uçan, F.; Ağçam, E.; Akyildiz, A. Bioactive Compounds and Quality Parameters of Natural Cloudy Lemon Juices. *J. Food Sci. Technol.* **2016**, *53* (3), 1465–1474.

(80) Buckow, R.; Kastell, A.; Terefe, N. S.; Versteeg, C. Pressure and Temperature Effects on Degradation Kinetics and Storage Stability of Total Anthocyanins in Blueberry Juice. *J. Agric. Food Chem.* **2010**, *58* (18), 10076–10084.

(81) Tinello, F.; Lante, A. Recent Advances in Controlling Polyphenol Oxidase Activity of Fruit and Vegetable Products. *Innov. Food Sci. Emerg. Technol.* **2018**, *50*, 73–83.

(82) Putnik, P.; Kresoja, Ž.; Bosiljkov, T.; Režek Jambrak, A.; Barba, F. J.; Lorenzo, J. M.; Roohinejad, S.; Granato, D.; Žuntar, I.; Bursać Kovačević, D. Comparing

the Effects of Thermal and Non-Thermal Technologies on Pomegranate Juice Quality: A Review. *Food Chemistry*. Elsevier Ltd May 1, 2019, pp 150–161.

(83) Martín-Belloso, O.; Morales-de la Peña, M. Fruit Preservation by Ohmic Heating and Pulsed Electric Fields. In *Food Engineering Series*; Springer, 2018; pp 441–456.

(84) Negri Rodríguez, L. M.; Arias, R.; Soteras, T.; Sancho, A.; Tacca, H.; Aimaretti, N.; Rojas Cervantes, M. L.; Szerman, N. Comparison of the Quality Attributes of Carrot Juice Pasteurized by Ohmic Heating and Conventional Heat Treatment. *LWT* **2021**, 111255.

(85) Cappato, L. P.; Ferreira, M. V. S.; Guimaraes, J. T.; Portela, J. B.; Costa, A. L. R.; Freitas, M. Q.; Cunha, R. L.; Oliveira, C. A. F.; Mercali, G. D.; Marzack, L. D. F.; et al. Ohmic Heating in Dairy Processing: Relevant Aspects for Safety and Quality. *Trends Food Sci. Technol.* **2017**, *62*, 104–112.

(86) Sakr, M.; Liu, S. A Comprehensive Review on Applications of Ohmic Heating (OH). *Renew. Sustain. Energy Rev.* **2014**, *39*, 262–269.

(87) Ioannou, I.; Ghoul, M. Prevention of Enzymatic Browning in Fruit and Vegetables. *Eur. Sci. J.* **2013**, *9* (30), 1857–7881.

(88) Kuijpers, T. F. M.; Narváez-Cuenca, C.-E.; Vincken, J.-P.; Verloop, A. J. W.; Berkel, W. J. H. van; Gruppen, H. Inhibition of Enzymatic Browning of Chlorogenic Acid by Sulfur-Containing Compounds. *J. Agric. Food Chem.* **2012**, *60* (13), 3507–3514.

(89) Jukanti, A. Polyphenol Oxidase(s): Importance in Food Industry. In *Polyphenol Oxidases (PPOs) in Plants*; Springer Singapore, 2017; pp 93–106.

(90) Joint FAO/WHO Expert Committee on Food Additives (JECFA). *Evaluation of*

Certain Food Additive- Sixty-Ninth Report of the Joint FAO/WHO Expert Committee on Food Additive; 2008.

(91) Rocha, A. M. C. N.; De Morais, A. M. M. B. Polyphenoloxidase Activity of Minimally Processed "Jonagored ' Apples (Malus Domestica). *J. Food Process. Preserv.* **2005**, *29* (1), 8–19.

(92) Serpen, A.; Gökmen, V. Reversible Degradation Kinetics of Ascorbic Acid under Reducing and Oxidizing Conditions. *Food Chem.* **2007**, *104* (2), 721–725.

(93) Laurila, E.; Kervinen, R.; Ahvenainen, R. The Inhibition of Enzymatic Browning in Minimally Processed Vegetables and Fruits: Review. *Postharvest News Inf.* **1998**, *9* (4), 53N-66N.

(94) Komthong, P.; Igura, N.; Shimoda, M. Effect of Ascorbic Acid on the Odours of Cloudy Apple Juice. *Food Chem.* **2007**, *100* (4), 1342–1349.

(95) Zolghadri, S.; Bahrami, A.; Hassan Khan, M. T.; Munoz-Munoz, J.; Garcia-Molina, F.; Garcia-Canovas, F.; Saboury, A. A. A Comprehensive Review on Tyrosinase Inhibitors. *J. Enzyme Inhib. Med. Chem.* **2019**, *34* (1), 279–309.

(96) Queiroz, C.; Ribeiro Da Silva, A. J.; Lúcia, M.; Lopes, M.; Fialho, E.; Valente-Mesquita, V. L. Polyphenol Oxidase Activity, Phenolic Acid Composition and Browning in Cashew Apple (Anacardium Occidentale, L.) after Processing. *Food Chem.* **2011**, *125*, 128–132.

(97) Derardja, A. eddine; Pretzler, M.; Kampatsikas, I.; Barkat, M.; Rompel, A. Inhibition of Apricot Polyphenol Oxidase by Combinations of Plant Proteases and Ascorbic Acid. *Food Chem. X* **2019**, *4*.

(98) Wang, S.; Lin, T.; Man, G.; Li, H.; Zhao, L.; Wu, J.; Liao, X. Effects of Anti-

Browning Combinations of Ascorbic Acid, Citric Acid, Nitrogen and Carbon Dioxide on the Quality of Banana Smoothies. *Food Bioprocess Technol.* **2014**, *7* (1), 161–173.

(99) İyidoğan, N. F.; Bayındırlı, A. Effect of L-Cysteine, Kojic Acid and 4-Hexylresorcinol Combination on Inhibition of Enzymatic Browning in Amasya Apple Juice. *J. Food Eng.* **2004**, *62* (3), 299–304.

(100) Ali, H. M.; El-Gizawy, A. M.; El-Bassiouny, R. E. I.; Saleh, M. A. Browning Inhibition Mechanisms by Cysteine, Ascorbic Acid and Citric Acid, and Identifying PPO-Catechol-Cysteine Reaction Products. *J. Food Sci. Technol.* **2015**, *52* (6), 3651–3659.

(101) Lim, W. Y.; Cheun, C. F.; Wong, C. W. Inhibition of Enzymatic Browning in Sweet Potato (*Ipomoea Batatas* (L.)) with Chemical and Natural Anti-browning Agents. *J. Food Process. Preserv.* **2019**, *43* (11).

(102) Pinto, M. S. T.; Siqueira, F. P.; Oliveira, A. E. A.; Fernandes, K. V. S. A Wounding-Induced PPO from Cowpea (Vigna Unguiculata) Seedlings. *Phytochemistry* **2008**, *69*, 2297–2302.

(103) Güray, M. Z.; Şanlı-Mohamed, G. A New Thermophilic Polyphenol Oxidase from Bacillus Sp.: Partial Purification and Biochemical Characterization. *J. proteins proteomics* **2013**, *4* (1), 11–20.

(104) Oshima, H.; Ueno, E.; Saito, I.; Matsumoto, H. Determination of Sodium Azide in Beverages by Ion Chromatography. *J. AOAC Int.* **2000**, *83* (6), 1410–1414.

(105) Arabaci, G. *Effects of Metals and Anti-Browning Agents on Polyphenol Oxidase Activity from Sorrel (Rumex Acetosa)*; 2015; Vol. 2.

(106) Alexandre, E. M. C.; Pinto, C. A.; Moreira, S. A.; Pintado, M.; Saraiva, J. A.

Nonthermal Food Processing/Preservation Technologies. In *Saving Food*; Elsevier, 2019; pp 141–169.

(107) Juarez-Enriquez, E.; Salmeron-Ochoa, I.; Gutierrez-Mendez, N.; Ramaswamy, H. S.; Ortega-Rivas, E. Shelf Life Studies on Apple Juice Pasteurised by Ultrahigh Hydrostatic Pressure. *LWT - Food Sci. Technol.* **2015**, *62* (1), 915–919.

(108) Dolas, R.; Saravanan, C.; Kaur, B. P. Emergence and Era of Ultrasonic's in Fruit Juice Preservation: A Review. *Ultrasonics Sonochemistry*. Elsevier B.V. November 1, 2019.

(109) Bot, F.; Calligaris, S.; Cortella, G.; Plazzotta, S.; Nocera, F.; Anese, M. Study on High Pressure Homogenization and High Power Ultrasound Effectiveness in Inhibiting Polyphenoloxidase Activity in Apple Juice. *J. Food Eng.* **2018**, *221*, 70–76.

(110) Manzocco, L.; Quarta, B.; Dri, A. Polyphenoloxidase Inactivation by Light Exposure in Model Systems and Apple Derivatives. *Innov. Food Sci. Emerg. Technol.* **2009**, *10*, 506–511.

(111) Antonio-Gutiérrez, O. T.; López-Díaz, A. S.; López-Malo, A.; Palou, E.; Ramírez-Corona, N. UV-C Light for Processing Beverages: Principles, Applications, and Future Trends. In *Processing and Sustainability of Beverages*; Elsevier, 2019; pp 205–234.

(112) Ravindran, R.; Jaiswal, A. K. Wholesomeness and Safety Aspects of Irradiated Foods. *Food Chemistry*. Elsevier Ltd July 1, 2019, pp 363–368.

(113) Kostelac, D.; Putnik, P.; Markov, K.; Frece, J.; Bursać Kovačević, D. Effects of Electrotechnologies on Enzymes in Foods and Food Model Systems. *Current*

Opinion in Food Science. Elsevier Ltd February 1, 2020, pp 47–56.

(114) Bhattacharjee, C.; Saxena, V. K.; Dutta, S. Novel Thermal and Non-Thermal Processing of Watermelon Juice. *Trends in Food Science and Technology*. Elsevier Ltd November 1, 2019, pp 234–243.

(115) Odriozola-Serrano, I.; Soliva-Fortuny, R.; Martín-Belloso, O. Impact of High-Intensity Pulsed Electric Fields Variables on Vitamin C, Anthocyanins and Antioxidant Capacity of Strawberry Juice. *LWT - Food Sci. Technol.* **2009**, *42*, 93–100.

(116) Chen, Y.; Yu, L. J.; Rupasinghe, H. V. Effect of Thermal and Non-Thermal Pasteurisation on the Microbial Inactivation and Phenolic Degradation in Fruit Juice: A Mini-Review. *Journal of the Science of Food and Agriculture*. March 30, 2013, pp 981–986.

(117) Yang, N.; Huang, K.; Lyu, C.; Wang, J. Pulsed Electric Field Technology in the Manufacturing Processes of Wine, Beer, and Rice Wine: A Review. *Food Control* **2016**, *61*, 28–38.

(118) Zhao, L.; Qin, X.; Wang, Y.; Ling, J.; Shi, W.; Pang, S.; Liao, X. CO2-Assisted High Pressure Processing on Inactivation of Escherichia Coli and Staphylococcus Aureus. *J. CO2 Util.* **2017**, *22*, 53–62.

(119) Benito-Román; Sanz, M. T.; Illera, A. E.; Melgosa, R.; Beltrán, S. Polyphenol Oxidase (PPO) and Pectin Methylesterase (PME) Inactivation by High Pressure Carbon Dioxide (HPCD) and Its Applicability to Liquid and Solid Natural Products. *Catal. Today* **2019**.

(120) Crowley, S. V.; Gazi, I.; Kelly, A. L.; Huppertz, T.; O'Mahony, J. A. Influence of Protein Concentration on the Physical Characteristics and Flow Properties of

Milk Protein Concentrate Powders. *J. Food Eng.* **2014**, *135*, 31–38.

(121) Crowley, S. V.; O'Callaghan, T. F.; Kelly, A. L.; Fenelon, M. A.; O'Mahony, J. A. Use of Ultrafiltration to Prepare a Novel Permeate for Application in the Functionality Testing of Infant Formula Ingredients. *Sep. Purif. Technol.* **2015**, *141*, 294–300.

(122) Rascon Escajeda, L. F.; Cruz Hernandez, M.; Rodriguez Jasso, R. M.; Charles Rodriguez, A. V.; Robledo Olivo, A.; Contreras Esquivel, J. C.; Belmares Cerda, R. Discussion between Alternative Processing and Preservation Technologies and Their Application in Beverages: A Review. *J. Food Process. Preserv.* **2018**, *42* (1), e13322.

(123) Vu, A.; Darvishmanesh, S.; Marroquin, M.; Husson, S. M.; Wickramasinghe, S. R. Fouling of Microfiltration Membranes by Biopolymers. *Sep. Sci. Technol.* **2016**, *51* (8), 1370–1379.

(124) Ma, L.; Zhang, M.; Bhandari, B.; Gao, Z. Recent Developments in Novel Shelf Life Extension Technologies of Fresh-Cut Fruits and Vegetables. *Trends Food Sci. Technol.* **2017**, *64*, 23–38.

2. HYPOTHESIS AND OBJECTIVES

2. Hypothesis and Objectives

Up to date, food industry does not have a perfect methodology to avoid and control enzymatic browning without affecting the nutritional, physicochemical and organoleptic properties of juices and without compromising food safety or price. The approach explored in the present thesis is based on the current advances in the field of nanomaterials and supramolecular chemistry that can potentially be used to develop better anti-browning strategies in fruit juices and other foodstuffs.

Thus, the main goal of this doctoral thesis is to design, develop, and validate a novel anti-browning process for juice production based on the use of two innovative strategies (mesoporous silica particles and macrocyclic ligands) for inhibiting the activity of polyphenol oxidase (PPO).

This thesis is presented in two parts depending on the nature of the inhibitor explored. The first one is based on the use of macrocycle polyamines compounds and the other one is based on the use of mesoporous silica particles. According to these, the following research questions and specific objectives were defined for each of them.

Research Question 1: Could macrocyclic polyamines alter PPO activity as a result of the supramolecular interactions between both species?

- To select from a suite of molecular structures the most suitable for inhibiting the polyphenol oxidase enzyme.
- To analyse the influence of different parameters such as pH and contact time to establish the best process conditions.
- To determine the kinetic parameters and the mechanism of inhibition performed by the selected inhibitors.

- To evaluate the effect of the selected macrocyclic polyamine over the enzymatic browning and bioactive compounds on apple juice.

Research Question 2: Would it be possible to synthesise a functionalized silica-based material able to interact with the PPO immobilizing it, blocking its activity and easily removable from the medium?

- To determine the most efficient silica-based material type for the inhibition of polyphenol oxidase enzyme.
- To establish if any additional functionalization of these materials is capable of improving the inhibition of polyphenol oxidase enzyme.
- To analyse the immobilization capacity of these materials for an efficient removal of PPO from the medium after a certain processing time.
- To create a magnetic silica material that allows us to remove the material from the medium without filtration.
- To validate the effectiveness of the selected materials in apple juice as real food system.

3. WORK PLAN

3. Work plan

In order to accomplish the objectives previously exposed, the following experimental plan was carried out.

3.1. Strategy 1: Use of azamacrocyclic compounds for PPO inhibition

The first stage of the research consisted of studying the use of macrocyclic ligands as a first strategy to inhibit the PPO.

Despite the existence of a great variety of macrocyclic compounds, for this study, macrocycle polyamines were chosen as they can perform non-covalent interactions. The amine groups give the molecules a strong basic character capable of binding anions and very effective as chelators. Moreover, they have the ability to interact with amino acids through hydrogen bonds or electrostatic interactions that makes them great candidates as PPO inhibitors.

It should be noted that to carry out this part of the study the collaboration with Professor Enrique García España and his group from the University of Valencia was essential. They are specialists in supramolecular chemistry and, particularly, in the synthesis and study of these molecules. In this way, they led the synthesis and characterization of the azamacrocyclic compounds, and we focused on the study of their performance as inhibitors.

PPO characterization was required in advance to determine the optimal pH and substrate for further analysis. Afterwards, we made an initial screening and selected the best inhibitors based on their inhibition properties and the influence of the pH or the contact time. Once we selected the compounds with the best inhibition potential over the PPO, we carried out the corresponding kinetic studies in order to learn more about the interactions between the ligands and the enzyme and find out

the type of inhibition. Finally, we explored the enzymatic browning on freshly apple juice with added macrocycles to validate their inhibition capacity in a real food system, as well as the impact in some bioactive compounds usually found in fruit juices.

The different processes and determinations corresponding to this chapter are schematically shown below (Figure 3.1):

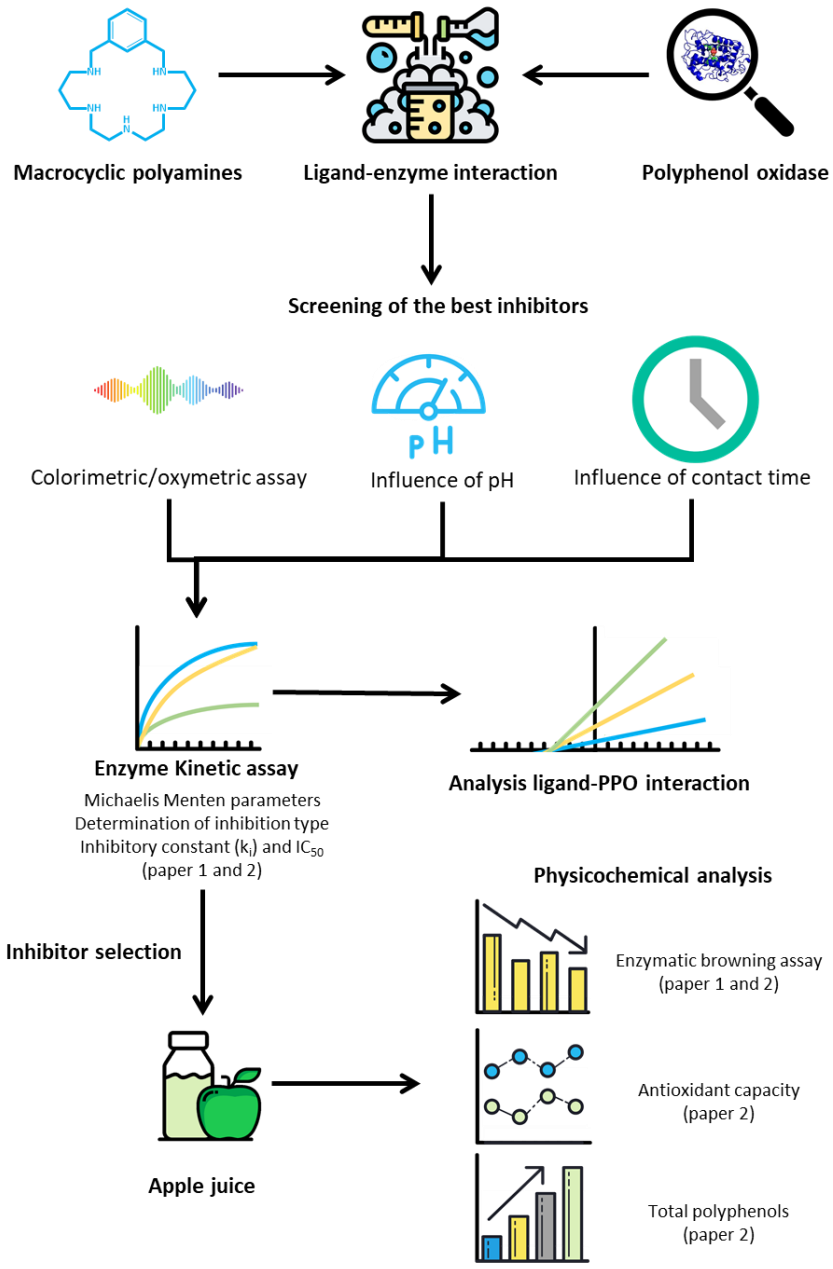

Figure 3.1. *Diagram of the experimental plan applied that led to the results reported in chapter 1.*

3.2. Strategy 2: Use of mesoporous silica particles for PPO inhibition.

The second stage consisted of studying the use of mesoporous silica particles to inhibit the PPO.

Among all the possible inorganic material options, the selection of mesoporous silica-based particles was based on their advantages including high stability, high specific surface area (>700 m^2/g), and large specific pore volume (>0.6 cm^3/g). First, we synthesised diverse materials with different morphologies and porosities to analyse and understand which are the best physical characteristics to interact with the PPO. Then, in order to provide the materials with specific active groups for PPO inhibition, several organo-alkoxysilanes were used for material surface functionalization.

After the property materials characterization, we proceeded to study the silica particles' power as inhibitors varying their concentration, pH, and time of contact. In addition, their ability to immobilise and capture the polyphenol oxidase was also analysed.

Finally, we test the best materials on freshly apple juice as a real food system to validate their effectiveness.

The different processes and determinations corresponding to this chapter are schematically shown below (Figure 3.2):

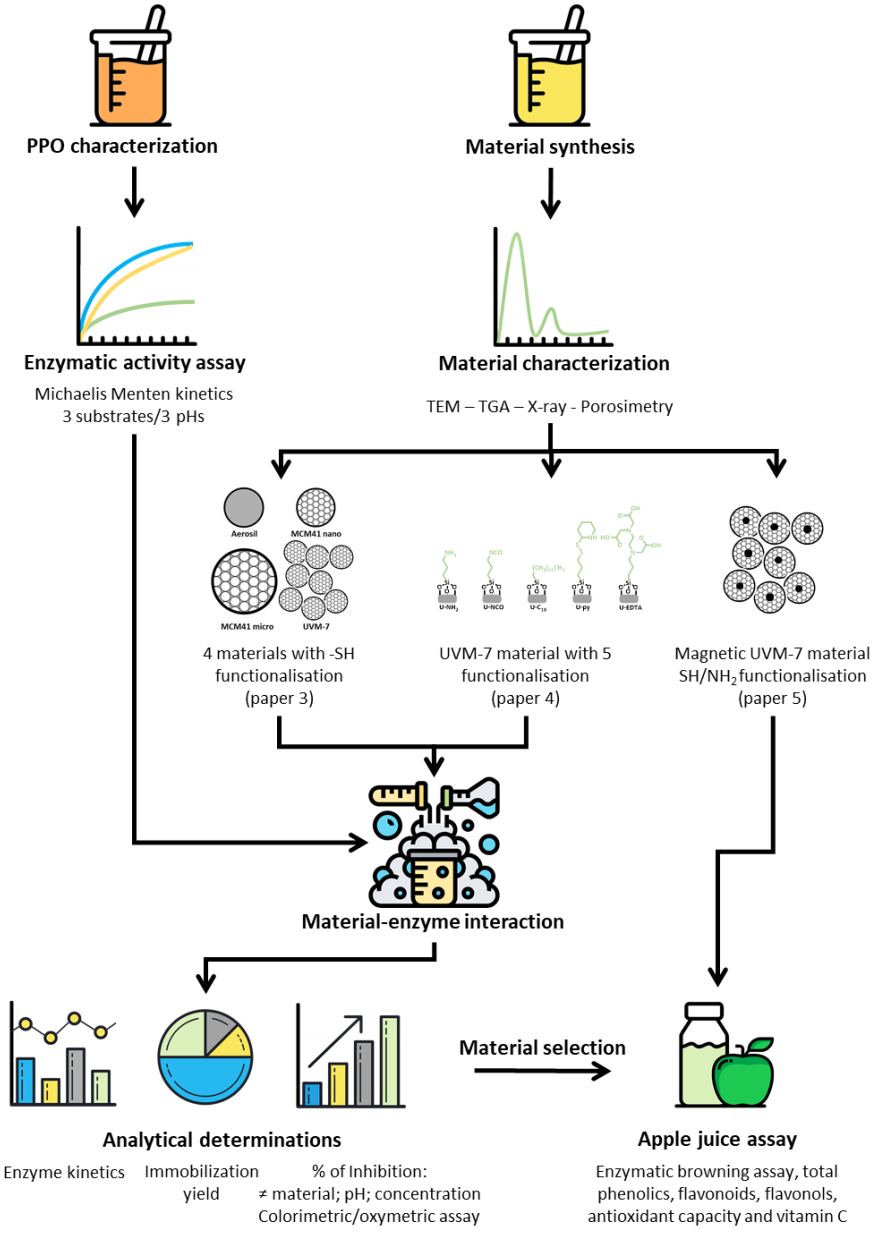

Figure 3.2. *Diagram of the experimental plan applied that led to the results reported in chapter 2.*

4. EXPERIMENTAL METHODOLOGY

4. Experimental methodology

This section includes the materials and methods employed in the experimental plan carried out in this doctoral thesis. It is divided into four subsections: synthesis and characterization of mesoporous silica materials, enzyme kinetics assays, enzyme-inhibitor interactions and inhibitory effect over apple juice.

4.1. Mesoporous silica materials synthesis and characterization

The studies developed in Papers III and IV analyse the potential of different mesoporous silica particles. For Paper III, four different mesoporous materials were tested, of which one was commercial and the other three were synthesized in the laboratory. In the first place, mesoporous microparticles called MCM-41 were synthesised by the so-called "atrane route". In a typical synthesis, 4.68 g of CTABr are added to a solution of $TEAH_3$ (25.79 g) that contains 0.045 mol of TEOS and NaOH at 118ºC. Next 80 mL of water are slowly added with vigorous stirring at 70ºC. This mixture is aged in an autoclave at 100 ºC for 24 h. According to the method described by Zhao et al. (2009)[1], the same type of material was also synthesized, but at nanometer size (MCM-41 nanoparticles). In a typical synthesis, 2.74 mmol of 1.00 g of CTABr was dissolved in 480 mL of distilled water, followed by the addition of 3.5 mL of a solution of NaOH 2 M. Then the solution was heated to 80ºC and 5 mL of TEOS was added drop-wise to the surfactant solution. The mixture is stirred for 2 h at this temperature.

The material called UVM-7 was also prepared[2]. Following as well the so-called "atrane route", a mixture of 0.05 mol of TEOS and 0.17 mol of $TEAH_3$ was heated at 120°C until no condensation of ethanol was observed in a Dean-Stark apparatus. The mixture was cooled down to 90ºC and 4.56 g CTABr were added, followed by 80 mL of water. The mixture was aged at room temperature for 24 h.

Lastly, in the last paper, the material UVM-7 was magnetized incorporation magnetite inside its structure. For this, first, the small superparamagnetic iron oxide nanoparticles were synthesized following the method presented by Sánchez-cabezas et al. (2019)[3]. Briefly, 50 mL of distilled water were heated at 80 °C followed by the addition of 12 g of $FeCl_3 \cdot 6H_2O$ and 4.9 g of $FeCl_2 \cdot 4H_2O$ followed by 19.53 ml of ammonia 32%. After 30 min, 2.13 mL of oleic acid was included in the mixture and kept under stirring for another 90 min at 80 °C. Finally, the blend was centrifuged at 12100 g for 10 min. The precipitate was washed with water and ethanol. The resulting magnetic black material was dried under vacuum overnight and resuspended in chloroform to avoid oxidation. The size of the nanoparticles was adjusted by centrifugation at 13400 g for 20 min. Once the small iron oxide nanoparticles (FeNPs) in the form of magnetite were synthesised, we proceeded to its coating with silica forming the UVM-7. A traditional UVM-7 synthesis with modification was followed. Instead of the usual addition of 80 mL of H_20, in this case 80 mL of a water-FeNPs mixture was added. For the mixtute, 1.6 g of CTAB were dissolved in the 80 mL of distilled water followed by the addition of 16 mL of the FeNPs suspended in chloroform (6.5 mg/mL). Then the two-phase solution was micro-emulsified using a probe sonicator. Finally, the emulsion was heated at 65 °C under constant stirring until chloroform was completely evaporated, giving a clear suspension of nanoparticles in water.

For all mesoporous materials, after the resulting white precipitate was collected by centrifugation, it was washed several times with distilled water. Finally, the different solids were dried at 70ºC and calcined at 550ºC in an oxidant atmosphere for 5 h to remove the template phase.

After synthesis, all supports were functionalised with several organo-alkoxysilanes groups. In Paper III, the thiol functionalisation was tested, and for

Paper IV, UVM-7 support was functionalised with two different amines (primary amine and pyridine), a carboxylic acid (EDTA), an alkane (C_{18}), and an isocyanate (NCO). In a typical assay[4], 1.0 g of each support was suspended in 30 mL of acetonitrile with an excess (10 mmol) of the selected organo-alkoxysilane (3-mercaptopropyltriethoxysilane, 3-aminopropyltriethoxysilane, 3-(Triethoxysilyl)propylisocyanate, trimethoxy (octadecyl)silane, and N-[(3-Trimethoxysilyl)propyl]ethylenediamine triacetic acid trisodium salt 40% in water). The final mixtures were stirred for 16 h at room temperature. The functionalised materials were isolated by centrifugation, washed with acetonitrile and dried at 37 ºC overnight. In some cases, a solvent change to toluene (C_{18} functionalisation) or methanol (carboxylic acid functionalisation) was necessary. In the case of the pyridyl disulfide functionalization, 250 mg of the thiol functionalised solid were resuspended in 8.5 mL of ACN containing 2.5 mmol of 2,2'-Dipyridyl disulphide and aged for 12 h. Lastly, the solid was isolated by centrifugation and subsequent washing with ACN and dried at 37 ºC overnight.

The morphology of the silica materials was characterised by standard procedures such as low-angle X-ray powder diffraction (Bruker D8 Advance CuKα radiation), transmission electron microscopy (JEOL–jem-1010), nitrogen adsorption/desorption isotherms and thermogravimetric analysis. Nitrogen adsorption/desorption isotherms were carried out in a Micromeritics ASAP 2010 automated sorption analyser at the liquid nitrogen temperature (-196°C.). Samples were prior degassed at 120°C in a vacuum overnight. The specific surface area was determined by applying the BET model[5] from the adsorption data within the low-pressure range. Pore size was calculated following the Barret-Joyner-Halenda model (BJH)[6].

4.2. Enzyme kinetics assays

To test our inhibitors we developed a model system using commercial PPO (tyrosinase from mushroom). Enzyme kinetic assays with different substrates (dopamine, L-tyrosine and chlorogenic acid) and pHs (3.5, 4.5 and 5.5) were carried out to select the best working parameters. In a typical experiment, 1.25 mL of a solution that contained 0.05 to 2.5 mM of the substrate in the presence of 10 mM phosphate buffer was mixed with 0.25 mL of the enzyme to a final concentration of 93.75 U. The absorbance at 420 nm was measured every 10 s for 10 min in a Spectrophotometer Beckman Coulter DU-730 Life Science UV/Vis Spectrophotometer. Afterwards, the initial reaction rate was calculated from the slope of the linear part of the absorbance-time curves. Since tyrosinase enzymatic reaction follows the Michaelis-Menten equation[7,8], the corresponding kinetic parameters, Km and Vmax, were obtained from the Lineweaver-Burk plot[9]. Afterwards, the catalytic constant (K_{cat}) and the specific constant were calculated from the kinetic parameters for each substrate and pH. Enzyme kinetic studies were performed at 20ºC by duplicate.

In order to study and determine the kinetic parameters in presence of the azamacrocycles (papers I and II), same enzymatic assay was carried out at pH 5.5. In this scenario, the different concentrations of inhibitor tested were previously mixed with the enzyme. Afterwards, this inhibitor/enzyme mixture was added to the substrate solution to start the enzymatic reaction.

The same protocol was performed in Paper III to study the type of inhibition caused by the nanomaterial but slightly modified. One mg of material was prior put in contact with the enzyme. Subsequently, the substrate was added and the absorbance at 420 nm was measured.

In all cases, the type of inhibition was determined using the Lineweaver-Burk representation. Furthermore, the inhibition constant (K_i) for an enzyme-ligand complex was analyzed by a Dixon plot[10] and the determination of IC_{50} was calculated.

4.3. Enzyme-inhibitor interactions

Relative activity in presence of the inhibitors

To study the influence of the different inhibitors tested in this thesis, kinetic studies were carried out to determine the initial power of each one following the procedure described by Siddiq et al. (2017)[11] with modifications.

The relative activity of tyrosinase was tested in presence of the macrocycles (Chapter 1). In this case, 1 mL of the inhibitor solution in a phosphate 10 mM buffer (5.5) was mixed with 0.25 mL of the PPO solution, then the substrate dopamine was added to let the reaction start. The final concentrations were 0.67 mM, 93.75 U y 2.5 mM respectively. The dopamine oxidation reaction was followed spectrophotometrically at 420 nm by a Beckman Coulter DU-730 Life Science UV/Vis spectrophotometer. The assays were done by triplicate at 24 °C measuring the absorbance each 10 s during 10 min. From the absorption-time curves, the initial speed of the reaction was determined from the slope of the linear stretch of the absorption-time curves. The different slopes were used to compare the inhibitory effect of the tested compounds against the control (see Equation (1)). Besides different pHs (4.5 and 6.5) and the influence of the previous contact time between the enzyme and the inhibitor (0 and 60 min) was also tested.

$$PPO\ inhibition\ (\%) = \left(\frac{V_{0i}}{V_{00}} * 100\right) \qquad (1)$$

Where Vo_0 is the control initial rate and Vo_i is the initial rate obtained for the different samples.

In the presence of the nanomaterials, same protocol with slightly modifications was carried out. The assay was performed by mixing 0.25 mL of the enzyme solution (375 U/mL) with 1 mL of phosphate buffer 10 mM that contained 1 mg of the mesoporous material. The resulting suspension was kept under stirring and afterwards, 0.25 mL of dopamine was added. The variables pH, time of contact and concentration both of material and substrate were changed to study their influence over the inhibition power. After 60 minutes of reaction, the samples were filtrated through a 0.45 µm PTFE filter and absorbance was measured at 420 nm. The same experiment was performed in the absence of the material and was used as a reference. Enzymatic inhibition was calculated according to Equation (2), where Abs_0 and Abs_i were the absorbances at 420 in the absence and presence of the material, respectively.

$$PPO\ Inhibition\ (\%) = \frac{Abs_0 - Abs_i}{Abs_0} * 100 \qquad (2)$$

Relative oxygen consumption activity

As mentioned in the introduction, the enzymatic browning process comprises two phases, the enzymatically catalysed oxidation and then a non-enzymatic polymerization reaction that is the one that generates the brown colour. Generally, the appearance of colour is used to follow the enzymatic browning reaction given the simplicity and accessibility of the necessary equipment (a spectrophotometer). Nevertheless, studying directly the oxygen consumption rate allows us to determine whether the effect of the inhibitors is directly related to the enzymatic activity (in the presence of oxygen) or to the non-enzymatic polymerization of quinones. Thus, in Papers I and IV the initial oxygen consumption rate was followed by an Oxyview System from Hansatech during the oxidation reaction of dopamine. The apparatus consisted on a Clark-type polarographic oxygen

electrode disc mounted within a DW1/AD electrode chamber and connected to the Oxyview electrode control unit.

For this assay, in 1 mL of phosphate buffer (10 mM, pH 5.5), which contained either the azamacrocyclic ligand dissolved (final concentration 0.67 mM) or the material (3 mg), was mixed with 0.25 mL of the PPO solution (final concentration of 93.75 U) in the reaction vessel. After stirring the sample for 10 minutes, 0.25 mL of dopamine was added (final concentration of 2.5 mM). The initial reaction rate was obtained from the slope of the linear part of the oxygen consumption curve during the first minutes, and was used to calculated the inhibitory capacity of the tested compounds against the control following the Equation (2).

Immobilisation assay

The Bradford assay[12] was performed to study the capability of the materials to immobilise PPO in Paper III and IV. Tyrosinase enzyme (93.75 U) was allowed to come into contact with the corresponding mesoporous material suspended in 1 mL of phosphate buffer. The resulting suspension was stirred for two different times (10 and 120 minutes) and then centrifuged (9600 RCF, 3 min). Absorbance measures were taken with a JASCO model V-630 at 595 nm using 2-mL plastic spectrophotometer cuvettes. The immobilisation yield was calculated according to Equation (3), where P_0 and P_i were the amounts of protein present in the solution in the presence and absence of the material, respectively, calculated from the previous calibration line.

$$Immobilisation\ yield\ (\%) = \frac{P_0 - P_i}{P_0} * 100 \qquad (3)$$

4.4. Inhibitory effect over apple juice

Apple juice was used as a real food system to test the best inhibitors studied during this doctoral thesis as apples are one of the fruits more affected by the PPO. The tests were done on freshly liquefied apples, obtained in a local store in Valencia. Apples were first washed and then liquefied in a Moulinex centrifugal JU200045.

PPO activity and Enzymatic browning assay

Polyphenol oxidase from the cloudy apple juice was determined spectrophotometrically measuring the increase of absorbance at 420 nm during 120 s. For this, 100 µL of the apple juice was mixed with 2.9 mL of catechol solution (0.05 M) previously prepared in a 0.1 M phosphate buffer at pH 6.5[13]. The PPO activity was taken as the slope of the linear stretch of the reaction curve.

With the purpose of studying the effect of the nanomaterials on the enzymatic browning, an aliquot of 2 mL of juice was combined with the nanomaterials (10 mg/mL). These mixtures were stirred at 200 rpm for 60 minutes and colour changes were followed by taking photographs of apple samples. Furthermore, in order to test browning inhibition persistence after removing the material, these blends were stirred at 400 rpm for 1 minute and then filtered off under vacuum using Whatman filter paper grade 41. In Paper III, the filtrate was separated into two aliquots. One was kept at room temperature and the other one was placed in the refrigerator to test the change of colour during storage. In paper II, 200 µL of the filtered juice were diluted in 1 mL of water and the colour change was followed by measuring the absorbance at 420 nm in a Thermo scientific Helios-zeta. In all cases, a sample without any inhibitor was used as the control.

In the case of the azamacrocyclic compounds (Paper I and II), a 2 mL aliquot of juice was put in contact with different concentration of the inhibitors. All samples

were kept under agitation (400 rpm) for 60 minutes to accelerate the oxidation process. Photographs were taken at different times to monitor and visualize the enzymatic browning. In Paper I, CIE L*a*b* (CIELAB) coordinates were measured in the images using Adobe® Photoshop while in paper III the colour change was measured with a spectrophotometer Minolta (CM-3600 d) using a D65 illuminant and 10° observer as a reference system.

The total colour difference (ΔE*) between the juice at time 0 and treated samples was calculated following the Equation (4).

$$\Delta E^* = \sqrt{(\Delta L^*)^2 + (\Delta a^*)^2 + (\Delta b^*)^2} \quad (4)$$

Bioactive compounds

Total phenolic content and the antioxidant capacity were also determined in paper IV and V to analyse the effect of the inhibitor on bioactive compounds. In the first place, using the Folin-Ciocalteu method, total phenolic content was measured[14,15]. Briefly, 10 µL of juice sample (treated and untreated) was diluted into 1.58 mL of deionized water and then mixed well with 100 µL of the Folin-Ciocalteu. After reacting for 3 min, 300 µL of Na_2CO_3 (20% w/v) was added to the mixture and left in dark for 60 min before measuring the absorbance at 765nm. A blank with the inhibitors was also measured and subtracted if present. The calibration curve was prepared with standard solutions of gallic acid (from 0 to 500 mg/L) by following the same method. The results were expressed as gallic acid equivalent (GAE) (mg GAE/L).

Regarding the antioxidant activity, three different methods were conducted: FRAP, DPPH· and $ABTS^{\bullet+}$. DPPH· was determined based on the method described by Wu et al. (2020)[16] with slight modifications. A sample of 10 µL of juice was added to 1 mL of methanolic solution of DPPH· (100 µM). Then, the mixture was kept in the dark for 30 min and absorbance was measured at 517 nm using UV/vis, Beckman

Coulter du 730. The results were determined based on the standard calibration curve from 0 to 200 mg/L of Trolox. Antioxidant capacity by means of the FRAP assay was performed following the method described by Thaipong et al. (2006) [17]. In brief, an aliquot of 25 µL of the juices was reacted with 2850 µL of FRAP solution and 125 µL of distilled water for 30 min in dark condition. Then the absorbance was measured at 593 nm. FRAP reagent was prepared mixing in a ratio 10:1:1 a solution of 300 mM acetate buffer (pH 3.6), 20 mM ferric chloride and 10 mM TPTZ in 40 mM HCl. A standard curve of Trolox was set and the results were stated as mg of Trolox equivalent per L (mg Trolox/L). Finally, the capacity to scavenge the $ABTS^{\bullet+}$ free radical was tested by the established $ABTS^{\bullet+}$ assay[17]. A 1:1 solution of 7.4 mM $ABTS^{\bullet+}$ solution and 2.6 mM potassium persulfate solution was prepared and left in the dark to react for 12h at room temperature. Then, 1 mL of the solution was diluted in 60 mL of methanol. For the assay, 10 µL of the apple juice was mixed with 140 µL of distilled water and 2890 µL of the $ABTS^{\bullet+}$ for 2h in dark conditions. Then the absorbance was taken at 734 nm in the same spectrophotometer. Three standard curves of Trolox were set for each procedure and the results were stated as mg of Trolox equivalent per L (mg Trolox/L). All assays were done by triplicate.

The total content on flavonoids and flavonols was estimated following the methodology published by Abid et al. (2013)[18,19]. For flavonoids, 100 µL aliquot of juice sample was mixed with 1.4 mL of deionized water and 75 µL of a 5% $NaNO_2$. Afterwards, the sample was left for 6 min and 150 µL of a 10% $AlCl_3$ was included and then after 5min, 0.50 mL of 1 M NaOH was added. Finally, the absorbance was measured at 510 nm previous a calibration curve of (+)-catechin. The results were reported as mg of catechin equivalent/L. For the total flavonols content, a 0.5 mL of diluted sample was mixed with 0.5 mL of 2% $AlCl_3$ solution, followed by the addition of 0.5 mL sodium acetate solution (50 g/L). The mixture was left for 150 min at 20

°C, and then, the absorbance was read at 440 nm. A standard curve of quercetin from 0 to 150 mg/L was prepared and the results were reported as mg of quercetin equivalent/L.

Finally, the content of ascorbic acid was also measured on the apple juices to determine the influence of the different inhibitors. A sample of 50 µL was mixed with 1.95 mL of 1.13 mM of sodium oxalate dissolved in a potassium dihydrogenphosphate (30mM)/ disodium hydrogenphosphate (0.8 mM) buffer solution (pH = 5.4) [20]. Subsequently, the absorbance was measured at 266 nm and data was confronted to a standard curve of L-ascorbic acid.

REFERENCES

(1) Zhao, Y.; Trewyn, B. G.; Slowing, I. I.; Lin, V. S. Y. Mesoporous Silica Nanoparticle-Based Double Drug Delivery System for Glucose-Responsive Controlled Release of Insulin and Cyclic AMP. *J. Am. Chem. Soc.* **2009**, *131* (24), 8398–8400.

(2) El Haskouri, J.; Zarate, D. O. de; Guillem, C.; Latorre, J.; Caldes, M.; Beltran, A.; Beltran, D.; Descalzo, A. B.; Rodriguez-Lopez, G.; Martinez-Manez, R.; et al. Silica-Based Powders and Monoliths with Bimodal Pore Systems. *Chem. Commun.* **2002**, No. 4, 330–331.

(3) Sánchez-Cabezas, S.; Montes-Robles, R.; Gallo, J.; Sancenón, F.; Martínez-Máñez, R. Combining Magnetic Hyperthermia and Dual T1/T2 MR Imaging Using Highly Versatile Iron Oxide Nanoparticles. *Dalt. Trans.* **2019**, *48* (12), 3883–3892.

(4) Garrido-Cano, I.; Candela-Noguera, V.; Herrera, G.; Cejalvo, J. M.; Lluch, A.;

Marcos, M. D.; Sancenon, F.; Eroles, P.; Martínez-Máñez, R. Biocompatibility and Internalization Assessment of Bare and Functionalised Mesoporous Silica Nanoparticles. *Microporous Mesoporous Mater.* **2021**, *310*, 110593.

(5) Brunauer, S.; Emmett, P. H.; Teller, E. Adsorption of Gases in Multimolecular Layers. *J. Am. Chem. Soc.* **1938**, *60* (2), 309–319.

(6) Barrett, E. P.; Joyner, L. G.; Halenda, P. P. The Determination of Pore Volume and Area Distributions in Porous Substances. I. Computations from Nitrogen Isotherms. *J. Am. Chem. Soc.* **1951**, *73* (1), 373–380.

(7) Munjal, N.; Sawhney, S. . Stability and Properties of Mushroom Tyrosinase Entrapped in Alginate, Polyacrylamide and Gelatin Gels. *Enzyme Microb. Technol.* **2002**, *30* (5), 613–619.

(8) Espín, J. C.; Varón, R.; Fenoll, L. G.; Gilabert, M. A.; García-Ruíz, P. A.; Tudela, J.; García-Cánovas, F. Kinetic Characterization of the Substrate Specificity and Mechanism of Mushroom Tyrosinase. *Eur. J. Biochem.* **2000**, *267* (5), 1270–1279.

(9) Doran, P. M. *Principios de Ingeniería de Los Bioprocesos*; Acribia, 1998.

(10) Dixon, M. The Determination of Enzyme Inhibitor Constants. *Biochem. J.* **1953**, *55* (1), 170–171.

(11) Siddiq, M.; Dolan, K. D. Characterization and Heat Inactivation Kinetics of Polyphenol Oxidase from Blueberry (Vaccinium Corymbosum L.). *Food Chem.* **2017**, *218*, 216–220.

(12) Bradford, M. M. A Rapid and Sensitive Method for the Quantitation of Microgram Quantities of Protein Utilizing the Principle of Protein-Dye Binding. *Anal. Biochem.* **1976**, *72* (1–2), 248–254.

(13) Illera, A. E.; Chaple, S.; Sanz, M. T.; Ng, S.; Lu, P.; Jones, J.; Carey, E.; Bourke, P. Effect of Cold Plasma on Polyphenol Oxidase Inactivation in Cloudy Apple Juice and on the Quality Parameters of the Juice during Storage. *Food Chem. X* **2019**, *3*, 100049.

(14) Andrew L Waterhouse. Determination of Total Phenolics. In *Current protocols in food analytical chemistry*; John Wiley & Sons, Inc., 2002; Vol. 6, p I1.1.1-I1.1.8.

(15) Aranibar, C.; Pigni, N. B.; Martinez, M.; Aguirre, A.; Ribotta, P.; Wunderlin, D.; Borneo, R. Utilization of a Partially-Deoiled Chia Flour to Improve the Nutritional and Antioxidant Properties of Wheat Pasta. *LWT - Food Sci. Technol.* **2018**, *89*, 381–387.

(16) Wu, C.; Li, T.; Qi, J.; Jiang, T.; Xu, H.; Lei, H. Effects of Lactic Acid Fermentation-Based Biotransformation on Phenolic Profiles, Antioxidant Capacity and Flavor Volatiles of Apple Juice. *LWT* **2020**, *122*, 109064.

(17) Thaipong, K.; Boonprakob, U.; Crosby, K.; Cisneros-Zevallos, L.; Hawkins Byrne, D. Comparison of ABTS, DPPH, FRAP, and ORAC Assays for Estimating Antioxidant Activity from Guava Fruit Extracts. *J. Food Compos. Anal.* **2006**, *19* (6–7), 669–675.

(18) Abid, M.; Jabbar, S.; Wu, T.; Hashim, M. M.; Hu, B.; Lei, S.; Zhang, X.; Zeng, X. Effect of Ultrasound on Different Quality Parameters of Apple Juice. *Ultrason. Sonochem.* **2013**, *20* (5), 1182–1187.

(19) Abid, M.; Jabbar, S.; Wu, T.; Hashim, M. M.; Hu, B.; Lei, S.; Zhang, X.; Zeng, X. Effect of Ultrasound on Different Quality Parameters of Apple Juice. *Ultrason. Sonochem.* **2013**, *20* (5), 1182–1187.

(20) Selimović, A.; Salkić, M.; Selimović, A. Direct Spectrophotometric Determination of L-Ascorbic Acid in Pharmaceutical Preparations Using Sodium Oxalate as a Stabilizer. *Eur. J. Sci. Res.* **2011**, *53* (2), 193–198.

5. RESULTS AND DISCUSSION

CHAPTER 1: Macrocyclic ligands for PPO inhibition

PAPER 1

Muñoz-Pina, S. et al. (2020). Inhibitory Effect of Azamacrocyclic Ligands on Polyphenol Oxidase in Model and Food Systems. *Journal of Agricultural and Food Chemistry*, 68 (30), 7964-7973.

PAPER 2

Muñoz-Pina, S. et al. (2021). A tetraazahydroxypyridinone derivative as inhibitor of apple juice enzymatic browning and oxidation. LWT – Food Science and Technology (submitted).

Noncovalent interactions underlie the most impressive functions of living systems from enzymes to nucleic acids. Since 1950, scientists began to explore the unlimited possibilities of such interactions in the framework called supramolecular chemistry[1]. This field studies from a multidisciplinary chemical perspective the complex assembly of two or more chemical species that bond by noncovalent intermolecular forces[2].

Among all non-covalent interactions (e.g., hydrogen bonding, electrostatic interactions, Van der Waals force) that can be used to create advanced materials, the host-guest interactions display great potential in several fields[3]. Those interactions are usually given by macrocycles (a "host") binding another molecule (a "guest") to produce a "host-guest" complex or supermolecule. Commonly, the host is a large molecule like an enzyme or cyclic compound which sizeable, central hole or cavity capable of enclosing smaller molecules. They can be from natural sources, semisynthetic, or completely synthetic molecules. In the case of the guest, they are smaller molecules such as simple inorganic ions or metals, bigger molecules like amino acids, or more sophisticated molecules like hormones[4].

An example of a typical host-guest supramolecular complex already used in the food industry either as part of the final product or during the processing would be the cyclodextrin ($C_{42}H_{70}O_{35}$). Cyclodextrins are natural cyclic oligosaccharides formed by the enzymatic degradation of starch, which, due to their hydrophobic-hydrophilic structure, are ideal for binding aromatic organic or as dietary fibre[5,6].

It was not until 1967 when the first macrocycle was discovered by Charles J. Pedersen, a crown-ether with cation-binding properties. He postulated that cations would place into the cavity of the molecule as a "crown" for the cation (see Figure 5.1)[7]. Pedersen synthesised and characterised 50 crown-ether giving rise to a field

that has progressed greatly, winning two Nobel Prizes, and seeing the implementation of many practical applications.

Since then, numerous types of macrocycles have been synthesised containing combinations of oxygen (oxa-), nitrogen (aza-), and even sulphur (sulfo-) (see Figure 5.1). In the case of nitrogen atoms, when they replace the oxygen atoms of the crown ethers, a new class of host is formed called macrocyclic polyamines [8]. The main advantage of the macrocycle polyamines among others is that the amine groups give the molecule a strong basic character with unique properties as a host. The protonation of the macrocyclic polyamines makes them capable of binding anions and very effective as chelators forming thermodynamically stable complexes with metal ions[9,10]. Besides, they have the ability to interact with amino acids through hydrogen bonds or electrostatic interactions. Macrocycle polyamines have shown their potential in many applications such as in catalysis[11], sensors, gas storage[12] as well as in biomedical applications as contrast agents especially for their chelating properties[9].

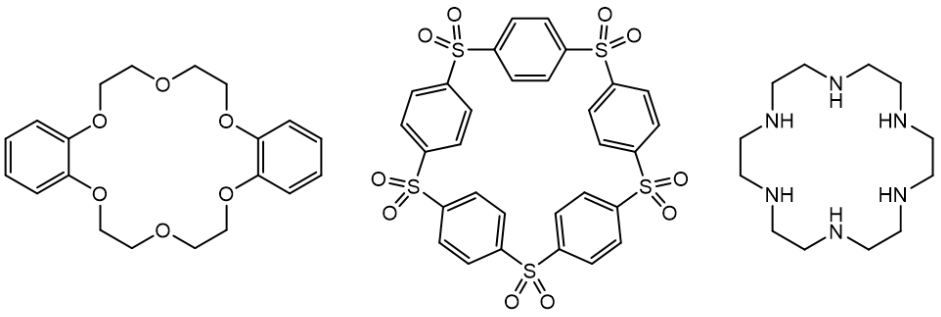

Figure 5.1. *Example of the different families of macrocycles.*

Besides, as they are characteristic for their interactions with metals, they have been used to mimic metalloenzymes related to the molecular oxygen metabolism[13,14]. On the other hand, it can be found in the literature some examples of this compound as enzyme inhibitors over iron and copper/zinc superoxide dismutase[15,16]

Despite its great potential as chelating agents and their interactions with amino acids, so far there are no studies about this type of molecules as possible inhibitors of PPO for developing new anti-browning agents.

PAPER 1: INHIBITORY EFFECT OF AZA-MACROCYCLIC LIGANDS ON POLYPHENOL OXIDASE IN MODEL AND FOOD SYSTEMS.

INHIBITORY EFFECT OF AZA-MACROCYCLIC LIGANDS ON POLYPHENOL OXIDASE IN MODEL AND FOOD SYSTEMS.

Sara Muñoz-Pina[1], José V. Ros-Lis[2], Estefanía Delgado-Pinar[3], Alvaro Martínez-Camarena[3], Begoña Verdejo[3], Enrique García-España[3], Ángel Argüelles[1], Ana Andrés[1]

[1]*Instituto Universitario de Ingeniería de Alimentos para el Desarrollo (IUIAD-UPV). Universitat Politècnica de València Camino de Vera s/n, 46022, Valencia, Spain*

[2]*Inorganic Chemistry Department, Universitat de València. 46100, Burjassot, Valencia Spain.*

[3]*Instituto de Ciencia Molecular, Universidat de València. C/Catedrático José Beltrán 2, Paterna (Valencia), Spain.*

SUMMARY

The first strategy to stop the enzymatic browning in this doctoral thesis consists of using macrocyclic polyamines compounds as enzyme inhibitors. In this regard, this work seeks to prove whether these molecules are capable of inhibiting the PPO.

Aza-macrocyclic ligands consist of big macromolecules synthesised by the combination of atoms of nitrogen and carbon. The amine group gives the molecule a basic character and has the advantage of binding several species such as metal ions, organic anions, and amino acids by non-covalent interactions. Besides, onto these molecules other chemical groups could be added to give them other functionalities, making them more polyvalent. Its high reactivity with proteins and metals become them, good candidates, to interact with metallic enzymes such as polyphenol oxidase (PPO). PPO enzyme is a family of copper-containing enzymes

that catalyse the oxidation of phenolic compounds into brown melanoid pigments. This reaction, known as enzymatic browning, occurs mainly in fruits and vegetables, although it can also be found in the animal kingdom. Yet this colour change in some cases is desirable (in coffee or tea), in most cases, there is a detriment on the colour, taste, and nutritional value of the food. Since the physical aspect is one of the main parameters that affect consumers when choosing a certain food, the food industry has been reducing the enzymatic browning through physical and chemical processes. However, all the disadvantages found in the current methodologies have encouraged researchers to keep looking for new and better ways to avoid this reaction.

Taking into account that azamacrocycles can interact with the PPO enzyme and so far, there are no studies aimed at the interaction of both compounds, this work aims to analyse the behaviour of several ligands with different structures over the PPO. To address the study, an initial screening of ten different compounds using commercial tyrosinase was carried out in order to analyse their influence over the enzymatic activity. Furthermore, their interactions were studied deeper analysing the oxygen consumption during the oxidation, the effect of the contact time and kinetic parameters. Finally, the power of the best inhibitor on enzymatic browning was directly verified in apple juice.

According to the obtained results, it has been demonstrated that in general terms all azamacrocyclic ligands alter the initial PPO reaction rate (from 10 to 95 %), nevertheless, this effect strong varies depending on the chemical structure. The ring size, as well as total nitrogen and the presence of anthracenes, are the principal components when it comes to obtaining a good inhibitor. Furthermore, the inhibition of the enzymatic browning is mainly due to the deactivation of the PPO and slightly improve when increasing the contact time between enzyme-ligand.

Kinetic parameters of the best inhibitors showed how mostly all compounds present a non-competitive inhibition, revealing the compound L2 with an S-parabolic-I-parabolic non-competitive inhibition. L2 showed a remarkable inhibition at a micromolar concentration (IC_{50}=10 µM) and their strength was verified on a real enzymatic browning. The change of colour (ΔE_{ab}*) generated by the enzymatic browning in an apple juice was significantly reduced by L2 by 90 % after 30 min and 60 % after 1 h. This work concludes, therefore, demonstrating how aza-macrocyclic compounds can be potential inhibitors of PPO. In addition, a potent inhibitor has been found (L2) which is capable of making structural changes on the protein collapsing its catalytic activity.

Key words: PPO, tyrosinase, inhibition, UVM-7, amines, apple juice.

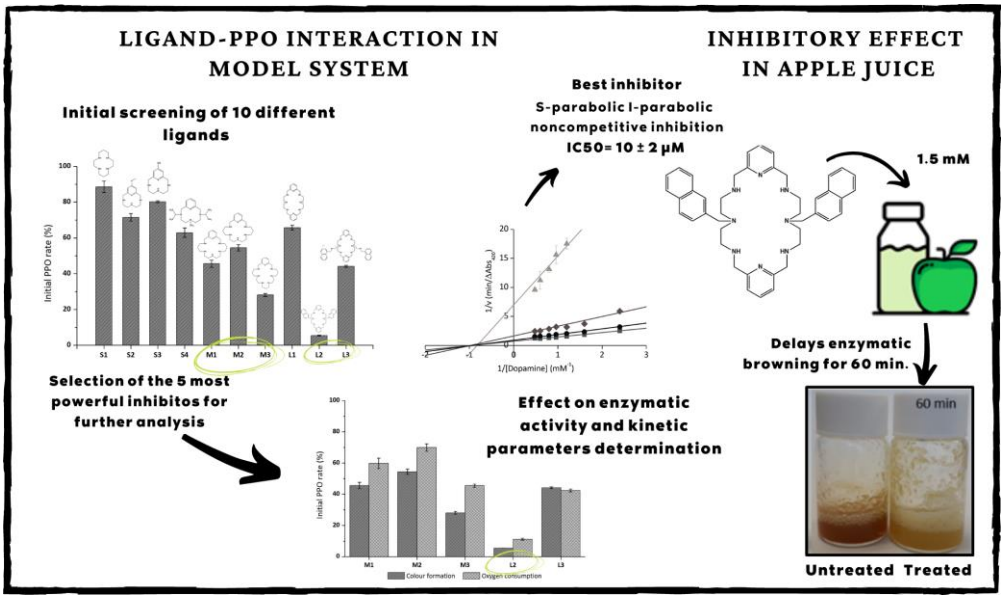

Figure 5.2. *Graphical abstract of the inhibitory effect of several azamacrocyclic ligands on polyphenol oxidase enzyme.*

1. Introduction

There is currently a growing tendency to consume fresh, cut, ready-to-eat fruits and vegetables or minimally processed fresh juices as there is a great concern for maintaining a healthy diet and preserve their sensory and nutritional properties. Therefore, maintaining the stability of the product and ensuring the natural colour is one of the main objectives of the food industry [17,18].

The main cause of colour modification of fruits and vegetables can be associated with the activity of the enzyme polyphenol oxidase (PPO, EC 1.14.18.1 or EC 1.10.3.1). The PPO catalyse the *o*-hydroxylation of monophenols into *ortho*-phenols and its posterior oxidation to *o*-quinones followed by a non-enzymatic polymerization of reactive quinones leading to the enzymatic browning of foods[19]. This reaction starts when the PPO enzyme and the atmospheric oxygen meet, usually during cell disruptions of the raw food in their harvesting, handling and post-harvest processing. The colour change, yet it is a desirable process in some foods[20], is inversely correlated with the acceptability of fruit and vegetable products by the consumer[21] which causes a considerable increase in food waste economic losses[22,23].

Since the factors that most influence enzymatic browning are the concentration of both the active enzyme and the phenolic compounds (plus the pH, the temperature and the presence of oxygen)[24] the processing of foods with high concentrations of PPO and polyphenols leads to a high risk of enzymatic browning in this type of food. A clear example would be the case of apple juices, which contain considerable amounts of polyphenols and polyphenol oxidases linked to suspended particles[25].

Food waste is a major humanitarian and environmental problem (Food and Agriculture Organization of the United Nations, 2011)[26] so it is not unexpected that

the food processing industry has been using different methods to prevent enzymatic browning based on both physical and chemical treatments. Traditionally, one of the methods most used by the industry has been thermal treatment. But heat induces changes in taste, colour, smell and nutritional properties due to the decomposition of volatile and thermosensitive compounds, such as aromas, vitamins, carotenoids and anthocyanins[27,28]. Regarding chemical treatments, the use of acidifying agents, chelators or sulphites have also been used as preventive for browning, but the fact that they can interfere with the taste or even cause allergies in the population (sulphites) has restricted their use in foods and beverages[29,30]. These drawbacks encourage researchers to still look for a novel strategies of PPO inhibitors, as could be the use of the nanomaterial technology[31,32].

From another point of view, supramolecular chemistry is a research subject of great interest at present. It studies the non-covalent interactions between molecules, usually named host and guest. The host molecules, in general, are large molecules capable of enclosing smaller molecules and they can be natural, semi-synthetic or completely synthetic molecules. On the other hand, the smaller guest molecules can be cationic, anionic or neutral like amino acids, organic anions and some metals[33].

Within the receptors designed for supramolecular studies, macrocyclic polyamines are especially relevant[34]. Polyamines offer a high potential as PPO inhibitors since these compounds can interact with metal cations with biological relevance such as Cu^{+2} [35–37] and have also the ability to interact with amino acids through hydrogen bonds or electrostatic interactions. In addition, these ligands can be functionalized with different chemical groups like aromatic groups or alkyl groups that can change their response over the PPO.

So far there are no studies aimed at studying the interactions between this type of compounds and polyphenol oxidase as a strategy for their inhibition in food systems. We can hypothesize that azamacrocycles can interact with the copper atoms in the active centre of the external part of the enzyme modifying its activity. Therefore, this work aims at analysing the behaviour of different azamacrocyclic compounds in the inhibition or modulation of the polyphenol oxidase enzyme activity in model and real systems, as a starting point to develop an alternative strategy for the industrial processing of fruits and vegetables.

2. Materials and methods

2.1. Chemicals

Commercial mushroom tyrosinase enzyme (2687 U/mg), dopamine hydrochloride ($(HO)_2C_6H_3CH_2NH_2 \cdot HCL$) and HEPES ($C_8H_{18}N_2O_4S$) were purchased all from Sigma-Aldrich (Sigma-Aldrich, USA). For the buffers, sodium bisphosphate (NaH_2PO_4) and disodium phosphate (Na_2HPO_4) were acquired from Scharlau (Sharlab S.L., Spain) and anhydrous sodium acetate ($NaCH_3COO$) from Panreac AppliChem (Panreac AppliChem, Barcelona, Spain).

The ligand S1 (cyclam) was purchased from Sigma-Aldrich (Sigma-Aldrich, USA). The others tested ligands were synthesised according to known procedures and the characterisation agrees with published data: S2[38], S3[39], S4[40], M1[41], M2[42], M3[43], L1[44], L2[45] and L3[46]. The different chemical structures are summarized in Figure 5.3.

The juices used in the tests were obtained in the laboratory by directly liquefying apples (Golden Delicious variety, Val Venosta) obtained in a local store.

2.2. Screening of the best inhibitors over tyrosinase from mushroom

Polyphenol oxidase activity in the presence of the ligands was determined following the protocol published by Muñoz-Pina et al. (2020)[16] and with some modifications from Siddiq and Dola (2017)[47]. Tyrosinase from mushroom (93.75 U) was put in contact with dopamine (2.5 mM) in presence of the ligand (0.67 mM) in a phosphate buffer 10 mM at pH 5.5. A control without inhibitor was used. The oxidation of the dopamine by the PPO produces an orange colour that is followed spectrophotometrically at 420 nm measuring the absorbance each 10 s during 10 min.

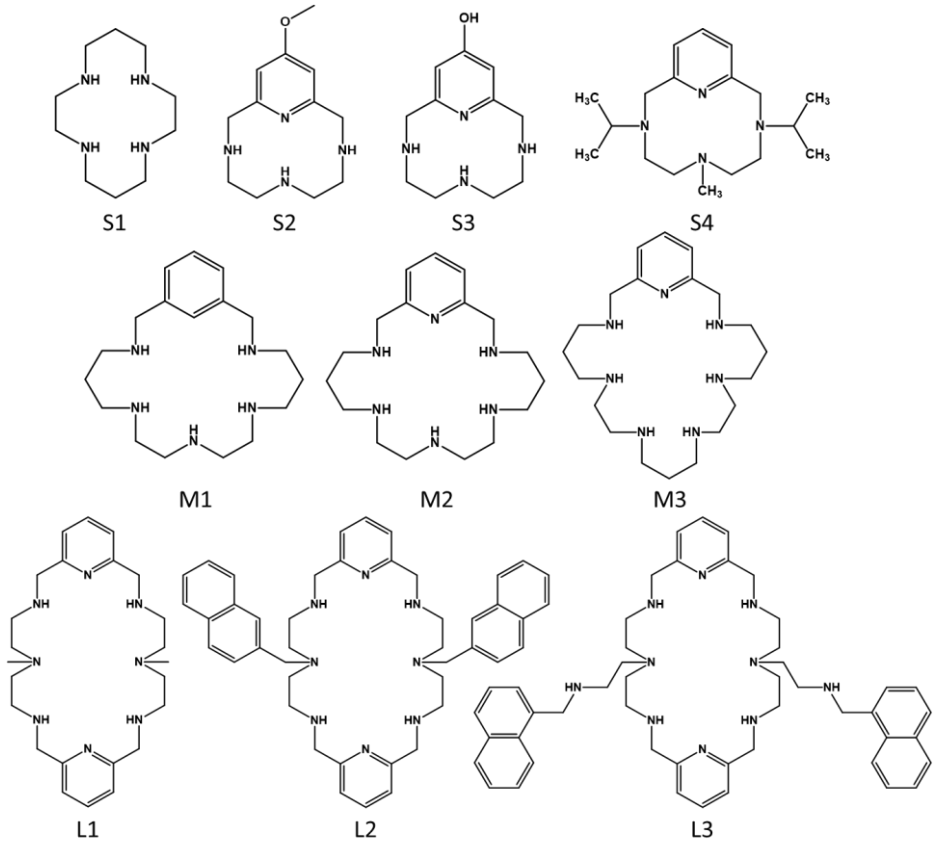

Figure 5.3. *Molecular structure of the ten studied azamacrocyclic ligand.*

As in the case of fruits and their respective juices, the typical pH found is between 3.5 and 5.5, to perform the assays it was chosen pH=5.5, in which the PPO continued to have a high activity (around 85%) but was similar to the pH found in fruit juices[48]. From the absorption-time curves, the slope of the linear stretch is obtained, related to the initial speed of the reaction. The different slopes were used to compare the inhibitory effect of the ligands against the control (see Equation (1)). The reaction was followed by a Beckman Coulter DU-730 Life Science UV/Vis spectrophotometer in triplicate at 24 °C. PPO inhibition was calculated according to Equation (1), where V_{00} is the control initial rate and V_{0i} is the initial rate obtained for the different samples.

$$PPO\ inhibition\ (\%) = 100 - \left(\frac{V_{0i}}{V_{00}} * 100\right) \qquad (1)$$

2.3. Enzyme-ligand interaction

To evaluate the influence of the contact time between the enzyme and the ligands, the enzyme was put in contact with the ligand at time 0 min and at 60 min. The azamacrocyclic compounds selected for the assay were M1, M2, M3, L2 and L3 (all at 0.67 mM). The reaction mixture was the same as in 2.2 and in both times a control without inhibitor was prepared.

The absorbance was then measured at 420 nm every 10 s for 10 min in a Beckman Coulter DU-730 Life Science UV/Vis spectrophotometer and the effect of the contact time on the initial rate was compared. PPO inhibition was calculated according to Equation (1), where V_{00} is the control initial rate and V_{0i} is the initial rate obtained for the different samples.

The oxygen consumption during the enzymatic catalysed oxidation was measured to monitor the PPO activity. The oxygen concentration in solution was measured with a Oxyview 1 measuring system of Hansatech Instruments, which

contains an S1 Clark-type polarographic oxygen electrode disc mounted within a DW1/AD electrode chamber and connected to the Oxyview electrode control unit. The oxygen consumption vs time curve was plotted and the initial rate of oxygen consumption measured from the positive slope of the initial part. PPO inhibition was calculated then according to Equation (1), where V_{o0} is the control positive initial rate of oxygen consumption and V_{oi} is the initial rate of oxygen consumption obtained for the different samples.

2.4. Enzyme kinetics in model systems

The five compounds with more inhibitory capacity were chosen to make a deeper study of enzymatic activity. For the determination of the kinetic parameters, the reaction was carried out at pH 5.5 under phosphate buffer 10 mM at ten different concentrations of the substrate dopamine (from 0.033 mM to 1.66 mM). The inhibitor/enzyme mixture was subsequently added to start the enzymatic reaction. The final concentration of enzyme in the assay was 93.75 U and the inhibitor concentration varied depending on its response. A control without inhibitor was also carried out. The absorbance at 420 nm was measured every 10 s for 10 min in a Spectrophotometer Beckman Coulter DU-730 Life Science UV / Vis Spectrophotometer. The production of dopamine was determined using a molar extinction coefficient for dopachrome of ε = 3700 M^{-1} cm^{-1} [49].

Since the enzymatic reaction of polyphenol oxidase follows Michaelis-Menten kinetics[50], K_M and v_{max} constants were calculated using the Lineweaver-Burk representation as a linearization method and compared to the representation of Langmuir[51]. The type of inhibition was also determined. Furthermore, the inhibition constant (K_i) for an enzyme-ligand complex were analysed by Dixon plot, which is a graphical method plot of 1/enzyme velocity (1/V) versus inhibitor concentration (I) with varying concentrations of the substrate. For the determination of IC_{50} values,

the concentration of individual ligand to achieve 50% PPO inhibition were calculated. Besides, GraphPad Prism 5.00.288 program was used to carry out various statistical analyses such as the analysis of variance (ANOVA) of one factor and two factors, depending on the case.

2.5. Fluorescence quenching analysis

The fluorescence assay was performed with a PTI fluorescence instrument. Same inhibitor/enzyme mixture as in section 2.2. was used in this study at the three ligand concentrations. Tyrosinase was excited at 274 nm and the emission spectrum over the range of 280 nm to 400 nm was recorded through a 3 nm slit. The emission spectrum of the tyrosinase solution was also directly measured.

2.6. Inhibitory effect over apple juice

Apple juice from cv. Golden Delicious obtained in the laboratory was selected to verify their inhibitory effects of the compounds on real samples. For each compound, a 2 mL aliquot of juice was put in contact with 2 mg and 4 mg of compound and another 2 mL of apple juice was used as a control sample. All samples were kept under agitation (400 rpm) for 60 minutes and photographs were taken at 0, 1 and 2 minutes and then at 5-minute intervals, in order to monitor and visualize the enzymatic browning. Furthermore, CIE L*a*b* (CIELAB) coordinates were measured in the images and colour differences were calculated using Adobe® Photoshop®.

2.7. Data analysis

Data are reported as mean ± standard deviation. Origin was used to perform the analysis of variance (One-Way ANOVA) and the LSD procedure (least significant difference). Partial least squares regression studies (PLS) were carried out with the R 3.6.0 software using the Kernel algorithm. Scale and center were used as parameters

to build the model. Leave one out (LOO) cross-validation was used to evaluate the adequacy of the experimental data and to select the quantity of latent variables.

3. Results and discussion

3.1. Selection of the best inhibitors

A macrocyclic ligand can interact directly with enzymes via supramolecular interactions, but at the same time, it is able to bind a metal atom within its central cavity. Besides, this cavity can be branched or functionalized with other chemical groups to stimulate the interactions with further spices as enzymes[40]. The size and spatial arrangement of the coordinating groups are of great importance since it significantly influences the properties of the complexes and this affects their selectivity[52]. First on this study, diverse compounds with different chemical structures were chosen in order to evaluate the effect of their presence in the oxidation reaction of dopamine by polyphenol oxidase (see Figure 5.3). The selected compounds have in common a macrocyclic unit. The size of the cavity varies depending on the number of atoms in the ring. Therefore, for clarity in the discussion, the ligands were divided according to the number of nitrogen groups in the macrocycle in small (S1, S2, S3, and S4), medium (M1, M2, and M3) and large (L1, L2, and L3).

An initial screening of the inhibitory activity was accomplished measuring the absorbance at 420 nm in presence of the ligand at pH 5.5 with dopamine as a substrate (Figure 5.4). In general terms, all the ligands reduce the initial reaction rate, which can be translated as a partial inhibition of the enzymatic activity. The degree of inhibition varies strongly among the ligands with a decrease in the initial PPO rate from 11.4 to 94.5 % depending on the chemical structure. On a fist sight, it can be

seen how the smallest cycles (S1, S2, S3, and S4) were not able to reduce the enzymatic activity of the PPO more than 40%. Besides, M1, M2, and M3, bigger in structure, presented better inhibition power with M3 inhibiting 70% of the PPO activity. Finally, L2 induces the greatest inhibition over the PPO (almost 95%) seeming that the functionalization with the two naphth-2-ylmethyl plays an important role. However, not only the naphth-2-ylmethyl units makes the difference as L3 present less inhibition (70%) having the same units but with an amine between the macrocycle and the naphthalene. If we compare these values with those reported by Wei Liu and co-workers[53] using citric acid as a typical tyrosinase inhibitor we can observe that these ligands present higher power of inhibition. In the case of citric acid, it was necessary a concentration superior to 10 mM to reach an inhibition of the 20% over tyrosinase from mushroom. They also report that the minimum of citric acid was 10 mM to strongly inhibit the PPO from bananas.

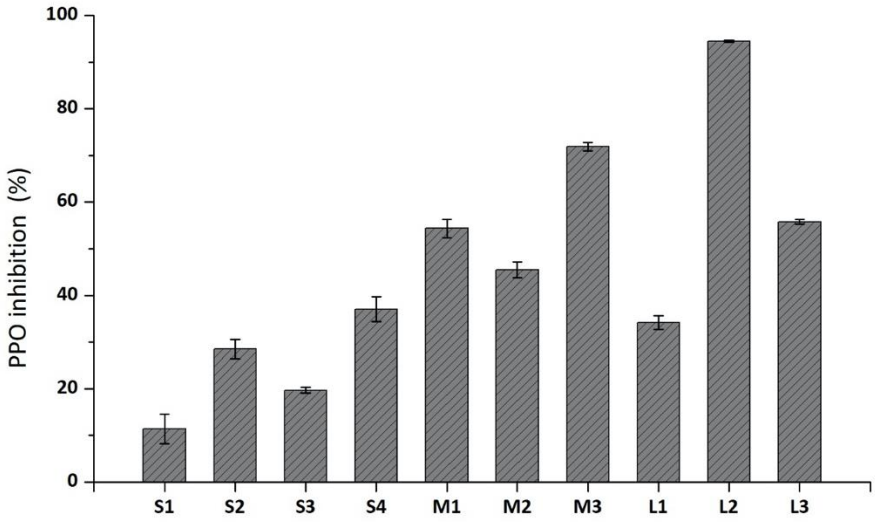

Figure 5.4. *Polyphenol oxidase (94 U) inhibition in presence of the ten different azamacrocyclic ligands (0.67 mM) using dopamine as substrate (2.5 mM).*

Even though this behaviour depends on the substrate source (catechol vs dopamine), in our case all the ligands present 10 times superior inhibition power with only 0.67 mM. Regarding to others commonly used organic acids, such as oxalic acid, Son et al. (2020)[54] pointed out that a concentration of approximately 1 mM could inhibit the PPO 50%, and 5 mM could inhibit the PPO 80%. Similar behaviour is reported for benzoic acid[55] over mushroom PPO where a concentration of 5.20 mM is needed to reach 50% inhibition. In our case, most of the ligands from the M and L family report the greatest inhibitory force, as they need less concentration than 1 mM to reach more than 50%.

In order to gain insight about the influence of the chemical structure in the PPO activity, the ligands were parametrised (see Table 5.1), and the degree of inhibition was modelized with the partial least-squares regression (PLS) technique. The PLS is a multivariate projection method that models the relation between an array of dependent variables (Y) and another array of independent variables (X) to find the components that allow the highest correlation with Y. In our case the independent variables were the parametrised data contained in Table 5.1, and the dependent variable was the degree of inhibition shown in Figure 5.4. All the data/ligands were included in the training set because the number of molecules was small, and we were interested in understanding the influence of the functional groups in the inhibitory activity measured during the screening.

To check the quality of the model, the leave one out (LOO) method was used, and four latent variables selected. Figure 5.5 contains a graph with the measured vs. the predicted values of the inhibitory activity for each ligand. The measured and predicted values were plotted together to evaluate the accuracy and precision of the created prediction models. Ideally, the predicted values should lie along the diagonal line, indicating that the predicted and actual values are the same.

Table 5.1. *Parametrised values of the ligands used in the PLS and squared values of the first four principal components*

Ligand / Loading	Ntot[a]	Pyr[b]	NH[c]	Nter[d]	Ant[e]	Amac[f]	OH[g]	Met[h]	Nmac[i]	Rsize[j]	Benz[k]	Sch[l]	Lch[m]	Inhib[n]
S1	4	0	4	0	0	0	0	0	4	14	0	0	0	11,4
S2	4	1	3	0	0	0	0	1	4	12	0	0	0	28,5
S3	4	1	3	0	0	0	1	0	4	12	0	0	0	19,7
S4	4	1	0	3	0	0	0	0	4	12	0	1	2	37,1
M1	5	0	5	0	0	0	0	0	5	20	1	0	0	54,4
M2	6	1	5	0	0	0	0	0	6	20	0	0	0	45,5
M3	7	1	6	0	0	0	0	0	7	24	0	0	0	71,4
L1	8	2	4	2	0	0	0	0	8	24	0	2	0	34,2
L2	8	2	4	2	2	2	0	0	8	24	0	0	2	94,5
L3	10	2	6	2	2	0	0	0	8	24	0	0	2	55,8
PC1[+]	0,1								0,08	0,77				
PC2[+]		0,05	0,52*	0,48	0,15	0,12				0,05*			0,45	
PC3[+]	0,16*	0,09*	0,19	0,29*					0,06*			0,16*		
PC4[+]	0,43*		0,61*		0,36*					0,21		0,26	0,13*	

[a] Ntot: total number of nitrogens. [b] Pyr: number of pyridine units. [c] NH: number of NH groups [d] Nter: number of tertiary amines [e] Ant: number of anthracene units [f] Amac: number of anthracene units attached to the macrocycle. [g] OH: number of OH groups. [h] Met: number of methoxy groups. [i] Nmac: number of N in the macrocycle. [j] Rsize: number of atoms that compose the macrocycle. [k] Benz: number of benzene units. [l] Sch: number of small chains attached to the macrocycle. [m] Lch: number of big chains attached to the macrocycle. [n] Inhib: % of inhibition calculated as 100-initial PPO rate. [+] Values lower than 0,05 have been omitted for clarity. * loadings with negative.

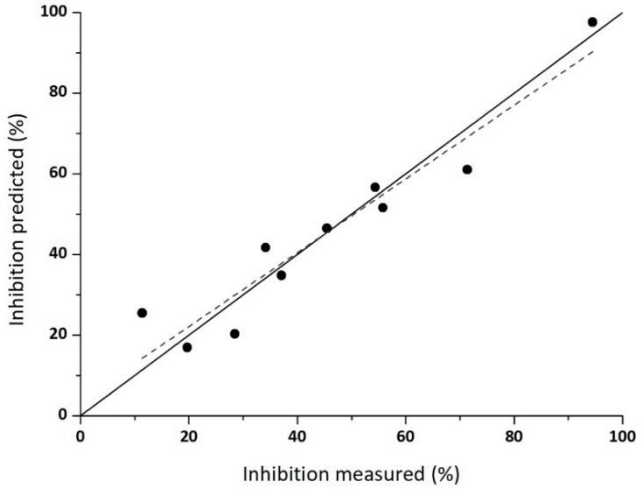

Figure 5.5. *Experimental versus predicted values by using a PLS statistical model (dashed lines) for the PPO inhibition. The solid line represents ideal behaviour..*

As can be seen in Figure 5.5, in general, a good fit is obtained and most of the points remain next to the solid line. Furthermore, a linear fitting by using the points in the graph with a simple linear model (y = ax + b) offered values of 0.915, 3.86 and 0.915 for the slope, the intercept, and R^2, respectively. The effect of the chemical structure parameters defined in Table 5.1 in the inhibitory activity was analyzed from the squared loadings for the first four principal components (PCs) (Table 5.1).In PLS the first principal component (PC1) contains the highest explained variance and explains most of the inhibitory response; PC2 contains the second-highest explained variance, and so on. In this case, PC1 suggest that the ring size is the main factor responsible of the inhibitory response. Also, high values are found for the total number of nitrogens (Ntot) and the number of nitrogens in the macrocycle (Nmac), suggesting that together with the ring size, the amino groups are highly relevant for the inhibitory activity. However, as the number of nitrogen

atoms in the ligand is high correlated with the macrocycle size, the inhibitory effect can be assigned neither to the ring size nor to the total number of nitrogens separately.

As can be seen in Table 5.1, we can assign as a second main factor in the ligand activity (PC2) to the macrocycle functionalization (Nter, Ant, Amac), with preference for the big size substituents (Lch) over the little groups (Sch). Also, the presence of the pyridine moiety seems to improve the response. Regarding the other two principal components, the number of NH (PC3) and methyl groups (PC4) have a positive but minor effect. Other functional groups such as the presence of benzene, the hydroxy or methoxy groups do not seem to offer any advantage.

From the structure of the ligands and the PLS analysis, we can conclude that the key factor of the inhibitory activity is the presence of a big macrocycle containing several amino groups and it improves with the presence of bulky hydrophobic substituents (i.e. i-Pr or anthracene) directly attached to the ring.

3.2. Ligand-PPO interaction

Since the ligands M1, M2, M3, L2, and L3 had reported the greatest power of inhibition over the PPO (at least 50%), we selected them to analyse their interaction more thoroughly.

As previously mentioned, the enzymatic browning process comprises two phases, firstly, the enzymatically catalysed oxidation takes place, followed by a non-enzymatic polymerization reaction that generates the brown colour[56]. Although the appearance of colour is generally used to follow the enzymatic browning reaction, the speed of oxygen consumption allows us to prove that the effect of azamacrocyclic compounds is directly related to the enzymatic activity (oxidation) and not associated with the non-enzymatic polymerization of the quinones.

As seen in Figure 5.6, the initial rates of oxygen consumption and colour formation were compared for the five inhibitors selected. Despite being different methodologies, both techniques reveal an appreciable increase on the inhibition of the browning process. The behaviour observed is that, although similar, the inhibition over the colour formation is higher than the inhibition of the oxygen consumption. This suggests that their mechanisms would not only involve the enzyme but an interfere with the polymerization reaction. By contrast, L2 shows a slight variance (5%) between both techniques, and L3 does not show any meaningful difference between the initial velocity of oxygen consumption and colour formation. These results suggest that for L2 and L3 the decrease in browning is mainly due to a decrease in the PPO activity.

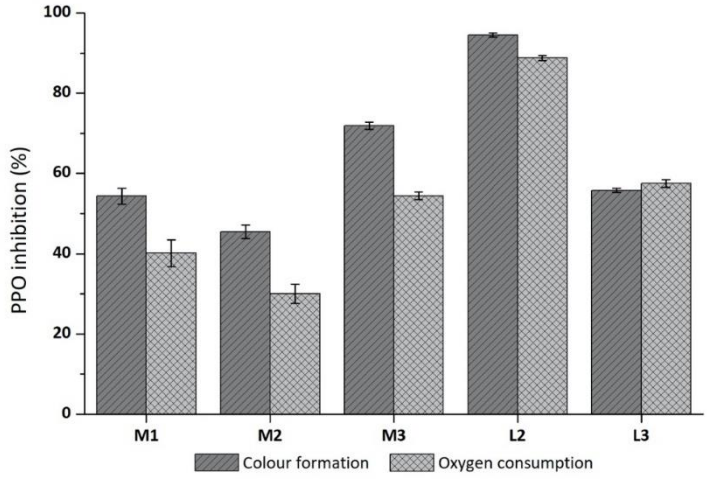

Figure 5.6. *PPO (94 U) inhibition (%) based on colour formation (dark grey) and based on oxygen consumption (light grey) for the five selected ligands (0.67 mM).*

Furthermore, the influence of the contact time between the enzyme and the different compounds should be considered as it might affect the inhibitory capacity over the PPO. Thus, the responses of the five selected ligands were analysed by varying the previous contact time between the ligand and the PPO prior to substrate addition (0 min and 60 min). With the exception of M3 (see Figure 5.7), the speed decreases as the contact time increases being that the differences are significant (p <0.0001). This would indicate that if the enzyme and the inhibitor are previously in contact in solution, they are able to interact to a greater extent, obtaining higher inhibition values.

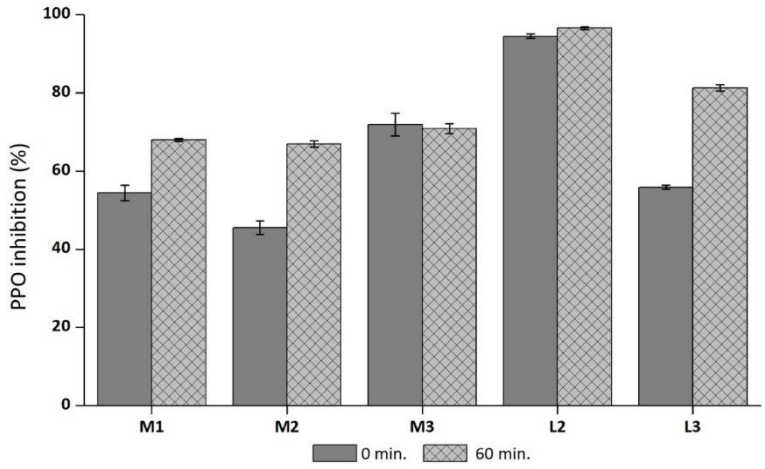

Figure 5.7. *Effect of contact time between polyphenol oxidase (94 U) and the different ligands on their inhibitory capacity prior to substrate addition. Without previous contact time (0 min; dark grey) and with 60 minutes of previous contact time (light grey).*

3.3. Kinetic parameters determination

As tyrosinase from mushroom follows Michaelis-Menten kinetics, in order to understand and compare the nature of the enzyme-inhibitor interaction, the classical method of Lineweaver-Burk plots was used to determine the kinetic parameters and the inhibition mechanism for each inhibitor (see Table 5.2). In the case of the Michaelis-Menten K_M constant, the value for the control was K_M = 1.05 ± 0.05 mM and 0.3321 mMmin^{-1} for v_{max}.

It is noticeable that the compounds M1 and M2, both similar in their structure, perform a similar inhibition over PPO with no statistical differences between them. The Michaelis-Menten constant maintains the values of the control, yet the v_{max} drops off as the amount of inhibitor increases in the solution. This behaviour indicates that both ligands M1 and M2 act as noncompetitive inhibitors. Also, it seems that the presence of the pyridine in the structure of M2 does not offer additional inhibitory capability to the ligand. It was also calculated the inhibition constant (K_i) and the IC_{50} for both M1 and M2 ligands were about 0.25 mM in both cases. In the case of noncompetitive inhibition, K_i and IC_{50} parameters must be equal or almost identical, as in the case of M1 and M2. Both ligands behave almost identically, as there is almost no differences between their constants.

In comparison with M1 and M2, M3 offers an extra inhibition power and also a change in the interaction on the PPO. It seems that the increase in the ring size and the extra nitrogen in its structure improve the inhibitory activity of the PPO. In this case, it was necessary to decrease the concentration to 0.33 mM to obtain the same v_{max} as M1 and M2 with double the concentration (0.66 mM). Furthermore, K_M also drops off with a significant difference from the control meaning that the inhibition would be mixed type in contrast to M1 and M2.

The next ligand with more inhibition power was L3, which has a 24-membered macrocycle ring, 10 nitrogens in total and 2 naphtha-2-ylmethyl units in its structure. With a concentration of 0.1 mM the maximum rate of the tyrosinase decreases approximately to 0.03 mM min^{-1}, also decreasing the catalytic constant and the catalytic efficiency in a substantial way. Thus, L3 is 4 times more active than M3 and 13 times more active than M2 and M1. It supports that when the macrocycle size and the number of nitrogens in the macrocycle are increased, together with the presence of the naphth-2-ylmethyl units, the inhibition power rises as deduced from the PLS analysis.

Lastly, L2 has also two naphth-2-ylmethyl units but in contrast with L3, they are directly attached to the ring by removing two NH units. This ligand is the most powerful inhibitor of the 10 tested ligands. The values of K_M and v_{max} were calculated for three different concentrations of L2 (see Table 5.2 and Figure 5.8A). In all the cases a value of K_M around 1.0 mM was obtained, with no statistically significant differences for $p<0.05$ in any case. However, the value of v_{max} decreases from 0.29 to 0.038 mM min^{-1} when increasing the concentration of L2 in the medium. K_M does not vary with the concentration of inhibitor, but v_{max} decreases. Thus, we can conclude that L2 induces a noncompetitive inhibition over the PPO enzyme, where there is no coordination with the active centre. The catalytic efficiency (k_{cat}/K_M) and the turnover number (k_{cat}) follow the same trend as the v_{max}, with values close to 1400 mM min^{-1} in absence of the inhibitor that dropped off up to 150 mM min^{-1} indicating that the efficiency of the enzyme is much lower in the presence of L2 at 0.04 mM, the lowest concentration of all the compounds. Furthermore, the IC_{50} parameter was also estimated at 10 ± 2 μM (n=3) statistically equal to kojic acid in the same conditions.

Table 5.2. *Kinetic parameters and type of inhibition of the enzyme Tyrosinase from mushroom (94 U) in presence of the five selected ligands at different concentrations.*

Compound (mM)		K_M[a](mM)	v_{max}[b] (mM min^{-1})	k_{cat}[c](min^{-1})	Catalytic efficiency[d] (mM^{-1} min^{-1})	IC_{50} (mM)	K_i (mM)	Inhibition type
Control		1.05 ± 0.05*	0.3324 ± 0.0108	1700 ± 50	1620 ± 140			
M1	0.67	1.01 ± 0.06*	0.091 ± 0.004^{+}	467 ± 19	460 ± 40	0.23 ± 0.02	0.28 ± 0.03	Non-competitive
	1.33	1.007 ± 0.118*	0.03 ± 0.002§	160 ± 10	160 ± 30			
M2	0.67	1.01 ± 0.03*	0.099 ± 0.002^{+}	510 ± 10	500 ± 20	0.25 ± 0.04	0.28 ± 0.02	Non-competitive
	1.33	1.02 ± 0.05*	0.0587 ± 0.0016§	303 ± 8	300 ± 20			
M3	0.1	0.71 ± 0.05	0.119 ± 0.005	610 ± 20	860 ± 80	0.09 ± 0.03	0.133 ± 0.009	Mixed type
	0.33	0.73 ± 0.03	0.073 ± 0.002^{+}	377 ± 14	520 ± 40			
L3	0.1	1.08 ± 0.05*	0.032 ± 0.002$^{§¥}$	164 ± 5	150 ± 10	0.014 ± 0.001	0.0106 ± 0.0008	Non-competitive
	0.67	0.97 ± 0.17*	0.02 ± 0.002	100 ± 10	100 ± 30			
L2	0.005	1.08 ± 0.14*	0.29 ± 0.04	1490 ± 190	1380 ± 50	0.010 ± 0.002	0.015 ± 0.003[e]	Non-competitive
	0.01	1.011 ± 0.014*	0.162 ± 0.005	840 ± 30	830 ± 20			
	0.04	1.2 ± 0.2*	0.038 ± 0.008$^{¥}$	200 ± 40	167 ± 4			

[a] Michaelis-Menten constant, dependent of enzyme concentration. [b] Reaction rate, dependent on enzyme concentration. [c] Catalytic constant, $k_{cat}=v_{max}/[E]$. [d] Catalytic efficiency, calculated by k_{cat}/K_M. [e] For L2, K_i cannot be determined directly from the usual Dixon plot, "K_i" is a more complex function which varies with [I] (K_i^{slope}). $^{*+§¥}$ There are no statistically significant differences for p <0.05.

This result indicates that, in general, the interaction of the compounds with the enzyme is not carried out in the active centre, as only M3 presents a mixed type inhibition. This absence of direct interaction could be explained since copper is found in the active site of the enzyme, within a biological structure with a complex quaternary structure and not as a free ion. Although the interaction of the inhibitor with the enzyme is not carried out in the active centre, it is likely to modify the interaction of the substrate with the active centre, avoiding or delaying the formation of products of the reaction[57].

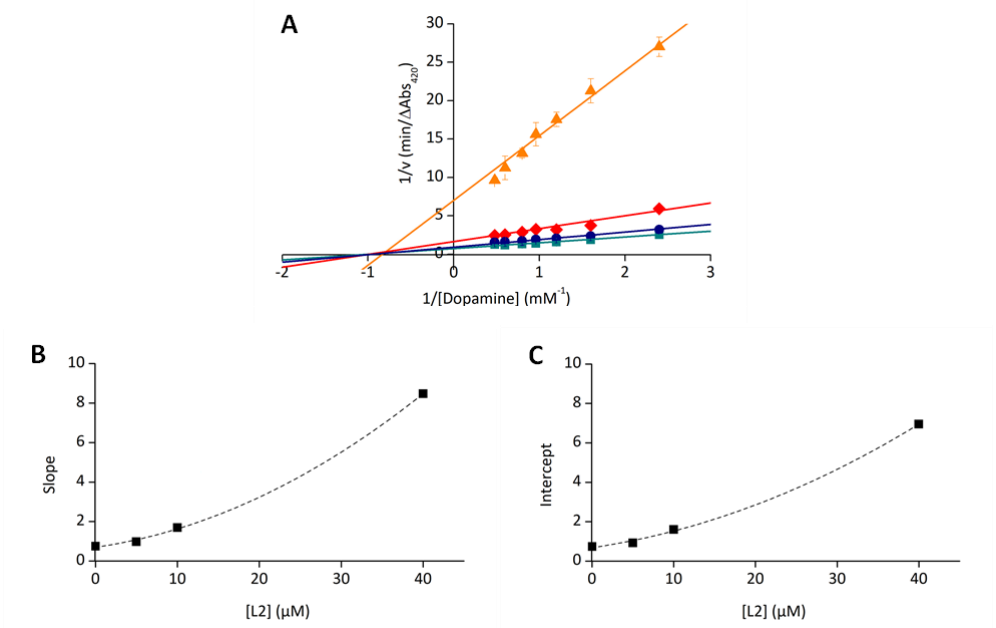

Figure 5.8. *A) Lineaweaver-Burk plot of dopamine oxidation in presence and absence of L2. The concentrations of L2 are (■) 0 μM, (●) 5 μM (◆) 10 μM and (▲) 40 μM. B) Secondary replot of Slope (KM/vmax) vs. [L2]. C) Secondary replot of intercept (1/vmax) vs [L2]). Data of (B) and (C) are obtained from (A).*

3.4. Analysis of L2-mushroom tyrosinase interaction

The influence of the inhibitor in the enzymatic activity was analysed through the study of the variation of the slope and the intercept values with the concentration of L2. In case of conventional Michaelis-Menten systems, a linear relationship is found. As can be seen in Figure 5.8b and 5.8c, both the slope (K_M/v_{max}) and the intercept ($1/v_{max}$) vs [L2] show an excellent fitting to parabolic (R^2 in both cases is 0.999) instead of linear functions. This indicates that the mechanism is rather S-parabolic I-parabolic inhibition[58] where there is either a complex noncompetitive inhibition with multiple inhibitor sites for one enzyme or complex conformational changes[59,60]. In these cases, K_i cannot be determined directly from the usual plots like Dixon; however, "K_i" as a more complex function, which varies with [I][61,62] , was determined from Equation (2) where K_i is K_i^{slope}.

$$slope = \frac{K_M}{V_{max}} * (1 + \frac{[I]}{K_i})^2 \qquad (2)$$

Applying Equation (2), the K_i^{slope} calculated is 15 ± 3 µM.

Fluorescence studies were also performed in order to get more insight into the nature of the enzyme-inhibitor interactions. It was observed that the intensity of the fluorescence decreases progressively when increasing the amount of L2, although without any significant shift in the maximum intensity. The Stern-Volmer equation was applied to calculate the Stern-Volmer quenching constant (K_{sv}) and the k_q (biomolecular quenching rate constant), determining whether the mechanism was static or dynamic[63]. The corresponding value for K_{sv} is 7.8 x 10^4 M^{-1} and 7.8 x 10^{12} $M^{-1}s^{-1}$ for k_q. Assuming that the collision quenching constant of biomolecules is about 2.0 x 10^{10} $M^{-1}s^{-1}$, our k_q is two order of magnitude higher, suggesting that the inhibition process provoked for L2 shows a static nature with a binding between the

enzyme and the inhibitor[64]. In this case, the number of binding sites can be obtained by Equation (3)[62,65]:

$$\frac{F_0}{F_0 - F} = \frac{1}{n} + \frac{1}{K}\frac{1}{[L1]} \quad (3)$$

Where F_0 and F are the relative fluorescence intensities of the enzyme with and without the inhibitor respectively, [L2] is the concentration of L2, K is the binding constant and n is the number of binding sites. A good correlation was obtained (R^2=0.999) and a value close to 1 (n = 0.860 ± 0.005) was calculated, which indicates the binding of one molecule of L2 to each tyrosinase is enough to change the conformation of the enzyme lowering its activity. In addition, a high binding constant was obtained ((1.869 ± 0.018) x 10^5 M^{-1}) in agreement with the great affinity between the enzyme and the inhibitor.

3.5. Inhibitory assays on apple juices as real matrices

Encouraged by the good results offered by L2 as an inhibitor of tyrosinase in model systems, its performance was checked in a real food system, as it is the case of freshly obtained apple juice. For that purpose, apples of the c.v. Golden Delicious variety were liquefied and put in contact with two different concentrations (0.5 mM and 1.5 mM) of L2; afterwards, the samples were left stirring for one hour. In general terms, once the apples liquefy, the enzymatic browning process begins quickly. The colour change is perceptible to the human eye within the first 5-10 minutes. As we can see in Figure 5.9a, in absence of inhibitor, the juice suffers a strong oxidation of the polyphenols even in the first 10 minutes, changing from bright yellow to an orange colour that becomes reddish after 30 minutes and reaches almost a full oxidative browning after 1 hour.

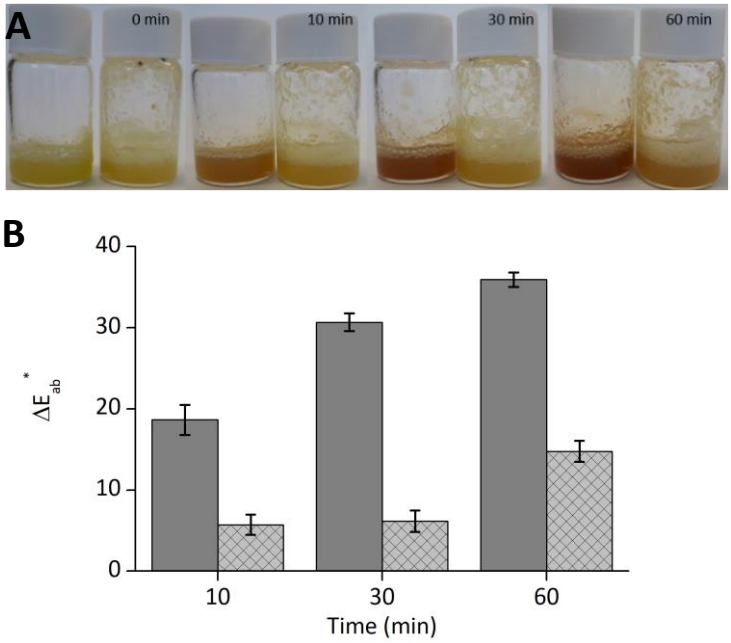

Figure 5.9. *A) Colour evolution in apple juice without the inhibitor (left) and in the presence of 1.5 mM of L2 (right). B) Measurements of colour difference ΔE over time: control (grey) and with 1.5 mM L2 (striped).*

When the juice is put in contact with the lowest concentration of L2 (0.5 mM) the enzymatic browning is delayed during the first 10 minutes; however, the reaction is not completely stopped, and the colour of the juice reaches a browning intensity similar to that observed in the absence of inhibitor at longer times (60 minutes). Raising the concentration of L2 in the juice to 1.5 mM, the inhibiting effect of the azamacrocyclic ligand was strong enough to stop the process. The colour change of the juice mixed with the 1.5 mM of L2 is almost inappreciable during the first 30 min, darkening slightly after 60 minutes.

Figure 5.9b collects the colour change differences (ΔE_{ab}^*) for the apple juice in presence and absence of inhibitor, taking the freshly prepared juice as reference.

In agreement with the naked eye colour changes, it can be noticed how after the first 10 min, the control reaches a ΔE_{ab}^{*} close to 20, which continues growing, while the one with inhibitor barely has a ΔE_{ab}^{*} of 5 that is maintained during the 30 min. At longer times (1 h) the control shows a colour similar to the 30 min, indicating that the oxidation is almost complete. However, the sample containing L2 (1.5 mM) holds a significant reduction in the enzymatic browning, although a slight increase in the ΔE_{ab}^{*} is observed, suggesting that a residual activity is maintained at long times.

4. Conclusions

In conclusion, during the present study, the influence over the enzymatic browning of 10 aza-macrocyclic ligands with diverse functionalisation has been tested, showing that they can be potentially used as inhibitory products of PPO to a greater or lesser extent. Their chemical structures strongly influence the inhibitory activity, the ring size and the number of nitrogens in the macrocycle (both correlated) being the main factor. Also, the presence of bulky aromatic groups attached to the macrocycle was relevant. The inhibition of the enzymatic browning is mainly due to the deactivation of the PPO and suffers a significant rise if the contact time between the enzyme the ligand increases. For L2, the most active inhibitor, kinetic studies indicate that ligands interact with the tyrosinase enzyme with a noncompetitive mechanism in a molar proportion of 1:1 giving rise to structural change on the protein that provokes an abrupt decrease in its activity. The high inhibitory activity of L2 was verified on a real sample showing how it can reduce the enzymatic browning in apple juice when used at 1.5 mM. L2 opens the door to a new strategy based on systems that conjugate polyamines and aromatic groups as tyrosinase inhibitors.

Acknowledgements

Financial support by the Spanish Ministerio de Ciencia, Innovación y Universidades (project RTI2018-100910-B-C44), Ministerio de Economía y Competitividad (projects CTQ2016-78499-C6-1-R, Unidad de Excelencia MDM 2015-0038 and CTQ2017-90852-REDC) and Generalitat Valenciana (Project PROMETEOII2015-002) is gratefully acknowledged.

PAPER 2: A TETRAAZAHYDROXYPYRIDINONE DERIVATIVE AS INHIBITOR OF APPLE JUICE ENZYMATIC BROWNING AND OXIDATION

A TETRAAZAHYDROXYPYRIDINONE DERIVATIVE AS INHIBITOR OF APPLE JUICE ENZYMATIC BROWNING AND OXIDATION

Sara Muñoz-Pina[1], Aitana Duch-Calabuig[1], José V. Ros-Lis[2], Begoña Verdejo[3], Enrique García-España[3], Ángel Argüelles[1], Ana Andrés[1]

[1] Instituto Universitario de Ingeniería de Alimentos para el Desarrollo (IUIAD-UPV). Universitat Politècnica de València Camino de Vera s/n, 46022, Valencia, Spain.

[2] REDOLí, Departamento de Química Inorgánica, Universitat de València, 46100, Burjassot, Valencia Spain.

[3] Instituto de Ciencia Molecular, Universitat de València. C/Catedrático José Beltrán 2, Paterna (Valencia), Spain.

SUMMARY

Once it has been proven that azamacrocyclic ligands are good candidates as anti-browning agents, we dug into the same strategy studying a compound similar in structure to the inhibitor kojic acid.

Enzymatic browning caused by polyphenol oxidase (PPO) is one of the main obstacles encountered in fruit and vegetable's industrialization. This poses a challenge to the food industry to apply appropriate inhibitors to control the enzymatic browning maintaining the food quality. Thermal inhibition processes do already exist, nonetheless, they tend to reduce the nutritional value of the product. Therefore, chemical inhibitors that do not alter these parameters have also been used. One of the most powerful chemical inhibitors of PPO is kojic acid, yet its difficulty of large-scale production, high cost and toxicity has restricted its use.

Macrocyclic polyamines are a class of compounds that comprise a special group of heterocycles able to bind different guests such as metals or amino acids. In addition, it is possible to branch or functionalised the central ring with different chemical groups creating new compounds. In this case, it can be functionalised with a group similar to the inhibitor kojic acid.

Thus, this study aims to evaluate three different inhibitors based on aza-macrocyclic compounds. First, a tetraazamacrocycle unit only; second, the same macrocycle with an aminoalkyl chain, and finally, the macrocycle functionalised with a pyridinone group similar to kojic acid. Moreover, its effect on enzymatic browning, total polyphenols and antioxidant activity in apple juice has been assessed.

As a first approach, to analyse their inhibitory power, a screening was carried out in the pH range where PPO is active: 4.5, 5.5 and 6.5. Even though all the tested substances reduce the PPO activity, the unfunctionalized macrocycle (I3) reduces it in a lower range (only 30 %). On the contrary, the 3-hydroxy-4-pyridinone functional group of I1 increases the inhibition, especially at pH 5.5 and 6.5 where almost a completely inhibition is found (85%). In order to determine the inhibition type for the different compounds, commercial PPO was reacted with the inhibitor (0.66 and 1.5 mM) at pH 5.5. The type of inhibition was determined by calculating KM and vmax constants using the Lineweaver-Burk representation. Apparently, the pyridinone group (in I1) offers an extra inhibition power that the amine group (in I2) is not able to perform; nonetheless, both have a mixed type of inhibition. Contrary to them, only the macrocycle, with a non-competitive inhibition capacity, is not able to perform a strong inhibition over the PPO. In fact, the IC50 parameter for I1 was 0.30 mM, much lower than the calculated for the other inhibitors.

Since I1 showed good results, its anti-browning capacity was studied by measuring colour change throughout time in cloudy apple juice. The enzymatic

browning process without inhibitor starts quickly, and the juice's colour change is visible. However, in presence of the I2 at 2.25 mM the colour change is barely noticeable. Regarding the effects of I1 over total phenolic content it was found that in the control, the phenols content was reduced nearly 40% after 60 min of stirring. However, in samples treated with 2.25 mM of inhibitor, the total phenolic content was stopped and remained stable. On the other hand, the antioxidant activity of the juice was reduced by more than 50% at least during the first 30 min.

In short, the presence of hydroxypyridinone attached to the macrocycle is relevant to enhance the inhibitor power and to reduce the enzymatic browning in a real matrix as a cloudy apple juice.

Key words: PPO, inhibition, macrocyclic polyamines, apple juice, physicochemical properties

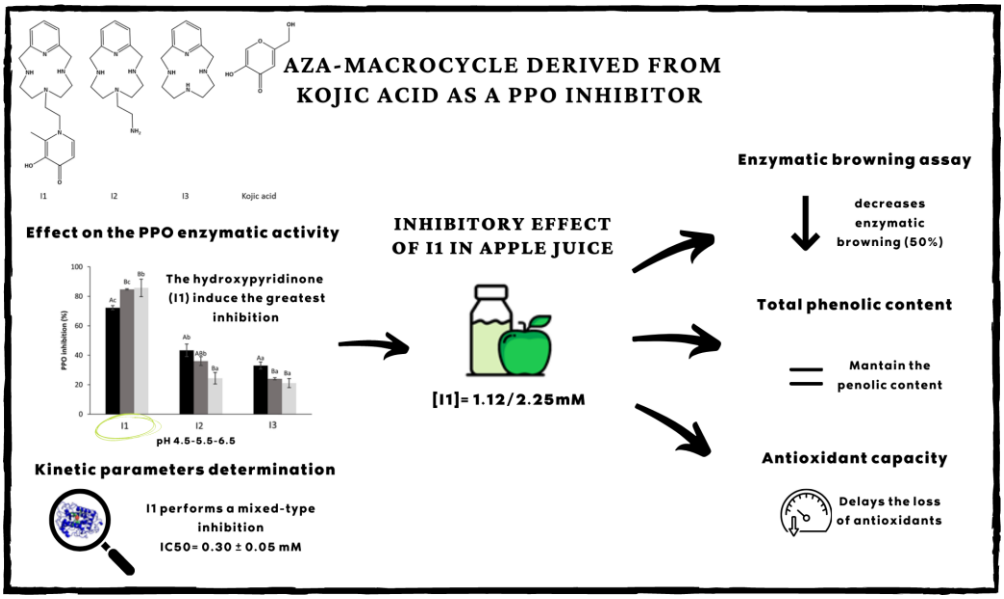

***Figure 5.10**. Graphical abstract of a polyamine macrocycle as an inhibitor of apple juice enzymatic browning and oxidation*

1. Introduction

Enzymatic browning is induced by mechanical and physical stresses taking place during post-harvest processing and storage in a wide range of products including fruits (e.g., apple, bananas and grapes), vegetables (e.g., potatoes, mushrooms and lettuce) and even in seafood (e.g., shrimps, spiny lobsters and crabs) [66]. It generates not only colour changes, but also adverse effects on taste, flavour, and nutritional value losing polyphenols and antioxidants, among others.

Enzymatic browning is one of the main obstacles encountered in the industrialization of some fruit/vegetables products [67]. Polyphenol oxidase (PPO), which is the main responsible of the enzymatic browning, is a copper-containing enzyme belonging to the oxidoreductase family. The Enzyme Commission (EC), according to its substrate specificity, has classified them into EC1.14.18.1 (cresolase or tyrosinase) and EC1.10.3.1 (diphenol oxidase or catechol oxidase) [68,69]. In enzymatic browning, PPO catalyses the oxidation of monophenols into o-quinones which is followed by a non-enzymatic polymerization. The polymerization of the quinones gives rise to reddish-brownish pigments called melanonids, which are the reason for colour change [70].

Apples (*Malus Domestica*) are the third more cultivated fruit worldwide, with a production of around 86 million tons in 2018 (FAOSTAT, 2018). From all production, a significant part of apples is meant for apple juice (e.g. in the U.S. was approximately 12 % of the total in 2018) [71]. Apple juices are highly susceptible to this deteriorative mechanism since apples contain both active PPO and high polyphenol content [72,73].

Nowadays, there is an upward tendency to consume fresher and minimally processed foods in a way that preserves the sensory and nutritional properties of

raw foods. Colour changes derived from enzymatic browning cause rejection by the consumers, leading to high amounts of food waste and economic losses for the industry. It is not surprising the food industry has developed different methods for the prevention of the enzymatic browning [32]. Thermal treatments are the most widely used physical method in the food industry, especially in beverages production. However, it has major drawbacks since it affects the nutritional quality of food, affecting thermosensitive nutrients such as vitamins, carotenoids, and anthocyanins. Other technologies have been explored as an alternative to thermal processing for fruits and vegetables, and especially for apple juice, such as ultra-high-pressure homogenization, high-pressure carbon dioxide, or cold plasma [74]. Nonetheless, its application in the industry is still scarce as they have some limitations such as negative effects on the nutritional quality of products or high cost.

Chemical inhibitors offer an interesting alternative due to their lower cost, manageability, and scarce alteration of the bioactive compounds. Among all the possibilities, only sulphites or acidifiers are a real alternative to thermal treatments in the food industry. In the case of acidifiers, such as citric acid and ascorbic acid, they inactivate the PPO by lowering the pH value. On the other hand, a reducing agent like sulphites and its derivatives act as irreversible inhibitors of PPO. Nevertheless, the taste alteration and the allergies in the population (sulphites) have restricted their use.

Therefore, the challenge for the food industry is to apply appropriate inhibitors to control enzymatic browning maintaining the quality and extending their shelf life while meeting current consumer needs.

Inhibitors from synthetic origin have been reported to inhibit the PPO, from synthetic polyphenols like deoxybenzoins to synthetic isoflavones,

thiosemicarbazones or chalcones. Showing great potential as PPO inhibitors, having in some cases greater inhibiting power than their natural analogues [75].

Polyamines like chitosan, a polymer containing several organic groups, has demonstrated its effectiveness as inhibitors of enzymatic browning [76]. Furthermore, macrocyclic polyamines have also shown great PPO inhibition depending on the number of amine groups and the chemical structure [77]. On the other hand, kojic acid is a very known powerful inhibitor that acts as a reducing agent and as a non-competitive inhibitor becoming a positive reference when testing new PPO inhibitors [75]. Having into mind these features, we hypothesize that the combination of a polyamine with a functional group like kojic acid could be an interesting approach to the development of a new family of PPO inhibitor. Thus, a PPO inhibitor including a tetraazamacrocyle modified with a hydroxypyridinone similar to kojic acid has been prepared (I1) and its effect on enzymatic browning, total polyphenols and antioxidant activity of apple juice studied.

2. Materials and methods

2.1. Chemicals

Commercial tyrosinase enzyme (2687 U/mg), dopamine hydrochloride, Kojic acid, 1,1-Diphenyl-2-picrylhydrazyl radical (DPPH·) and Folin Ciocalteu reagent (2N) were purchased from Sigma-Aldrich (Sigma-Aldrich, USA). Sodium bisphosphate, disodium phosphate and sodium carbonate were acquired from Scharlau (Sharlab S.L., Spain) and anhydrous sodium acetate from Panreac AppliChem (Panreac AppliChem, Barcelona, Spain). Lastly, methanol (99.9%) was purchase from Honeywell (Honeywell, France). The apple juices used in the tests were obtained in

the laboratory by liquefying apples (Golden Delicious variety) obtained in a local store.

The inhibitors I1, I2, and I3 were synthesised according to known procedures: Verdejo et al. (2007)[14] and López-Martínez et al. (2016)[15].

2.2. Study of enzyme-inhibitor interaction over tyrosinase

The effect of the inhibitors (0.67 mM) over tyrosinase (93.75 U) was tested in presence of dopamine (2.5 mM) at different pH (4.5, 5.5 and 6.5) in a phosphate-acetate buffer of 10 mM [77]. For each pH, a sample in absence of inhibitor was used as control. The dopamine oxidation reaction was followed spectrophotometrically at 420 nm by a Beckman Coulter DU-730 Life Science UV/Vis spectrophotometer. The assays were done in triplicate at 24 °C measuring the absorbance each 10 s during 5 min. From the absorption-time curves, the initial speed of the reaction was determined from the slope of the linear stretch of the absorption-time curves. The different slopes were used to compare the inhibitory effect of the tested compounds against the control (see Equation (1)).

$$PPO\ inhibition\ (\%) = \left(\frac{V_{oi}}{V_{oo}} * 100\right) \qquad (1)$$

Where V_{o0} is the control initial rate and V_{oi} is the initial rate obtained for the different samples.

2.3. Enzyme kinetics in model system

To determine the inhibition type for the different compounds, it was designed a model system where commercial PPO was reacted with the inhibitor at pH (5.5) using phosphate-acetate buffer 10mM. One millilitre solution of varying concentrations of dopamine with a final concentration of 0.08 mM to 2 mM were prepared. Then, 0.50 mL of inhibitor/enzyme mixture was subsequently added. The

final concentration of enzyme in the assay was 94 U and two inhibitor concentration were tested (0.66 and 1.5 mM). Enzyme activity was determined by the formation of dopachrome following the increase in absorbance at 420 nm for 5 min (ε =3700 M^{-1} cm^{-1}) in a Spectrophotometer Beckman Coulter DU-730 Life Science UV/Vis spectrophotometer [49]. The type of inhibition was determined by calculating K_m and v_{max} constants using the Lineweaver-Burk representation as polyphenol oxidase follows kinetics of Michaelis Menten.

2.4. Inhibitory effect of enzymatic browning over apple juice

Apple juice from cv. Golden Delicious obtained in the laboratory was selected to verify the effect of the best inhibitor on real samples. The inhibitory effect was measured following the procedure reported by Muñoz-Pina, Ros-Lis, Argüelles, Martínez-Máñez, & Andrés, 2020 with slight modifications. Briefly, two millilitres of an aliquot of the cloudy juice were put in contact with 1 mL of a I1 solution, to get a final concentration of 1.12 mM and 2.25 mM. These blends were kept under agitation (400 rpm) for 60 minutes to accelerate the oxidation process and the colour change was measured with a spectrophotometer Minolta (CM-3600 d) at 0, 5, 10, 20, 30, and 60 min. CIE L*a*b* (CIELAB) colour space which comprises L* (lightness), a* (red to green) and b* (yellow to blue) coordinates were obtained using a D65 illuminant and 10° observer as a reference system. The total colour difference (ΔE_{ab}*) between the juice at time 0 and treated samples was calculated following Equation (2)

$$\Delta E^* = \sqrt{(\Delta L^*)^2 + (\Delta a^*)^2 + (\Delta b^*)^2} \qquad (2)$$

The colour difference between the initial colour and the samples can be classified as not noticeable (0-0.5), slightly noticeable (0.5-1.5), noticeable (1.5-3.0), well visible (3.0-6.0) and great (6.0-12.0), depending on the value of ΔE_{ab}^* [80].

2.5. Determination of total phenolic content (TPC) and antioxidant activity

Total phenolic content was determined using the Folin-Ciocalteu method [81,82]. Briefly, 10 µL of juice sample (see section 2.4) was diluted into 1.58 mL of deionized water and then mixed well with 100 µL of the Folin-Ciocalteu. After reacting for 3 min, 300 µL of Na_2CO_3 (20% w/v) was added to the mixture and left in dark for 60 min before measuring the absorbance at 765 nm. A blank with the inhibitors was also measured and subtracted if present. The calibration curve was prepared with standard solutions of gallic acid (from 0 to 500 mg/L) by following the same method. The results were expressed as gallic acid equivalent (GAE) (mg GAE/L).

The antioxidant activity of the juices by the DPPH· method was determined following the method described by Wu et al. (2020)[83] with slight modifications. A sample of 10 µL of juice (see section 2.4) was added to 1 mL of methanolic solution of DPPH· (100 µM). Then, the mixture was kept in the dark for 30 min and absorbance was measured at 517 nm using UV-VIS spectrophotometer (Thermo scientific Helios-zeta). The results were determined based on the standard calibration curve from 0 to 200 mg/L of Trolox. The data were expressed as Trolox equivalent (mg Trolox/L). All assays were done in triplicate.

2.6. Software and data analysis

Species distribution curves were calculated with Hyss2009 software of Hyperquad using the protonation constants published in López-Martínez et al. (2016)[15]. Data are reported as mean ± standard deviation. Statgraphics Centurion XVII software was used to perform the analysis of variance (One-Way ANOVA) and Multiple Range Tests by the LSD procedure (least significant difference) of the Fisher test to identify homogeneous groups. A confidence level of 95% (p-value < 0.05) was used.

3. RESULTS AND DISCUSSION

3.1 Impact of pH on inhibitor-PPO interaction

As noted above, aza-macrocyclic compounds have proved their efficiency in binding PPO via supramolecular interactions. The central cavity can be branched and/or functionalized to produce a wide variety of new compounds with different chemical properties enhancing their supramolecular interactions. 1-(2-(3,6,9-triaza-1(2,6)-pyridinacyclodecaphane-6-yl)ethyl)-3-hydroxy-2methylpyridin-4(1H)-one (I1) was synthesised as a model by a combination of a pyridine group (similar to kojic acid) with a tetraazamacrocycle. In order to gain insight into the influence of the chemical structure in the activity of the inhibitor, also the compounds 3,6,9-triaza-1(2,6)-pyridinacyclodecaphane (I3) containing the macrocycle unit only, and 2-(3,6,9-triaza-1(2,6)-pyridinacyclodecaphane-6-yl)ethan-1-amine (I2) including an aminoalkyl chain were synthesised (see Figure 5.11).

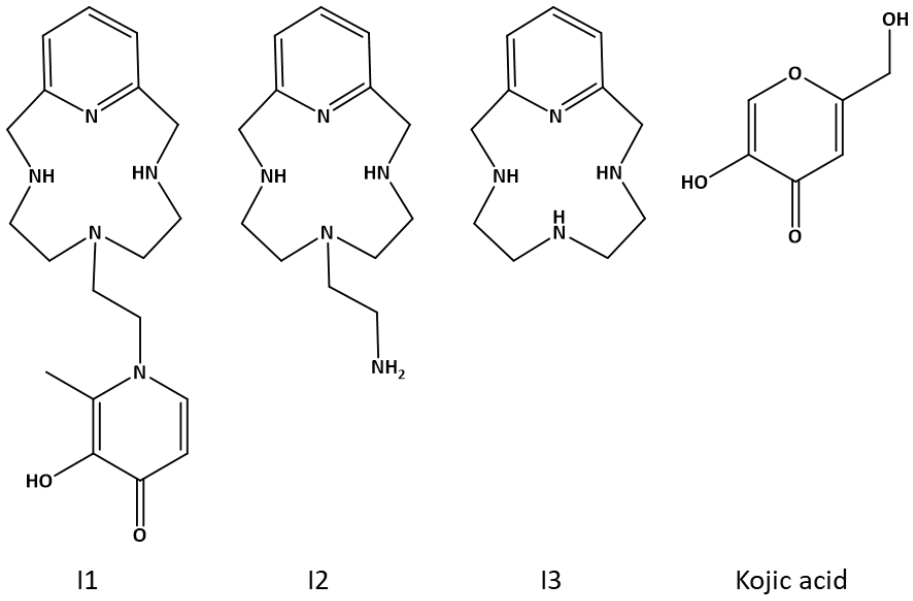

Figure 5.11. *Molecular structures of the inhibitors I1, I2, I3 and kojic acid.*

As a first approach, to analyse their inhibitory power, a preliminary screening was carried out in the pH range where PPO is active (4.5, 5.5, 6.5). The pHs were selected considering that the behaviour of polyamines is pH-dependent and most of the fruits that show enzymatic browning present a pH in this range.

In general terms, all the tested substances reduce the initial reaction rate, which can be translated as a partial inhibition of the enzymatic activity. The degree of inhibition varies strongly among the assays with a decrease in the initial PPO rate from 20 to 85% depending on the pH and the inhibitor (Figure 5.12). At a first sight, it can be seen how the unfunctionalized macrocycle (I3) reduces the PPO activity but to a lesser extent than the other inhibitors.

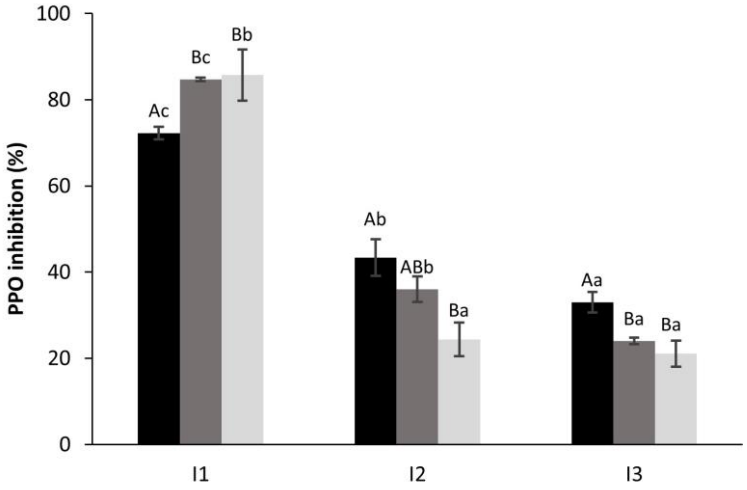

Figure 5.12. *Polyphenol oxidase (94 U) inhibition in presence of the three different aza-macrocyclic inhibitors (0.67 mM) using dopamine as substrate (2.5 mM) at different pH: 4.5 (black), 5.5 (grey) and 6.5 (light grey). A-C: different letters indicate significant differences in PPO inhibition between pH. a-c: different letters indicate significant differences between inhibitors ($p < 0.05$).*

The effect decreases as the pH increases reaching 20% at pH 6.5. Similar behaviour is reported by I2, however, the extra alkyl amino chain enhances its inhibitory power, especially at pH 4.5 showing a 40% of inhibition. Finally, it is noticeable how the presence of the 3-hydroxy-4-pyridinone functional group (similar to kojic acid) in I1 increases the inhibition inducing the greatest inhibition among the inhibitors. At pH 5.5 and 6.5, it reaches an almost complete PPO inhibition (85%) yet at low pH, the inhibition slightly decreases (72%). Having in mind that the tested inhibitors can be present as diverse species depending on the pH, the species distribution diagram at the studied pH range can be found in Figure 5.13 [78]. I1, I2 and I3 share the tetraaza macrocycle unit that contains two protonated amines at slightly acidic pH because the third protonation needs highly acidic conditions due to electrostatic repulsions with the other cationic groups. I2 also contains a primary amine (pK_a > 9) that generates a positive charge. The 3-hydroxypyridinone unit is able to lose one proton at basic pH, thus it is neutral under the pH of study. In the 4.5 - 6.5 pH range, the main species are $[H_2I1]^{2+}$, $[H_3I2]^{3+}$ and $[H_2I3]^{2+}$. Since the isoelectric point of PPO is placed around pH 4.5-5[84] certain repulsion between the PPO and the positive charges could be expected in particular at pH 4.5.

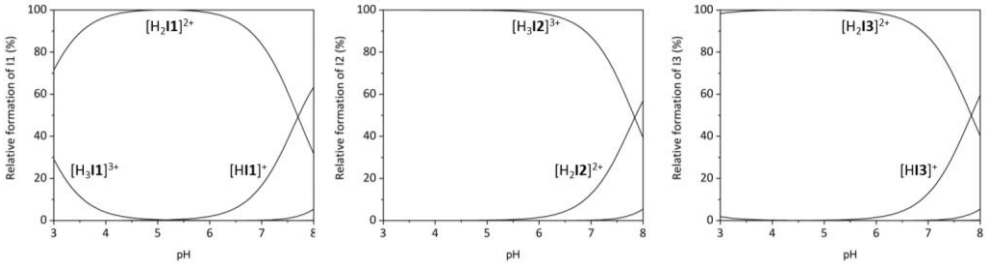

Figure 5.13. *Species distribution curves calculated for the aqueous solution of the inhibitor. Per cent values represent concentrations relative to the total amount of inhibitor at an initial value of 0.67 mM.*

However, the inhibition studies indicate that electrostatic repulsion is not the main factor. For I2 and I3 the percentage of PPO inhibition increases as the pH moves from 6.5 to 4.5, and I3, with an additional positive charge (+3) offer a degree of inhibition stronger than I2. By contrast, at pH 6.5 a minor concentration of the partially protonated compounds $[HI1]^{+}$, $[H_2I2]^{2+}$ and $[HI3]^{+}$ is present that could explain the slight reduction of inhibition found for I2 and I3 at this pH. These results suggest that the molecule interacts with the enzyme through complex interactions. In agreement with the behaviour observed for similar systems based on cyclic polyamines, an increment in the number of nitrogens improves the inhibition activity [77]. In any case, the most remarkable is that the pyrone group present in I1 quadruples the inhibitory activity (an 85% in comparison with the 21% of I3 at pH 6.5). Nevertheless, the macrocyclic cavity, although to a lesser degree compared to the pyrone, also exhibits an inhibitor effect.

Taken into account these results and in order to get a deeper insight, the pH 5.5 was selected because this pH is found in many fruits juices where PPO activity (around 85%) causes many browning problems[48].

3.3. Inhibition mechanisms of aza-macrocyclic compounds.

The Lineweaver-Burk plot was used to determine the kinetic parameters to identify the inhibition mechanism for each inhibitor (see Table 5.3).

The kinetics parameters for the control were, in the case of Michaelis-Menten constant, K_m = 1.52 mM and 0.26 mM min^{-1} for v_{max}. As expected, the reaction rate v_{max} of the PPO dramatically dropped in the presence of high concentrations of I1 (0.0157 mM min^{-1}) achieving almost a total inhibition. Besides, the Michaelis-Menten constant values also diminished progressively as increasing inhibitor concentration with statistically significant differences to the control.

Therefore, as the inhibitor favours binding to the enzyme-substrate complex the observed inhibition can be considered a mixed type non-competitive-uncompetitive inhibition [85]. The catalytic constant (K_{cat}) and the catalytic efficiency (K_{cat}/Km) of the enzyme also plummeted from values close to 1000 to values below 250 for both constants. In fact, the catalytic constant drops 94 % when the concentration of I1 in de medium is 1.5 mM implying that the efficiency of the enzyme is much lower in its presence. Same v_{max} and K_m parameters were found (with no statistical differences) for I2 at double concentration (1.50 mM) compared to those found for I1 at 0.65 mM. Although the type of inhibition is assumed to be the same (mixed type), it appears that the pyrone group offers an extra inhibition power that the amine group is not able to perform (see Table 5.3). However, I2 also achieves high inhibition over the PPO in the concentrations studied since it manages to reduce the catalytic constant of the enzyme (1350 min^{-1}) to almost half when the concentration is 0.67 mM. However, the last compound, I3, behaves differently, exhibiting a non-competitive inhibition over the PPO enzyme. The Michaelis−Menten constant maintains the values of the control when altering the inhibition concentration, yet the v_{max} drops off. Contrasted with the other two inhibitors, I3 is not able to perform a strong inhibition over the PPO, being necessary to double the concentration to perform an equal K_{cat} as I2.

Besides, the IC_{50} parameter for I2 and I3 is much higher than for I1 which was calculated at 0.30 mM. The IC_{50} value for I1 is worse than the one calculated for kojic acid under the same conditions (0.011 mM) [77]. Nevertheless, it is substantially better than the value found for other commonly used organic acids found in literature, such as citric (20 mM), cinnamic (2.10 mM), or benzoic acid (5.2 mM)[53,55,86]

Table 5.3. *Kinetic parameters and type of inhibition of the enzyme tyrosinase (94 U) in presence of the inhibitors at different concentrations.*

Compound (mM)		K_M[a](mM)	v_{max}[b] (mM min^{-1})	k_{cat}[c](min^{-1})	Catalytic efficiency[d] (mM^{-1} min^{-1})	IC_{50} (mM)	Inhibition type
Control		1.52^{*} ± 0.09	0.259 ± 0.014	1350 ± 80	888 ± 108		
I1	0.67	$1.02^{+\S}$ ± 0.07	0.064^{+} ± 0.003	329 ± 14	320 ± 40	0.30 ± 0.05 (0.18 mg/mL)	Mixed type
	1.50	0.33 ± 0.03	0.0157 ± 0.0008	81 ± 4	250 ± 30		
I2	0.67	$1.35^{*+¥}$ ± 0.19	0.151^{*} ± 0.008	780 ± 40	577 ± 108	0.79 ± 0.06 (0.45 mg/mL)	Mixed type
	1.50	$0.77^{\S}$ ± 0.08	0.035^{+} ± 0.003	178 ± 16	230 ± 50		
I3	0.67	1.85^{*} ± 0.08	0.222 ± 0.008	1140 ± 50	620 ± 50	1.82 ± 0.16 (0.81mg/mL)	Non-competitive
	1.50	$1.7^{*¥}$ ± 0.2	0.151^{*} ± 0.019	784 ± 108	460 ± 140		

[a] Michaelis-Menten constant. [b] Reaction rate. [c] Catalytic constant, $k_{cat}=v_{max}/[E]$. [d] Catalytic efficiency, calculated by k_{cat}/K_M. $^{*+\S¥}$ There are no statistically significant differences for p <0.05.

3.4. Browning inhibition of I1 on apple juice

Considering the good results obtained for I1 in model system studies with PPO, we further studied its anti-browning capacity in freshly apple juice as a real food system. It is also worth notice that preliminary studies of I1 with two cell lines, HeLa and ARPE-19, do not reveal any toxicity[79]. The liquified juice was mixed with two different concentration of I1 (1.12 mM and 2.25 mM) and the change of colour was followed over time. Figure 5.14 collects the colour differences (ΔE_{ab}^{*}) over time using the initial colour as reference. Once the apples liquefy, the enzymatic browning process begins quickly, and the colour change of the control (in absence of inhibitor) is well visible to the human eye in 5 minutes (ΔE_{ab}^{*}= 3). However, in presence of the inhibitor at 2.25 mM the colour barely changes being not noticeable.

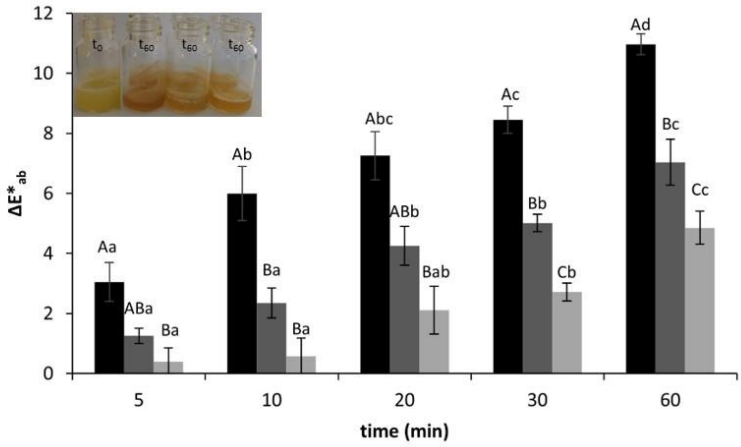

Figure 5.14. *Colour evolution in apple juice of control (black), in presence of 1.12 mM of I1 (grey) and 2.25 mM of I1 (light grey) over time. A-C: different letters indicate significant differences in ΔE_{ab}^{*} between I1 concentrations. a-c: different letters indicate significant differences between times ($p < 0.05$).*

At a lower concentration (1.12 mM), the inhibitor delayed the enzymatic browning reaching a noticeable change of colour with a ΔE_{ab}^{*} close to 2.5 at 10 minutes, similar to the control at 5 min.

Even though the speed of PPO decreased in presence of the inhibitor, the enzymatic browning reaction did not stop completely. The colour change in the juice treated with the lowest I1 concentration (1.12 mM) varies among the 40 and 65% when compared to the untreated sample at the same time. By raising the inhibitor concentration in the juice to 2.25 mM, the enzymatic browning is further delayed with a ΔE_{ab}^{*} of 0.6 after 10 min of stirring compared to 6.0 found for the control. The threshold of colour change to be qualified as "great" is trespassed within 10 minutes in absence of inhibitor and 60 min at 1.12 mM. However, it is not reached if a [I1] = 2.25 mM is used even after 1 hour of exposition to the air under stirring. When measuring the initial browning rate, values for the slope of 0.601, 0.219 and 0.084 ΔE_{ab}^{*} min^{-1} were calculated for the control and the juices containing 1.12 mM and 2.25 mM respectively ($R^2 > 0.95$). Thus, reductions in the initial enzymatic browning rate of an 86% can be observed in presence of [I1] equal to 2.25 mM.

3.5. Effect of I1 on total phenolic content (TPC) and and antioxidant capacity (DPPH·) on apple juice

Apple and their juices contain high concentrations of diverse phenolic compounds such as chlorogenic acid, gallic acid, catechin and quercetin, which are well known for their beneficial effects on human health[87]. Thus, the effect of the inhibitor over total phenolic content and antioxidant capacity (DPPH·) was measured.

As depicted in Figure 5.15, the initial content of total phenols was about 600 mg of GAE L^{-1} just after liquefying the apple which is in concordance with the range

presented in the literature for the same apple variety [88,89]. However, this value decreased significantly ($p < 0.05$) as time evolved progressively, reducing the content of phenols by almost 40% after 60 min of stirring. This trend was repeated when the samples were treated with 1.12 mM inhibitor, however, the degradation rate of phenol was slowed down and only 15% was lost after 60 minutes. Nonetheless, the decrease in the total phenolic content in the apple juice was stopped and remained stable after 60 min in presence of 2.25 mM of I1 ($p < 0.05$). The results also showed a good negative correlation (-0.756) between the TPC and enzymatic browning (ΔE_{ab}^{*}) for $p<0.05$, as expected by the oxidation of phenolic compounds used as PPO substrates. This correlation is stronger for the control (-0.926) than for the juices containing inhibitor (-0.636 for 1.12 mM and -0.266 for 2.25 mM). Suggesting that the PPO inhibition induced by I1 could be more intense than we can deduct from the enzymatic browning.

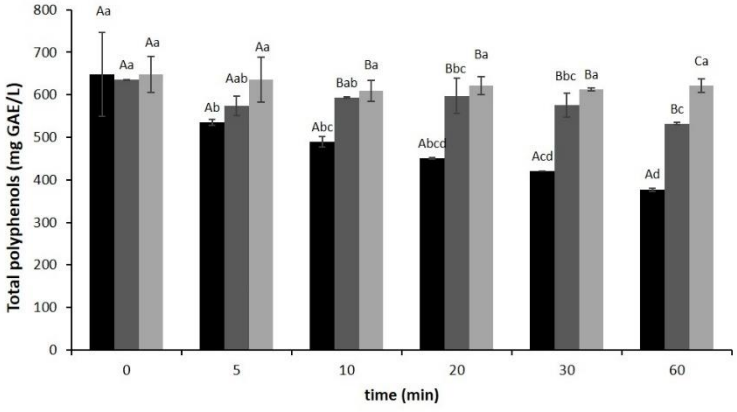

Figure 5.15. *Total phenol content of apple juice of control (black), in presence of 1.12 mM of I1 (grey) and 2.25 mM of I1 (light grey) during the time. A-C: different letters indicate significant differences in total polyphenols between concentrations. a-c: different letters indicate significant differences between times ($p < 0.05$).*

The antioxidant capacity measured with DPPH· can be found in Figure 5.16. As time increases and oxidation occurs, the antioxidant activity of freshly squeezed cloudy apple juice decreased significantly. When I1 is added, even though after 20 and 30 minutes this effect is significantly diminished, at longer times the loss of radical scavenging species is comparable to the control.

According to Pearson's correlations, the reduction in the antioxidant properties expressed by the DPPH· method is significantly correlated with enzymatic browning for the control (-0.931) and both concentrations of inhibitor (-0.871 for 1.12 mM and -0.906 for 2.25 mM). However, if we analyse the correlation with total phenolic content in the presence of 2.25 mM of I1 no significant correlation is found (0.139 $p > 0.05$). This behaviour can be explained by having in mind that the DPPH· assay measures not only phenols but also other compounds present in the apple juice such as vitamins (vitamin C and E), heteropolysaccharides and polypeptides. Similar results were found on fresh lettuce when testing citric acid and oxalic acid as inhibitors. Where no correlation was found between antioxidant activity and total phenolic content in presence of the inhibitors[90]. Besides, in a recently published article [83] the authors correlated the content of nine different phenolic compounds found in apple juice and the antioxidant activity determined by the DPPH· method. The study showed how significant positive correlations were only obtained for the content of caffeic acid and phlorizin for $p < 0.05$ (0.677 and 0.532 respectively). Although no correlation was found for either the chlorogenic acid or epicatechin, which were the most abundant phenolic compound besides the phlorizin in apple juice. Thus, the oxidation process in presence of I1 could damage more polyphenols such as caffeic acid that have more impact on the antioxidant activity than on the TPC.

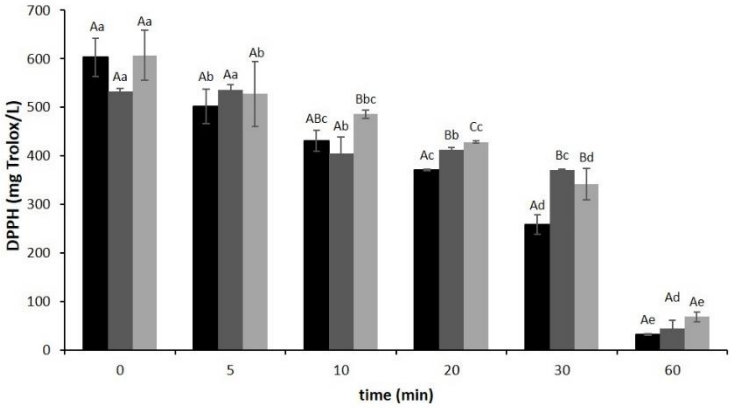

Figure 5.16. *Antioxidant activity (DPPH·) of apple juice of control (black), in presence of 1.12 mM of I1 (grey) and 2.25 mM of I1 (light grey) during the time. A-C: different letters indicate significant differences in DPPH between I1 concentrations. a-c: different letters indicate significant differences between times ($p < 0.05$).*

4. CONCLUSION

The effect on the PPO enzyme of three different azamacrocyclic inhibitors has been tested. The inhibition studies at different pHs suggest that the interaction with the PPO enzyme is not due to electrostatic forces but through other complex interactions. Besides, the presence of hydroxypyridinone attached to the macrocycle was relevant to enhance the inhibitor power especially at pH 5.5 and 6.5. Kinetic studies denote a mixed type of inhibition of I1 with an IC_{50} (0.30 mM) much higher than the one calculated for I2 and I3. The inhibitory activity of I1 was validated on freshly obtained apple juice as a real food system. The inhibitor can reduce the enzymatic browning by more than 50% and the decrease in total phenolic content in apple juice was stopped r when used 2.25 mM. Furthermore, I1 delays, at least during the first 30 min, the antioxidant capacity measured with DPPH.

REFERENCES OF THE CHAPTER 1

(1) Schneider, H.-J. Introduction and Overview. In *Applications of Supramolecular Chemistry*; CRC Press, 2012; pp 14–23.

(2) Steed, J. W.; Atwood, J. L.; Gale, P. A. Definition and Emergence of Supramolecular ChemistryAdapted in Part from Supramolecular Chemistry , J. W. Steed and J. L. Atwood, Wiley: Chichester, 2nd Ed., 2009. In *Supramolecular Chemistry*; John Wiley & Sons, Ltd: Chichester, UK, 2012; pp 3–8.

(3) Yu, G.; Chen, X. Host–Guest Chemistry in Supramolecular Theranostics. *Theranostics* **2019**, *9* (11), 3041–3074.

(4) Steed, J. W.; Atwood, J. L. *Supramolecular Chemistry: Second Edition*; John Wiley and Sons: Chichester, UK, 2009.

(5) Zakharova, L.; Mirgorodskaya, A.; Gaynanova, G.; Kashapov, R.; Pashirova, T.; Vasilieva, E.; Zuev, Y.; Synyashin, O. Supramolecular Strategy of the Encapsulation of Low-Molecular-Weight Food Ingredients. In *Encapsulations*; Elsevier, 2016; pp 295–362.

(6) Buschmann, H.-J. Applications in the Food and Textile Industries. In *Applications of Supramolecular Chemistry*; Schneider, H.-J., Ed.; 2012; pp 417–429.

(7) Pedersen, C. J. Cyclic Polyethers and Their Complexes with Metal Salts. *J. Am. Chem. Soc.* **1967**, *89* (26), 7017–7036.

(8) Ariga, K.; Kunitake, T. The Chemistry of Molecular Recognition — Host Molecules and Guest Molecules. In *Supramolecular Chemistry — Fundamentals and Applications*; Springer-Verlag, 2006; pp 7–44.

(9) Mewis, R. E.; Archibald, S. J. Biomedical Applications of Macrocyclic Ligand Complexes. *Coord. Chem. Rev.* **2010**, *254* (15–16), 1686–1712.

(10) Renard, I.; Archibald, S. J. CXCR4-Targeted Metal Complexes for Molecular Imaging. In *Advances in Inorganic Chemistry*; Academic Press Inc., 2020; Vol. 75, pp 447–476.

(11) Moreno-Mañas, M.; Pleixats, R.; Sebastián, R. M.; Vallribera, A.; Roglans, A. Organometallic Chemistry of 15-Membered Tri-Olefinic Macrocycles: Catalysis by Palladium(0) Complexes in Carbon-Carbon Bond-Forming Reactions. *J. Organomet. Chem.* **2004**, *689* (23), 3669–3684.

(12) Stackhouse, C. A.; Ma, S. Azamacrocyclic-Based Metal Organic Frameworks: Design Strategies and Applications. *Polyhedron*. Elsevier Ltd May 1, 2018, pp 154–165.

(13) Mapuskar, K. A.; Anderson, C. M.; Spitz, D. R.; Batinic-Haberle, I.; Allen, B. G.; E. Oberley-Deegan, R. Utilizing Superoxide Dismutase Mimetics to Enhance Radiation Therapy Response While Protecting Normal Tissues. *Semin. Radiat. Oncol.* **2019**, *29* (1), 72–80.

(14) Muscoli, C.; Cuzzocrea, S.; Riley, D. P.; Zweier, J. L.; Thiemermann, C.; Wang, Z. Q.; Salvemini, D. On the Selectivity of Superoxide Dismutase Mimetics and Its Importance in Pharmacological Studies. *Br. J. Pharmacol.* **2003**, *140* (3), 445–460.

(15) Marín, C.; Inclán, M.; Ramírez-Macías, I.; Albelda, M. T.; Cañas, R.; Clares, M. P.; González-García, J.; Rosales, M. J.; Urbanova, K.; García-España, E.; et al. In Vitro Antileishmanial Activity of Aza-Scorpiand Macrocycles. Inhibition of the Antioxidant Enzyme Iron Superoxide Dismutase. *RSC Adv.* **2016**, *6* (21), 17446–17455.

(16) Olmo, F.; Clares, M. P.; Marín, C.; González, J.; Inclán, M.; Soriano, C.; Urbanová, K.; Tejero, R.; Rosales, M. J.; Krauth-Siegel, R. L.; et al. Synthetic Single and Double Aza-Scorpiand Macrocycles Acting as Inhibitors of the Antioxidant Enzymes Iron Superoxide Dismutase and Trypanothione Reductase in Trypanosoma Cruzi with Promising Results in a Murine Model. *RSC Adv.* **2014**, *4* (110), 65108–65120.

(17) Simpson, B. K. *Food Biochemistry and Food Processing*; Wiley-Blackwell, 2012.

(18) İyidoğan, N. F.; Bayındırlı, A. Effect of L-Cysteine, Kojic Acid and 4-Hexylresorcinol Combination on Inhibition of Enzymatic Browning in Amasya Apple Juice. *J. Food Eng.* **2004**, *62* (3), 299–304.

(19) Croguennec, T. Enzymatic Browning. In *Handbook of Food Science and Technology 1*; John Wiley & Sons, Inc.: Hoboken, NJ, USA, 2016; pp 159–181.

(20) Brütsch, L.; Rugiero, S.; Serrano, S. S.; Städeli, C.; Windhab, E. J.; Fischer, P.; Kuster, S. Targeted Inhibition of Enzymatic Browning in Wheat Pastry Dough. *J. Agric. Food Chem.* **2018**, *66* (46), 12353–12360.

(21) Ma, L.; Zhang, M.; Bhandari, B.; Gao, Z. Recent Developments in Novel Shelf Life Extension Technologies of Fresh-Cut Fruits and Vegetables. *Trends Food Sci. Technol.* **2017**, *64*, 23–38.

(22) Queiroz, C.; Mendes Lopes, M. L.; Fialho, E.; Valente-Mesquita, V. L. Polyphenol Oxidase: Characteristics and Mechanisms of Browning Control. *Food Rev. Int.* **2008**, *24* (4), 361–375.

(23) Marshall, M.; Kim, J.; Wei, C. Enzymatic Browning in Fruits, Vegetables and Seafoods. *Food Agric. Organ.* **2000**, *41*, 259–312.

(24) Seo, S.-Y.; Sharma, V. K.; Sharma, N. Mushroom Tyrosinase: Recent

Prospects. *J. Agric. Food Chem.* **2003**, *51* (10), 2837–2853.

(25) Tronc, J.-S.; Lamarche, F.; Makhlouf, J. Enzymatic Browning Inhibition in Cloudy Apple Juice by Electrodialysis. *J. Food Sci.* **1997**, *62* (1), 75–78.

(26) Jiang, S.; Penner, M. H. The Nature of β-Cyclodextrin Inhibition of Potato Polyphenol Oxidase-Catalyzed Reactions. *Food Chem.* **2019**, *298*, 125004.

(27) Buckow, R.; Kastell, A.; Terefe, N. S.; Versteeg, C. Pressure and Temperature Effects on Degradation Kinetics and Storage Stability of Total Anthocyanins in Blueberry Juice. *J. Agric. Food Chem.* **2010**, *58* (18), 10076–10084.

(28) Massini, L.; Rico, D.; Martin-Diana, A. B. Quality Attributes of Apple Juice: Role and Effect of Phenolic Compounds. In *Fruit Juices*; Rajauria, G., Tiwari, B. K., Eds.; Academic Press, 2018; pp 45–57.

(29) McEvily, A. J.; Iyengar, R.; Otwell, W. S. Inhibition of Enzymatic Browning in Foods and Beverages. *Crit. Rev. Food Sci. Nutr.* **1992**, *32* (3), 253–273.

(30) Iyengar, R.; McEvily, A. J. Anti-Browning Agents: Alternatives to the Use of Sulfites in Foods. *Trends Food Sci. Technol.* **1992**, *3*, 60–64.

(31) Muñoz-Pina, S.; Ros-Lis, J. V.; Argüelles, Á.; Coll, C.; Martínez-Máñez, R.; Andrés, A. Full Inhibition of Enzymatic Browning in the Presence of Thiol-Functionalised Silica Nanomaterial. *Food Chem.* **2018**, *241*, 199–205.

(32) Muñoz-Pina, S.; Ros-Lis, J. V.; Argüelles, Á.; Martínez-Máñez, R.; Andrés, A. Influence of the Functionalisation of Mesoporous Silica Material UVM-7 on Polyphenol Oxidase Enzyme Capture and Enzymatic Browning. *Food Chem.* **2020**, *310*, 125741.

(33) Fraschetti, C.; Filippi, A.; Crestoni, M. E.; Marcantoni, E.; Glucini, M.; Guarcini, L.; Montagna, M.; Guidoni, L.; Speranza, M. Protonated Hexaazamacrocycles

as Selective K Receptors. *J. Am. Soc. Mass Spectrom.* **2015**, *26* (7), 1186–1190.

(34) Yu, X.; Zhang, J. *Macrocyclic Polyamines : Synthesis and Applications*; WILEY-VCH Verlag, 2017.

(35) Castillo, C. E.; Máñez, M. A.; Basallote, M. G.; Clares, M. P.; Blasco, S.; García-España, E. Copper (II) Complexes of Quinoline Polyazamacrocyclic Scorpiand-Type Ligands: X-Ray, Equilibrium and Kinetic Studies. *Dalt. Trans.* **2012**, *41* (18), 5617.

(36) Santra, S.; Mukherjee, S.; Bej, S.; Saha, S.; Ghosh, P. Amino-Ether Macrocycle That Forms Cu ^{II} Templated Threaded Heteroleptic Complexes: A Detailed Selectivity, Structural and Theoretical Investigations. *Dalt. Trans.* **2015**, *44* (34), 15198–15211.

(37) Malthus, S. J.; Wilson, R. K.; Vikas Aggarwal, A.; Cameron, S. A.; Larsen, D. S.; Brooker, S. Carbazole-Based N 4 -Donor Schiff Base Macrocycles: Obtained Metal Free and as Cu (II) and Ni (II) Complexes. *Dalt. Trans.* **2017**, *46* (10), 3141–3149.

(38) Fan, R.; Serrano-Plana, J.; Oloo, W. N.; Draksharapu, A.; Delgado-Pinar, E.; Company, A.; Martin-Diaconescu, V.; Borrell, M.; Lloret-Fillol, J.; García-España, E.; et al. Spectroscopic and DFT Characterization of a Highly Reactive Nonheme FeV-Oxo Intermediate. *J. Am. Chem. Soc.* **2018**, *140* (11), 3916–3928.

(39) Lincoln, K. M.; Gonzalez, P.; Richardson, T. E.; Julovich, D. A.; Saunders, R.; Simpkins, J. W.; Green, K. N. A Potent Antioxidant Small Molecule Aimed at Targeting Metal-Based Oxidative Stress in Neurodegenerative Disorders. *Chem. Commun.* **2013**, *49* (26), 2712–2714.

(40) Martínez-Camarena, Á.; Liberato, A.; Delgado-Pinar, E.; Algarra, A. G.; Pitarch-Jarque, J.; Llinares, J. M.; Mañez, M. Á.; Domenech-Carbó, A.; Basallote, M. G.; García-España, E. Coordination Chemistry of Cu $^{2+}$ Complexes of Small N-Alkylated Tetra-Azacyclophanes with SOD Activity. *Inorg. Chem.* **2018**, *57* (17), 10961–10973.

(41) Algarra, A. G.; Basallote, M. G.; Belda, R.; Blasco, S.; Castillo, C. E.; Llinares, J. M.; García-España, E.; Gil, L.; Máñez, M. Á.; Soriano, C.; et al. Synthesis, Protonation and Cu ^{II} Complexes of Two Novel Isomeric Pentaazacyclophane Ligands: Potentiometric, DFT, Kinetic and AMP Recognition Studies. *Eur. J. Inorg. Chem.* **2009**, *2009* (1), 62–75.

(42) Díaz, P.; Basallote, M. G.; Máñez, M. A.; García-España, E.; Gil, L.; Latorre, J.; Soriano, C.; Verdejo, B.; Luis, S. V. Thermodynamic and Kinetic Studies on the Cu (II) Coordination Chemistry of a Novel Binucleating Pyridinophane Ligand. *Dalt. Trans.* **2003**, No. 6, 1186–1193.

(43) Basallote, M. G.; Doménech, A.; Ferrer, A.; García-España, E.; Llinares, J. M.; Máñez, M. A.; Soriano, C.; Verdejo, B. Synthesis and Cu(II) Coordination of Two New Hexaamines Containing Alternated Propylenic and Ethylenic Chains: Kinetic Studies on PH-Driven Metal Ion Slippage Movements. *Inorganica Chim. Acta* **2006**, *359* (7), 2004–2014.

(44) Acosta-Rueda, L.; Delgado-Pinar, E.; Pitarch-Jarque, J.; Rodríguez, A.; Blasco, S.; González, J.; Basallote, M. G.; García-España, E. Correlation between the Molecular Structure and the Kinetics of Decomposition of Azamacrocyclic Copper(II) Complexes. *Dalt. Trans.* **2015**, *44* (17), 8255–8266.

(45) Alarcón, J.; Albelda, M. T.; Belda, R.; Clares, M. P.; Delgado-Pinar, E.; Frías, J. C.; García-España, E.; González, J.; Soriano, C. Synthesis and Coordination

Properties of an Azamacrocyclic Zn(II) Chemosensor Containing Pendent Methylnaphthyl Groups. *Dalt. Trans.* **2008**, No. 46, 6530–6538.

(46) Clares, M. P.; Aguilar, J.; Aucejo, R.; Lodeiro, C.; Albelda, M. T.; Pina, F.; Lima, J. C.; Parola, A. J.; Pina, J.; Seixas de Melo, J.; et al. Synthesis and H^{+}, Cu^{2+}, and Zn^{2+} Coordination Behavior of a Bis(Fluorophoric) Bibrachial Lariat Aza-Crown. *Inorg. Chem.* **2004**, *43* (19), 6114–6122.

(47) Siddiq, M.; Dolan, K. D. Characterization and Heat Inactivation Kinetics of Polyphenol Oxidase from Blueberry (Vaccinium Corymbosum L.). *Food Chem.* **2017**, *218*, 216–220.

(48) Munjal, N.; Sawhney, S. . Stability and Properties of Mushroom Tyrosinase Entrapped in Alginate, Polyacrylamide and Gelatin Gels. *Enzyme Microb. Technol.* **2002**, *30* (5), 613–619.

(49) Vermeer, L. M.; Higgins, C. A.; Roman, D. L.; Doorn, J. A. Real-Time Monitoring of Tyrosine Hydroxylase Activity Using a Plate Reader Assay. *Anal. Biochem.* **2013**, *432* (1), 11–15.

(50) Espín, J. C.; Varón, R.; Fenoll, L. G.; Gilabert, M. A.; García-Ruíz, P. A.; Tudela, J.; García-Cánovas, F. Kinetic Characterization of the Substrate Specificity and Mechanism of Mushroom Tyrosinase. *Eur. J. Biochem.* **2000**, *267* (5), 1270–1279.

(51) Doran, P. M. *Principios de Ingeniería de Los Bioprocesos*; Acribia, 1998.

(52) Marcantoni, E.; Petrini, M. Recent Developments in the Stereoselective Synthesis of Nitrogen-Containing Heterocycles Using *N* -Acylimines as Reactive Substrates. *Adv. Synth. Catal.* **2016**, *358* (23), 3657–3682.

(53) Liu, W.; Zou, L.; Liu, J.; Zhang, Z.; Liu, C.; Liang, R. The Effect of Citric Acid on

the Activity, Thermodynamics and Conformation of Mushroom Polyphenoloxidase. *Food Chem.* **2013**, *140* (1–2), 289–295.

(54) Son, S. M.; Moon, K. D.; Lee, C. Y. Kinetic Study of Oxalic Acid Inhibition on Enzymatic Browning. *J. Agric. Food Chem.* **2000**, *48* (6), 2071–2074.

(55) Öz, F.; Colak, A.; Özel, A.; Sağlam Ertunga, N.; Sesli, E. Purification And Characterization Of A Mushroom Polyphenol Oxidase And Its Activity In Organic Solvents. *J. Food Biochem.* **2013**, *37* (1), 36–44.

(56) Ayaz, F. A.; Demir, O.; Torun, H.; Kolcuoglu, Y.; Colak, A. Characterization of Polyphenoloxidase (PPO) and Total Phenolic Contents in Medlar (Mespilus Germanica L.) Fruit during Ripening and over Ripening. *Food Chem.* **2008**, *106* (1), 291–298.

(57) Harvey, R. A.; Ferrier, D. R. *Biochemistry*, 5th ed.; Wolters Kluwer Health/Lippincott Williams & Wilkins, 2011.

(58) Fromm, H. J. Chapter 10: Reversible Enzyme Inhibitors as Mechanistic Probes. In *Contemporary enzyme kinetics and mechanism: Reliable Lab Solutions*; Purich, D. L., Ed.; Elsevier/Academic Press: Ney York, 2009; pp 279–302.

(59) Segel, I. H. *Enzyme Kinetics : Behavior and Analysis of Rapid Equilibrium and Steady State Enzyme Systems*; Wiley Classics Library: New York, 1993.

(60) Qin, X.-Y.; Lee, J.; Zheng, L.; Yang, J.-M.; Gong, Y.; Park, Y.-D. Inhibition of α-Glucosidase by 2-Thiobarbituric Acid: Molecular Dynamics Simulation Integrating Parabolic Noncompetitive Inhibition Kinetics. *Process Biochem.* **2018**, *65*, 62–70.

(61) Chakrabarty, S. P.; Ramapanicker, R.; Mishra, R.; Chandrasekaran, S.; Balaram, H. Development and Characterization of Lysine Based Tripeptide

Analogues as Inhibitors of Sir2 Activity. *Bioorg. Med. Chem.* **2009**, *17* (23), 8060–8072.

(62) Gou, L.; Lee, J.; Yang, J.-M.; Park, Y.-D.; Zhou, H.-M.; Zhan, Y.; Lü, Z.-R. Inhibition of Tyrosinase by Fumaric Acid: Integration of Inhibition Kinetics with Computational Docking Simulations. *Int. J. Biol. Macromol.* **2017**, *105*, 1663–1669.

(63) Tang, H.; Cui, F.; Li, H.; Huang, Q.; Li, Y. Understanding the Inhibitory Mechanism of Tea Polyphenols against Tyrosinase Using Fluorescence Spectroscopy, Cyclic Voltammetry, Oximetry, and Molecular Simulations. *RSC Adv.* **2018**, *8* (15), 8310–8318.

(64) Dewey, T. G. *Biophysical and Biochemical Aspects of Fluorescence Spectroscopy*; Plenum Press, 1991.

(65) Gou, L.; Lee, J.; Hao, H.; Park, Y.-D.; Zhan, Y.; Lü, Z.-R. The Effect of Oxaloacetic Acid on Tyrosinase Activity and Structure: Integration of Inhibition Kinetics with Docking Simulation. *Int. J. Biol. Macromol.* **2017**, *101*, 59–66.

(66) Aksoy, M. A New Insight into Purification of Polyphenol Oxidase and Inhibition Effect of Curcumin and Quercetin on Potato Polyphenol Oxidase. *Protein Expr. Purif.* **2020**, *171*, 105612.

(67) Es-Safi, N.-E.; Eronique Cheynier, V.; Moutounet, M. Implication of Phenolic Reactions in Food Organoleptic Properties. *J. Food Compos. Anal.* **2003**, *16*, 535–553.

(68) Derardja, A. eddine; Pretzler, M.; Kampatsikas, I.; Barkat, M.; Rompel, A. Inhibition of Apricot Polyphenol Oxidase by Combinations of Plant Proteases and Ascorbic Acid. *Food Chem. X* **2019**, *4*.

(69) Moon, K. M.; Kwon, E. Bin; Lee, B.; Kim, C. Y. Recent Trends in Controlling the Enzymatic Browning of Fruit and Vegetable Products. *Molecules* **2020**, *25* (12).

(70) Kanteev, M.; Goldfeder, M.; Fishman, A. Structure-Function Correlations in Tyrosinases. *Protein Sci.* **2015**, *24* (9), 1360–1369.

(71) Bortolini, D. G.; Benvenutti, L.; Demiate, I. M.; Nogueira, A.; Alberti, A.; Zielinski, A. A. F. A New Approach to the Use of Apple Pomace in Cider Making for the Recovery of Phenolic Compounds. *LWT* **2020**, *126*, 109316.

(72) Martino, E.; Vuoso, D. C.; D'Angelo, S.; Mele, L.; D'Onofrio, N.; Porcelli, M.; Cacciapuoti, G. Annurca Apple Polyphenol Extract Selectively Kills MDA-MB-231 Cells through ROS Generation, Sustained JNK Activation and Cell Growth and Survival Inhibition. *Sci. Rep.* **2019**, *9* (1), 1–15.

(73) Bondonno, N. P.; Bondonno, C. P.; Ward, N. C.; Hodgson, J. M.; Croft, K. D. The Cardiovascular Health Benefits of Apples: Whole Fruit vs. Isolated Compounds. *Trends in Food Science and Technology*. Elsevier Ltd November 1, 2017, pp 243–256.

(74) Tinello, F.; Lante, A. Recent Advances in Controlling Polyphenol Oxidase Activity of Fruit and Vegetable Products. *Innov. Food Sci. Emerg. Technol.* **2018**, *50*, 73–83.

(75) Zolghadri, S.; Bahrami, A.; Hassan Khan, M. T.; Munoz-Munoz, J.; Garcia-Molina, F.; Garcia-Canovas, F.; Saboury, A. A. A Comprehensive Review on Tyrosinase Inhibitors. *J. Enzyme Inhib. Med. Chem.* **2019**, *34* (1), 279–309.

(76) Sapers, G. M. Chitosan Enhances Control of Enzymatic Browning in Apple and Pear Juice by Filtration. *J. Food Sci.* **1992**, *57* (5), 1192–1193.

(77) Muñoz-Pina, S.; Ros-Lis, J. V.; Delgado-Pinar, E. A.; Martı Nez-Camarena, A.; Verdejo, B.; Garcı A-España, E.; Argüelles, Á.; Andrés, A. Inhibitory Effect of Azamacrocyclic Ligands on Polyphenol Oxidase in Model and Food Systems. *J. Agric. Food Chem.* **2020**, *68* (30), 7964–7973.

(78) Verdejo, B.; Ferrer, A.; Blasco, S.; Castillo, C. E.; González, J.; Latorre, J.; Máñez, M. A.; Basallote, M. G.; Soriano, C.; García-España, E. Hydrogen and Copper Ion-Induced Molecular Reorganizations in Scorpionand-like Ligands. A Potentiometric, Mechanistic, and Solid-State Study. *Inorg. Chem.* **2007**, *46* (14), 5707–5719.

(79) López-Martínez, L. M.; Pitarch-Jarque, J.; Martínez-Camarena, À.; García-España, E.; Tejero, R.; Santacruz-Ortega, H.; Navarro, R. E.; Sotelo-Mundo, R. R.; Leyva-Peralta, M. A.; Doménech-Carbó, A.; et al. Synthesis, Characterization, and Cu2+ Coordination Studies of a 3-Hydroxy-4-Pyridinone Aza Scorpiand Derivative. *Inorg. Chem.* **2016**, *55* (15), 7564–7575.

(80) Xiang, Q.; Fan, L.; Zhang, R.; Ma, Y.; Liu, S.; Bai, Y. Effect of UVC Light-Emitting Diodes on Apple Juice: Inactivation of Zygosaccharomyces Rouxii and Determination of Quality. *Food Control* **2020**, *111*, 107082.

(81) Aranibar, C.; Pigni, N. B.; Martinez, M.; Aguirre, A.; Ribotta, P.; Wunderlin, D.; Borneo, R. Utilization of a Partially-Deoiled Chia Flour to Improve the Nutritional and Antioxidant Properties of Wheat Pasta. *LWT - Food Sci. Technol.* **2018**, *89*, 381–387.

(82) Andrew L Waterhouse. Determination of Total Phenolics. In *Current protocols in food analytical chemistry*; John Wiley & Sons, Inc., 2002; Vol. 6, p I1.1.1-I1.1.8.

(83) Wu, C.; Li, T.; Qi, J.; Jiang, T.; Xu, H.; Lei, H. Effects of Lactic Acid Fermentation-

Based Biotransformation on Phenolic Profiles, Antioxidant Capacity and Flavor Volatiles of Apple Juice. *LWT* **2020**, *122*, 109064.

(84) Fan, Y.; Flurkey, W. H. Purification and Characterization of Tyrosinase from Gill Tissue of Portabella Mushrooms. *Phytochemistry* **2004**, *65* (6), 671–678.

(85) Palmer, T.; Bonner, P. L. Enzyme Inhibition. In *Enzymes*; Elsevier, 2011; pp 126–152.

(86) Shi, Y.; Chen, Q. X.; Wang, Q.; Song, K. K.; Qiu, L. Inhibitory Effects of Cinnamic Acid and Its Derivatives on the Diphenolase Activity of Mushroom (Agaricus Bisporus) Tyrosinase. *Food Chem.* **2005**, *92* (4), 707–712.

(87) Barreira, J. C. M.; Arraibi, A. A.; Ferreira, I. C. F. R. Bioactive and Functional Compounds in Apple Pomace from Juice and Cider Manufacturing: Potential Use in Dermal Formulations. *Trends in Food Science and Technology*. Elsevier Ltd August 1, 2019, pp 76–87.

(88) Suárez-Jacobo, Á.; Rüfer, C. E.; Gervilla, R.; Guamis, B.; Roig-Sagués, A. X.; Saldo, J. Influence of Ultra-High Pressure Homogenisation on Antioxidant Capacity, Polyphenol and Vitamin Content of Clear Apple Juice. *Food Chem.* **2011**, *127* (2), 447–454.

(89) Sauceda-Gálvez, J. N.; Codina-Torrella, I.; Martínez-García, M.; Hernández-Herrero, M. M.; Gervilla, R.; Roig-Sagués, A. X. Combined Effects of Ultra-High Pressure Homogenization and Short-Wave Ultraviolet Radiation on the Properties of Cloudy Apple Juice. *LWT* **2020**, *136*, 110286.

(90) Altunkaya, A.; Gökmen, V. Effect of Various Inhibitors on Enzymatic Browning, Antioxidant Activity and Total Phenol Content of Fresh Lettuce (Lactuca Sativa). *Food Chem.* **2008**, *107* (3), 1173–1179.

CHAPTER 2: Mesoporous silica particles for PPO inhibition

PAPER 3

Muñoz-Pina, S. et al. (2018). Full inhibition of enzymatic browning in the presence of thiol-functionalised silica nanomaterial. *Food chemistry*, 241, 199-205.

PAPER 4

Muñoz-Pina, S. et al. (2020). Influence of the functionalisation of mesoporous silica material UVM-7 on polyphenol oxidase enzyme capture and enzymatic browning. *Food chemistry*, 310, 125741.

PAPER 5

Muñoz-Pina, S. et al. (2021). Bioactive compounds and enzymatic browning inhibition in cloudy apple juice by a new magnetic UVM-7-SH mesoporous material (under preparation).

Nanotechnology has opened new research areas in many fields such as medicine, physics, material science, pharmacology, and also the food industry[1]. Focusing on the food industry, nanotechnology has been implanted more often on the bioactive compounds encapsulations or in the designing of active packaging but applications in industrial processes are still scarce.

Among all the possible inorganic material options, silica-based materials present several advantages including specific manufacturing technique, high stability, robustness, and ease of modification[2]. In the food industry, silica oxide materials are allowed as an additive (E551) which is mainly used as an anti-caking agent, food pigment, or health supplements[3].

It was not until 1990 that it was described the first porous silica material with uniform pore size called folder sheet mesoporous material[4]. Two years later, researchers of the Mobil Company reported the synthesis of a family of mesoporous silica materials called M41S with different pore geometry[5]. Since then, the development of new types of mesoporous silica materials with different applications has grown exponentially.

Mesoporous silica particles (MSPs) are structures chemically composed of silicon dioxide (SiO_2) with a pore diameter in the range between 2 and 50 nm[6]. The order in which these structural pores are distributed gives rise to the different types of mesoporous materials. Apart from the mesopores, these particles present a high specific surface area (>700 m^2/g) and large specific pore volume (>0.6 cm^3/g)[7]. Furthermore, both structure and morphology of these materials are easily modifying through the synthesis parameters allowing to create new materials at request[8]. The siliceous structure also provides the material with thermal and chemical stability as well as minor toxicity and low cost[9]. Regarding the biocompatibility of the MSPs, although it is a difficult issue to evaluate since many factors influence, the range in

size is a key point. Whereas small MSPs can penetrate biological membranes and be distributed in the body, larger particles cannot and are well tolerated and excreted by the organism. Thus, these are preferred in food research[10].

The current synthetic methodology most used is based on sol-gel reaction where there are two main elements: a) the surfactant, whose function is to form a structure-directing template and build a high ordered porous net; b) the silica precursor, which after hydrolysis and condensation upon the template polymerises becoming the final rigid material[11]. In a typical example, the reaction starts after the surfactant micelle is formed in an aqueous solution (e.g., cylindrical when using N-cetyltrimethylammonium bromide, CTABr). Then, the precursor (e.g., tetraethyl orthosilicate, TEOS) is added and starts to hydrolyse and polymerise around the micelles. Finally, the surfactant is removed either by extraction or under calcination leaving cylindrical empty channels of approximately 3 nm in diameter (using CTABr) arranged in a hexagonal distribution (see Figure 5.17).

As stated before, changes in the synthesis route (pH, type of surfactant, concentration, temperature, silica precursor, solvent, etc.) lead to infinity of materials with different morphologies and porosities[12]. Furthermore, chelator agents ($TEAH_3$) can be added during the synthesis to harmonize the hydrolysis and condensation rates of the precursor modifying the final size of the material[13].

In literature, it is easy to find many mesoporous silica materials with different mesoporous sizes, pores distribution, particle size, shape, or density. Some of them are Mobil Composition of Matter No. 41 (MCM-41)[5], Santa Barbara amorphous silica (SBA-15)[14], Universidad Valencia material (UVM-7)[15], or anionic-templated mesoporous silica material (AMS-6)[16].

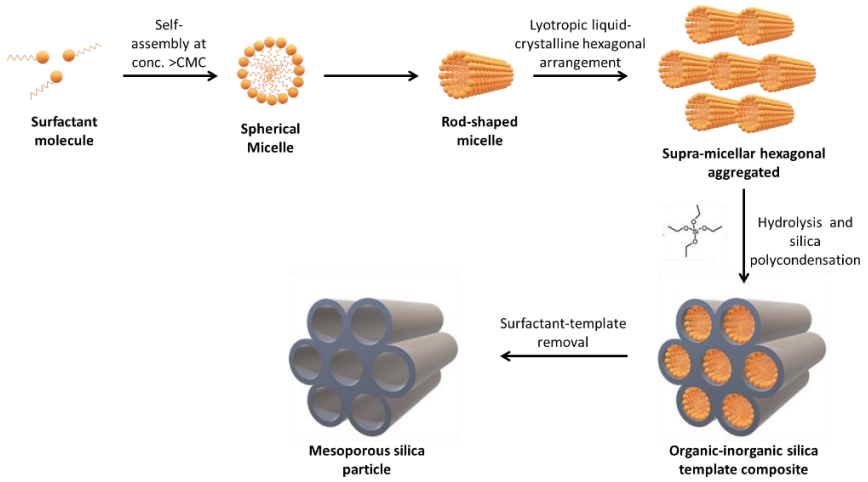

Figure 5.17. *Schematic representation of the synthesis of mesoporous silica-based materials with ordered hexagonal porous structure (e.g., MCM41).*

Apart from the physical characteristics of the materials, the MSPs surface is full of silanol groups (Si-OH) which can easily react with organo-alkoxysilanes ($(R´O)_3$-Si-R) generating organic-inorganic hybrids materials (Si-O-Si-R)[17]. Currently, there is a wide variety of organosilanes with different physicochemical properties (anions, cations, neutral molecules, etc.), which allow us to develop materials with specific functionalities for each application.

With so many options provided by these materials, is not unexpected that they have been employed in wildly different applications. From developing several sensors (pesticides, mercury, etc.)[18] to delivery systems (drugs, bioactive compounds, etc.)[19], or even for food preservation in packaging or as liquid disinfection systems[20]. Regarding its application in enzymology, they have been mainly used for enzyme immobilization and so enhance their enzymatic activity, and their pH-temperature stability[21]. Although this technology has been barely studied to inactivate enzymes, and in particular the PPO, their unique features make them excellent candidates for developing new anti-browning agents.

PAPER 3: FULL INHIBITION OF ENZYMATIC BROWNING IN THE PRESENCE OF THIOL-FUNCTIONALISED SILICA NANOMATERIAL

FULL INHIBITION OF ENZYMATIC BROWNING IN THE PRESENCE OF THIOL-FUNCTIONALISED SILICA NANOMATERIAL

Sara Muñoz-Pina[1], José V. Ros-Lis[2]*, Ángel Argüelles[1], Carmen Coll[3,4], Ramón Martínez-Máñez[3,4], Ana Andrés[1]

[1] Instituto Universitario de Ingeniería de Alimentos para el Desarrollo (IUIAD-UPV). Universitat Politècnica de València Camino de Vera s/n, 46022, Valencia, Spain

[2] Inorganic Chemistry Department, Universitat de València. 46100, Burjassot, Valencia Spain.

[3] Instituto Interuniversitario de Investigación de Reconocimiento Molecular y Desarrollo Tecnológico. Universitat Politècnica de València - Universitat de València. Camino de Vera s/n, 46022, Valencia, Spain.

[4] CIBER de Bioingeniería, Biomateriales y Nanomedicina (CIBER-BBN).

SUMMARY

The first work of chapter 2 of this thesis explores different types of mesoporous silica materials in order to evaluate their possible use as anti-browning agent and polyphenol oxidase inhibitor.

In the food industry, one of the main problems responsible for the high waste each year is the change of colour occasioned on fruits, vegetables, and their juices by the enzymatic browning. Thus, the industry has tried to mitigate this effect by inactivating the PPO, either using physical treatments like pasteurization or chemical treatments such as sulphites. Nevertheless, these treatments present several drawbacks as altering some of their nutritional parameters or even induction of allergic reactions. In this context, mesoporous silica materials could be also used

as potential application in industrial processes as inhibitors of the PPO. The high variety existing of mesoporous materials with different sizes, pores, and structural properties, makes them ideal for hosting and interacting with enzymes. Besides, these materials have the ability to functionalize their surface by attaching diverse chemical groups depending on the application. Although some of these materials have been proved to immobilise various enzymes, they have been not studied as a strategy to avoid enzymatic browning yet.

Thus, the present work focuses on the evaluation of the four silica mesoporous materials as PPO inhibitors, first on a model system and secondly on a fresh apple juice. In this sense, apple juice was selected for the study since apples are one of the most produced and consumed fruits globally. Besides, they contain high levels of phenolic compounds (hydroxycinnamic acids and flavan-3-ols among others) making them highly susceptible to enzymatic browning.

The four materials chosen consisted of MCM-41 (MCM-41 micro and MCM-41 nano), UVM-7, and the commercial material Aerosil. All of them present different structural properties such as different sizes and mesopore configurations. Afterwards, these materials were functionalized with thiol groups and characterized. Afterwards, these materials were functionalized with thiol groups and were characterized, and their inhibition potential were tested.

Despite all supports inhibit to some extent the tyrosinase activity, thiol functionalization enhanced in all cases the inhibition potential. UVM-7 was the support with the strongest inhibitory power (>50%) mainly due to the synergetic effect of the bimodal pore system. Besides, it was demonstrated that all materials, in particular UVM-7-SH, could immobilize the PPO allowing its removal from the medium. On the other hand, kinetic studies showed how UVM-7-SH performed a non-competitive inhibition mechanism causing a similar enzyme inhibition to that

accomplished by an acidic pH. The UVM-7-SH concentration needed to accomplish a total inhibition was 3 mg/93.75 U.

The most relevant result of this study was found when tested UVM-7-SH on fresh apple juice. Even though the concentration had to be raised to 10 mg/mL mainly due to the high PPO activity in the juice, UVM-7-SH led to a total PPO inhibition stopping the enzymatic browning even at long times.

From the obtained results, it can be concluded that mesoporous materials are good candidates to develop processes stop the enzymatic browning, yet this effect is dependent on the material's structure and functionalization. Nevertheless, UVM-7-SH material was capable of inhibiting the PPO activity in model system and stopping the enzymatic browning in a real apple juice.

Key words: PPO, tyrosinase, inhibition, UVM-7, thiols, apple juice.

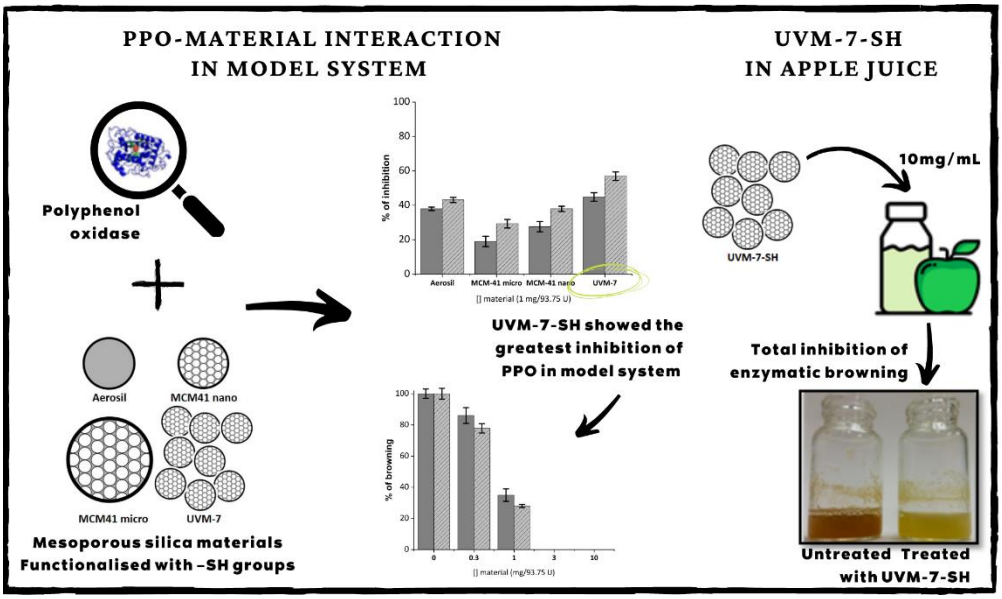

Figure 5.18. *Graphical abstract of the study of enzymatic browning in the presence of thiol-functionalised silica nanomaterial.*

1. Introduction

Consumer acceptance of new food products depends on their organoleptic properties, with appearance and colour being the most important factors when making buying decisions, especially about fruits and vegetables. Therefore, maintaining food colour during shelf life is a main objective in the food industry given its possible economic impact. The main reason for colour change with fruits and vegetables is known as enzymatic browning, and it has been estimated that this process is responsible for more than 50% of waste[22].

Enzymatic browning is a complex chemical reaction that is divided into several phases, enzymatic hydroxylation, enzymatic oxidation and non-enzymatic polymerisation. The two first steps are catalysed by polyphenol oxidase (PPO). This process transforms phenolic compounds into polymeric structures, which produce the characteristic brown colour[23].

The polyphenol oxidase (PPO) enzyme (EC 1.14.18.1 o EC 1.10.3.1), also known as tyrosinase, catechol oxidase, monophenol oxidase and cresolase, has two copper (II) ions, and each is linked to three histidines (type 3 copper enzyme). In nature, the PPO enzyme can be found in two different forms to catalyse two distinct reactions. In the first reaction, the hydroxylation of mono-phenols generates *ortho*-phenols, while the enzyme oxidises these *ortho*-phenols into quinones in the second one. These forms are met-tyrosinase and oxi-tyrosinase, but only oxi-tyrosinase is able to hydroxylate mono-phenols[24,25]. The last enzymatic browning process step consists in the non-enzymatic polymerisation of quinones, which gives rise to melanoides[26] that are responsible for colour changes.

The main factors that affect food enzymatic browning are: pH, temperature, enzyme activity, quantity of polyphenols, and presence of oxygen[27]. For this reason,

processing vegetal foods with large amounts of active PPO and polyphenols involves the risk of enzymatic browning, which causes colour changes and reduces consumer acceptability.

It is important to note that in Europe, and according to FAOSTAT, apple (*Malus Pumila*) is the second fruit in consumption and production terms and is also one of the most important polyphenol sources in diet. Given their high polyphenols content, apples are one of the fruits most affected by enzymatic browning[28]. Apples contain several forms of polyphenols, of which chlorogenic acid is the most important given its high concentration in this fruit[29]. Another is L-tyrosine[30], which is also found in other foods such as mushrooms and crustaceans, and it provokes the same browning problems as in apples.

Over the years, the industry has adopted different chemical and physical strategies to lessen enzymatic browning and to, therefore, reduce fruit and vegetable losses. Traditionally, heat treatment has been used as an enzymatic inactivation method[31]. However, this process has many problems since fruits and vegetables have a considerable amount of thermosensitive compounds, such as vitamins[32], carotenoids and anthocyanins[33], which may be affected during treatment. Besides, temperature applications must be fast and enzymatic inhibition must be complete or the browning process accelerates[34].

When chemical treatments are applied, acidulants that lower pH, or chelating agents that interact on the active centre of the enzyme, have been used to inactivate PPO[35]. Sulphites have also been employed to prevent colour change, but the potential induction of allergenic reactions in consumers has limited their use in food and beverages[36].

Other non-thermal treatments, such as ultrasounds[37], CO_2 supercritical[38], electrical pulses[39], high hydrostatic pressure (HHP)[40] and ultraviolet light[41] having shown good results to inactivate PPO, they have their limitations, such as high cost and large machinery requirements.

From another point of view, nanotechnology is opening up new research areas in several fields, such as medicine and pharmacology[42], and also in the food industry[43]. However in the food industry, the use of nanoparticles has focused on developing encapsulated bioactive compounds and designing active packaging, but applications in industrial processes are still scarce. Silica mesoporous materials are nanomaterials that are synthesised by combining surfactant micellar aggregates with reactive silica precursors[5]. Depending on the surfactant being used, the resultant materials have different structures and pore sizes, which vary between 2 nm and 50 nm. These materials can also be functionalised easily with diverse chemicals groups. Many silica mesoporous materials have been developed in the last 25 years when the M41S family was discovered by a scientist at Mobil Oil[5]; e.g., MCM-41 is one of the most investigated materials and has a 2D hexagonal structure. UVM-7 is also a mesoporous material that was synthesised at the University of Valencia in 2002 based on the "atrane route"[15]. This material is characterised by having both intra-particle and inter-particle pores, which provide the material with a large surface area and a stable pore distribution. These features make these supports ideal for hosting and interacting with enzymes[44]. Nevertheless, the interactions between silica mesoporous materials and polyphenol oxidase have barely been studied as a strategy to avoid enzymatic browning in food systems[45], with only a partial inhibition in model systems and no tests available in real samples.

The aim of this work is to study interactions between four silica mesoporous materials (MCM-41 nanometric size, MCM-41 micrometric size, UVM-7 and Aerosil

200), and their parent materials functionalised with thiol groups, with the PPO enzyme, to evaluate their ability to inhibit enzymatic browning in both model systems and apple juice.

2. Materials and methods

2.1. Chemicals

Aerosil 200 was purchased from Evonic industries. Mushroom tyrosinase, Dopamine hydrochloride, L-tyrosine, chlorogenic acid, sodium dihydrogen phosphate and disodium hydrogen phosphate were acquired from Sigma-Aldrich and were used without further purification. Finally, two different varieties of apples (cv. Granny Smith & cv. Golden Delicious), obtained from a local retailer, were used to prepare juice.

2.2. Synthesis and characterisation of silica materials

Materials were prepared following known procedures. A detailed description of the synthesis of the three mesoporous nanomaterials, the functionalisation with the thiol groups and their characterisation can be found in the Supplementary Material.

Silica materials characterisation was done by low-angle X-ray powder diffraction (XRD) in a Bruker D8 Advance using CuKα radiation. A JEOL –jem-1010 was employed for the transmission electron microscopy (TEM) characterisation. The amount of thiol groups in the four materials was measured by a TGA/SDTA 851e Mettler Toledo (TGA).

The nitrogen adsorption/desorption isotherms were measured in a volumetric adsorption analyser (Micromeritics ASAP 2020) at a liquid nitrogen

temperature (-196ºC). The Barret-Joyner-Halenda (BJH) model[46] was fitted to estimate pore size distribution and pore volume, while the specific surface area was calculated by the BET model[47] within the low-pressure range. Wall thickness and a_0 cell were calculated from the porosity and XRD data[48].

2.4. Enzyme kinetics in model systems

Mushroom tyrosinase was used to prepare the model systems. Dopamine, L-tyrosine and chlorogenic acid were tested as substrates. In a typical experiment, 1.25 mL of a solution that contained 0.005 to 2.5 mM of substrate in the presence of 10 mM phosphate buffer at pH 5.5 is mixed with 0.25 mL of the enzyme solution (0.14mg/mL-375 U/mL). Absorbance is measured every 20 seconds at 420 nm. Enzyme kinetic studies were performed at 20ºC in duplicate. Solutions at pH 3.5 and 4.5 were also prepared for dopamine.

The initial reaction rate was calculated from the slope of the linear part of the absorbance-time curves. The saturation curve was obtained by plotting the reaction rate values *versus* the different substrate concentrations. Since tyrosinase enzymatic reaction follows the Michaelis-Menten equation[49], the corresponding kinetic parameters, K_M and v_{max}, were obtained from the Lineweaver-Burk plot[50]. Afterwards, the catalytic constant (K_{cat}) and the specific constant were calculated from the kinetic parameters for each substrate and pH. A one-way analysis of variance (ANOVA) was applied to determine the influence of the different substrates and the influence of pH in the case of dopamine.

2.5. Study of enzyme-material interactions in model systems

In order to determine the nature of the enzyme-material interaction, two types of studies were conducted: enzyme kinetics in the presence of the material and quantification of enzyme immobilisation. In the kinetic studies, 0.25mL of the

enzyme solution (375 U/mL) were added to 1 mL of phosphate buffer 10 mM (pH=4) that contained 1 mg of material. The resulting suspension was stirred for 2 h to ensure that the interactions between the enzyme and the material were as high as possible. Afterwards, 0.25 mL of dopamine 0.12 mM were added, and colour enhancement was monitored after 60 min by measuring absorbance, after filtration through a 0.45 μm PTFE filter in a JASCO V-630 model at 420. The same experiment was performed in the absence of the material and was used as a reference. Enzymatic browning inhibition can be calculated from absorbance values according to Equation (1), where Abs_0 and Abs_i were the absorbances at 420 in the absence and presence of the material, respectively.

$$\%\, Inhibition = \frac{Abs_0 - Abs_i}{Abs_0} * 100 \qquad (1)$$

The kinetic study with UVM-7-SH at pH 4.5 was performed following the same procedure, which was slightly modified since the stock substrate solution changed from 0.5 to 10 mM to obtain the same final concentration as shown above. The inhibition type caused by the UVM-7-SH material was studied with the Lineweaver-Burk plot, and by following the protocol and equations described in De Arriaga, 1979[51]. The free protein concentration was measured by the Bradford method[52], based on binding the protein to the dye to form a blue complex. As a control, an enzyme solution (375 U/mL) that contained 1 mg of the material in phosphate buffer at pH=3.5 was used. The calibration line was formed with bovine serum albumin. Absorbance measures were taken with a JASCO model V-630 at 595 nm using 2-mL plastic spectrophotometer cuvettes. Both, the kinetic studies and the Bradford method were run in triplicate.

2.6. Material testing in apple juice

Apple juice was used as a real food system to test the material selected in the kinetic studies. The test was run on liquefied apples, obtained in the laboratory from two varieties of apple, cv. Granny Smith and cv. Golden Delicious. Three apple juice aliquots of 2 mL were taken from each variety. One of each was combined with 20 mg of either UVM-7 or UVM-7-SH, and the other one was used as the control sample. These mixtures were stirred at 200 rpm for 60 min. Colour changes were followed by taking photographs of apple samples.

Furthermore, in order to test browning inhibition persistence after removing the material, 4 mL of Golden Delicious juice were placed so they came into contact with 40 mg of UVM-7-SH and were stirred for 5 min. Afterwards, the sample was filtered off and the filtrate was separated in two aliquots. One was kept at room temperature and the other one was placed in the refrigerator. Moreover, a sample without the material was used as the control.

3. Results and discussion

3.1. Materials characterisation and selection

Eight materials were prepared as potential inhibitors of PPO. They involved the combination of four supports (MCM-41 micro, MCM-41 nano, UVM-7 and Aerosil 200) with two functionalities: silanols (naturally present on the surface of silica materials), or thiol groups (which were covalently attached to the material's surface). Mesoporous materials have shown the ability to immobilise PPO up to 30% upon enzyme loading[45]. The pore size and pore volume of the materials appeared to be the most relevant factor when immobilising PPO. Therefore, a variety of particle size and topologies were selected. MCM-41 and UVM-7 are characterised by an

ordered mesoporous bidimensional structure, with a pore diameter of a few nanometers. With MCM-41, two kinds of supports with diverse particle sizes (MCM-41-micro and MCM-41-nano) were prepared to study the effect of particle size on the nanomaterial-enzyme interaction. UVM-7 is a bimodal porous silica material made from the aggregation of pseudo-spherical mesoporous nanoparticles (12–17 nm) developing intra-nanoparticles pores (mesopore) of 2–4 nm (a pseudo-hexagonal disordered array) and 20–70 nm inter-particle macro pores (textural porosity) that improve diffusion[15]. Finally, Aerosil is characterised by the absence of the mesoporous system, although a certain porosity can be observed between particles (textural porosity).

The silica supports were covalently modified with thiol groups (-SH). This modification was inspired by the knowledge that cysteine is a well-known PPO inhibitor, and the thiol group in cysteine is the active moiety[53,54]. The use of covalent bonding offers greater stability to final systems compared with other possibilities, such as occlusion or electrostatic interactions.

X-ray powder diffraction and TEM confirmed that the mesoporous structure was maintained during calcination (while preparing the unfunctionalised materials) and during the functionalisation of the materials with thiols (see the Supplementary Material, Table S5.1 and Figure S5.1 and S5.2). The BET analysis of the N_2 adsorption/desorption isotherms (see Figure S5.3) offered specific surface values for all the materials that came close to 1,000 m^2g^{-1} after calcination (see Table 5.4). The specific surface value of the materials functionalised with thiols groups was strikingly similar to the unfunctionalised ones because the thiol chain is not long enough to stop N_2 from entering pores. This tendency was also observed when the BJH model was applied to calculate the specific pore volume of all the solids.

Table 5.4. *Textural properties and organic content of the different silica matrix as-made, calcined and functionalised: UVM-7, MCM-41 nano, MCM-41 micro and Aerosil 200.*

Material		Area [a] (m^2g^{-1})	Mesopore volume [b] (cm^3g^{-1})	Mesopore diameter [b] (nm)	Textural pore diameter [b] (nm)	Textural pore volume [b] (cm^3g^{-1})	mmol SH/g SiO_2
UVM-7	calcined	866.8	0.66	2.69	41.3	1.02	-
	-SH	842.7	0.64	2.58	36.4	0.80	0.55
MCM-41 nano	calcined	1029.9	0.81	2.56	14.0	0.12	-
	-SH	902.8	0.55	2.48	14.2	0.11	0.78
MCM-41 micro	calcined	1030.7	0.67	2.38	-	-	-
	-SH	1035.5	0.74	2.36	-	-	0.56
Aerosil	calcined	195.9	-	-	14.9	0.25	-
	-SH	181.8	-	-	17.3	0.34	0.32

[a] BET specific surface calculated from the N2 adsorption-desorption isotherms.

[b] Pore volumes and pore size (diameter) calculated from the N_2 adsorption-desorption isotherms for the selected materials.

In all cases values of around 0.6-0.8 m^3g^{-1} were obtained for the specific mesopore volume in the calcined and functionalised particles. In addition, the calculated pore diameter values were 2.69 nm for UVM-7 and 2.58 for UVM-7-SH. With MCM-14, the calculated pore diameter values were about 2.5 nm for MCM-41 nano and 2.3 for MCM-41 micro for both the unfunctionalised and functionalised supports. As the Aerosil structure does not present mesopores, the only calculated parameter was surface (195.92 m^2g^{-1} for Aerosil and 181.78 m^2g^{-1} for Aerosil-SH). As we can see, the specific surface for Aerosil is much lower than that found for the other supports as its structure lacks mesopores (see Table 5.4).

In addition to mesopores, the materials can also show textural porosity due to the aggregation of smaller sized particles. As observed in Table 5.4, the prepared supports present textural porosity with pore diameters that fall within the range of 15 nm (MCM-41-nano and Aerosil) or 40 nm (UVM-7), as well as specific textural pore volumes from 0.11 to 1.0 $cm^3\ g^{-1}$.

Lastly, the amount of the thiol group present in the mesoporous materials was estimated by a TGA analysis (see Table 5.4). Values of 0.32, 0.55, 0.75 and 0.54 mmol of thiol/g SiO_2 for Aerosil-SH, MCM41-micro-SH, MCM-41-nano-SH and UVM-7-SH were respectively found. These results fall in line with the expected degree of functionalisation for the silica materials[55]. It seems that the smaller specific surface of Aerosil allowed a lower degree of functionalisation, which resulted in the smallest amount of thiol. For the mesoporous materials, which have larger surfaces, thiol functionalisation increased from 70% (MCM-41-micro and UVM-7) to 140% (MCM-41-nano) compared with Aerosil.

3.2. Enzyme kinetics in model systems

As pH in fruits and their resultant juices usually ranges from 3.5 to 5.5, the PPO kinetics was measured within this interval. Three substrates that are typically found in the literature for PPO (dopamine, chlorogenic acid and tyrosine) were studied. Among the different substrates, dopamine was clearly the substrate with the greatest enzymatic activity since L-tyrosine and chlorogenic acid had a lower v_{max} (Table 5.5). In both cases, the turnover number was lower than that for dopamine; however, with chlorogenic acid, affinity was almost as high as it was for dopamine. All the constants statistically differed from one another, with a 99.95% probability. Therefore, dopamine was selected for the other experiments as it exhibited the most intense response. pH is one of the most relevant parameters to affect biological processes (e.g., enzymatic activity) both in food systems and during food processing. The results in Table 5.5 show enzyme activity evolution with pH (from 3.5 to 5.5), with almost no activity at pH 3.5. Munjal and Sawhney[56] reported similar results in 2002. With the enzyme-dopamine model system, v_{max}, K_{cat} and the specific constant parameters increased with pH (p<0.05), but no significant differences were found for K_M (p<0.05). The affinity of the enzyme for dopamine (K_{cat}/K_M) reached values above 3800 $\Delta Abs_{420} min^{-1} mM^{-1}$ at pH 5.5, which came close to 40 $\Delta Abs_{420} min^{-1} mM^{-1}$ at pH 3.5. Thus, a pH of around 4.5 was selected for the assays run in the presence of the materials.

Table 5.5. *Tyrosinase from the mushroom kinetics parameters (93,75U) in the presence of different substrates (Dopamine, L-tyrosine and chlorogenic acid) at different pHs and in the presence of 1mg of UVM-7-SH.*

Substrate	K_M[a](mM)	v_{max}[b] ($\Delta Abs_{420} min^{-1}$)	K_{cat}[c] (ΔAbs_{420} mM^{-1} min^{-1})	Specific constant[d] (ΔAbs_{420} min^{-1} $(mM^2)^{-1}$)
Chlorogenic acid pH 5.5	0.31 ± 0.02	0.201 ± 0.006	1000 ± 30	3400 ± 100
L-tyrosine pH 5.5	0.19 ± 0.07	0.050 ± 0.007	260 ± 40	1500 ± 400
Dopamine pH 5.5	1.0 ± 0.2*	0.78 ± 0.09	3800 ± 500	3800 ± 400
Dopamine pH 4.5	0.87 ± 0.17*+	0.43 ± 0.07	2200 ± 300	2500 ± 100
Dopamine pH 3.5	0.5 ± 0.3*	0.0041 ± 0.0012	21 ± 6	40 ± 20
Dopamine + UVM-7-SH pH 4.5	1.0 ± 0.6+	0.009 ± 0.004	40 ± 20	44 ± 6

[a] Michaelis-Menten constant, dependent on enzyme concentration.

[b] Reaction rate, dependent on enzyme concentration.

[c] Catalytic constant, $K_{cat}=v_{max}/[E]$

[d] Specific constant, calculated by K_{cat}/K_M

* There are no statistically significant differences for p <0.05 for the K_M constant at different pH.

+ There are no statistically significant differences for p <0.05 between K_M from dopamine at pH 4.5 in the absence and presence of UVM-7-SH.

3.3. The material-enzyme interaction

The material-enzyme interaction was studied by analysing PPO activity inhibition in the presence of the eight prepared materials (four supports, with and without thiols). Enzyme activity was quantified through the browning measured at 420 nm 1 hour after adding the substrate to the enzyme solution, with or without the material. All the tested materials, even those non-functionalised with thiols, were able to inhibit enzymatic activity to a certain extent and went from 19% to 58% (Figure 5.19). For the calcined materials, which are covered with silanol groups, inhibitory power decreased in this order: UVM-7 > Aerosil > MCM-41-nano > MCM-41-micro. After taking their structure into account (Table 5.4), it can be concluded that neither surface nor mesopore volume is a relevant characteristic for enzyme inactivation. The influence of the mesopore diameter could not be ruled out since UVM-7 had wider pores, followed by MCM-41-nano and MCM-41 micro. However, the pore size differences between them were relatively small, and they did not exist in Aerosil, which proved more active than the MCM-41-based materials. So, although mesopores seemed to be responsible for certain browning inhibition, they were not the main driver.

Presence of textural pores is probably the main structural factor responsible for the differences noted in enzyme activity inhibition between materials. As we can see in Table 5.4, it seems that an increase in either the textural pore diameter or the textural pore volume enhances inhibitory power. The migration of the enzyme to the material is a diffusion-controlled process[45], and the smaller the pore diameter, the more difficult it is for the enzyme to enter pores, particularly pores below 3 nm. The experimental results suggested that the enzyme was able to interact with mesopores, but a combined interaction with mesopores and textural pores was probably the most effective approach to inactivate it.

When the materials were functionalised with thiols, PPO inhibition increased with values between 29% for MCM-41-micro-SH and 58% for UVM-7-SH (Figure 5.19). The inhibitory effect of the diverse materials followed the same order as that found for the calcined materials, but the additional effect accomplished by thiol groups differed depending on the support type. While inhibition respectively increased by 12.2%, 11.15 and 10.1% for UVM-7-SH, MCM-41-nano-SH and MCM-41-micro-SH compared to the calcined material, this increment with Aerosil was only 4%. It would appear that thiol functionalisation improved PPO inhibition in particular materials which contained mesopores, and then induced a similar increase for all three materials. On the contrary for Aerosil, the effect of the material without mesopores was significantly weaker (p<0.01).

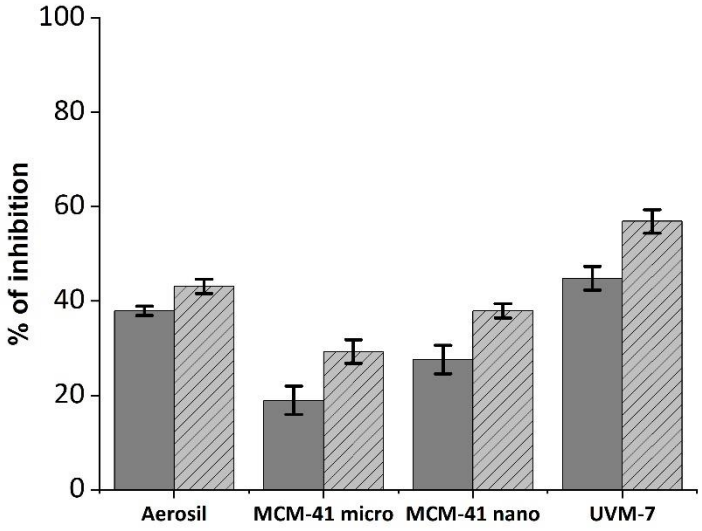

Figure 5.19. *Percentage of enzymatic activity inhibition after 1-hour reaction at an enzyme concentration of 93.75 U and in the presence of 1 mg of the material. Dark grey: calcined material; light grey: thiol-functionalised materials.*

It is feasible to think that the weaker effect of thiol in Aerosil could be attributed to its lower thiol loading compared to the mesoporous supported materials. However, a regression coefficient (R^2) as low as 0.0023 was obtained for the other three materials when we performed a correlation after removing Aerosil-SH, which refutes such a hypothesis. Therefore, the results suggested that UVM-7-SH was the material with the strongest inhibitory power due to the synergetic effect of the bimodal pore system with the strong effect of thiols.

In order to gain further insight into the inhibition mechanism, the amount of enzyme captured by the material was determined indirectly by quantifying the amount of free enzyme present in the solution by the Bradford method. The results showed that 2 h after coming into contact with 1 mg of the material, the percentage of immobilised enzyme fell within the 50-71% range (Figure 5.20). In this case, the type of material also affected the % of immobilised enzyme, but these differences were narrower than for enzymatic activity. Furthermore, the thiol groups improved enzyme immobilisation, and this effect was observed only in those materials that contained mesopores. However, an unsatisfactory correlation was found among the concentration of thiols and the increase of the enzyme immobilization (R^2 = 0.211).

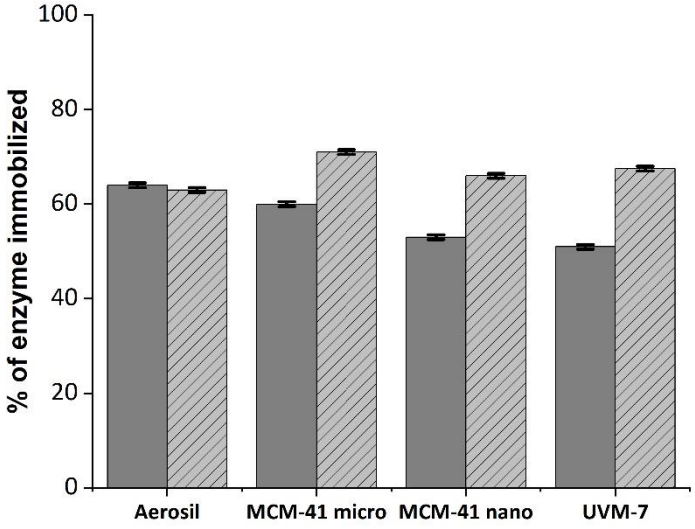

Figure 5.20. *Percentage of immobilisation of enzymatic activity after a 2-hour reaction at an enzyme concentration of 93.75 U and in the presence of 1 mg of the material. Dark grey: calcined material; light grey: thiol-functionalised materials.*

3.4. The tyrosinase-UVM-7-SH interaction

Since UVM-7-SH offered the best performance in overall PPO activity reduction and the highest percentage of inhibition for the immobilised enzyme, a kinetic study was performed at pH 4.5. The aim of this set of experiments was to compare the results with the previous results obtained in Section 3.2, and to understand the type of inhibition by using the Lineweaver–Burk plot. As expected, the reaction rate v_{max} was much lower in the presence of 1 mg of UVM-7-SH than that at the same pH without the material. A slight reduction in enzyme affinity was also observed (K_M) for the substrate (Table 5.5). In the presence of UVM-7-SH, both the turnover number (K_{cat}) and catalytic efficiency (K_{cat}/K_M) of the enzyme plummeted from values near 2500 to some of around 40 for both constants. These

findings indicated that enzyme activity significantly decreased in the presence of UVM-7-SH. It was also noted that these values were similar to those obtained for the enzyme at pH 3.5, which demonstrated that UVM-7 functionalised with thiol groups caused a similar enzyme inhibition to that accomplished by an acidic pH. This indicates a clear advantage of using UVM-7 to control enzyme activity instead of the acidification strategy, as the sensorial properties of the food system remain unaltered.

The K_M and v_{max} values suggested that the inhibition mechanism was non-competitive as no statistically significant differences were observed for K_M, while v_{max} lowered. This result indicated that although the UVM-7-SH-enzyme interaction did not occur in the enzyme active centre, it seemed to modify the interaction between the substrate and the active centre by stopping the product formation reaction[57].

As the final objective of obtaining a PPO inhibitor material was to avoid enzymatic browning in fruit juice, the material-enzyme ratio was tested at pH 4.5 and 5.5. No test was performed at pH 3.5 as activity at this pH was too low and it was difficult to spectrophotometrically follow inhibition. As the enzyme was more active at pH 5.5 than it was at pH 4.5, and in order to facilitate interpretation, the results are shown as a percentage of inhibition, and refer to the control at the corresponding pH.

UVM-7-SH was unable to prevent browning when used at low concentrations (0.3 and 1 mg of the material), and concentrations above 3 mg were needed to inhibit the generation of brown pigments (see Figure 5.21). Similar results were obtained for the two pH conditions, which suggests that inhibition does not depend on the pH of the solution, at least not for the studied interval.

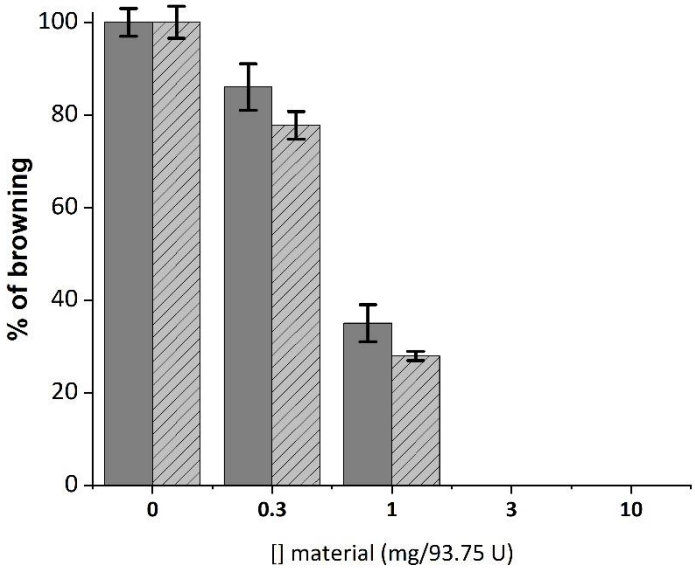

Figure 5.21. *Influence of the material concentration and pH on the enzymatic browning reaction using dopamine 0,12mM as a substrate after a one-hour reaction. Dark grey: pH 4.5; light grey: pH 5.5*

The pKa of the thiol groups (pKa ≅10) was far from the pH of the trials, and no relevant change in the material's surface properties was expected between pH 4.5 and 5.5.

The influence of the substrate on the material-enzyme interaction was also tested. For this purpose, L-tyrosine and chlorogenic acid were used as substrates instead of dopamine, and a similar response was observed (see supplementary material, Figure S5.4). Increasing the quantity of UVM-7-SH in the model system enhanced inhibition, and total inhibition was accomplished with 3 mg per 93.75 U. The results suggest that the material's capacity to inhibit enzyme activity is independent of the substrate and pH, and the material-enzyme ratio is the only critical variable for the inhibition process.

Lastly, it should be considered that the enzyme and substrate would be present in the same matrix in a real application. Therefore, the enzymatic reaction will start as soon as cellular content is exposed to oxygen. Thus, it is advisable that the material is able to interact with the enzyme as quickly as possible, ideally no sooner than the material is added. In order to evaluate the requirement of the contact time between the enzyme and the material, diverse contact times were tested before adding the substrate (0, 1, 10 min and 2 h). The assay was performed at pH 4.5 at a 3 mg/93.75 U ratio since these were the conditions at which full enzyme inhibition was achieved. The obtained results showed that the previous contact time only had a minor effect on the material response, and 97% inhibition was achieved in short times, with 100% inhibition for longer times.

The results confirmed that combining the UVM-7 structure with thiol groups was able to empower inhibition, and up to a point at which enzymatic browning was no longer significant. This scenario suggests that a suitable UVM-7-SH:enzyme ratio could stop enzymatic reactions and could, therefore, avoid enzymatic browning in real food systems.

3.5. UVM-7-SH performance in apple juice

Once the good response of UVM-7-SH particles had been proved in model systems, the effect of mesoporous particles on real juice was studied. Two apple varieties were chosen for the test. Golden Delicious was chosen, as this is the most widely consumed cultivated variety in Europe. Granny Smith was selected for its homogeneous composition between different batches and origins, which guarantees reproducibility in the results[58].

Diverse UVM-7-SH concentrations were added to the fresh liquefied apple juice. The results showed that 1 mg/mL of the material added to apple juice was

insufficient to stop enzymatic browning. When the concentration was increased to 5 mg/mL, the browning reaction was delayed and progressed similarly to the control after 10 min. The addition of 10 mg/mL to both varieties led to the total PPO enzyme inhibition of juice samples. According to the literature[59], the enzymatic activity in both apple varieties was similar, which explains why the same amount of mesoporous material was needed to ensure inhibition for both varieties. Besides, these outputs suggested a direct dependency between the UVM-7-SH concentration and PPO enzyme activity.

Persistence of inhibition is shown in Figure 5.22a and 5.22b; the vials on the left contain natural apple juice with no added material, while those on the right contain 10 mg/mL of UVM-7-SH. The enzymatic browning process, which is characteristic of fresh apple juice, is observed in the samples on the left. Colour change was observed in the early stages (under 1 minute) due to the speed of the oxidation process. After a 5-minute exposure to oxygen, juice became red-copper, which vastly differed from its original yellow colour. However, no enzymatic browning was observed in these fresh juice samples when the UVM-7-SH material was added. The inhibiting effect of the mesoporous material was strong enough to completely stop the process; as we can see, the juices without the material had completely oxidised after 60 min.

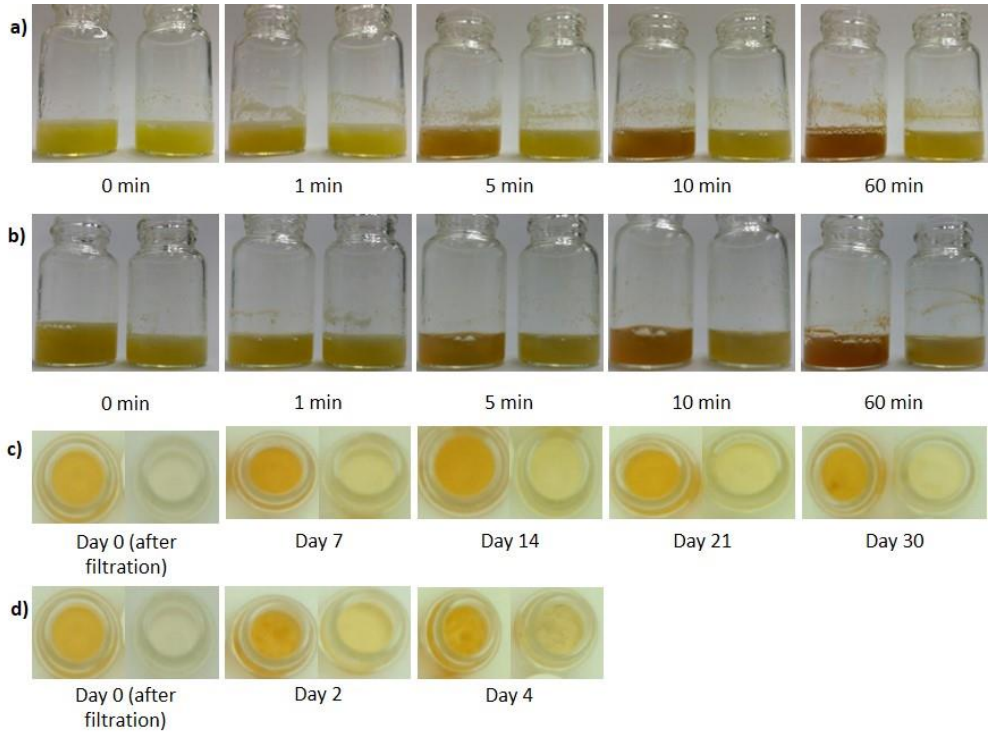

Figure 5.22. *Colour evolution in an apple smoothie. (a) Golden Delicious without the material (left) and in the presence of 10 mg/mL of UVM-7-SH (right). (b) Granny Smith without the material (left) and in the presence of 10 mg/mL of UVM-7-SH (right). (c) Golden Delicious in the presence of 10 mg/mL of UVM-7-SH filtered after 5 min and stored at 4°C (d) Golden Delicious in the presence of 10 mg/mL of UVM-7-SH filtered after 5 min and stored at room temperature.*

The same test was performed, but UVM-7 was used to check the effect of the thiol groups present in the functionalised particles of UVM-7-SH. In this case, enzymatic browning was slightly slowed down by the presence of UVM-7 during the first min. A few min later, the oxidation process progressed to an advanced stage, even at high concentrations of the material (10 mg/mL) (see supplementary

material, Figure S5.5). This observation evidence that the –SH groups are essential for developing enzyme inhibition, and therefore for avoiding enzymatic browning.

A last experiment was carried out by removing the UVM-7-SH from real juice after a 5-minute contact step. The aim of this trial was to explore the possibility of recovering the material and then obtaining a final juice free of particles. After removing the material, two sets of samples were stored at 4°C (Figure 5.22c) and at room temperature (20°C) (Figure 5.22d). The browning of the refrigerated samples was monitored for 30 days. while the samples stored at room temperature were thrown away after 4 days due to mould growth. We can observe how the freshly filtered sample, previously treated with UVM-7-SH, became colourless and slightly darkened (almost imperceptible to the naked eye) throughout the experiment. As the control sample, a juice solution without the material, but also filtered after being stirred for 5 min, was prepared. It was already orange after the 5-minute step, and darkened with time. Therefore, it can be stated that the UVM-7-SH material has the functionality of inhibiting browning and does not need to remain in the system since inhibition endures, and even after it has been removed from an early stage.

4. Conclusions

It has been demonstrated that mesoporous materials are good candidates to immobilise and inhibit PPO. The effect on the enzyme is dependent on not only the material's structure, but also on functionalisation. It would appear that the mesopores and micropores combination (observed in materials such as UVM-7), together with thiol groups, offers the best inhibitory properties. UVM-7-SH is capable of inhibiting the PPO enzyme and, therefore, of stopping the enzymatic oxidation process when used at concentrations that equal or exceed 3 mg of UVM-

7-SH per 93.75 enzymatic units, and does not seem to depend on the substrate. The experiments were performed in both model systems and fresh apple juice, obtained from the Golden Delicious and Granny Smith varieties. Enzymatic browning inhibition in juices remained up to 30 days, even after the material was removed by filtration after a contact stage that lasted only 5 min.

Acknowledgements

The authors thank the financial support obtained from the Spanish Government (Project MAT2015-64139-C4-1-R) and the Generalitat Valenciana (Project GVA/2014/13).

SUPPLEMENTARY MATERIAL

Materials synthesis

Mesoporous silica materials synthesis

Mesoporous microparticles MCM-41 silica was synthesised by the so-called "atrane route", a simple preparative technique based on the use of "silatranes" ligands as hydrolytic inorganic precursors and surfactants as porogen species. The molar ratio of the reagents for this synthesis was set at 8 $TEAH_3$:2 TEOS: 0.52 CTAB: 0.5 NaOH: 180 H_2O. In a typical synthesis, 4.68 g of CTABr are added to a solution of $TEAH_3$ (25.79 g) that contains 0.045 mol of TEOS and NaOH at 118ºC. Next 80 mL of water are slowly added with vigorous stirring at 70ºC. After a few min, a white suspension form. This mixture is aged in an autoclave at 100 ºC for 24 h.

Mesoporous MCM-41 nanoparticles (MSN) were synthesised according to the method described by Zhao, Trewyn, Slowing and Lin[41]. In a typical synthesis, 1.00

g of N-cetyltrimethylammoniumbromide (CTABr, 2.74 mmol) is dissolved in 480 mL of distilled water, followed by the addition of 3.5 mL of a solution of NaOH 2.00 M. Then the solution is heated to 80ºC and TEOS (5 mL, 2.57x10-2mol) is added drop-wise to the surfactant solution. The mixture is stirred for 2 h at this temperature.

The synthesis strategy for preparing UVM-7 silicas was a modification of the so-called "atrane" route. A mixture of TEOS (10.7 mL, 0.05 mol) and TEAH3 (22.3mL, 0.17 mol) was heated to 120ºC until no elimination of ethanol was observed. The mixture was cooled down to 90ºC and 4.56 g CTABr were added, followed by water. The mixture was aged at room temperature for 24h[42].

For all the mesoporous materials, the resulting white precipitate was collected by centrifugation and washed with distilled water. Finally, the solid was dried at 70ºC. To prepare the final porous material, the as-synthesised solid was calcined at 550ºC in an oxidant atmosphere for 5 h to remove the template phase.

Thiol functionalisation

Firstly, 1.0 g of each support was suspended in 30 mL of acetonitrile and an excess of 3-mercaptopropyltriethoxysilane (1.86 mL, 10 mmol) was added. The final mixtures were stirred for 16 h at room temperature. The four functionalised materials (MCM-41-micro-SH, MCM-41-Nano-SH, UVM-7-SH and Aerosil-SH) were isolated by centrifugation, washed with acetonitrile and dried at 37 ºC overnight.

Materials characterisation

The morphology of the MCM-41- and UVM-7-based materials was characterised by standard procedures, such as low-angle X-ray powder diffraction and TEM. TGA was performed in the thiol-containing products. Nitrogen adsorption/desorption isotherms were also executed in all the materials.

XRD studies

The XRD patterns (Figure S5.1) showed the expected four peaks indexed as (100), (110), (200) and (210) Bragg reflections, which are characteristic of the hexagonal ordered array of the MCM-41 material (Figure S1A and S1B). For UVM-7, the XRD patterns showed only one peak, indexed as (100) and related with a disordered hexagonal array (Figure S1C). Nevertheless, the peak between 2º and 2.5º 2θ (indexed as d_{100}) was not only present in the as-synthesised sample, but also in the calcined and functionalised samples. The fact that the (100) peak existed in the XRD patterns and in all cases indicated that the hexagonal ordered array was not modified throughout the process in any case. For UVM-7, the principal plane d_{100} spacing of the as-made particle was 43.07 Å, 38.61 Å for the calcined material and 40.69 Å for the synthesised particle (Table S5.1).

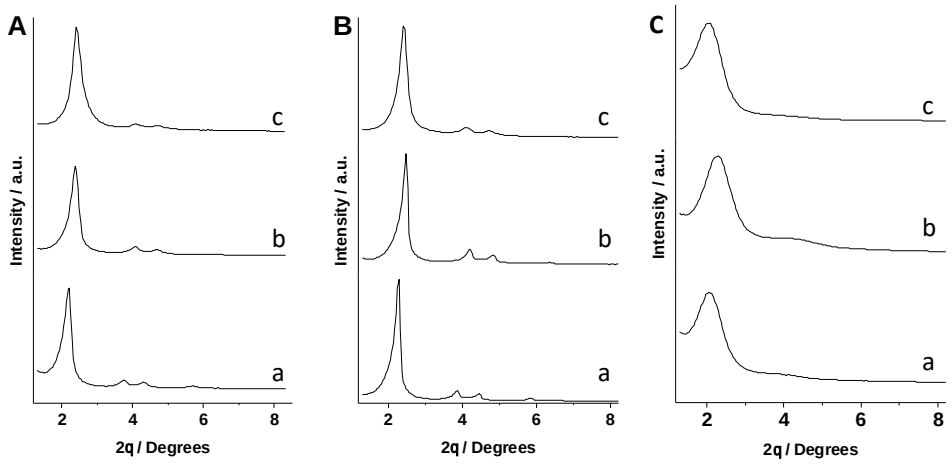

Figure S5. 1. *The powder X-ray diffraction patterns of the a) as-made material, b) the calcinated material and c) the material that contained 3-mercaptopropyltrimethoxysilane for the A) MCM-41, B) MSN and C) UVM-7 materials.*

Figure S5.1. The powder X-ray diffraction patterns of the a) as-made material, b) the calcinated material and c) the material that contained 3-mercaptopropyltrimethoxysilane for the A) MCM-41, B) MSN and C) UVM-7 materials

Based on these results, the a_0 cell parameter was calculated for both the UVM-7 synthesised (49.7 Å) and UVM-7 calcined samples (44.59 Å). A significant cell contraction of 5.1 Å was observed, which was most likely related to the condensation of silanols in the calcination step[43]. The parameters calculated for MCM-41 nano and MCM-41 micro were almost the same as each other as the only difference between them was particle size. The d_{100} spacing values were about 36 to 40 Å, depending on whether as was as-made, calcinated or functionalised. However, in general terms, they were slightly smaller than those calculated for UVM-7.

Table S5. 1. *Pore structure data of the used supports*

Material		d_{100}[a](Å)	2θ[b] (^{0})	Area[c] (m^2g^{-1})	a_0[d] (Å)	dw[e] (Å)
UVM-7	as-made	43.07	2.05	99.24	49.7	-
	calcined	38.61	2.29	866.8	44.59	17.69
	functionalised	40.69	2.17	842.7	50.68	23.56
MCM-41 nano	as-made	39.99	2.21	55.01	46.18	
	calcined	37.33	2.37	1029.9	43.10	17.48
	functionalised	36.68	2.41	902.8	42.36	17.51
MCM-41 micro	as-made	38.61	2.29	10.24	44.59	
	calcined	35.55	2.40	1030.7	41.05	17.23
	functionalised	36.68	2.41	1035.5	42.36	18.80
Aerosil	as-made	-	-	-	-	-
	calcined	-	-	195.9	-	-
	functionalised	-	-	181.8	-	-

[a] Diffraction peak of the reticular plane 100

[b] Angle of incidence for the reflection plane.

[c] The BET specific surface calculated from the N2 adsorption-desorption isotherms.

[d] The cell parameter calculated by $a_0=2d_{100}*(\sqrt{3})-1$

[e] Wall thickness was calculated by $d_w= a_0 - d_p$, where d_p is the pore diameter.

The distance between the two pore centres was also calculated for both MCM-41 nano and MCM-41 micro, which are shown in Table S5.1. Besides, the same cell contraction was observed as in UVM-7, with 3.54 Å for MCM-41 micro and 3.08 Å for MCM-41 nano due to the condensation of silanols when the sample was calcined.

TEM studies

Figure S5.2 is a representative image of the different mesoporous materials, where the typical disordered hexagonal porosity of the MCM-41 and MSN matrix can be clearly seen. In addition, the prepared MSN material was obtained as spherical particles with diameters that ranged from 80 nm to 110 nm, as shown in Figure S5.2b. Figure S5.2c depicts the characteristic hierarchic bimodal pore organisation of the UVM-7 material. The presence of the mesoporous structure in the final functionalised solids was also confirmed with the TEM analysis, in which the typical channels or pores of the materials were visualised after the functionalised process (data not shown).

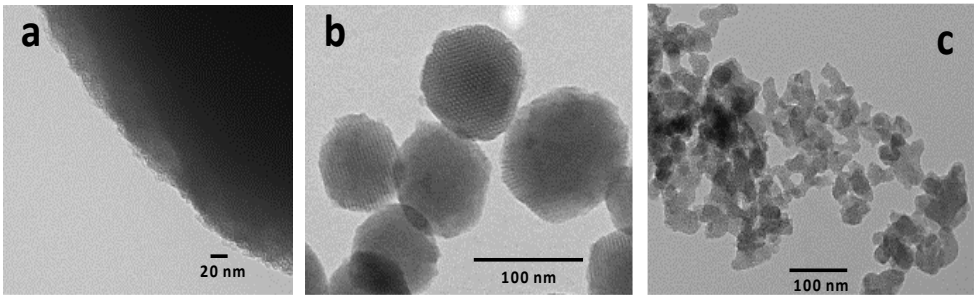

Figure S5. 2. *Representative TEM images of the a) calcined MCM-41, 2) calcined MSN and 3) calcined UVM-7 materials*

Nitrogen adsorption/desorption studies

The N_2 adsorption/desorption isotherms are type IV for all the supports, except Aerosil, which is typical of mesoporous materials with a narrow pore size distribution according to IUPAC. By employing the Brunauer, Emmett and Teller (BET) model on the adsorption curves, the specific surface was obtained. With the UVM-7 as-made, the specific surface was very low (99.24 m^2g^{-1}) due to the presence of surfactant in the pores that block the N_2 entrance. With both MCM-41s, the response was similar, but with a small specific surface (55.01 m^2g^{-1} for MCM-41 nano and 10.24 m^2g^{-1} for MCM-41 micro). Once all the organic matter was removed after calcinations, and also after functionalisation, the specific surface increased to values that came close to 1,000 m^2g^{-1}. This tendency was also observed when the BJH model was applied to calculate the pore volume of all the solids. Therefore, in the case of particles as-synthesised was almost non-existent (0.007 to 0.07 m^3g^{-1}).

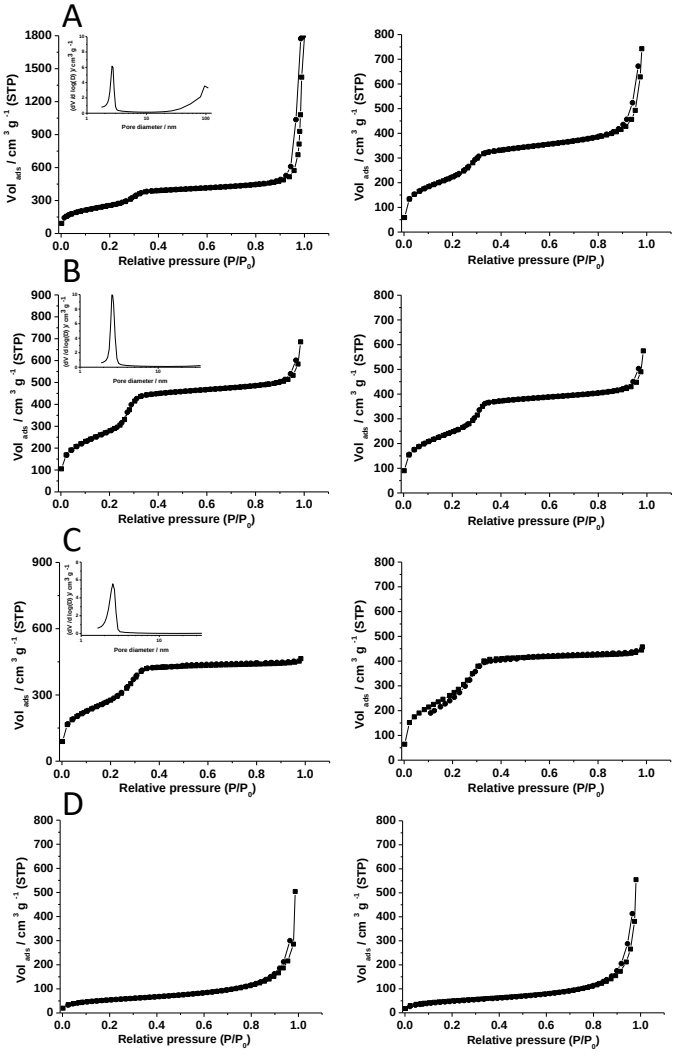

Figure S5. 3. *The N2 adsorption-desorption isotherms of the supports. UVM-7 (A), Nano (B), Micro (C) and Aerosil (D). Non-functionalised (left) and functionalised with thiol groups (right). Inset: the pore size distribution of the calcined mesoporous material.*

Influence of UVM7-SH in the enzymatic browning in presence of other substrates

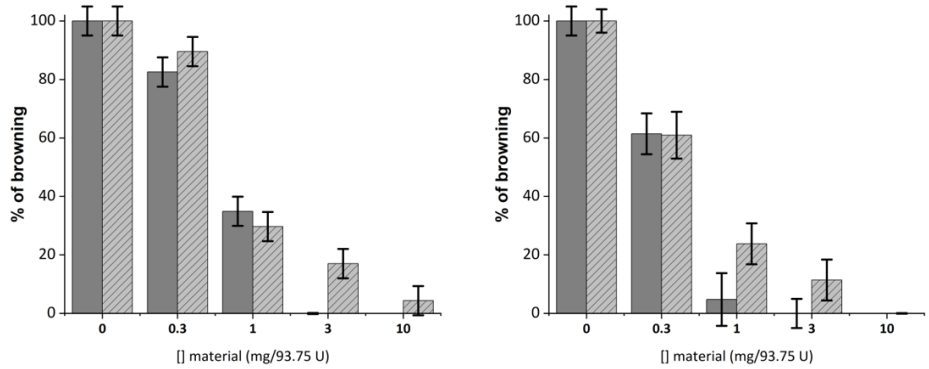

Figure S5. 4. *Influence of the material concentration and pH on the enzymatic browning reaction using L-tyrosine (left) or chlorogenic acid (right) 0.12mM as substrate after a one-hour reaction. Dark grey: pH 4.5; light grey: pH 5.5*

Influence of UVM7 in the enzymatic browning in apple smoothie

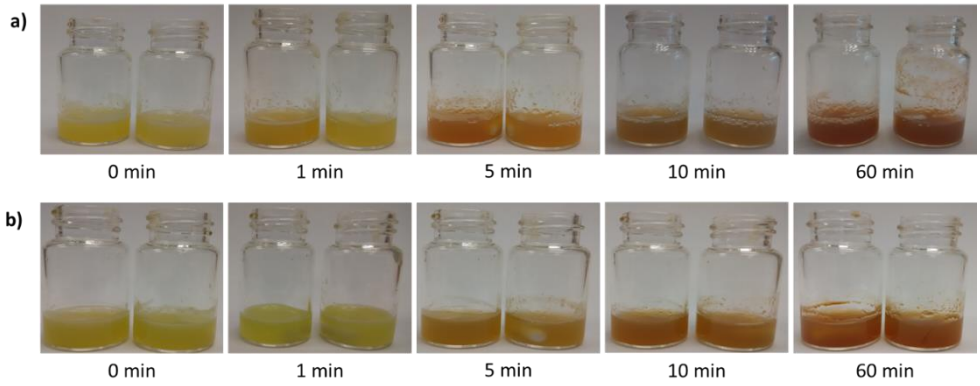

Figure S5. 5. *Colour evolution in an apple smoothie. (a) Golden Delicious without the material (left) and in the presence of 10 mg/mL of UVM7 (right). (b) Granny Smith without the material (left) and in the presence of 10 mg/mL of UVM7 (right).*

PAPER 4: INFLUENCE OF THE FUNCTIONALISATION OF MESOPOROUS SILICA MATERIAL UVM-7 ON POLYPHENOL OXIDASE ENZYME CAPTURE AND ENZYMATIC BROWNING

INFLUENCE OF THE FUNCTIONALISATION OF MESOPOROUS SILICA MATERIAL UVM-7 ON POLYPHENOL OXIDASE ENZYME CAPTURE AND ENZYMATIC BROWNING

Sara Muñoz-Pina[1], José V. Ros-Lis[2,3], Ángel Argüelles[1], Ramón Martínez-Máñez[3,4], Ana Andrés[1]

[1]*Instituto Universitario de Ingeniería de Alimentos para el Desarrollo (IUIAD-UPV). Universitat Politècnica de València Camino de Vera s/n, 46022, Valencia, Spain*

[2]*Inorganic Chemistry Department, Universitat de València. 46100, Burjassot, Valencia Spain.*

[3]*CIBER de Bioingeniería, Biomateriales y Nanomedicina (CIBER-BBN).*

[4]*Instituto Interuniversitario de Investigación de Reconocimiento Molecular y Desarrollo Tecnológico. Universitat Politècnica de València - Universitat de València. Camino de Vera s/n, 46022, Valencia, Spain.*

SUMMARY

Delving into the same strategy and chapter, this second article studies the influence of the functionalization of the UVM-7 on enzymatic browning.

Silica mesoporous materials have been proved to immobilise and inhibit the polyphenol oxidase enzyme, yet this effect is dependent both on the structural properties and on the functionalization of the supports. This enzyme is responsible for the enzymatic browning which happens in some fruit and vegetables causing adverse alterations in organoleptic, nutritional and colour. Since the acceptability of products by consumers is primarily dependent on colour and appearance, enzymatic browning has become an important goal of food processing. The drawbacks found

in the current techniques used to prevent the enzymatic browning have done those researchers still investigate new methodologies that do not alter food quality. Thus, the use of silica mesoporous materials could lead to a new type of PPO inhibitors.

As the modification of the surface of silica mesoporous materials influences their capability of interaction with the PPO, the aim of this work is to evaluate the impact of five different UVM-7 surface coating on the enzymatic browning. Model systems allow better control of experimental work and a better understanding of the influence of different factors. Thus, the effect of the support's functionalization on the inhibition power, the immobilization, and the pH over PPO were evaluated. Afterwards, the material with the best response was checked in apple juice.

The five functionalization groups selected for the study were two different amines, a carboxylic acid, an alkane, and an isocyanate for they diverse reactivity properties. The effect of these materials on enzymatic browning was studied in two different ways. First, it was observed whether the inhibitory effect occurred directly in the oxidation step of the substrate, thereby reducing the oxygen consumption; secondly, whether they interact more in the non-enzymatic polymerization reaction that forms melanoid compounds. In this scenario, it was found that 3 mg of U-NH_2 was capable of inhibiting by 50% the rate of oxygen consumption, thus interacting directly with the PPO enzyme. However, despite delaying the initial rate, the enzymatic browning did not change dramatically after one hour. On the other hand, functionalization had a positive effect on the reduction of time necessary to immobilize the PPO. All materials, except for U-EDTA, retained the PPO almost completely after 10 min of stirring, with an immobilization yield of 100% for U-NH_2. Nevertheless, this immobilization activity does not affect the PPO activity as supported by the result in the oxygen consumption and colour formation. U-NH2 was selected to study the effect of pH on enzyme-material interactions. In this case,

there was a clear dependence on the pH, being more abrupt when increasing the amount of material to 10 mg per 94 U. At pH 6.5 this material, although no capable of inhibiting the PPO, was able to crosslink the o-quinones formed by Michael-type addition of Schiff-base reaction leaving the solution colourless again. This effect was tested on a just made apple juice where again, the material could not stop the PPO but after removing it barely any change of colour was observed after 90 min.

Therefore, it has been proven that the functionalization of these materials is a key point in the interaction with polyphenol oxidase. By choosing well the functionalization of the material, not only the enzyme can be trapped, but also the products generated. In particular, UVM-7 functionalized with amino groups is well suited for this purpose.

Key words: PPO, tyrosinase, inhibition, UVM-7, amines, apple juice.

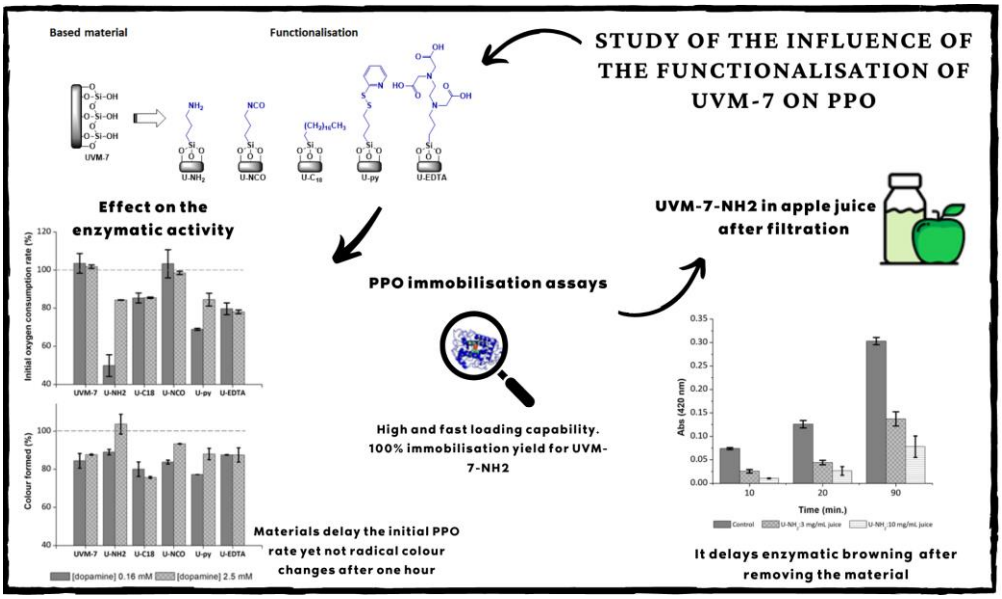

***Figure 5.23**. Graphical abstract of the influence of the functionalisation of UVM-7 on PPO*

1. Introduction

The polyphenol oxidase (PPO) enzyme, also known as tyrosinase (monophenolase activity EC 1.14.18.1 and diphenolase activity EC 1.10.3.1), is a relevant type 3 copper protein responsible for catalysing the O-hydroxylation of monophenols and converting them into O-diphenols and, subsequently, catalysing the oxidation of O-diphenols to produce O-quinones[60]. These *ortho*-quinones are particularly reactive and their polymerisation produces different coloured pigments (e.g. black, brown, or even red), which, in turn, cause enzymatic browning. Polyphenol oxidase was first discovered in the mushroom by Schoenbein in 1856. Since then, it has been subject to numerous studies[61]. Some of the main topics approached in those works are: PPO characterisation[62], medical interest[63], sensors[64], wastewater regeneration[65] or protein cross-linking and immobilisation[66].

In food technology[67], PPO is present in a wide variety of foods. Polyphenol oxidase can be one of the causes, for example, of changes in colour when fruit flesh and juice come into contact with oxygen. Enzyme mediated colour change is known as enzymatic browning and causes significant modifications in organoleptic, nutritional and colour properties, mostly in those foods with high percentages of tyrosinase and polyphenols.

Even though this reaction in some foods, like chocolate or tea, is essential and desirable[68], browning is undesirable in fruits or vegetable that have notable amounts of polyphenols. As consumers' acceptability of products depends mostly on colour and appearance, enzymatic browning has become a crucial target for food processing and, therefore, for the food industry.

Among the available techniques to prevent or avoid the enzymatic browning reaction, pasteurisation is the most widely used industrial method because it can

inactivate enzymes and destroy microorganisms simultaneously. Although pasteurisation guarantees the safety and shelf life of fruits and vegetables, application of high temperatures (between 60-90°C) may destroy some thermosensitive nutrients that are very common in these food matrices, such as vitamins, carotenoids and anthocyanins[33].

To avoid the negative effects of pasteurisation, the food industry has developed alternative methods to inactivate PPO, including high pressure[69], supercritical carbon dioxide[70], ultrasound[71], gamma irradiation[72] and adding certain chemical agents, such as acidulants[73]. Nonetheless, some of these techniques have not been completely transferred to the industry given their high cost and, in some cases, their major machinery requirements. Only the addition of some chemical agents, such as sulphites or acids that lower pH, has been widely used as an alternative to pasteurisation. Even though sulphites are powerful inhibitors of PPO, their use as food additives is not recommended because these compounds might cause allergenic reactions. In this scenario, research that has focused on finding new methodologies capable of inhibiting enzymatic browning without altering food quality is a relevant field.

From another point of view, nanotechnology has enabled much progress to be made in many fields, such as biomedicine[74], chemical sensors[75], etc. The food technology sector is no stranger to this revolution and has also shown an interest in finding nanotechnological solutions for a number of applications[76]. For instance, the interactions between nano-scale materials and proteins have been well studied[77] given the possibility of modulating enzyme activity or of modifying the enzyme structure and function[78]. Although the use of nano-scale materials, such as nanoparticles, can be an interesting tool to stop enzymatic browning in industrial food processing, this has been rarely addressed to date. In this context, Corell Escuin

et al. (2017)[45] reported the ability of mesoporous silica materials to immobilise the PPO enzyme, where pore size and pH were the major factors that affected their immobilising capacity. Along the same line, Muñoz-Pina et al. (2018)[79] studied the PPO inhibitory capacity of several thiol-functionalised mesoporous silica materials with different shapes and pore sizes. The UVM-7 material, a silica based MCM-41 type mesoporous material, which contains both mesopores and textural pores, has also been reported to be able to immobilise and inhibit polyphenol oxidase in both model and real systems[79].

Based on the hypotheses that the modification of the surface of the nanomaterials can influence the ability of the UVM-7 nanomaterials to immobilise PPO and to inhibit enzymatic browning, the aim of this work is to evaluate the influence of the surface coating in the modulation of the enzyme activity in model systems and the inhibition of enzymatic browning in apple juice.

2. Materials and methods

2.1. Chemicals

Tetraethyl orthosilicate (TEOS) reagent grade 98%, triethanolamine ($TEAH_3$) reagent grade 98%, N- cetyltrimethylammonium bromide (CTABr) for molecular biology ≥99%, 3-aminopropyl triethoxysilane (APTES) ≥98%, trimethoxy(octadecyl)silane technical grade 90% (GC), 3-triethoxysilyl propyl isocyanate 95%, 3-mercaptopropyl trimethoxysilane 95%, 2,2'-dipyridyl disulphide 98%, acetic acid glacial ReagentPlus ≥99%, mushroom tyrosinase lyophilized powder ≥1000 unit/mg solid, dopamine hydrochloride were provided by Sigma-Aldrich (Sigma-Aldrich, USA) and used without further purification. N-[(3-trimethoxysilyl) propyl]ethylenediamine triacetic acid trisodium salt 40% in water was provided by

Fluorochem (Fluorochem, UK). Sodium dihydrogen phosphate anhydrous extra pure and di-sodium hydrogen phosphate anhydrous extra pure were supplied by Scharlau (Sharlab S.L., Spain) and sodium acetate anhydrous for analysis ACS by Panreac (Panreac AppliChem, Barcelona, Spain). The mesoporous material UVM-7 was prepared following known procedures[80]. Following a modification of the so-called "atrane" route, a mixture of 0.05 mol of TEOS and 0.17 mol of $TEAH_3$ was heated at 120°C until no condensation of ethanol was observed in a Dean–Stark apparatus. Afterwards, the mixture was cooled down to 90°C and 4.56 g of CTABr were added, followed by 80 mL of water. The mixture was aged at room temperature for 24 h. The resulting precipitate was collected by centrifugation and washed with water. Lastly, the solid was dried at 70°C and calcined at 550°C under static air atmosphere, as an oxidant atmosphere, for 5 h to remove the CTABr surfactant.

Apples of the variety Golden Delicious were obtained from a local retailer and used to prepare juice.

2.2. Synthesis of the UVM-7 functionalised materials

Five materials were prepared with diverse functionalisations.

2.2.1 Synthesis of U-NH_2

One gram of calcined UVM-7 was treated with excess APTES (10 mmol) in 30 mL of acetonitrile (ACN). The suspension was allowed to react for 16 h at room temperature. Then the resultant solid was isolated by centrifugation, washed with ACN and finally dried at 37°C.

2.2.2 Synthesis of U-NCO

Solid U-NCO was prepared by allowing 1 g of calcined UVM-7 to come into contact with excess 3-(Triethoxysilyl) propyl isocyanate (10 mmol) in 30 mL of

acetonitrile. The suspension was allowed to react for 16 h at room temperature. Then U-NCO was isolated by centrifugation, washed with ACN and finally dried at 37°C.

2.2.3 Synthesis of U-py

For the synthesis of U-py, 1 gram of UVM-7 was reacted with 10 mmol of (3-Mercaptopropyl) trimethoxysilane in 30 mL of acetonitrile for 16 h. After isolation by centrifugation, the solid was washed with ACN and dried at 37°C. Afterwards, 250 mg of the resultant solid were resuspended in 8.5 mL of ACN containing 2.5 mmol of 2,2'-Dipyridyl disulphide and aged for 12 h. Lastly, the solid was isolated by centrifugation and subsequent washing with ACN.

2.2.4 Synthesis of U-C_{18}

Solid U-C_{18} was obtained by reacting 10 mmol of trimethoxy(octadecyl)silane and 1 g of UVM-7 in 30 mL of toluene. The mixture was reacted at room temperature for 16 h. The resulting solid was washed with methanol and dried at 37°C.

2.2.5 Synthesis of U-EDTA

Solid U-EDTA was prepared by adding 10 mmol of 40%n-[(3-trimethoxysilyl) propyl] ethylenediamine triacetic acid trisodium salt in water to 30 mL of a suspension of methanol containing 1 g of UVM-7. Four drops of acetic acid glacial were poured and the mix was aged for 16 h at room temperature. The solid was washed with water and acetone and was dried at 37°C.

2.3. Characterisation of the UVM-7 functionalised materials

The characterisation of the UVM-7 functionalised materials was carried out by low-angle X-ray powder diffraction (XRD), Bruker D8 Advance CuKα radiation), transmission electron microscopy (TEM, JEOL–jem-1010), nitrogen

adsorption/desorption isotherms and thermogravimetric analysis (TGA) and FTIR spectroscopy was carried out with a Bruker Tensor-27. Nitrogen adsorption/desorption isotherms were carried out in a Micromeritics ASAP 2010 automated sorption analyser at the liquid nitrogen temperature (-196°C.). Samples were degassed at 120°C in a vacuum overnight. The specific surface area was determined by applying the BET model[47] from the adsorption data within the low-pressure range. Pore size was calculated following the Barret-Joyner-Halenda model (BJH)[46] . From the XRD analysis[48], the a_0 cell parameter and the wall thickness of the silica materials were calculated (see Table 5.6). A TGA was used to estimate the concentration of the different functionalised chemical groups on the UVM-7 surface using an oxidant atmosphere (air, 80 mL/min) with a heating programme (10°C/min from 393 to 1273 K and an isothermal heating step at this temperature for 30 min).

2.4. Oxygen consumption

The initial oxygen consumption rate was followed by an Oxyview System from Hansatech during the oxidation reaction of the dopamine using a Clark Type Oxygen electrode. For this assay, the different synthesised materials (UVM-7, U-NH_2, U-NCO, U-py, U-EDTA and U-C_{18}) were used at the 3 mg/mL ratio in phosphate buffer (10 mM, pH 5.5). Solutions were sonicated for 5 minutes to acquire the materials' correct dispersion. One millilitre of the solution was allowed to come into contact with 0.25 mL of the PPO solution of 375 U/mL in the reaction vessel to be stirred for 10 minutes. Afterwards, 0.25 mL of dopamine was added. Two different dopamine concentrations were tested: 0.16 mM and 2.5 mM. The initial reaction rate was obtained from the slope of the linear part of the oxygen consumption curve during the first minutes. A control with no material was also studied. Assays were done in triplicate at 25°C.

2.5. Colorimetric determination of PPO activity

In a typical experiment, 3 mg of material were suspended in 1 mL of phosphate or buffer 10 mM at a defined pH of 5.5. After sonication, 0.25 mL of a tyrosinase solution of 375 U/mL was added and the mixture was aged for 10 min by stirring. Subsequently, 0.25 mL of dopamine solution 0.16 mM or 2.5 mM was/were added and the enzymatic reaction was left for 1 h. Then the suspension was centrifuged, and the supernatant was measured by spectrophotometry (Thermo scientific Helios-zeta) at 420 nm using 2.5 mL plastic cuvettes. The assays done in the absence of material were also carried out as the control. To test the influence of the pH, the same protocol was followed using phosphate-acetate 10 mM as buffer at pH 4.5, 5.5 and 6.5, to study the influence of pH. Assays were done in duplicate.

2.6. Material immobilisation capacity

The Bradford assay[52] was performed to study the capability of UVM-7 and the UVM-7 functionalised materials to immobilise PPO. For this purpose, 0.25 mL of a tyrosinase solution of 375 U/mL was allowed to come into contact with 3 mg of the corresponding mesoporous material suspended in 1 mL of phosphate buffer at pH 5.5. The resulting suspension was stirred for two different times (10 and 120 minutes) and then centrifuged (9600 RCF, 3 min). From the supernatant, two 100-mL aliquots were taken to perform the Bradford assay. The amount of free enzyme in solution was obtained by interpolation in a calibration line, obtained using tyrosinase from mushroom. The immobilisation yield was calculated according to Equation (1), where P_0 and P_i were the amounts of protein present in the solution in the presence and absence of the material, respectively, calculated from the calibration line. An ANOVA test was used to determine significant differences.

$$Immobilisation\ yield\ (\%) = \frac{P_0 - P_i}{P_0} * 100 \qquad (1)$$

From the rest of the supernatant, 900 mL were taken and allowed to come into contact with 180 mL of dopamine 15 mM to determine residual enzyme activity. Measurements were taken every 10 seconds at 420 nm. Assays were done in triplicate. Relative activity was calculated according to Equation (2), where V_{o0} is the control initial rate and V_{oi} is the initial rate obtained for the different samples.

$$Relative\ activity\ (\%) = \left(\frac{V_{0i}}{V_{0_0}}\right) * 100 \qquad (2)$$

2.8. Material testing in apple juice

Apples of the cv. Golden Delicious variety were first washed and then liquefied in a Moulinex centrifugal JU200045. A 2-mL aliquot of the freshly liquefied juice was taken and mixed with two different amounts of U-NH_2 (20 mg and 6 mg). Simultaneously, another 2-mL aliquot with no material was used as the control sample. These blends were stirred at 400 rpm for 1 minute. Subsequently, the different samples were filtrated under vacuum using Whatman filter paper grade 41 to eliminate the mesoporous material. The new aliquots continued to be stirred and colour changes were followed by image taking. In order to measure enzymatic browning, 200 µL of the filtered juice were diluted in 1 mL of water and the colour change was followed by measuring the absorbance at 420 nm in a Thermo scientific Helios-zeta. An ANOVA test was used to determine significant differences.

3. Results and discussion

3.1. Materials selection and characterisation

We recently reported that calcined UVM-7 material can inhibit enzymatic browning better than other silica-based mesoporous materials such as MCM-41 with nanometric or micrometric particle size or aerosil[45]. We also observed that this

browning inhibition can be modulated by the functionalisation of the silica surface. Furthermore, silica materials functionalised with thiol groups can fully inhibit enzymatic browning in apple juice[79]. In order to gain further insight into the enzymatic browning process and in an attempt to improve the use of the UVM-7 mesoporous support to immobilise and inhibit enzymatic browning, five materials were herein prepared that consisted of UVM-7 supports functionalised with two different amines (APTES and pyridine; materials U-NH_2 and U-py, respectively), carboxylic acid (EDTA; material U-EDTA), an alkane (C_{18}; material U-C_{18}) and an isocyanate (material U-NCO) (see Figure 5.24). These functional groups showed diverse charge, reactivity and supramolecular binding properties. Propyl isocyanate was chosen for its ability to react with different nucleophiles, including the amines and alcohols usually present in the residues of proteins[81]. The functionalisation with amines or carboxylic acids resulted in polar charged surfaces that can be modified with variations in the pH of the solution. In this context, APTES has been widely used to immobilise proteins[82]. The metal chelating properties of the amino and carboxylate groups can result in the coordination, or eventually in the demetallation, of the two copper active centres in PPO, with the consequent decrease in the enzymatic activity. Also, the long chain alkane derivative (C_{18}) offers to study the influence of a hydrophobic surface.

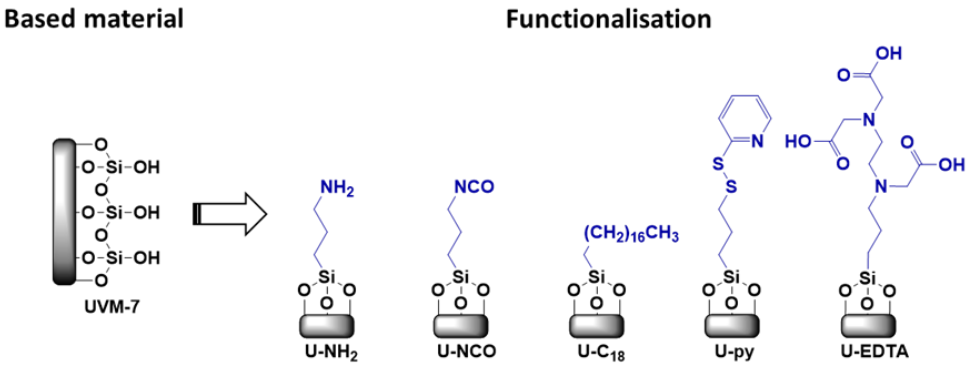

Figure 5.24. *Illustration of the functional groups attached to the UVM-7 support and tested against the PPO enzyme.*

X-ray powder diffraction and TEM techniques were used to confirm the mesoporous structure of the starting UVM-7 and the final functionalised materials. The XRD pattern of the UVM-7 solid showed low-angle reflection, which is related to a hexagonal array of pores indexed as a (100) Bragg reflection, and characteristic of UVM-7 materials. The five surface-modified materials (U-NH_2, U-py, U-NCO, U-EDTA and U-C_{18}) maintained the X-ray powder diffraction pattern observed for the calcined support (UVM-7), which agrees with the maintenance of the mesoporous structure during the functionalisation process (Figure S5.6). d_{100} spacing was calculated for all the materials using the data from the X-ray powder diffraction experiments. As seen in Table 5.6, the d_{100} spacing values were around 43 Å in all cases, which coincides with other reported values[83]. The hexagonal porous structure was also confirmed by TEM (Supplementary Material, Figure S5.7). The TEM images also indicated that no substantial changes occurred in the structure of the support after functionalisation.

The TGA (Supplementary Material, Figure S5.8) revealed that the amount of organic content varied among the diverse materials. As seen in Table 5.6, the amount of organic matter ranged from 0.16 to 2.95 mmol (g SiO_2)$^{-1}$ for U-NCO and U-NH_2,

respectively, which are similar values to those found for other reported UVM-7-functionalised materials[75]. Although functionalisation did not modify the structure of the support, it strongly impacted the specific surface area and porosity. The calcined material (UVM-7) had a specific surface area that came close to 900 $m^2\ g^{-1}$, which had a bimodal porous system with pores of 2.7 nm (mesopores) and 40 nm (textural porosity). The specific area slightly reduced due to the organic functionalisation for U-C_{18}, U-NCO and U-py. However, the material with the highest number of moles of organic molecules per gram of solid (U-NH_2) drastically dropped in the total specific area, with a value of 216 m^2g^{-1}. Even stronger is the blocking effect observed for U-EDTA (119 m^2g^{-1}), a material with an organic content of only 0.97 mmol (g SiO_2)$^{-1}$). This behaviour can be explained keeping in mind that while the organic residue in the U-NH_2 contains three carbon and one nitrogen atoms, in the U-EDTA material the organic residue shows eleven carbon, two nitrogen and four oxygen atoms, therefore a much bigger molecular volume per molecule.

From Table 5.6, we can observe that this reduction in the specific area for both U-NH_2 and U-EDTA was also accompanied by a reduction in the mesopore volume, while only minor variations were noted for the textural pore volume. It seems that only those materials loaded with the highest amount of organic groups (U-NH_2 and U-EDTA) were able to block the little size mesopores with approximately 2.7 nm of diameter. However, they cannot block to the same extent big size textural pores with a diameter close to 40 nm (see Table 5.6). We must consider that the short length of the organic chains (up to 18 carbons) is not able long enough to block a pore with a radius close to 20 nm.

Table 5.6. *Textural properties and organic content of the UVM-7 silica matrix as-made, calcined, and functionalised.*

Material	Area [a] (m^2g^{-1})	Mesopore volume[b] (cm^3g^{-1})	Mesopore diameter[b] (nm)	Textural pore diameter[b] (nm)	Textural pore volume[b] (cm^3g^{-1})	mmol /g SiO_2	d_{100}[c](Å)	2θ[d] (^{0})	a_0[e] (Å)	dw[f](Å)
UVM-7 As made	-	-	-	-	-	-	44.8	1.97	51.7	-
UVM-7 calcined	909.4	0.72	2.71	39.6	0.96	-	43.9	2.01	50.7	23.6
U-NH_2	251.6	0.15	2.62	37.5	0.62	2.95	44.8	1.97	51.7	25.5
U-C_{18}	819.7	0.64	2.65	35.3	0.79	0.16	43.9	2.01	50.7	24.2
U-NCO	831.2	0.56	2.47	34.3	0.69	0.85	42.3	2.09	48.8	24.1
U-py	835.6	0.63	2.57	31.4	0.67	0.29	42.3	0.13	48.8	23.1
U-EDTA	118.5	0.07	2.74	36.0	0.36	0.97	43.1	0.93	49.8	22.3

[a] BET specific surface calculated from the N^2 adsorption-desorption isotherms.

[b] Pore volumes and pore size (diameter) calculated from the N^2 adsorption-desorption isotherms.

[C] Diffraction peak of the reticular plane 100 calculated by $2d_{100}\,sen\theta=n\lambda$

[d] Angle of incidence for the reflection plane

[e] The cell parameter calculated by $a_0=2d_{100}*(\sqrt{3})^{-1}$

[f] Wall thickness was calculated by $dw= a_0 - d_p$, where d_p is the pore diameter.

3.2. Studies of PPO activity in the presence of the UVM-7 functionalised materials

Enzymatic browning is a two-step process comprising first the PPO-mediated oxidation of the substrate (typically phenols or catechols) to quinones by oxygen, followed by non-enzymatic polymerisation that generates the final brown melanoid products. Thus, to characterise the PPO enzymatic response in the presence of the functionalised UVM-7 materials, two sets of assays were carried out. Firstly, oxygen consumption due to the PPO catalysed dopamine oxidation was determined by the Oxyview system and the main kinetic parameters of the reaction were calculated from the initial reaction rate. Secondly, the colour formed during the 1-hour reaction was measured as an approach to see the effect of inhibition in the long term. Similar experiments were run with the non-functionalised UVM-7 material. Moreover, measurements were taken in the absence of nanomaterials and were included as a reference.

Figure 5.25a and 5.25b contain the enzymatic activity measured by the two methodologies. The activity in the absence of material was used as a reference (100%). For the sake of clarity, a dashed line was added to indicate this value.

As seen in Figure 5.25a, the initial oxygen consumption rate in the presence of the non-functionalised UVM-7 led to no significant differences in the values observed in the absence of material (100%). This indicates that the presence of UVM-7 does not interfere in the first enzymatic browning stage when oxygen is consumed during polyphenols oxidation. The same behaviour was observed for U-NCO. However, when PPO came into contact with U-C_{18} or U-EDTA, the oxidation rate of dopamine dropped by 20-25% regardless of the amount of the substrate present in the medium. On the contrary, U-py or U-NH_2 showed differences with the substrate (i.e. dopamine) concentration. At high dopamine concentrations, over the Michaelis

constant (K_M), the initial reaction rate dropped by around 20%, but the rate fell 50% for U-NH_2 and 30% for U-py at lower dopamine concentration.

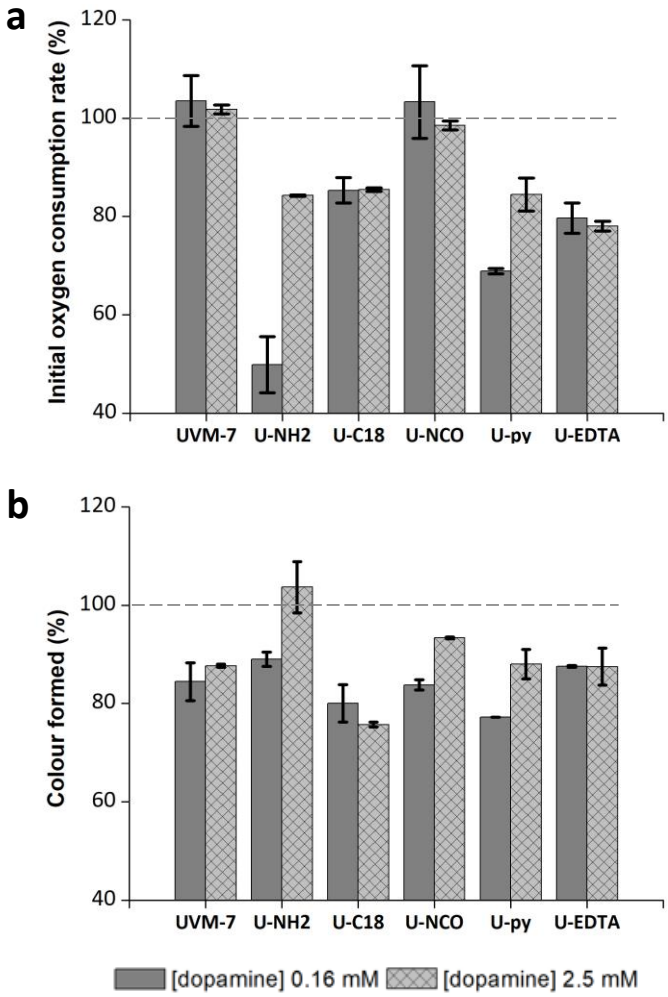

Figure 5.25. *PPO enzymatic response (93.75U) in the presence of 3 mg of functionalised and non-functionalised UVM-7 in the presence of two different substrate concentrations. (a) Initial oxygen consumption speed. (b) Colour formed*

after a 1-hour reaction between PPO and dopamine in the presence of the different materials.

The dependence of the rate inhibition on the substrate concentration found for U-NH_2 and U-py, and the fact that inhibition was greater when the substrate concentration was low, suggests a competitive inhibition mechanism. In this kind of mechanism, the material and substrate would compete for access to the binuclear copper active centre and the formation of the enzyme-substrate or the enzyme-inhibitor complex. In this kind of systems, the increase in the substrate concentration displaces the inhibitor modifying the relative activity. Otherwise, the inhibition rate would be the same, regardless of the substrate concentration, as observed for U-C_{18}, for example. Furthermore, this evidences that U-NH_2, in particular, can lower the initial rate of the PPO-mediated oxidation reaction by slowing down the process, at least for short times.

In order to evaluate the enzymatic response for long times in the presence of mesoporous materials, the enzymatic reaction between dopamine and PPO was allowed to continue for 1 h and the absorbance at 420 nm measured after centrifugation (Figure 5.25b). Even though the initial conversion rate of polyphenols was delayed in some cases, it would seem that enzymatic browning did not dramatically change after 1 h with any of the studied materials. Once again, supports UVM-7, U-C_{18} and U-EDTA showed the same response with both large and small amounts of substrate in the medium (about 85 %). In contrast, U-py and U-NH_2 responses were substrate/concentration-dependent.

3.3. PPO immobilisation assays

As noted above, the UVM-7 mesoporous material is characterised by having a bimodal porous system that renders material advantages for enzyme

immobilisation compared to other mesoporous materials. By way of example, the well-known mesoporous silica MCM-41 has difficulties to immobilise large enzymes given its relatively small pore size[84]. In contrast, Tortajada et al. (2005)[85] reported the ability of UVM-7 to load small enzymes into its mesopores, and also the ability to immobilise larger proteins in the textural pores between nanoparticles. These authors also showed a fast adsorption rate and high enzyme loading for bimodal UVM-7 silica. The advantage of this special topology of the UVM-7 material with PPO has also been demonstrated in calcined and thiol functionalised UVM-7[79].

To better understand the mechanism of inhibition and to evaluate the capacity of the materials to immobilise PPO, the Bradford method was used to quantify the amount of protein that remained in the solution after coming into contact with the supports. Two contact times (10 and 120 minutes) between the enzyme and silica materials were evaluated.

Table 5.7 provides the results of the immobilisation tests. In general, all the functionalised materials (except for U-EDTA) offered immobilisation yields higher than 80%, even at times as short as 10 minutes. Thus, the materials show an interesting ability to capture the mushroom tyrosinase from the solution.

Table 5.7. *Percentage of the immobilisation of enzymatic activity and the residual activity of the enzyme in the supernatant.*

Material	Immobilisation yield (%)		Relative activity (%)[a]	
	10 min	2h	10 min	2 h
UVM-7	59 ± 6	92 ± 10	5.9 ± 1.4	1.52 ± 0.16
U-NH_2	100 ± 2	104 ± 8	0.4 ± 0.05	0.40 ± 0.10
U-C_{18}	90 ± 10	90 ± 4	0.07 ± 0.05	0.09 ± 0.05
U-NCO	88 ± 3	88 ± 6	1.1 ± 0.2	0.47 ± 0.09
U-py	80 ± 10	104 ± 18	0.31 ± 0.06	0.25 ± 0.05
U-EDTA	-	-	63 ± 3	70.0 ± 1.6

[a] Activity measured in the supernatant after the removal of the material loaded with the immobilised enzyme.

The different behaviour noted for U-EDTA could be due to the high concentration of the carboxylic groups in the nanomaterial, which would endow the particle a negative charge under the given conditions. This charge could influence the interaction between the material and the enzyme, which would hinder adsorption. It seems that the functionalisation could have a positive effect on the reduction of the time necessary to immobilize the tyrosinase. For the non-functionalised UVM-7, the immobilisation of PPO is slower than for the functionalised materials, with an immobilization yield of 59 % at 10 minutes that reach 90% when the contact time was 2 h (see Table 5.7). No significant differences for $p < 0.005$ were found in the immobilisation yield between both contact times for the other materials. This implies that the functionalisation of UVM-7 improves the speed of enzyme's immobilisation with values over 80% for U-C18, U-NCO and U-py, which was complete (100%) for U-NH_2. This result agrees with other authors who, for instance, achieved the almost complete immobilisation of other enzymes using supports functionalised with amino groups as anchors[84,86].

Furthermore, we performed an experiment to verify if the solution had free enzyme and it maintained its activity in solution after the exposition to the material. For this purpose, tyrosinase was exposed to the material, followed by the material removal loaded with the immobilized enzyme. The activity assay of the supernatant (900 µL) was tested by adding 180 µL of dopamine 15 mM and measuring the initial activity rate spectrophotometrically with the variation of absorbance at 420 nm. As seen in Table 5.7 (% relative activity columns), those materials with high immobilisation capabilities (i.e U-NH_2, U-C_{18}, U-NCO and U-py) offered minimal residual enzyme activity in the supernatant, which coincides with the results obtained in the immobilisation tests. For the assay carried out with non-functionalised UVM-7, the supernatant showed certain activity after at a 10-minute contact time, which confirms that this material needs longer times to completely immobilise the enzyme. Furthermore, as expected from the immobilisation yield, U-EDTA presented the most activity, but also a drop of about 35% in relative activity compared to the sample that did not come into contact with the materials. This finding suggests that the material could induce certain enzyme inhibition, even if not immobilised.

As can be deduced from the data the materials offer a strong tendency to capture the tyrosinase, but the enzyme maintains a significant activity, even when it was immobilised on the UVM-7 functionalised materials. This is supported by the high immobilisation yields close to 90-100 % (see Table 5.7) but a reduction in the oxygen consumption and absorbance at 420 nm (see Section 3.2) of only 20 to 50 %. Moreover, the confirmation of the activity of the enzyme on the material is supported by an inhibition around 99% for the supernatant after removing the material loaded with the enzyme for most of the materials.

3.4 Effect of pH on the material-PPO interaction.

Mesoporous material U-NH_2 showed the best PPO inhibitory properties and was the only support to slow down the initial oxygen consumption due to the oxidation of dopamine up to 50% at a low substrate concentration. Its immobilising power was the highest effective and fastest of all the studied materials. For this reason, this functionalised UVM-7 support (U-NH_2) was selected for further study the effect of pH on the nanomaterial-enzyme interaction. Three different pH values were evaluated using phosphate-acetate 10 mM buffer (4.5, 5.5 and 6.5) to explore the usual pH range in fruits and vegetables. Furthermore, U-C_{18}, a material lacking pH-sensitive groups, was also used for comparison purposes. Two concentrations of material were used (3 mg/93.75U, Figure 5.26a) or high (10 mg/93.75U, Figure 5.26b) to study the influence of the concentration of the material in the inhibition capability. In all the cases the material, the enzyme and the substrate were put in contact together and the browning measured in the supernatant after centrifugation.

The results are summarized in Figure 5.26. At a first glance, we can observe that the material U-NH_2 offers a behaviour much more dependent on the pH than the alkyl functionalised homologous U-C_{18}. As the pH basifies the absorbance at 420 nm in solution decreases. It shows the same tendency at the two concentrations of material, although the variation with the pH increases with the amount of material present.

As can be seen in Figure 5.26 and the picture inserted in Figure 5.26b, at pH 4.5 and after centrifugation, the solution shows values of relative absorbance close to 100% and the U-NH_2 material presents a white colour. This suggests that at pH 4.5 the U-NH_2 material would offer a weakened tendency to immobilise the enzyme. The isoelectronic point of PPO is sited around pH 5[87] and, therefore at pH 4.5, a certain

repulsion between the PPO enzyme and the positive charges of protonated amino groups was expected to preclude immobilisation. This effect would diminish at less acidic pH. At pH 6.5 the suspension containing 10 mg of U-NH_2 developed an intense dark brown colour. However, upon centrifugation, a black precipitate and a slightly coloured solution were obtained, which suggests that the brown molecules generated during polymerisation remained adsorbed in the material. This behaviour can be observed also in the system containing 3 mg of U-NH_2 although to a minor extension. This unexpected phenomenon can be explained by the reaction that can take place between the catechol and the primary amines in the support. In fact, Yang et al. (2016)[88] described that the crosslinking between o-quinones and primary amines results in the formation of more than 60 compounds in just a few minutes via Michael-type addition or Schiff-base reactions.

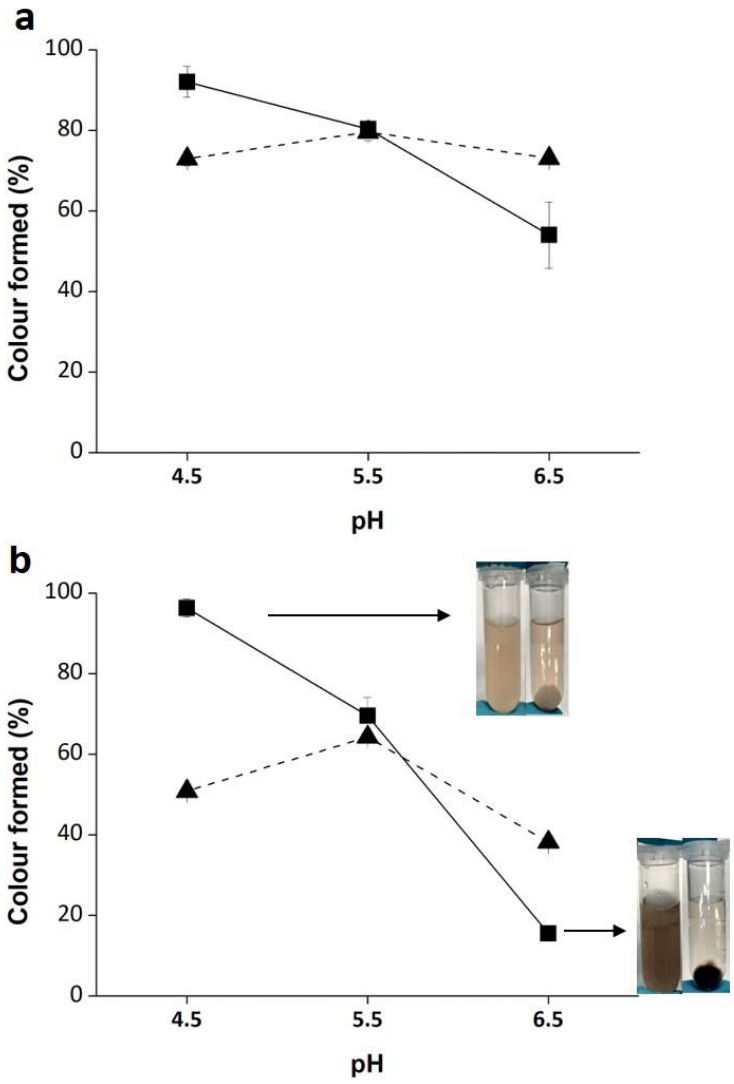

Figure 5.26. *Colour formed after a 1-hour reaction between 93.75U of PPO and 0.16 mM of dopamine in the presence of the different materials and after centrifugation. (a) [material]= 3mg. (b) [material]= 10mg. Material: (■) U-NH_2, and (▲) U-C18.*

These processes are both fast and complex and have been employed to synthesise polymers[89]. Hence the o-quinones formed in our sample could react with the primary amine from U-NH_2 to form polymers that remain attached to particles by leaving the solution colourless when the material is removed. Therefore, the U-NH_2 immobilisation capability to immobilise the PPO enzyme was complemented with the ability of the anchored amines to react with the oxidized quinones to leave the solution colourless after centrifugation or filtration.

3.5 U-NH_2 performance in apple juice

The performance of U-NH_2 particles in apple juice was tested to estimate the enzymatic browning inhibition of this material in food samples. When the mesoporous particles coated with amino groups were stirred with the recently made liquefied apple juice (3 mg/mL), no differences could be seen by the naked eye, and the measured colour differences were not significant ($p < 0.05$). This indicates that U-NH_2 is unable to inhibit enzymatic browning in apple juice when the nanomaterial is added to the liquefied sample.

However, when considering the great immobilisation power of this material as explained above, another test was done by removing particles from the medium by vacuum filtration using Whatman filter paper grade 41 after 1 minute. The result (Figure 5.27A and 5.27B) revealed that, in the presence of 3 mg/mL of U-NH_2, the colour generated by enzymatic browning (measured as the absorbance at 420 nm) diminished by more than 50% after 90 minutes compared with the control. Furthermore, when the amount of material was increased to 10 mg, no change in colour by the naked eye was observed in the filtered juice for the first 20 minutes and absorbance values went below 0.5. Only after 90 minutes was a light orange colour noted which corresponded to an absorbance of 0.8, which was only 25% of the control after the same reaction time.

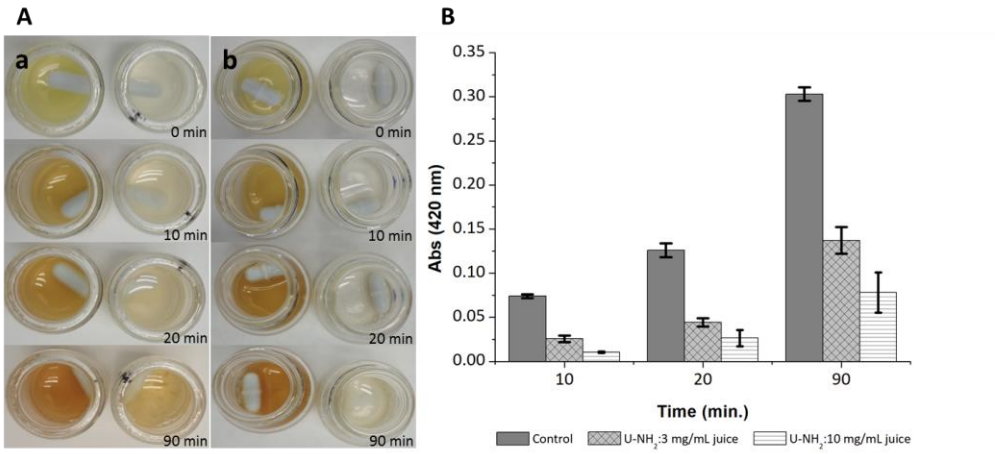

Figure 5.27. *A) Colour evolution in the Golden delicious apple juice filtered, followed by images. (a) 3 mg of U-NH_2/mL juice. (b) 10 mg of U-NH2/mL juice. B) Colour difference of the filtered apple juice over time, and previously treated with 3 mg of U-NH_2/mL juice and 10 mg of U-NH_2/mL juice versus the control measured spectrophotometrically.*

The absence of significant enzymatic browning after the filtering of the material reveals that particles remove the enzyme from the juice by avoiding the oxidation and polymerisation of substrates.

4. Conclusions

Five UVM-7-based materials with diverse functionalities (amine, carboxylic acid, alkane and isocyanate) were prepared and their influence on the enzymatic browning process was studied. Functionalisation strongly influenced the immobilisation of the enzyme. The negatively charged surface generated by carboxylic acid induced a reduction of immobilisation capability. On the contrary, the other functionalisations improved the immobilisation of the enzyme, particularly

with short contact times (10 minutes) by reaching 100% enzyme immobilisation for the U-NH_2 material. However, despite the fast and high loading capability, the enzyme immobilised on the material retained a certain degree of activity. When the materials continued to be in contact with solutions, PPO activity remained around 80% and only U-NH_2 offered inhibition that came close to 50% in oxygen consumption at a low dopamine concentration (0.16 mM). So this material is more suitable for tests done in food samples. When the material was removed from the solution, before adding the substrate, full enzymatic browning inhibition was observed for most of the materials, which agrees with the high PPO immobilisation yield. The experiments performed in fresh apple juice with U-NH_2 revealed that the material offered a suitable approach to inhibit enzymatic browning if the material came into contact with the liquefied apple juice when it was prepared and removed 1 minute later. Hence these materials can be used to immobilise and remove PPO from juices and to avoid the enzymatic browning process. In particular, the amine-containing material is well-suited for such purpose as it seems able to capture not only the enzyme, but also products from oxidation.

Acknowledgements

The authors are grateful to the Spanish Government (Projects RTI2018-100910-B-C44 and MAT2015-64139-C4-1) and the Generalitat Valencia (Project PROMETEO/2018/024) for support.

SUPPLEMENTARY MATERIAL

Materials synthesis

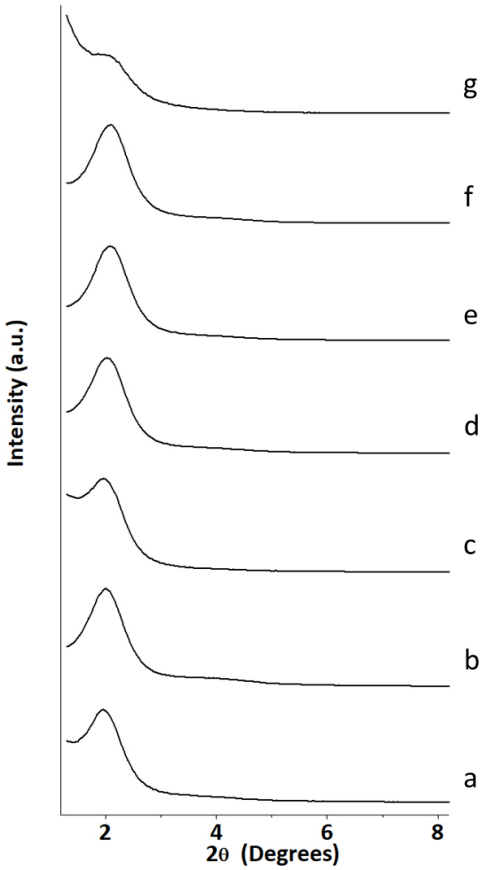

Figure S5. 6. *The powder X-ray diffraction patterns of the (a) UVM-7 as made, (b) calcinated UVM-7, (c) U-NH_2, (d) U-C_{18}, (e) U-NCO, (f) U-py and (g) U-EDTA.*

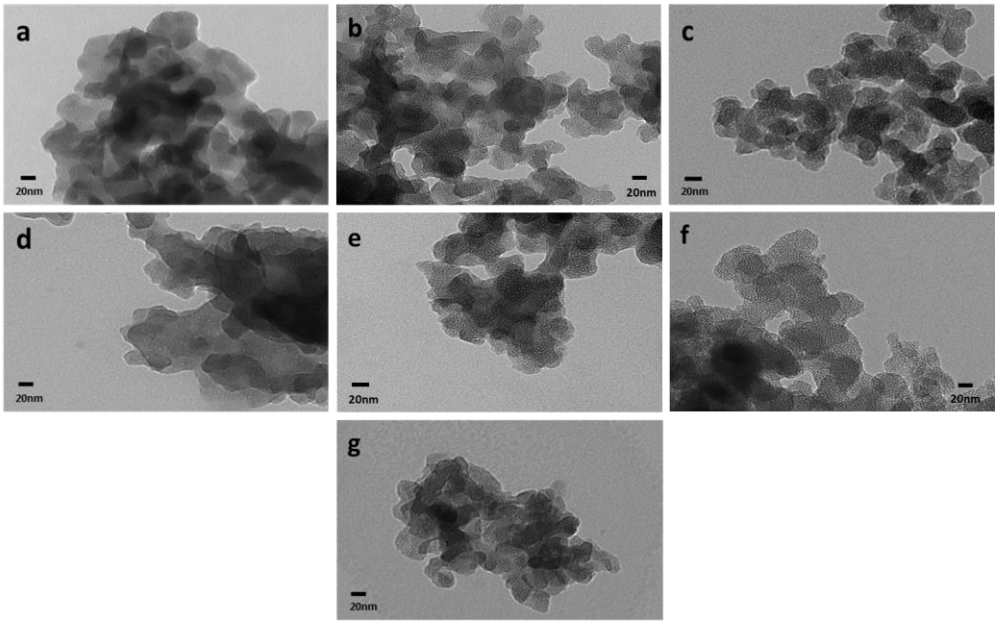

Figure S5. 7. *Representative TEM images of (a) UVM-7 as made, (b) calcinated UVM-7, (c) U-NH_2, (d) U-C_{18}, (e) U-NCO, (f) U-py and (g) U-EDTA.*

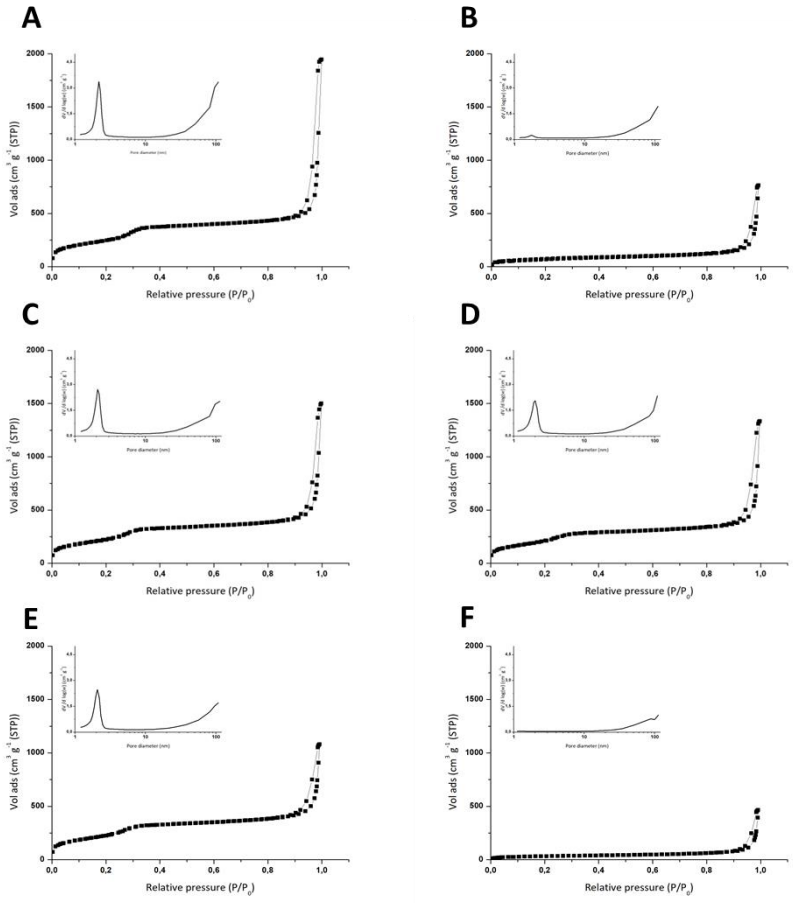

Figure S5. 8. *Nitrogen adsorption-desorption isotherms of the supports. (A) UVM-7, (B) U-7-NH_2, (C) U-7-C_{18}, (D) U-7-NCO, (E) U-7-py and (F) U-7-EDTA. Inset: BJH pore size distribution calculated from adsorption isotherm.*

PAPER 5: BIOACTIVE COMPOUNDS AND ENZYMATIC BROWNING INHIBITION IN CLOUDY APPLE JUICE BY A NEW MAGNETIC UVM-7-SH MESOPOROUS MATERIAL

BIOACTIVE COMPOUNDS AND ENZYMATIC BROWNING INHIBITION IN CLOUDY APPLE JUICE BY A NEW MAGNETIC UVM-7-SH MESOPOROUS MATERIAL.

Sara Muñoz-Pina[1], Aitana Duch-Calabuig[1], Elia Ruiz De Assín David[1], José V. Ros-Lis[2], Pedro Amoros[3], Ángel Argüelles[1], Ana Andrés[1]

[1] *Instituto Universitario de Ingeniería de Alimentos para el Desarrollo (IUIAD-UPV). Universitat Politècnica de València Camino de Vera s/n, 46022, Valencia, Spain.*

[2] *REDOLí, Departamento de Química Inorgánica, Universitat de València, 46100, Burjassot, Valencia Spain.*

[3] *Instituto de Ciencia de Materiales, Universitat de València, C/Catedrático José Beltrán 2, 46980 Paterna Valencia, Spain*

SUMMARY

Finally, the last work of this Doctoral thesis collects the two best functionalisation studied so far in a new synthesised magnetic material (M-UVM-7) to evaluate the effect of the treatment on the bioactive compounds of the juice.

Among the wide variety of foods on the market, fruits and vegetables are known for their high supply of dietary fibre, polyphenols, vitamins, and minerals. However, their elevated concentrations of polyphenols make them highly exposed to enzymatic browning. As this reaction, catalysed by the polyphenol oxidase enzyme, starts when there is a break on the food tissue, is not surprising that the juice industry has adopted different methodologies to prevent it. However, the filtration to clarify the juice provokes a significant loss of most bioactive compounds. On the other hand, the use of thermal treatments like pasteurization also affects thermosensitive compounds like vitamins. In this way, it has been proved the use of

mesoporous materials for the inhibition of the PPO as well as for delaying the enzymatic browning in apple juice. However, in order to remove the material, it is necessary to filtrates the juice, altering its nutritional value. Furthermore, the effect of these materials on bioactive compounds has not been evaluated either.

Therefore, the present work focuses on the synthesis of a magnetized UVM-7 material by incorporating magnetic nanoparticles into its structure to facilitates its elimination. In this sense, cloudy apple juice was selected to be treated with the material and its effect on the nutritional composition was measured. After properly characterizing the material, we proceeded to functionalize with the two best functionalization studied so far in this thesis.

As a first approach, the PPO of the juice was characterized. It was determined that the maximum PPO enzyme activity was reached after the first 10 minutes of its preparation. Besides, the optimal [material]/PPO ratio was determined to be 15 mg/mL. The effect of these materials on the physicochemical parameters of the juices was also studied. No significant changes in pH or TSS were detected for the non-functionalised and M-UVM-7-SH supports. However, a sharp rise in pH was noticed when the sample was treated with the amino-functionalized material. Regarding the effect of the enzymatic browning on the bioactive compounds, was revealed that the oxidation was highly correlated to the flavonoid content. Moreover, this undesirable reaction also impacted the total phenolic content, total flavonols, and total antioxidant capacity. The samples treated with the non-functionalized support, unfortunately, did not affect the process reaching similar values that those found for the control. In turn, the amine groups negatively affected the juice, since in some cases it accelerated the loss of bioactive compounds (DPPH, FRAP, flavonoids and flavonols). The only material capable of retarding by 70% the colour change was the M-UVM-7-SH. This reduction also causes a decrease

in the loss of nutrients from the juice. The oxidation of vitamin C is relieved as well as the loss of flavonoids. Finally, although the TPC and DPPH were still affected, the final content was higher than the control after treatment.

From the obtained results, it can be concluded that the magnetization of the UVM-7 facilitates the elimination of the material without removing the studied bioactive compounds of the juice. Moreover, the functionalization with thiol groups stopped the loss of vitamin C and the flavonoids of the juice, mitigating, also, the loss of total polyphenols and the antioxidant capacity.

Key words: Magnetic UVM-7, thiols, Enzymatic browning, Inhibition, Apple juice, Bioactive compounds.

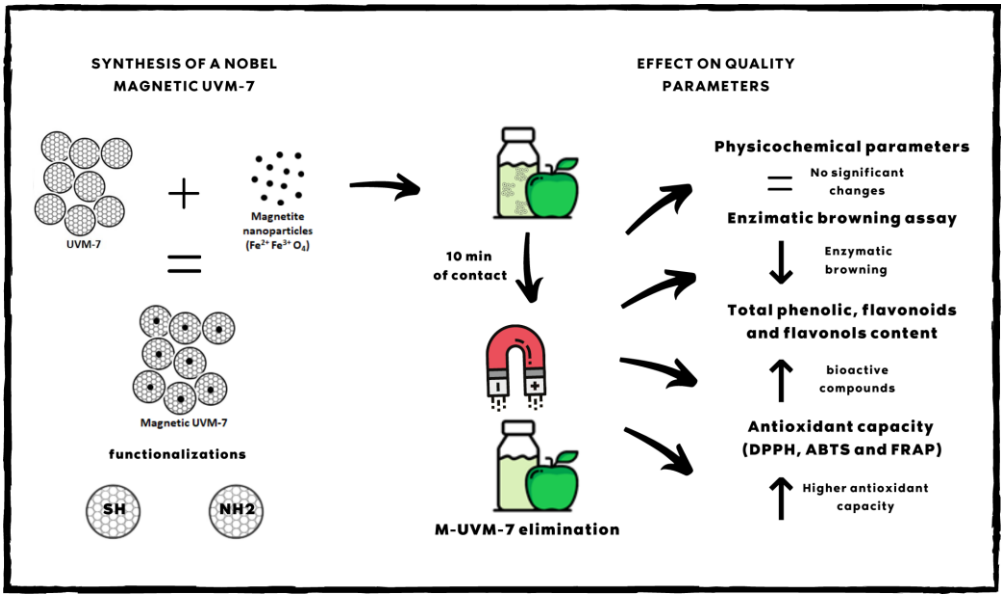

Figure 5.28. *Graphical abstract of the study of enzymatic browning and nutritional value in the presence of a new magnetic UVM-7-SH material.*

1. Introduction

Fruits and vegetables include a wide and diverse group of plant foods whose energy and nutritional content varies remarkably between the different species. Indeed, these type of food are known for they important concentrations of vitamins, minerals, and phytochemicals that function as antioxidants, and anti-inflammatory agents[90]. Within this wide variety, apples (*Malus Domestica*) are the second fruit most consumed in the European Union and the third most cultivated worldwide (86 million tons in 2018) (FAOSTAT, 2018). While a large portion of apples are consumed fresh (70%), 20 % of the total are meant for processed products as juices or dehydrated fruits[91]. Besides, apples are an important source of phenolic compounds including flavonoids (such as flavonols: principally quercetin glycosides and flavanols: catechins and epicatechins) and phenolic acids (such as chlorogenic acid, gallic acid, and caffeic acid)[92]. Traditionally, apple juice has been commonly consumed as clear juice, unfortunately, the clarification process implies the loss of about 50-90% of these compounds[93]. The growing tendency to consume fresher and minimally processed foods has increased sales of cloudy juices with a much higher concentration of polyphenols[94]. Nevertheless, the elevated amounts of these bioactive compounds make them highly susceptible to enzymatic browning and a problem for the industry to assure colour stability [93].

The browning of cloudy apple juices is mainly due to the polyphenol oxidase enzyme (PPO). PPO compromises diverse copper-containing enzymes (catechol oxidase (EC 1.10.3.1), tyrosinase (EC 1.14.18.1), and laccase (E.C. 1.10.3.2)), and is wildly distributed in nature: animals, plans, and fungi [60]. Depending on the nature of the PPO, this enzyme can catalyse two different reactions. In the first place the hydroxylation of monophenols to *o*-phenols, and in the second place the oxidation of the *o*-phenols into quinones. Quinones are very reactive compounds that

polymerise with other quinones, amino acids, or proteins generating reddish-brownish pigments called melanonids, which are the reason for colour change[95]. This process, known as enzymatic browning, is not unique to apples but is the main cause of colour change in fruits and vegetables. Since the main factors that enhance the PPO activity and therefore the enzymatic browning are the concentration of polyphenols and the active enzyme, fruits and vegetables are the most affected foods. This reaction starts when there is a cell disruption in the matrix and PPO, polyphenols, and oxygen meet[96]. This tissue damage usually happens during harvesting, handling, and post-harvest processing like in the juice industry.

The colour change caused by enzymatic browning can cause consumer rejection, leading to food waste and economic losses. To minimize the problem, the food industry has adopted different methodologies to prevent enzymatic browning. Thermal pasteurization has been the gold standard to prevent both enzymatic browning and destroying microorganisms. However, the application of temperatures between 60 and 90°C results in undesirable sensorial and nutritional changes due to the damage of volatile and thermosensitive compounds [97]. Other no-thermal treatments have been developed over the years to replace pasteurization. Ultrasounds, CO_2 supercritical, ultraviolet radiation, or high hydrostatic pressure are some of the alternatives, nonetheless, negative effect on food properties or the high cost have restricted their implementation [20].

In recent years, the implementation of nanotechnology in the food industry has had a prominent growth with good results. However, these studies have been focused mainly on encapsulation and packaging, but not on industrial processes. Thus, in order to find a new solution to this challenge, our working group has proved the use of silica mesoporous nanomaterials as candidates for PPO inhibition. The material UVM-7 functionalised with thiol groups was able to both immobilise and

inhibit polyphenol oxidase in model systems and to stop the enzymatic browning in apple juice [79]. Besides, in another recent publication [98], the material UVM-7 was functionalised with amine groups and it was proved that the material was capable of capturing not only the PPO but also the oxidation products.

However, the main drawback found was the need for filtration to remove the material losing most of the bioactive compounds present in the juice. Moreover, even proved their effectiveness against the PPO no studies were made of their influence on the other important quality parameters of apple juice that could meet the demands of consumers as well. Therefore, the main objective of the present study is to develop a new magnetic UVM-7 mesoporous silica material removable from the juice functionalised with thiol and amine groups. Besides, it was evaluated their effect on physicochemical (pH, °Brix, colour formation), bioactive compounds (ascorbic acid, total phenolics, flavonoids and flavonols) and the antioxidant capacity (DPPH, FRAP, and ABTS) of cloudy apple juice.

2. Materials and methods

2.1. Chemicals

Tetraethyl orthosilicate (TEOS) reagent grade 98%, triethanolamine (TEAH3) reagent grade 98%, N- cetyltrimethylammonium bromide (CTABr) for molecular biology ≥ 99%, 3-aminopropyl triethoxysilane (APTES) ≥ 98%, 3-mercaptopropyl trimethoxysilane 95%, sodium nitrite reagent grade 97%, 6-Hydroxy-2,5,7,8-tetramethylchromane-2-carboxylic acid (Trolox 97%), 2,2-Diphenyl-1-picrylhydrazyl (DPPH), gallic acid (97.5-102% titration), L-Ascorbic acid >99.%, 2,4,6-Tris(2-pyridyl)-s-triazine (TPTZ 98%), Quercetin >95%, chloroform >99%, (+)-Catechin hydrate 98%, 1,2-dihydroxybenzene >99%, sodium oxalate >99.5%, ammonia solution 32% and oleic acid 99% were provided by Sigma-Aldrich (Sigma-Aldrich, USA). Sodium

carbonate anhydrous, potassium dihydrogen phosphate, sodium bisphosphate, disodium phosphate and were acquired from Scharlau at reagent grade (>99%) (Sharlab S.L., Spain). Sodium acetate, iron (III) chloride hexahydrate 97%, iron (II) chloride tetrahydrate 97%, methanol 99.9%, Folin- Ciocalteu reagent, potassium persulfate >99% and aluminium chloride >99.0% were purchase from Honeywell (Honeywell, France). Finally, sodium hydroxide 1N standard volumetric solution came from Panreac AppliChem (Panreac AppliChem, Barcelona, Spain) and 2,2'-Azino-bis(3-ethylbenzthiazoline-6-sulfonic acid (ABTS) from Roche® Life Science Products.

Golden Delicious apples obtained in a local store were used to obtain the fresh juices used in the tests.

2.2. Synthesis and characterization of the magnetic UVM-7

Magnetic UVM-7 (M-UVM-7) was prepared following a two-step procedure. In a first step, small superparamagnetic iron oxide nanoparticles were synthesized following the method presented by Sánchez-Cabezas et al. (2019)[99]. Briefly, under a nitrogen atmosphere, 50 mL of distilled water were heated at 80 °C followed by the addition of 12 g of $FeCl_3 \cdot 6H_2O$ and 4.9 g of $FeCl_2 \cdot 4H_2O$. Then, 19.53 ml of ammonia 32% was added and the mixture was left under stirring for 30 min. Subsequently, 2.13 mL of oleic acid was included in the mixture and kept under stirring for another 90 min at 80 °C. Once the mixture was cool down to room temperature, the blend was centrifuged at 12100 g for 10 min. The precipitate was washed three cycles with distilled water and three more cycles with ethanol. The resulting magnetic black material was dried under vacuum overnight and resuspended in chloroform to avoid oxidation, forming a ferrofluid. In order to discard the largest nanoparticles and adjust the size of the final nanoparticles, the ferrofluid was centrifuged at 13400 g for 20 min.

Once the small iron oxide nanoparticles (FeNPs) in the form of magnetite were synthesised, we proceeded to its coating with silica forming the UVM-7. A traditional UVM-7 synthesis with modification was followed. A mixture of TEOS (0.05 mol) and $TEAH_3$ (0.17 mol) was heated to 140 °C until no condensation of ethanol was observed. The reaction was cooled to 90◦C and 2.96 g of CTAB was gradually added followed by 80 mL of the water-FeNPs mixture. The blend was aged at room temperature for 16 h and the resulting precipitate was collected by centrifugation (10000 g) and washed with water and ethanol. Lastly, the final magnetic silica UVM-7 was dried at 40 °C and calcined in an oxidant atmosphere at 550 °C for 5 h.

The water-FeNPs mixture was prepared previously with a phase-transfer of the ferrofluid to water[99]. First, 1.6 g of CTAB were dissolved in the 80 mL of distilled water followed by the addition of 16 mL of the FeNPs suspended in chloroform (6.5 mg/mL). Then the two-phase solution was micro-emulsified using a probe sonicator. Finally, the emulsion was heated at 65 °C under constant stirring until chloroform was completely evaporated, giving a clear suspension of nanoparticles in water.

The functionalisation with the thiol and amine groups were carried out following known procedures[79,98].

FeNPs were characterised by powder X-ray diffraction (PXRD) in a Bruker AXS D8 Advance diffractometer using CuKα radiation and working at 40 kV/40 mA. The diffraction pattern of FeNPs was analysed in the 2θ range between 25 and 65°. Furthermore, the size distribution of the nanoparticles was studied by dynamic light scattering (DLS) using a Malvern Zetasizer Nano-ZS equipment working at 25°C.

Magnetic mesoporous silica material (M-UVM-7) characterization was done by the same XRD diffractometer at a low angle. TEM images were recorded using transmission electron microscopy (JEOL JEM-1010 instrument). Specific surface area,

pore size distribution, and pore volume were measured from nitrogen adsorption-desorption isotherms in a Micromeritics ASAP 2020 instrument under nitrogen temperature (-196 °C). In order to determine the Si/Fe molar ratio (wt %) of the M-UVM-7 material the electron probe microanalysis (EDX-Philips SEM-515 instrument) was used. Finally, the amount of thiol and amine groups were measured by Thermal Gravimetric Analysis (TGA) in a TGA 550 Discovery from TA instruments.

2.3. Cloudy apple juice preparation and polyphenol oxidase (PPO) activity determination

Golden Delicious apples were first washed and then liquefied in a Moulinex centrifugal JU200045. The cloudy apple juice was analysed immediately after preparation. Polyphenol oxidase from the cloudy apple juice was determined following known procedures[100]. Briefly, 100 µL of the apple juice was mixed with 2.9 mL of catechol solution (0.05 M) previously prepared in a 0.1 M phosphate buffer at pH 6.5. The oxidation reaction was followed spectrophotometrically (UV/vis, Beckman Coulter du 730) measuring the increase of absorbance at 420 nm during 120 s. The PPO activity was taken as the slope of the linear stretch of the reaction curve. To determine the maximum PPO enzyme activity, the activity was measured at different times after making the juice (0, 5, 10, 20, and 30 min).

The best ratio material/[PPO] was determined by analysing the PPO activity in the presence of the M-UVM-7 functionalised and non-functionalised. For this, 15 mg of the material was mixed with 1 mL of three apple juice dilutions (1, ½, and ¼). The mixture was kept under stirring for 10 min and subsequently the same enzymatic assay was accomplished. Control without the material was also carried out. The assays were done in triplicate at 20°C.

2.5. M-UVM-7 treatment

An aliquot of 2 mL of apple juice was mixed with the three different materials (M-UVM-7, M-UVM-7-SH, and M-UVM-7-NH_2) in concertation of 15 mg/mL for 10 minutes. Afterwards, the material was removed by a neodymium magnet and the sample was kept under stirring for 30 min more. For all the assays, aliquots were taken after and before removing the material and after 30 min. The measurements were done in triplicate and a sample without material was used as a control. Besides, a blank with the inhibitors was also measured and subtracted if present.

2.5.1 Determination of total soluble solids (°Brix), pH and enzymatic browning

The pH of the juices was determined using a digital pH meter (Metler Toledo SevenEasy. Total soluble solids (TSS) were determined using a digital refractometer (Atago-3T) at 20 ± 1 °C and results were expressed in the standard °Brix unit.

2.5.2. Inhibitory effect of enzymatic browning

The oxidation process and the colour change were measured to assess the inhibitory effect by using a spectrophotometer Minolta (CM-3600 d). CIE L*a*b* (CIELAB) colour space which comprises L* (lightness), a* (red to green) and b* (yellow to blue) coordinates were obtained using a D65 illuminant and 10° observer as a reference system. The total colour difference (ΔE*) between the juice at time 0 and treated samples was calculated following the equation (2)

$$\Delta E^* = \sqrt{(\Delta L^*)^2 + (\Delta a^*)^2 + (\Delta b^*)^2} \qquad (2)$$

2.5.3. Determination of total phenolic content (TPC) and antioxidant activities analysis

Total phenolic content (TPC) of juices were performed according to the Folin-Ciocalteu method[101,102]. A mixture of 10 µL aliquot of the apple juice, 1.58 mL of

deionized water, and 100 µL of the Folin-Ciocalteu reagent was left for 3 min. Afterwards, 300 µL of Na_2CO_3 (20% w/v) was added and left in dark for 60 min before measuring the absorbance at 765 nm (UV/vis, Beckman Coulter du 730). A standard curve of gallic acid from 0 to 500 mg/L was prepared (r^2=0.997) and the results were reported as mg of gallic acid equivalent (GAE) (mg GAE/L).

For the antioxidant activities analysis, three different methods were conducted**.** One assay used to assess the antioxidant capacity was the ferric reducing antioxidant power assay (FRAP) following the method described by Thaipong et al. (2006)[103]. In brief, an aliquot of 25 µL of the juices was reacted with 2850 µL of FRAP solution and 125 µL of distilled water for 30 min in dark condition. Then the absorbance was measured at 593 nm in a UV/vis, Beckman Coulter du 730. FRAP reagent was prepared mixing in a ratio 10:1:1 a solution of 300 mM acetate buffer (pH 3.6), 20 mM ferric chloride and 10 mM TPTZ in 40 mM HCl. A standard curve of Trolox was set (r^2=0.999) and the results were stated as mg of Trolox equivalent per L (mg Trolox/L).

The antioxidant activity of the treated and untreated juices was also studied by DPPH· method investigating their ability to scavenge the $DPPH^{\bullet}$ free radical [104] with slight modifications. A sample of 10 µL of juice was added to 1 mL of methanolic solution of $DPPH^{\bullet}$ (100 µM). Then, the mixture was kept in the dark for 30 min and absorbance was measured at 517 nm using UV/vis spectrophotometer. The data were expressed as Trolox equivalent (mg Trolox/L) after getting the corresponding calibration curve (r^2=0.990).

Finally, the capacity to scavenge the $ABTS^{\bullet+}$ free radical was tested by the established $ABTS^{\bullet+}$ assay[103]. A 1:1 solution of 7.4 mM $ABTS^{\bullet+}$ solution and 2.6 mM potassium persulfate solution was prepared and left in the dark to react for 12h at room temperature. Then, 1 mL of the solution was diluted in 60 mL of methanol. For

the assay, 10 µL of the apple juice was mixed with 140 µL of distilled water and 2890 µL of the $ABTS^{\bullet+}$ for 2h in dark conditions. Then the absorbance was taken at 734 nm in the same spectrophotometer. The data were expressed as Trolox equivalent (mg Trolox/L) after getting the corresponding calibration curve (r^2=0.997).

2.5.4. Determination of total flavonoids and flavonols

The total content of flavonoids and flavonols was estimated following the methodology published by Abid et al. (2013)[37]. For flavonoids, 100 µL aliquot of juice sample was mixed with 1.4 mL of deionized water and 75 µL of a 5% $NaNO_2$. Afterwards, the sample was left for 6 min and 150 µL of a 10% $AlCl_3$ was included and then after 5min, 0.50 mL of 1 M NaOH was added. Finally, the absorbance was measured at 510 nm previous to a calibration curve of (+)-catechin (r^2=0.993). The results were reported as mg of catechin equivalent/L.

For the total flavonols content, a 0.5 mL of diluted sample was mixed with 0.5 mL of 2% $AlCl_3$ solution, followed by the addition of 0.5 mL sodium acetate solution (50 g/L). The mixture was left for 150 min at 20 °C, and then, the absorbance was read at 440 nm. A standard curve of quercetin from 0 to 150 mg/L was prepared (r^2=0.998) and the results were reported as mg of quercetin equivalent/L.

2.5.5. Determination of ascorbic acid

The content of ascorbic acid was measured according to the method reported by Selimović, Salkić, & Selimović, 2011[105]. A sample of 50 µL was mixed with 1.95 mL of 1.13 mM of sodium oxalate dissolved in a potassium dihydrogenphosphate (30mM)/ disodium hydrogenphosphate (0.8mM) buffer solution (pH = 5.4). Subsequently, the absorbance was measured at 266 nm and data was confronted to a standard curve of L-ascorbic acid (r^2=0.999).

2.6. Software and data analysis

Data are reported as mean ± standard deviation. Statgraphics Centurion XVII software was used to perform the analysis of variance (One-Way ANOVA) and Multiple Range Tests by the LSD procedure (least significant difference) of the Fisher test to identify homogeneous groups. Besides, data were subjected to a Pearson correlation analysis to find the linear relationship between variables. A confidence level of 95% (p-value < 0.05) was used in all cases.

3. RESULTS AND DISCUSSION

3.1 Description of the new magnetic mesoporous material

In recently published articles, we verified the use of mesoporous silica particles as a new tool for inhibiting the polyphenol oxidase enzyme and its potential use as an anti-browning agent. In particular, UVM-7 functionalized with thiol groups, which contains a bimodal pore system structure adequate for the PPO interaction, avoided the change of colour in apple juice[79]. Besides, when functionalised with amine groups, although no inhibition of the enzymatic browning occurred, the PPO was retained in the material delaying the enzymatic browning when the material was removed[98]. However, removing the material from the medium implies filtering the juice, thus eliminating the pulp and with it, many of its bioactive compounds. To solve this issue, a new UVM-7 magnetic material that allows us to remove it from the medium without having to filter the juice was herein developed and functionalised with thiol (-SH) and amine ($-NH_2$) groups.

To synthesise the new M-UVM-7, a two-steps route was designed. In the first place, it was necessary to develop small magnetic nanoparticles that were able to be introduced into the UVM-7 without breaking its morphology. PXRD powder diffraction and DLS were used to characterize the nanoparticles. The XRD pattern

(Figure 5.29) shows that the final FeNPs correspond to highly crystalline magnetite ($Fe^{2+}Fe^{3+}{}_2O_4$) presenting sharp diffraction peaks with 2θ values of 30.17, 35.46, 43.09, 53.28, 56.88, and 62.45. Furthermore, the relative intensities of the peaks agree with the Bragg reflections of magnetite which were indexed as [2 2 0], [3 1 1], [4 0 0], [4 2 2], [5 1 1] and [4 4 0]. The size distribution of the nanoparticles was measured using dynamic light scattering (DLS) with a particle size of 20 nm. Once the magnetite was synthesised, it proceeded to the synthesis of the M-UVM-7. For this, different Magnetite/Si ratios were tested, where small ratios generated slightly magnetic UVM-7 (only 4.6 ± 0.4 % wt of Fe) while large ratios caused a disruption of the UVM-7 in which its textural pore disappears (textural pore volume=0.13 cm^3/g; textural pore diameter=20 nm).

Nevertheless, an optimum Magnetite/Si ratio where the M-UVM-7 was magnetic enough to remove it from a solution was found (11 % wt of Fe). X-ray powder diffraction and TEM analysis confirmed the mesoporous structure of the M-UVM-7. The XRD pattern of the silica at a low angle with a peak at 2θ around 2° corresponding to the reticular plane 100 confirms the presence of the mesoporous

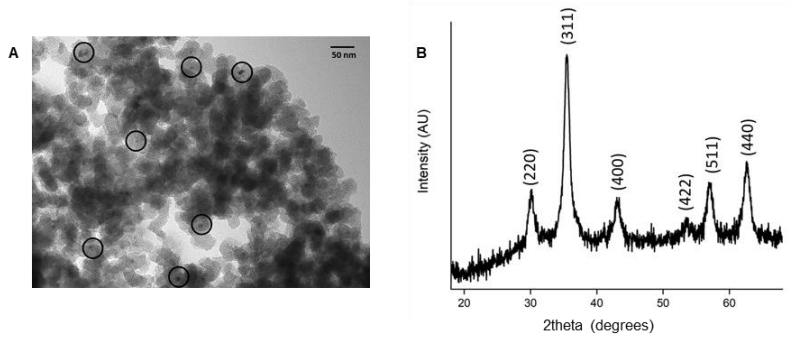

Figure 5.29. *Representative TEM image of M-UVM-7 with the magnetic nanoparticles enclosed by a circle (A). X-ray diffraction pattern of the small magnetite nanoparticles (FeNPs).*

ordered structure. As seen in Table 5.8, d_{100} spacing calculated from the PXRD data was around 40 Å which coincides with other reported values [83]. Besides, TEM images (Figure 5.29A) depicted the typical structure of the UVM-7 inorganic matrix in which can notice small black spots scattered throughout the material concerning the magnetite nanoparticles. Nitrogen adsorption/desorption isotherms of M-UVM-7 proved that the bimodal hierarchical porosity typical of the UVM-7 silica-based support was maintained after the incorporation of FeNPs (Table 5.8). The BET analysis found the specific surface value up to 1000 m^2g^{-1} with a mesopore volume close to 1 cm^3g^{-1} and a pore diameter of 2.83 nm. Regarding the textural porosity, the most influential parameter for the PPO inhibition, the textural pore volume and the textural pore diameter were 1.6 cm^3g^{-1} and 40 nm respectively. This data is in agreement with the ones found for a non-magnetized UVM-7[106–108].

Regarding the materials functionalised with thiol (-SH) and amine ($-NH_2$) groups, TGA analysis estimated an amount of organic content of 0.6 and 1.5 mmol $(g\ SiO_2)^{-1}$ respectively. These results fall in line with the expected degree of functionalization reported in our previous works. The functionalization did not modify the structure of the support as it maintains the X-ray diffraction pattern and confirmed by TEM images; however, it did affect the BET surface. In the case of M-UVM-7-SH, with a lower amount of -SH groups, the decrease in the specific area is less (1047 m^2g^{-1}) than for M-UVM-7-NH_2 (496 m^2g^{-1}).

Table 5.8. *Structural properties and organic content of the M-UVM-7, M-UVM-7-SH, and M-UVM-7-NH2*

Material	S_{BET}[a] (m^2/g)	Mesopore diameter (nm)[b]	Mesopore Volume (cm^3/g)[b]	Textural pore diameter (nm)[b]	Textural pore volume (cm^3/g)[b]	d_{100} (Å)[c]	2θ (°)[d]	mmol organic /g SiO_2	% Fe (wt %)
M-UVM-7	1059	2.83	0.92	40.03	1.62	40.69	2.17	-	
M-UVM-7-SH	1047	2.73	0.87	38.2	1.2	42.72	2.07	0.6	11.17 ± 1.7
M-UVM-7-NH_2	496	2.49	0.3	39.3	0.87	42.72	2.07	1.5	

[a] BET specific surface calculated from the N^2 adsorption-desorption isotherms.

[b] Pore volumes and pore size (diameter) calculated from the N^2 adsorption-desorption isotherms.

[C] Diffraction peak of the reticular plane 100 calculated by $2d_{100}\,sen\theta=n\lambda$

[d] Angle of incidence for the reflection plane

3.2 Apple PPO characterization and study of material/PPO ratio

The enzymatic activity of PPO in the golden delicious apple juice over time was studied. It was observed how the PPO activity grew during the first 10 minutes from 45% in recently liquefied juice until reaching its maximum activity after 10 min (100%). Afterwards, the activity of the enzyme began to slowly decrease, reaching 75% of the activity after 30 min under stirring. This can be explained as PPO is trapped in apple tissue plastids while polyphenols are found mainly in the vacuoles [109]. During juice making there is a cell disruption in the apple tissue releasing the PPO and the polyphenols leading to the enzymatic browning reactions. However, a lag time period is observed before the reaction. In addition, as it is cloudy apple juice, part of the PPO which is trapped in the pulp, slowly diffuses into the medium. Considering these results, 10 min was established as the contact time between the juice and the material before removing it from the juice with a neodymium magnet.

On the other hand, the optimal ratio material:[PPO] was determined by testing different ratios of juice/material (Table 5.9). The presence of the M-UVM-7 did not have a significant effect on the inhibition of PPO even when using the smallest ratio juice:material. This fall in line with our previous reports when it was tested in apple juice and the enzymatic browning occurred[79]. A little inhibition is performed in the presence of the support functionalised with amine groups with a slight increase after its removal. Although without overcoming more than 50% of inhibition. However, the magnetic material functionalised with -SH groups (M-UVM-7-SH) performed indeed a remarkable inhibition ranged from 30 to 65% depending on the ratio. The -SH groups attached to the material surface interact with PPO so, the higher the ratio of material used the less active residual enzyme would be. Additionally, an increase of the inhibition was observed after removing the M-UVM-7-SH from the medium reaching similar results regardless the ratio.

Table 5.9. *Inhibition (%) of the apple PPO by the M-UVM-7, M-UVM-7-SH, and M-UVM-7-NH_2, at pH 6.5 using catechol as substrate.*

material	ratio [material]/juice (mg/mL)	Inhibition (%)		
		10 min	10* min	30* min
M-UVM-7	15	0 ± 4^{aA}	2 ± 5^{aA}	5 ± 2^{aA}
	30	9 ± 5^{aA}	3 ± 5^{aA}	2 ± 6^{aA}
	60	5 ± 2^{aA}	2 ± 2^{aA}	0 ± 2^{aA}
M-UVM-7-SH	15	33 ± 4^{cC}	68 ± 5^{aA}	59 ± 2^{bA}
	30	55 ± 4^{bB}	68 ± 7^{aA}	55 ± 6^{bA}
	60	62 ± 3^{aA}	69 ± 6^{aA}	61 ± 2^{aA}
M-UVM-7-NH_2	15	11 ± 8^{aC}	14 ± 6^{aB}	9 ± 6^{aC}
	30	28 ± 2^{bA}	34 ± 2^{aA}	30 ± 2^{abB}
	60	23 ± 2^{bB}	37 ± 2^{aA}	35 ± 2^{aA}

*After removing the material after 10 min in contact with the cloudy apple juice.

These results point out M-UVM-7-SH manages to interact and retain both, active and inhibited PPO so when the material is removed, active PPO is eliminated thus increasing the inhibition.

Since the final inhibition is the same regardless of the ratio, 15 (mg/mL) was the ratio used for further analysis as well as the suggested one for the development of further industrial application of the M-UVM-7-SH for PPO inactivation purposes.

3.3. Effect of M-UVM-7-SH and M-UVM-7-NH_2 on physical-chemical properties of the cloudy apple juice

3.3.1. Colour, pH and total soluble solids (°Brix)

Results regarding the effect of the magnetic UVM-7 functionalised with thiol and amine groups on pH, total soluble solids (TSS), and colour change are summarized in Table 5.10. The initial values of TSS and pH of the cloudy apple juice (12.2 °Brix and 3.99 respectively) agreed with previously reported values for the juice of the same apple variety [97]. No significant changes (p<0.05) in TSS were observed

after the contact time and separation of the magnetic particles. No changes in the pH of the juice were observed after using non-functionalized and functionalised materials with -SH groups. In contrast, there was a significant increase in the pH (from 3.99 to 5.5) of those samples treated with M-UVM-7-NH_2. This rise in the pH might be not desirable as could negatively impact consumer acceptance. Similar result were found by Peña-Gómez et al. (2019)[20] when using silica mesoporous microparticles to filtrate apple juice. In this case, no alteration of pH or °Brix was found when using non-functionalized silica being also stable during time. However, they found an increase in the pH of the juice when filtrated with a particle functionalised with vanillin via amine moieties. They attributed this effect to the presence of unreacted amine groups with the vanillin on the surface of the particle that leads to an increase in the pH. In the present study, the high amount of -NH_2 groups attached to the surface of the particles could be responsible for the observed increase of pH.

Concerning the influence of the magnetic mesoporous materials on the enzymatic browning, significant colour differences were recorded between the control and the samples treated with M-UVM-7-SH as shown in Table 5.10. The enzymatic browning process in absence of an inhibitor is quite fast under agitation reaching a colour difference of 9 just after 10 min, or 12 after 30 min of stirring. The same tendency is followed when the juice is treated with the non-functionalized M-UVM-7 and with M-UVM-7-NH_2 with no significant differences for $p<0.05$. However, when the apple juice is treated with M-UVM-7-SH the enzymatic browning process slowed down dramatically with a colour difference of 1.8 after 10 min, 80% less than the control. At the end of the study (30 min), even without the presence of the material in the juice, the enzymatic browning did not reach the values of the control. A value of colour change of 3.8 is achieved by the treated sample in contrast to the

12.7 of the untreated sample. It has been reported that values greater than 12 indicated absolute colour differences by the human eye, while colour changes between $3 < \Delta E_{ab}^{*} > 4$ only trained eye can detected[110,111]. As said before, the double capacity of the M-UVM-7-SH to both inhibit and remove the PPO could explain the ability of this material to control enzymatic browning. While the material is in agitation in the apple juice, the PPO is inhibited by the thiol groups; once the material is removed, most PPO is separated from the juice. These results are in concordance with our previous works, showing that the magnetization of the UVM-7 does not affect its capacity of inhibiting the enzymatic browning in apple juice.

Table 5.10. *Effect of magnetic UVM-7 materials on pH, °Brix, colour change (ΔE_{ab}^{*}), and ascorbic acid content in apple juice at different times.*

Sample	Time (min)	pH	Total soluble solids (°Brix)	ΔE_{ab}^{*}	Ascorbic acid (mg/100 mL)
Control	0	3.99 ± 0.01^{b}	10.2 ± 0.01^{a}	0^{c}	22.5 ± 0.3^{a}
	10	3.99 ± 0.01^{b}	10.2 ± 0.01^{a}	9.24 ± 0.08^{bA}	21.0 ± 0.4^{bA}
	30	4.01 ± 0.01^{b}	10.2 ± 0.01^{a}	12.7 ± 0.6^{aA}	17.5 ± 1.8^{cAB}
M-UVM-7	10	4.13 ± 0.10^{b}	10.1 ± 0.01^{a}	-	20 ± 2^{abA}
	10*	4.01 ± 0.08^{b}	10.7 ± 0.07^{a}	9.80 ± 0.08^{bA}	21 ± 2^{aAB}
	30*	4.05 ± 0.02^{b}	10.3 ± 0.01^{a}	13.3 ± 0.07^{aA}	17 ± 1^{bAB}
M-UVM-7-SH	10	3.96 ± 0.03^{b}	10.2 ± 0.01^{a}	-	21 ± 2^{aA}
	10*	3.97 ± 0.03^{b}	10.2 ± 0.01^{a}	1.85 ± 0.03^{bC}	22 ± 2^{aA}
	30*	3.96 ± 0.01^{b}	10.2 ± 0.01^{a}	3.8 ± 0.2^{aB}	22 ± 2^{aA}
M-UVM-7-NH_2	10	5.56 ± 0.02^{a}	10.2 ± 0.00^{a}	-	20 ± 2^{abA}
	10*	5.59 ± 0.02^{a}	10.4 ± 0.01^{a}	8.1 ± 0.3^{bB}	18 ± 2^{bB}
	30*	5.56 ± 0.01^{a}	10.2 ± 0.01^{a}	12.1 ± 0.6^{aA}	15 ± 2^{bB}

After removing the material after 10 min in contact with the cloudy apple juice. $^{a-c}$ Different lowercase letters indicate significant differences among times for $p<0.05$ compared with the control t=0. $^{A-C}$ Different capital letters indicate significant differences among compounds at the same time for $p<0.05$; in this case, both time 10 and 10 (before and after removing the material) are compared with control t=10 min.

3.3.2. Ascorbic acid

Ascorbic acid is highly sensitive to thermal degradation during heat treatment and storage, so it is often used as a marker for product quality deterioration [112]. Thus, its content was also measured in the juices before and after the contact with and remotion of the materials (Table 5.10). The initial value of ascorbic acid found in the apple juice fall in concordance with the found in other apple juices [113,114] and it was observed a significant decrease after 30 min (p<0.05) from 22.5 to 17.5 mg/100 mL of juice. Besides a high negative correlation (r=-0.8482, p<0.05) was found between the enzymatic browning and the concentration of ascorbic acid present in the apple juice. Some authors have correlated the decrease in the vitamin with the enzymatic browning development in apples[115,116]. Ascorbic acid is oxidised to dehydroascorbic acid preventing the oxidation of other phenols present in the matrix[117].

Regarding the treated juices, the presence of the M-UVM-7 did not change the evolution of vitamin C concentration in the juice. Amine functionalization did not stop either the loss of vitamin C after 30 min reducing it significantly to 18 mg/100 mL. In fact, when the M-UVM-NH_2 was removed from the apple juice, a slight but significant decrease in the amount of vitamin C was detected. On the contrary, processing the juice with M-UVM-7-SH did not significantly affect the ascorbic acid content in the raw juice after 30 min. Despite other alternative treatments like UV irradiation on fruit juices do not prevent the loss of vitamin C[118], treatment with M-UVM-7-SH could reduce its.

3.3.3. Total phenolic (TPC), flavonoids, and flavonols content

A high initial value of phenolic compounds (760 ± 40 mg GAE/L) was found just after liquefying the apples (Figure 5.30), which is in agreement with those

reported by other authors for "Golden Delicious" apple juice [94]. The flavonoid content found in the raw juice was also high (400 ± 20 mg catechin/L) being in concordance with other studies [37]. On the other hand, the flavonols content in the juice was lower compared with their analogues (98 ± 8 mg quercetin/L). Flavan-3-ols are usually the most representative phenolics in apple juice (65%) nevertheless, flavonols are mainly found in the skin of the fruit appearing therefore in low quantities in the juice (6-15% of total phenolic compounds)[92,119].

A significant decrease (20%) in the total content of phenolic compounds was observed in the control samples 10 min after the juice extraction, reaching a concentration close to 500 mg GAE/L after 30 min. These reductions correlated for $p<0.05$ with the production of brown pigments and the loss of vitamin C over time (r=-0.8989 and 0.7631 respectively). Flavonoids were also affected by the enzymatic browning in the case of the control juice (r=-0.9438) as the initial concentration was reduced after 10 min. However, no significant changes in flavonols were found for the control over time. Similar results were obtained in the juice samples treated with M-UVM-7 and M-UVM-7-NH_2. These materials were not capable to block the oxidation of neither the phenolic compounds nor the flavonoids and flavonols. Furthermore, the UVM-7-NH_2 enhanced the loss of some phenolic (35% loss with respect to the control), flavonoids (50%) and flavonols (60%) compound probably because of the pH increase. Indeed, some authors[120,121] have shown PPO enzymatic activities in golden delicious apples rather higher at pH above 5 than close to 4.

On the other hand, the functionalized material with thiol groups was capable to stop the oxidation during the contact step and therefore the loss of the assessed bioactive compounds. Once removed from the medium, the residual enzyme did not affect the total flavonoid content, but it did affect the TPC and flavonols. It seems that the formed colour in the juice treated with -SH is mainly due to the loss of

flavonols, and polyphenols according to correlations (r=-0.664, and -0.5756 for p<0.05).

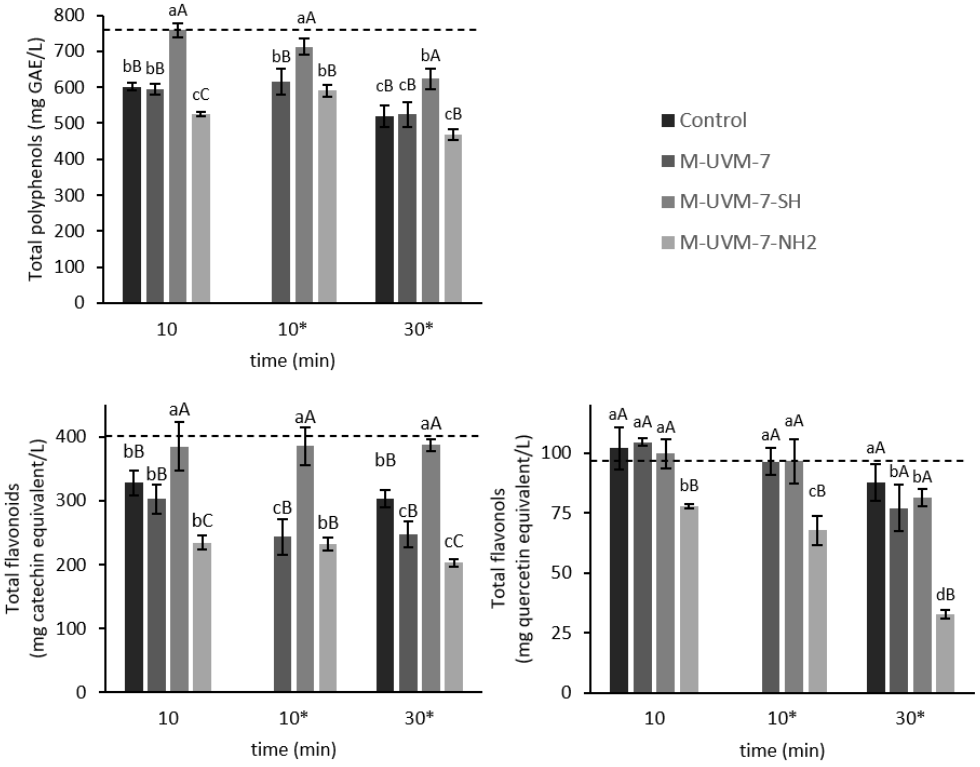

Figure 5.30. *Effect of the different materials on total phenolic content, flavonoids and flavonols in apple juice. Dotted line indicates the initial value in the juice at t=0. *After removing the material after 10 min in contact with the cloudy apple juice.a-c Different capital letters indicate significant differences among compounds at the same time for p<0.05; in this case both time 10 and 10* (before and after removing the material) are compared with control t=10 min.*

Noci et al., (2008)[122] reported a 50% of loss in the total phenolic content in apple juice after a short-time high-temperature treatment (94 °C for 26 s) and reducing the temperature to 72 °C only 10 % was recovered, still losing 40% of TPC. So, the results with M-UVM-7-SH are quite promising compared to those obtained by applying thermal treatments.

3.3.4. Total antioxidant capacity

Antioxidant activities based on DPPH, ABTS, and FRAP revealed a significant decrease ($p<0.05$) in the antioxidant capacity of untreated juice after 30 min (50% for DPPH and ABTS, and 25% for FRAP analysis) (Figure 5.31). A positive correlation was found between $DPPH^{\bullet}$, $ABTS^{\bullet+}$, and FRAP for $p<0.05$ ($r=0.9378$-0.9389), which is in accordance with other reported values[119]. Besides, correlations above -0.9 were achieved for the generation of browning pigments (ΔE_{ab}^{*}), DPPH and ABTS with a lower correlation but still significant for FRAP ($r=-0.8722$). Antioxidant capacity in the apple juice can be attributed to several antioxidants, being the contribution of polyphenols about 70-80% while vitamin C contribution is less than 5%. Regarding the polyphenols, the antioxidant capacity is mostly attributed to flavanols (proanthocyanidins and catechins) with a weak correlation for quercetin glycosides (flavonols)[92,93]. In this study, no significant correlation was found between the antioxidant activity and flavonols content, yet a significant correlation of 0.8247, 0.9071 and 0.7217 for DPPH, ABTS and FRAP respectively and the total flavonoids were found. This is in line with the previous results where the total flavonoid content decreased over time as does the antioxidant activity.

Treatment with mesoporous silica materials (M-UVM-7 and M-UVM-7-NH_2) did not preserve the antioxidant activity of juices. In fact, the M-UVM-7-NH_2

significantly decreased the total antioxidant capacity when measured by the DPPH and ABTS method similarly as was observed for total flavonoids and flavonols. No significant changes were found after removing these materials from the juice. These results indicate that the tested materials are not able to entrap and eliminate the antioxidants from the juice when they are magnetically removed.

The antioxidant capacity of juice samples treated with M-UVM-7-SH remained close to 1400 mg Trolox/L (in ABTS) even after it removed the medium. Only 20% of the antioxidant activity determined by DPPH was lost after the M-UVM-7-SH treatment in contrast with the 50% lost by the control. However, the antioxidant activity measured by FRAP decreased significantly to values close to the control (50% from the initial) despite not having decreased the flavonoid content. Differences in the antioxidant activity in samples treated with M-UVM-7-SH depending on the analytical method could be related to the different phenolic compounds contributing to each assay. Although flavonoids are the most influential in antioxidant activity, the decrease in antioxidant capacity after treatment with M-UVM-7-SH measured by FRAP may be due to the loss of non-flavonoid polyphenols also present in apples. Apart from the flavonoids, some acidic phenolic compounds may influence as well to the total antioxidant capacity. In this sense, Wu et al. (2020)[104] reported that the hydroxycinnamic acid with more influence in the DPPH assay was caffeic acid, while ABTS would better correlate with ferulic acid.

In short, both the Pearson's correlation coefficient and the results indicated that that for the cloudy apple juice, enzymatic browning was highly related to the loss of flavonoids, vitamin C and non-flavonoid phenols, largely affecting their antioxidant power. No positive changes were found in the concentration of the bioactive compounds when treating the juice with M-UVM-7 and M-UVM-7-NH_2. On the contrary, when the juice was treated with M-UVM-7-SH, no loss neither in

flavonoids nor vitamin C were observed. Consequently, the scarce enzymatic browning that occurs would be related to the loss of non-flavonoid polyphenols such as chlorogenic acid, caffeic acid, or ferulic acid.

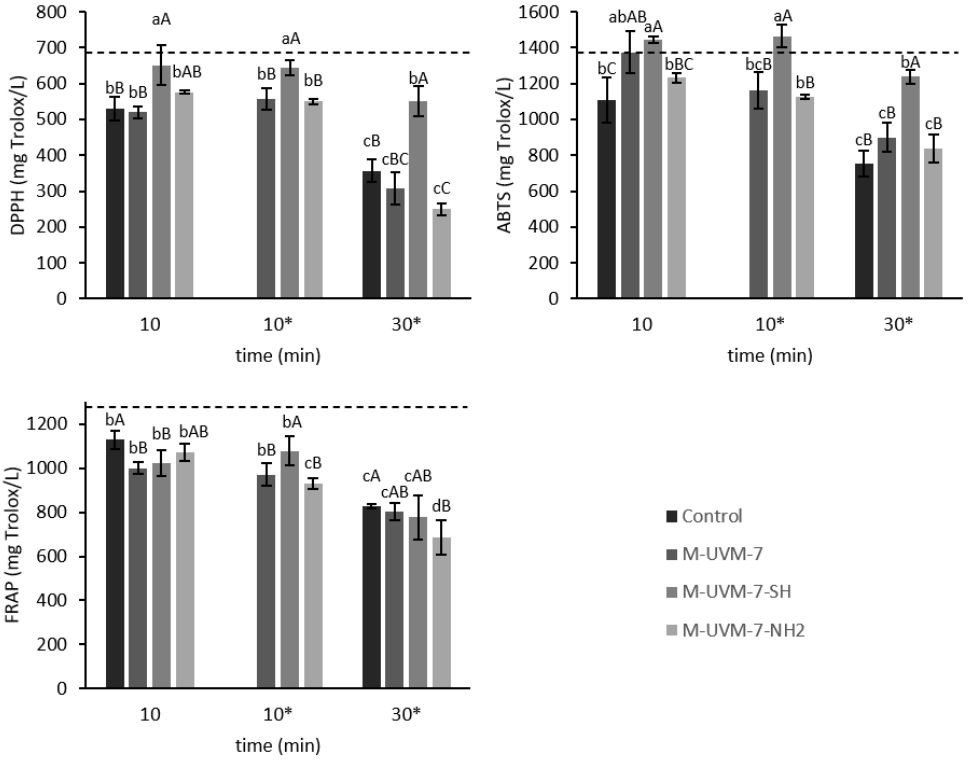

Figure 5.31. *Antioxidant capacity measured by three different methodologies (DPPH●, ABTS●+, and FRAP) of cloudy apple juice. Dotted line indicates the initial value in the juice at t=0. *After removing the material after 10 min in contact with the cloudy apple juice.* $^{a\text{-}c}$ *Different lowercase letters indicate significant differences among times for p<0.05 compared with the control t=0.* $^{A\text{-}C}$ *Different capital letters indicate significant differences among compounds at the same time for p<0.05; in this case both time 10 and 10* (before and after removing the material) are compared with control t=10 min.*

4. CONCLUSION

A novel UVM-7 magnetic material has been prepared for the first time in order to remove it from the apple juices after treating them. For this purpose, a two step-route synthesis was followed in which firstly ultra-small magnetic nanoparticles (Magnetite) were prepared followed by the synthesis of the Magnetic UVM-7 (M-UVM-7). This material was functionalized with both thiol and amine groups. The ratio selected was 15 mg of material per 1 mL. The results showed how the apple juice is oxidized quickly affecting the concentration of vitamin C, total polyphenols, and flavonoids, as well as the total antioxidant capacity measured by three different methods (DPPH, ABTS, and FRAP). This reaction was significantly delayed when applying the material M-UVM-7-SH which reduced the enzymatic browning by 70%. This fall also impacted positively the content of vitamin C, flavonoids and ABTS with no significant differences from the initial content of the juice. Besides, although the TPC and DPPH were still affected, the final content was higher than the control after treatment.

REFERENCES OF THE CHAPTER 2

(1) Nasrollahzadeh, M.; Sajadi, S. M.; Sajjadi, M.; Issaabadi, Z. Applications of Nanotechnology in Daily Life. In *Interface Science and Technology*; Elsevier B.V., 2019; Vol. 28, pp 113–143.

(2) Banerjee, S.; Dhir, A.; Gogoi, H.; Datta, A. Silica-Based Materials for Bioanalytical Chemistry and Optoelectronics. In *Chemistry of Silica and Zeolite-Based Materials*; Elsevier, 2019; pp 213–228.

(3) Wittig, A.; Gehrke, H.; Del Favero, G.; Fritz, E.-M.; Al-Rawi, M.; Diabaté, S.; Weiss, C.; Sami, H.; Ogris, M.; Marko, D. Amorphous Silica Particles Relevant in Food Industry Influence Cellular Growth and Associated Signaling Pathways in Human Gastric Carcinoma Cells. *Nanomaterials* **2017**, *7* (1), 18.

(4) Yanagisawa, T.; Shimizu, T.; Kuroda, K.; Kato, C. The Preparation of Alkyltrimethylammonium-Kanemite Complexes and Their Conversion to Microporous Materials. *Bull. Chem. Soc. Jpn.* **1990**, *63* (4), 988–992.

(5) Beck, J. S.; Vartuli, J. C.; Roth, W. J.; Leonowicz, M. E.; Kresge, C. T.; Schmitt, K. D.; Chu, C. T. W.; Olson, D. H.; Sheppard, E. W.; McCullen, S. B.; et al. A New Family of Mesoporous Molecular Sieves Prepared with Liquid Crystal Templates. *J. Am. Chem. Soc.* **1992**, *114* (27), 10834–10843.

(6) Narayan, R.; Nayak, U. Y.; Raichur, A. M.; Garg, S. Mesoporous Silica Nanoparticles: A Comprehensive Review on Synthesis and Recent Advances. *Pharmaceutics* **2018**, *10* (3), 118.

(7) Zhang, X.; Cresswell, M. Silica-Based Amorphous Drug Delivery Systems. In *Inorganic Controlled Release Technology*; Elsevier, 2016; pp 93–137.

(8) Verma, P.; Kuwahara, Y.; Mori, K.; Raja, R.; Yamashita, H. Functionalized

Mesoporous SBA-15 Silica: Recent Trends and Catalytic Applications. *Nanoscale* **2020**, *12* (21), 11333–11363.

(9) Ghaferi, M.; Koohi Moftakhari Esfahani, M.; Raza, A.; Al Harthi, S.; Ebrahimi Shahmabadi, H.; Alavi, S. E. Mesoporous Silica Nanoparticles: Synthesis Methods and Their Therapeutic Use-Recent Advances. *Journal of Drug Targeting*. Taylor and Francis Ltd. 2021, pp 131–154.

(10) Pérez-Esteve, É.; Ruiz-Rico, M.; De La Torre, C.; Villaescusa, L. A.; Sancenón, F.; Marcos, M. D.; Amorós, P.; Martínez-Máñez, R.; Barat, J. M. Encapsulation of Folic Acid in Different Silica Porous Supports: A Comparative Study. *Food Chem.* **2016**, *196*, 66–75.

(11) Pal, N.; Bhaumik, A. Soft Templating Strategies for the Synthesis of Mesoporous Materials: Inorganic, Organic-Inorganic Hybrid and Purely Organic Solids. *Advances in Colloid and Interface Science*. Elsevier B.V. 2013, pp 21–41.

(12) Pal, N.; Lee, J. H.; Cho, E. B. Recent Trends in Morphology-Controlled Synthesis and Application of Mesoporous Silica Nanoparticles. *Nanomaterials* **2020**, *10* (11), 1–38.

(13) Möller, K.; Bein, T. Talented Mesoporous Silica Nanoparticles. *Chem. Mater.* **2017**, *29* (1), 371–388.

(14) Zhao, D.; Feng, J.; Huo, Q.; Melosh, N.; Fredrickson, G. H.; Chmelka, B. F.; Stucky, G. D. Triblock Copolymer Syntheses of Mesoporous Silica with Periodic 50 to 300 Angstrom Pores. *Science (80-.).* **1998**, *279* (5350), 548–552.

(15) El Haskouri, J.; Zarate, D. O. de; Guillem, C.; Latorre, J.; Caldes, M.; Beltran,

A.; Beltran, D.; Descalzo, A. B.; Rodriguez-Lopez, G.; Martinez-Manez, R.; et al. Silica-Based Powders and Monoliths with Bimodal Pore Systems. *Chem. Commun.* **2002**, No. 4, 330–331.

(16) Garcia-Bennett, A. E.; Terasaki, O.; Che, S.; Tatsumi, T. Structural Investigations of AMS-n Mesoporous Materials by Transmission Electron Microscopy. *Chem. Mater.* **2004**, *16* (5), 813–821.

(17) Costa, J. A. S.; de Jesus, R. A.; Santos, D. O.; Neris, J. B.; Figueiredo, R. T.; Paranhos, C. M. Synthesis, Functionalization, and Environmental Application of Silica-Based Mesoporous Materials of the M41S and SBA-n Families: A Review. *J. Environ. Chem. Eng.* **2021**, *9* (3), 105259.

(18) Huang, J.; Liu, H. B.; Wang, J. Functionalized Mesoporous Silica as a Fluorescence Sensor for Selective Detection of Hg2+ in Aqueous Medium. *Spectrochim. Acta - Part A Mol. Biomol. Spectrosc.* **2021**, *246*, 118974.

(19) Poyatos-Racionero, E.; González-Álvarez, I.; González-Álvarez, M.; Martínez-Máñez, R.; Marcos, M. D.; Bernardos, A.; Aznar, E. Surfactant-triggered Molecular Gate Tested on Different Mesoporous Silica Supports for Gastrointestinal Controlled Delivery. *Nanomaterials* **2020**, *10* (7), 1–18.

(20) Peña-Gómez, N.; Ruiz-Rico, M.; Fernández-Segovia, I.; Barat, J. M. Study of Apple Juice Preservation by Filtration through Silica Microparticles Functionalised with Essential Oil Components. *Food Control* **2019**, *106*, 106749.

(21) Sannino, F.; Costantini, A.; Ruffo, F.; Aronne, A.; Venezia, V.; Califano, V. Covalent Immobilization of β-Glucosidase into Mesoporous Silica Nanoparticles from Anhydrous Acetone Enhances Its Catalytic Performance. *Nanomaterials* **2020**, *10* (1), 108.

(22) Whitaker, J. R.; Lee, C. Y. Recent Advances in Chemistry of Enzymatic Browning. *Enzym. browning its Prev. - ACS Symp. Ser. 600* **1995**, *45* (2), 2–7.

(23) Gutierrez, J. B. *Ciencia Bromatológica: Principios Generales de Los Alimentos*, 1st ed.; DIAZ DE SANTOS, Ed.; 2000.

(24) Sánchez-Ferrer, Á.; Neptuno Rodríguez-López, J.; García-Cánovas, F.; García-Carmona, F. Tyrosinase: A Comprehensive Review of Its Mechanism. *Biochim. Biophys. Acta - Protein Struct. Mol. Enzymol.* **1995**, *1247* (1), 1–11.

(25) Rolff, M.; Schottenheim, J.; Decker, H.; Tuczek, F. Copper-O2 Reactivity of Tyrosinase Models towards External Monophenolic Substrates: Molecular Mechanism and Comparison with the Enzyme. *Chem. Soc. Rev.* **2011**, *40* (7), 4077–4098.

(26) Rouet-Mayer, M.-A.; Ralambosoa, J.; Philippon, J. Roles of O-Quinones and Their Polymers in the Enzymic Browning of Apples. *Phytochemistry* **1990**, *29* (2), 435–440.

(27) Martinez, M. V.; Whitaker, J. R. The Biochemistry and Control of Enzymatic Browning. *Trends Food Sci. Technol.* **1995**, *6* (6), 195–200.

(28) Hertog, M. G. L.; Hollman, P. C. H.; Katan, M. B. Content of Potentially Anticarcinogenic Flavonoids of 28 Vegetables and 9 Fruits Commonly Consumed in the Netherlands. *J. Agric. Food Chem.* **1992**, *40* (12), 2379–2383.

(29) Picinelli, A.; Sua´rez, B.; Mangas, J. J. Analysis of Polyphenols in Apple Products. *Zeitschrift für Leb. und -forsch. A* **1997**, *204* (1), 48–51.

(30) Rocha, A. M. C. .; Morais, A. M. M. . Characterization of Polyphenoloxidase (PPO) Extracted from 'Jonagored' Apple. *Food Control* **2001**, *12* (2), 85–90.

(31) Williams, D. C.; Lim, M. H.; Chen, A. O.; Pangborn, R. M.; Whitaker, H. R.

Blanching of Vegetables for Freezing: Which Indicator Enzyme to Choose. *Foof Technol.* **1986**, *40* (6), 130–140.

(32) Bomben, J. L.; Dietrich, W. C.; Hudson, J. S.; Hamilton, H. K.; Farkas, O. F. Yields and Solids Loss in Steam Blanching Cooling and Freezing Vegetables. *J. Food Sci.* **1975**, *40* (4), 660–664.

(33) Buckow, R.; Kastell, A.; Terefe, N. S.; Versteeg, C. Pressure and Temperature Effects on Degradation Kinetics and Storage Stability of Total Anthocyanins in Blueberry Juice. *J. Agric. Food Chem.* **2010**, *58* (18), 10076–10084.

(34) Toribio, J. L.; Lozano, J. E. Heat Induced Browning of Clarified Apple Juice at High Temperatures. *J. Food Sci.* **1986**, *51* (1), 172–175.

(35) Sapers, G. M.; Hicks, K. B.; Phillips, J. G.; Garzarella, L.; Pondish, D. L.; Matulaitis, R. M.; McCormack, T. J.; Sondey, S. M.; Seib, P. A.; EI-Atawy, Y. S. Control of Enzymatic Browning in Apple with Ascorbic Acid Derivatives, Polyphenol Oxidase Inhibitors, and Complexing Agents. *J. Food Sci.* **1989**, *54* (4), 997–1002.

(36) Sapers, G. M. Chitosan Enhances Control of Enzymatic Browning in Apple and Pear Juice by Filtration. *J. Food Sci.* **1992**, *57* (5), 1192–1193.

(37) Abid, M.; Jabbar, S.; Wu, T.; Hashim, M. M.; Hu, B.; Lei, S.; Zhang, X.; Zeng, X. Effect of Ultrasound on Different Quality Parameters of Apple Juice. *Ultrason. Sonochem.* **2013**, *20* (5), 1182–1187.

(38) Gui, F.; Wu, J.; Chen, F.; Liao, X.; Hu, X.; Zhang, Z.; Wang, Z. Inactivation of Polyphenol Oxidases in Cloudy Apple Juice Exposed to Supercritical Carbon Dioxide. *Food Chem.* **2007**, *100* (4), 1678–1685.

(39) Ho, S. Y.; Mittal, G. S. Electroporation of Cell Membranes: A Review. *Crit. Rev.*

Biotechnol. **1996**, *16* (4), 349–362.

(40) Juarez-Enriquez, E.; Salmeron-Ochoa, I.; Gutierrez-Mendez, N.; Ramaswamy, H. S.; Ortega-Rivas, E. Shelf Life Studies on Apple Juice Pasteurised by Ultrahigh Hydrostatic Pressure. *LWT - Food Sci. Technol.* **2015**, *62* (1, Part 2), 915–919.

(41) Müller, A.; Noack, L.; Greiner, R.; Stahl, M. R.; Posten, C. Effect of UV-C and UV-B Treatment on Polyphenol Oxidase Activity and Shelf Life of Apple and Grape Juices. *Innov. Food Sci. Emerg. Technol.* **2014**, *26*, 498–504.

(42) Vallet-Regí, M.; Balas, F.; Arcos, D. Mesoporous Materials for Drug Delivery. *Angew. Chemie Int. Ed.* **2007**, *46* (40), 7548–7558.

(43) Pérez-Esteve, E.; Bernardos, A.; Martínez-Máñez, R.; Barat, J. M. Nanotechnology in the Development of Novel Functional Foods or Their Package. An Overview Based in Patent Analysis. *Recent Pat. Food. Nutr. Agric.* **2013**, *5* (1), 35–43.

(44) Ispas, C.; Sokolov, I.; Andreescu, S. Enzyme-Functionalized Mesoporous Silica for Bioanalytical Applications. *Anal. Bioanal. Chem.* **2009**, *393* (2), 543–554.

(45) Corell Escuin, P.; García-Bennett, A.; Vicente Ros-Lis, J.; Argüelles Foix, A.; Andrés, A. Application of Mesoporous Silica Materials for the Immobilization of Polyphenol Oxidase. *Food Chem.* **2017**, *217*, 360–363.

(46) Barrett, E. P.; Joyner, L. G.; Halenda, P. P. The Determination of Pore Volume and Area Distributions in Porous Substances. I. Computations from Nitrogen Isotherms. *J. Am. Chem. Soc.* **1951**, *73* (1), 373–380.

(47) Brunauer, S.; Emmett, P. H.; Teller, E. Adsorption of Gases in Multimolecular Layers. *J. Am. Chem. Soc.* **1938**, *60* (2), 309–319.

(48) Neimark, A. V; Ravikovitch, P. I.; Grün, M.; Schüth, F.; Unger, K. K. Pore Size Analysis of MCM-41 Type Adsorbents by Means of Nitrogen and Argon Adsorption. *J. Colloid Interface Sci.* **1998**, *207* (1), 159–169.

(49) Espín, J. C.; Varón, R.; Fenoll, L. G.; Gilabert, M. A.; García-Ruíz, P. A.; Tudela, J.; García-Cánovas, F. Kinetic Characterization of the Substrate Specificity and Mechanism of Mushroom Tyrosinase. *Eur. J. Biochem.* **2000**, *267* (5), 1270–1279.

(50) Doran, P. M. *Principios de Ingeniería de Los Bioprocesos*; Acribia, 1998.

(51) De Arriaga, M. D. *Cinética Enzimática: Manejo de Datos*; Universidad de Oviedo, 1979.

(52) Bradford, M. M. A Rapid and Sensitive Method for the Quantitation of Microgram Quantities of Protein Utilizing the Principle of Protein-Dye Binding. *Anal. Biochem.* **1976**, *72* (1), 248–254.

(53) Richard-Forget, F. C.; Goupy, P. M.; Nicolas, J. J. Cysteine as an Inhibitor of Enzymic Browning. 2. Kinetic Studies. *J. Agric. Food Chem.* **1992**, *40* (11), 2108–2113.

(54) İyidoğan, N. F.; Bayındırlı, A. Effect of L-Cysteine, Kojic Acid and 4-Hexylresorcinol Combination on Inhibition of Enzymatic Browning in Amasya Apple Juice. *J. Food Eng.* **2004**, *62* (3), 299–304.

(55) Ros-Lis, J. V.; Casasús, R.; Comes, M.; Coll, C.; Marcos, M. D.; Martínez-Máñez, R.; Sancenón, F.; Soto, J.; Amorós, P.; Haskouri, J. E.; et al. A Mesoporous 3D Hybrid Material with Dual Functionality for Hg^{2+} Detection and Adsorption. *Chem. - A Eur. J.* **2008**, *14* (27), 8267–8278.

(56) Munjal, N.; Sawhney, S. . Stability and Properties of Mushroom Tyrosinase

Entrapped in Alginate, Polyacrylamide and Gelatin Gels. *Enzyme Microb. Technol.* **2002**, *30* (5), 613–619.

(57) Harvey, R. A.; Ferrier, D. R. *Biochemistry*, 5th ed.; Wolters Kluwer Health/Lippincott Williams & Wilkins, 2011.

(58) Barrera, C.; Betoret, N.; Corell, P.; Fito, P. Effect of Osmotic Dehydration on the Stabilization of Calcium-Fortified Apple Slices (Var. Granny Smith): Influence of Operating Variables on Process Kinetics and Compositional Changes. *J. Food Eng.* **2009**, *92* (4), 416–424.

(59) Reinkensmeier, A.; Steinbrenner, K.; Homann, T.; Bußler, S.; Rohn, S.; Rawel, H. M. Monitoring the Apple Polyphenol Oxidase-Modulated Adduct Formation of Phenolic and Amino Compounds. *Food Chem.* **2016**, *194*, 76–85.

(60) Kanteev, M.; Goldfeder, M.; Fishman, A. Structure-Function Correlations in Tyrosinases. *Protein Sci.* **2015**, *24* (9), 1360–1369.

(61) Mayer, A. M. Polyphenol Oxidases in Plants and Fungi: Going Places? A Review. *Phytochemistry* **2006**, *67* (21), 2318–2331.

(62) Decker, H.; Schweikardt, T.; Tuczek, F. The First Crystal Structure of Tyrosinase: All Questions Answered? *Angew. Chemie Int. Ed.* **2006**, *45* (28), 4546–4550.

(63) Nakamura, Y.; Torikai, K.; Ohigashi, H. A Catechol Antioxidant Protocatechuic Acid Potentiates Inflammatory Leukocyte-Derived Oxidative Stress in Mouse Skin via a Tyrosinase Bioactivation Pathway. *Free Radic. Biol. Med.* **2001**, *30* (9), 967–978.

(64) Reza, K. K.; Ali, M. A.; Srivastava, S.; Agrawal, V. V.; Biradar, A. M. Tyrosinase Conjugated Reduced Graphene Oxide Based Biointerface for Bisphenol A

Sensor. *Biosens. Bioelectron.* **2015**, *74*, 644–651.

(65) Ba, S.; Haroune, L.; Soumano, L.; Bellenger, J.-P.; Jones, J. P.; Cabana, H. A Hybrid Bioreactor Based on Insolubilized Tyrosinase and Laccase Catalysis and Microfiltration Membrane Remove Pharmaceuticals from Wastewater. *Chemosphere* **2018**, *201*, 749–755.

(66) Liu, D.-M.; Chen, J.; Shi, Y.-P. Tyrosinase Immobilization on Aminated Magnetic Nanoparticles by Physical Adsorption Combined with Covalent Crosslinking with Improved Catalytic Activity, Reusability and Storage Stability. *Anal. Chim. Acta* **2018**, *1006*, 90–98.

(67) Mishra, B. B.; Gautam, S.; Sharma, A. Free Phenolics and Polyphenol Oxidase (PPO): The Factors Affecting Post-Cut Browning in Eggplant (Solanum Melongena). *Food Chem.* **2013**, *139* (1–4), 105–114.

(68) Macedo, A. S. L.; Rocha, F. de S.; Ribeiro, M. da S.; Soares, S. E.; Bispo, E. da S. Characterization of Polyphenol Oxidase in Two Cocoa (Theobroma Cacao L.) Cultivars Produced in the South of Bahia, Brazil. *Food Sci. Technol.* **2016**, *36* (1), 56–63.

(69) Kaushik, N.; Rao, P. S.; Mishra, H. N. Process Optimization for Thermal-Assisted High Pressure Processing of Mango (Mangifera Indica L.) Pulp Using Response Surface Methodology. *LWT - Food Sci. Technol.* **2016**, *69*, 372–381.

(70) Liu, Y.; Hu, X.; Zhao, X.; Song, H. Combined Effect of High Pressure Carbon Dioxide and Mild Heat Treatment on Overall Quality Parameters of Watermelon Juice. *Innov. Food Sci. Emerg. Technol.* **2012**, *13*, 112–119.

(71) Bhat, R.; Ming Goh, K. Sonication Treatment Convalesce the Overall Quality of Hand-Pressed Strawberry Juice. *Food Chem.* **2017**, *215*, 470–476.

(72) Kim, D.; Song, H.; Lim, S.; Yun, H.; Chung, J. Effects of Gamma Irradiation on the Radiation-Resistant Bacteria and Polyphenol Oxidase Activity in Fresh Kale Juice. *Radiat. Phys. Chem.* **2007**, *76*, 1213–1217.

(73) Jiang, G.-H.; Kim, Y.-M.; Nam, S.-H.; Yim, S.-H.; Eun, J.-B. Enzymatic Browning Inhibition and Antioxidant Activity of Pear Juice from a New Cultivar of Asian Pear (Pyrus Pyrifolia Nakai Cv. Sinhwa) with Different Concentrations of Ascorbic Acid. *Food Sci. Biotechnol.* **2016**, *25* (1), 153–158.

(74) Giner-Casares, J. J.; Henriksen-Lacey, M.; Coronado-Puchau, M.; Liz-Marzán, L. M. Inorganic Nanoparticles for Biomedicine: Where Materials Scientists Meet Medical Research. *Mater. Today* **2016**, *19* (1), 19–28.

(75) Pallás, I.; Marcos, M.; Martínez-Máñez, R.; Ros-Lis, J. Development of a Textile Nanocomposite as Naked Eye Indicator of the Exposition to Strong Acids. *Sensors* **2017**, *17* (9), 2134.

(76) Poyatos-Racionero, E.; Ros-Lis, J. V.; Vivancos, J.-L.; Martínez-Máñez, R. Recent Advances on Intelligent Packaging as Tools to Reduce Food Waste. *J. Clean. Prod.* **2018**, *172*, 3398–3409.

(77) Shemetov, A. A.; Nabiev, I.; Sukhanova, A. Molecular Interaction of Proteins and Peptides with Nanoparticles. **2012**, *6* (6), 4585–4602.

(78) Chen, M.; Zeng, G.; Xu, P.; Lai, C.; Tang, L. How Do Enzymes “Meet” Nanoparticles and Nanomaterials? *Trends Biochem. Sci.* **2017**, *42*, 914–930.

(79) Muñoz-Pina, S.; Ros-Lis, J. V.; Argüelles, Á.; Coll, C.; Martínez-Máñez, R.; Andrés, A. Full Inhibition of Enzymatic Browning in the Presence of Thiol-Functionalised Silica Nanomaterial. *Food Chem.* **2018**, *241*, 199–205.

(80) Comes, M.; Aznar , E.; Moragues, M.; Marcos, M. D.; Martínez-Máñez, R.;

Sancenón, F.; Soto, J.; Villaescusa, L. A.; Gil, L.; Amorós, P. Mesoporous Hybrid Materials Containing Nanoscopic “Binding Pockets” for Colorimetric Anion Signaling in Water by Using Displacement Assays. *Chem. - A Eur. J.* **2009**, *15* (36), 9024–9033.

(81) Canilho, N.; Jacoby, J.; Pasc, A.; Carteret, C.; Dupire, F.; Stébé, M. J.; Blin, J. L. Isocyanate-Mediated Covalent Immobilization of Mucor Miehei Lipase onto SBA-15 for Transesterification Reaction. *Colloids Surfaces B Biointerfaces* **2013**, *112*, 139–145.

(82) Liu, D.-M.; Chen, J.; Shi, Y.-P. Advances on Methods and Easy Separated Support Materials for Enzymes Immobilization. *TrAC Trends Anal. Chem.* **2018**, *102*, 332–342.

(83) Haskouri, J. El; Dallali, L.; Fernández, L.; Garro, N.; Jaziri, S.; Latorre, J.; Guillem, C.; Beltrán, A.; Beltrán, D.; Amorós, P. ZnO Nanoparticles Embedded in UVM-7-like Mesoporous Silica Materials: Synthesis and Characterization. *Phys. E Low-dimensional Syst. Nanostructures* **2009**, *42* (1), 25–31.

(84) Yiu, H. H. .; Wright, P. A.; Botting, N. P. Enzyme Immobilisation Using SBA-15 Mesoporous Molecular Sieves with Functionalised Surfaces. *J. Mol. Catal. B Enzym.* **2001**, *15* (1), 81–92.

(85) Tortajada, M.; Ramón, D.; Beltrán, D.; Amorós, P. Hierarchical Bimodal Porous Silicas and Organosilicas for Enzyme Immobilization. *J. Mater. Chem.* **2005**, *15* (35–36), 3859.

(86) Zou, B.; Hu, Y.; Cui, F.; Jiang, L.; Yu, D.; Huang, H. Effect of Surface Modification of Low Cost Mesoporous SiO2 Carriers on the Properties of Immobilized Lipase. *J. Colloid Interface Sci.* **2014**, *417*, 210–216.

(87) Fan, Y.; Flurkey, W. H. Purification and Characterization of Tyrosinase from Gill Tissue of Portabella Mushrooms. *Phytochemistry* **2004**, *65* (6), 671–678.

(88) Yang, J.; Saggiomo, V.; Velders, A. H.; Cohen Stuart, M. A.; Kamperman, M. Reaction Pathways in Catechol/Primary Amine Mixtures: A Window on Crosslinking Chemistry. *PLoS One* **2016**, *11* (12), e0166490.

(89) Wu, J.; Zhang, L.; Wang, Y.; Long, Y.; Gao, H.; Zhang, X.; Zhao, N.; Cai, Y.; Xu, J. Mussel-Inspired Chemistry for Robust and Surface-Modifiable Multilayer Films. *Langmuir* **2011**, *27* (22), 13684–13691.

(90) Slavin, J. L.; Lloyd, B. Health Benefits of Fruits and Vegetables. *Adv. Nutr.* **2012**, *3* (4), 506–516.

(91) Dhyani, P.; Bahukhandi, A.; Rawat, S.; Bhatt, I. D.; Rawal, R. S. Diversity of Bioactive Compounds and Antioxidant Activity in Delicious Group of Apple in Western Himalaya. *J. Food Sci. Technol.* **2018**, *55* (7), 2587–2599.

(92) Massini, L.; Rico, D.; Martin-Diana, A. B. Quality Attributes of Apple Juice: Role and Effect of Phenolic Compounds. In *Fruit Juices*; Rajauria, G., Tiwari, B. K., Eds.; Academic Press, 2018; pp 45–57.

(93) Kolniak-Ostek, J.; Oszmiański, J.; Wojdyło, A. Effect of L-Ascorbic Acid Addition on Quality, Polyphenolic Compounds and Antioxidant Capacity of Cloudy Apple Juices. *Eur. Food Res. Technol.* **2013**, *236* (5), 777–798.

(94) Marszałek, K.; Woźniak, Ł.; Barba, F. J.; Skąpska, S.; Lorenzo, J. M.; Zambon, A.; Spilimbergo, S. Enzymatic, Physicochemical, Nutritional and Phytochemical Profile Changes of Apple (Golden Delicious L.) Juice under Supercritical Carbon Dioxide and Long-Term Cold Storage. *Food Chem.* **2018**, *268*, 279–286.

(95) Jukanti, A. *Polyphenol Oxidases (PPOs) in Plants*; Springer Singapore, 2017.

(96) Singh, B.; Suri, K.; Shevkani, K.; Kaur, A.; Kaur, A.; Singh, N. Enzymatic Browning of Fruit and Vegetables: A Review. In *Enzymes in Food Technology: Improvements and Innovations*; Springer Singapore, 2018; pp 73–78.

(97) Sauceda-Gálvez, J. N.; Codina-Torrella, I.; Martinez-Garcia, M.; Hernández-Herrero, M. M.; Gervilla, R.; Roig-Sagués, A. X. Combined Effects of Ultra-High Pressure Homogenization and Short-Wave Ultraviolet Radiation on the Properties of Cloudy Apple Juice. *LWT* **2021**, *136*, 110286.

(98) Muñoz-Pina, S.; Ros-Lis, J. V.; Argüelles, Á.; Martínez-Máñez, R.; Andrés, A. Influence of the Functionalisation of Mesoporous Silica Material UVM-7 on Polyphenol Oxidase Enzyme Capture and Enzymatic Browning. *Food Chem.* **2020**, *310*.

(99) Sánchez-Cabezas, S.; Montes-Robles, R.; Gallo, J.; Sancenón, F.; Martínez-Máñez, R. Combining Magnetic Hyperthermia and Dual T1/T2 MR Imaging Using Highly Versatile Iron Oxide Nanoparticles. *Dalt. Trans.* **2019**, *48* (12), 3883–3892.

(100) Illera, A. E.; Chaple, S.; Sanz, M. T.; Ng, S.; Lu, P.; Jones, J.; Carey, E.; Bourke, P. Effect of Cold Plasma on Polyphenol Oxidase Inactivation in Cloudy Apple Juice and on the Quality Parameters of the Juice during Storage. *Food Chem. X* **2019**, *3*, 100049.

(101) Aranibar, C.; Pigni, N. B.; Martinez, M.; Aguirre, A.; Ribotta, P.; Wunderlin, D.; Borneo, R. Utilization of a Partially-Deoiled Chia Flour to Improve the Nutritional and Antioxidant Properties of Wheat Pasta. *LWT - Food Sci. Technol.* **2018**, *89*, 381–387.

(102) Andrew L Waterhouse. Determination of Total Phenolics. In *Current protocols in food analytical chemistry*; John Wiley & Sons, Inc., 2002; Vol. 6, p I1.1.1-I1.1.8.

(103) Thaipong, K.; Boonprakob, U.; Crosby, K.; Cisneros-Zevallos, L.; Hawkins Byrne, D. Comparison of ABTS, DPPH, FRAP, and ORAC Assays for Estimating Antioxidant Activity from Guava Fruit Extracts. *J. Food Compos. Anal.* **2006**, *19* (6–7), 669–675.

(104) Wu, C.; Li, T.; Qi, J.; Jiang, T.; Xu, H.; Lei, H. Effects of Lactic Acid Fermentation-Based Biotransformation on Phenolic Profiles, Antioxidant Capacity and Flavor Volatiles of Apple Juice. *LWT* **2020**, *122*, 109064.

(105) Selimović, A.; Salkić, M.; Selimović, A. Direct Spectrophotometric Determination of L-Ascorbic Acid in Pharmaceutical Preparations Using Sodium Oxalate as a Stabilizer. *Eur. J. Sci. Res.* **2011**, *53* (2), 193–198.

(106) Pérez-Esteve, É.; Ruiz-Rico, M.; Martínez-Máñez, R.; Barat, J. M. Mesoporous Silica-Based Supports for the Controlled and Targeted Release of Bioactive Molecules in the Gastrointestinal Tract. *J. Food Sci.* **2015**, *80* (11), E2504–E2516.

(107) Pérez-Cabero, M.; Hungría, A. B.; Morales, J. M.; Tortajada, M.; Ramón, D.; Moragues, A.; Haskouri, J. El; Beltrán, A.; Beltrán, D.; Amorós, P. Interconnected Mesopores and High Accessibility in UVM-7-like Silicas. *J. Nanoparticle Res.* **2012**, *14* (8), 1–12.

(108) Muñoz-Pina, S.; Amorós, P.; Haskouri, J. El; Andrés, A.; Ros-Lis, J. V. Use of Silica Based Materials as Modulators of the Lipase Catalyzed Hydrolysis of Fats under Simulated Duodenal Conditions. *Nanomaterials* **2020**, *10* (10), 1927.

(109) Falguera, V.; Sánchez-Riaño, A. M.; Quintero-Cerón, J. P.; Rivera-Barrero, C. A.; Méndez-Arteaga, J. J.; Ibarz, A. Characterization of Polyphenol Oxidase Activity in Juices from 12 Underutilized Tropical Fruits with High Agroindustrial Potential. *Food Bioprocess Technol.* **2012**, *5* (7), 2921–2927.

(110) Terra, A. L. M.; Moreira, J. B.; Costa, J. A. V.; Morais, M. G. de. Development of Time-PH Indicator Nanofibers from Natural Pigments: An Emerging Processing Technology to Monitor the Quality of Foods. *LWT* **2021**, *142*, 111020.

(111) King, K. A.; Derijk, W. G. Variations of L*a*b* Values among Vitapan® Classical Shade Guides: Basic Science Research. *J. Prosthodont.* **2007**, *16* (5), 352–356.

(112) Suárez-Jacobo, Á.; Saldo, J.; Rüfer, C. E.; Guamis, B.; Roig-Sagués, A. X.; Gervilla, R. Aseptically Packaged UHPH-Treated Apple Juice: Safety and Quality Parameters during Storage. *J. Food Eng.* **2012**, *109* (2), 291–300.

(113) Xu, J.; Zhou, L.; Miao, J.; Yu, W.; Zou, L.; Zhou, W.; Liu, C.; Liu, W. Effect of Cinnamon Essential Oil Nanoemulsion Combined with Ascorbic Acid on Enzymatic Browning of Cloudy Apple Juice. *Food Bioprocess Technol.* **2020**, *13* (5), 860–870.

(114) Dumbravă, D.-G.; Hădărugă, N.-G.; Moldovan, C.; Raba, D.-N.; Popa, M.-V.; Rădoi, B. Antioxidant Activity of Some Fresh Vegetables and Fruits Juices. *J. Agroaliment. Process. Technol.* **2011**, *17* (2), 163–168.

(115) Joshi, A. P. K.; Rupasinghe, H. P. V.; Pitts, N. L.; Khanizadeh, S. Biochemical Characterization of Enzymatic Browning in Selected Apple Genotypes. *Can. J. Plant Sci.* **2007**, *87* (5), 1067–1074.

(116) López-Nicolás, J. M.; Núñez-Delicado, E.; Sánchez-Ferrer, Á.; García-Carmona,

F. Kinetic Model of Apple Juice Enzymatic Browning in the Presence of Cyclodextrins: The Use of Maltosyl-β-Cyclodextrin as Secondary Antioxidant. *Food Chem.* **2007**, *101* (3), 1164–1171.

(117) Arora, B.; Sethi, S.; Joshi, A.; Sagar, V. R.; Sharma, R. R. Antioxidant Degradation Kinetics in Apples. *J. Food Sci. Technol.* **2018**, *55* (4), 1306–1313.

(118) Aguilar, K.; Garvín, A.; Lara-Sagahón, A. V.; Ibarz, A. Ascorbic Acid Degradation in Aqueous Solution during UV-Vis Irradiation. *Food Chem.* **2019**, *297*, 124864.

(119) Fernández-Jalao, I.; Sánchez-Moreno, C.; De Ancos, B. Effect of High-Pressure Processing on Flavonoids, Hydroxycinnamic Acids, Dihydrochalcones and Antioxidant Activity of Apple 'Golden Delicious' from Different Geographical Origin. *Innov. Food Sci. Emerg. Technol.* **2019**, *51*, 20–31.

(120) Liu, F.; Han, Q.; Ni, Y. Comparison of Biochemical Properties and Thermal Inactivation of Membrane-Bound Polyphenol Oxidase from Three Apple Cultivars (Malus Domestica Borkh). *Int. J. Food Sci. Technol.* **2018**, *53* (4), 1005–1012.

(121) Fu, Y.; Zhang, K.; Wang, N.; Du, J. Effects of Aqueous Chlorine Dioxide Treatment on Polyphenol Oxidases from Golden Delicious Apple. *LWT - Food Sci. Technol.* **2007**, *40* (8), 1362–1368.

(122) Noci, F.; Riener, J.; Walkling-Ribeiro, M.; Cronin, D. A.; Morgan, D. J.; Lyng, J. G. Ultraviolet Irradiation and Pulsed Electric Fields (PEF) in a Hurdle Strategy for the Preservation of Fresh Apple Juice. *J. Food Eng.* **2008**, *85* (1), 141–146.

6. CONCLUDING REMARKS

6. Concluding remarks

Enzymatic browning on fruits and vegetables as well as the main weaknesses of thermal treatments and their alternatives have been the starting point of this work. Concretely, fulfilling the main goal of this doctoral thesis, two anti-browning processes have been studied and designed based on two diverse strategies: mesoporous silica materials and macrocyclic compounds. Some concluding remarks related to the preliminary two research question and specific objectives are presented accordingly:

- Macrocyclic compounds: The factors influencing the interactions between both PPO and macrocyclic compounds altering the enzymatic activity have been explored in this thesis. It has been proven that both the ring size and the number of nitrogen are the main factors of the molecular structure affecting their inhibitory power. Furthermore, both contact time between the enzyme and the inhibitor and the pH of the solution would influence the inhibitory response. The ability to inhibit enzymatic browning is generally due to alterations not only on the PPO, but also, on the non-enzymatic polymerization of quinones.

  First, among the ten inhibitors studied at the beginning, the most active was an azamacrocyclic compound functionalized with two naphthyl units. This novel inhibitor is capable of inhibiting PPO in a non-competitive S-parabolic I-parabolic nature and performs conformational changes over the enzyme archiving a remarkable inhibition (IC_{50}= 10µM). Indeed, its performance was checked on a real enzymatic browning process using apple juice as a real matrix. The enzymatic browning was delayed a 60% after an hour.

  Second, a macrocyclic containing an hydroxypyridinone like kojic acid performs a mixed type of inhibition over the PPO in model system with an

IC_{50} of 0.30 mM. Moreover, it significantly reduces the enzymatic browning in freshly apple juice by more than 50% stopping the oxidation of the TPC and delaying the loss of the antioxidant capacity.

- Mesoporous silica materials: Silica-based material are able to interact with the PPO immobilizing it, blocking its activity, and can be easily removable from the medium. Of the four studied materials, the support UVM-7 offers the best inhibitory properties mainly due to its double mesopore-micropore combination in its structure. The functionalization of these materials plays a crucial role in their inhibition and/or immobilization yield power. The functionalization with thiol groups showed the greatest inhibitory power on the enzyme and the enzymatic browning. It enhances notably the PPO inhibition archiving a total inhibition at a ratio of 3 mg/93.75 U in model systems. Conversely, amine groups have proven to be the best to immobilize the enzyme, retaining 100% of the enzyme tyrosinase. In addition, in real samples, it can eliminate the enzyme from the medium when it is filtered decreasing the enzymatic browning.

  In order to eliminate the silica particles from the juice avoiding the filtration of food samples, a new magnetic UVM-7 has been developed. Its performance on apple juice has revealed that the new magnetic UVM-7 functionalised with thiol groups not only significantly slows the enzymatic browning (70%), but also remains stable the total flavonoids, vitamin C, and the antioxidant capacity (ABTS) even after its removal from the medium..

7. FUTURE PERSPECTIVES

7. Future perspectives

So far in this study, the results obtained have demonstrated the potential use as anti-browning of two innovative approaches when it comes to inhibiting and stopping enzymatic browning. However, more research is needed to enable scaling up the process to industry level. In the first place, the use of the azamacrocyclic inhibitors has only been tested in one type of food, apple juice. Nevertheless, knowing that the chemical characteristics of the enzyme vary remarkably from one fruit to another as well as the stages of ripeness, it would be necessary to extend these investigations to other types of fruits. On the other hand, sensory studies would be essential to validate its use and acceptance among consumers.

Regarding the use of nanomaterials as a new industrial methodology, our studies have been developed and validated to inhibit the enzymatic browning in apple juice. Nonetheless, same as in the previous case, test in more types of food would be needed. Moreover, it would be interesting to functionalise the UVM-7 support with the best azamacrocyclic compounds studied in this thesis. Taking into account that the consumer prefers more and more foods without additives, the merging of the two strategies studied could lead to an even more powerful inhibitor that is also eliminated from the medium.

Although the studied macrocyclic compounds and micro-sized silica materials have not shown toxicity in preliminary tests, more toxicity tests of the studied inhibitors should be done to ensure their safety. Moreover, test of residual magnetic material on juices has to be done to guarantee a final safe product.

Finally, taking into mind the objective of finding a more sustainable non-thermal process for the inhibition of enzymatic browning, the recovery and reuse of the material is a priority approach. The magnetic core facilitates the recovery of the

material through magnetic fields but optimising the process for the recovery of the material and determining the maximum cycles of reusability is crucial. On the other hand, given its ability to immobilize the PPO, another interesting line would be to study the possible extraction of the PPO from the material getting the PPO as by-product, which is a high price enzyme in the market.

Thus, this thesis has been a starting point for the implementation of two lines of research that had not previously been implemented as anti-browning agents but has a promising result.